The effect of *gw2* mutant alleles on grain weight and size in bread wheat

Aura Montemayor Lara

A thesis submitted to the University of East Anglia for the degree of Doctor of Philosophy

John Innes Centre

December 2022

Abstract

Food production must increase to meet consumer demands in a population that is growing at a faster pace than current yield increases. Grain weight and size are amongst the most important agronomical traits as they impact grain yield. To date, our understanding on how grain weight is genetically controlled in wheat is still growing. The overall aim of this thesis was to understand if the *GRAIN WIDTH 2* (*GW2*) mutant alleles play a role in increasing grain weight in different wheat genetic backgrounds tested under contrasting environments. To address this, a detailed characterisation of *GW2* single, double and triple mutant near isogenic lines (NILs) was conducted in UK and international field trials. Likewise, we also aimed to understand whether these increases were mediated by the plant hormones gibberellins.

Thousand grain weight (TGW) and protein content increased consistently with increasing number of mutant *GW2* copies in a dosage-dependent manner in cv Paragon under UK trials. Yield did not increase in the single and double mutants, but a significant decrease was found in the triple mutants. The effect of the *gw2* alleles in two wheat cultivars, Reedling and Kingbird, grown across contrasting field environments (irrigation, heat stress and drought) was also assessed. Contrasting effects were found, with the *gw2* allele having a positive effect on TGW and yield in Kingbird while in Reedling the effect was detrimental. Finally, two different glasshouse experiments were conducted to determine the effect of bioactive gibberellins and paclobutrazol applications on final seed weight and morphometrics. Our findings are relevant in the context of food security as they show the potential to increase grain size and grain protein content with a neutral effect on yield. Furthermore, we found that increases in yield are achievable during heat stress which is relevant in the context of climatic change.

Access Condition and Agreement

Acknowledgements

Index

VII

Index of figures

Table list

List of Abbreviations

ABA	abscisic acid
ARF2	AUXIN RESPONSE FACTOR 2
BB	Big Brother
BR	Brassinosteroids
CK	Cytokinin
dpa	Days post anthesis
DTA	Days to anthesis
DTH	Days to heading
DTM	Days to Maturity
DW	Dry weight
EMS	ethyl methanesulphonate
ET	Ethylene
GWAS	Genome Wide Association Studies
GA	Gibberellin
Gbp	Giga base pair
GN1	Grain number 1
GW2	GRAIN WIDTH 2
GPC	Grain protein content
GFP	Green filling duration
H	Haplotypes
HLW	Hecto Liter weight
JA	Jasmonic Acid
KASP	Kompetitive Allele Specific PCR
Mbp	Mega Base Pairs
Mya	Million years ago
MT	Mutant
NILs	Near Isogenic Lines
PAC	Paclobutrazol
PPD-D1	PHOTOPERIOD-D1
QTL	Quantitative trait loci
RIL	Recombinant Inbred Lines
Rht	Reduced height
RNAi	RNA interference
RNA-Seq	RNA sequencing
SA	Salicylic Acid
SEM	Scanning electron microscope
SNPs	Single Nucleotide Polymorphisms
TCP	TEOSINTE, CYCLOIDEA and PROLIFERATING CELL FACTORS
TF	Transcription Factor
TGW	Thousand Grain Weight
TILLING	Targeting Induced Local Lesions in Genomes
UHPLC-MS	Ultra-high performance liquid chromatography tandem mass spectrometry
WT	Wild type

1. General introduction

1.1. Crop production must increase to tackle world hunger

The production of cereal grains is critical for food security. Crop production must increase to meet the demands of a global population estimated to exceed nine billion by 2050 (FAO, 2021). By 2050, crop production must increase by at least 50%, however, present rates of yield growth won't be enough to meet the demands from consumers, farmers and food industry (Reynolds et al., 2022 ; Ray et al., 2013). Furthermore, the arable land decreased in all regions for the past 20 years while population grows faster than production and cropland areas (FAO, 2021). Therefore, it is essential and urgent that we find methods to boost crop yields. Higher yield lowers agricultural commodity prices, which leads to lower numbers of malnourished people at risk of hunger (Rosegrant et al., 2013). Genetic improvements in yield potential have boosted wheat production in the past decades; however, the current genetic gains are not enough to overcome the challenges of a growing population without increasing the amount of land under arable use. Understanding how crop yield and yield components are affected by the environment and genetics across the life cycle of wheat is needed to achieve the increasing food demands (Reynolds et al., 2009).

1.2. The role of wheat for global food security

Cereal grain production is essential for ensuring food security. Wheat (*Triticum aestivum*), rice (*Oryza sativa*), and maize (*Zea mays*) are some of the grasses produced for their edible grains or their derived products. Only 15 crop plants, out of more than 50,000 edible plant species in the world, are responsible for 90% of the world's food energy consumption (Stewart and Lal, 2018b). Close to 87% of the world's cereal production are made up of rice, maize, and wheat (Figure1.1) (FAO, 2021). Wheat alone provides around 20% of the daily calories and protein intake. Globally, wheat is grown in more than 200 million hectares of arable land in all five continents, with Russia, China and India as the world's biggest producers (Figure 1.2) (FAO, 2021).
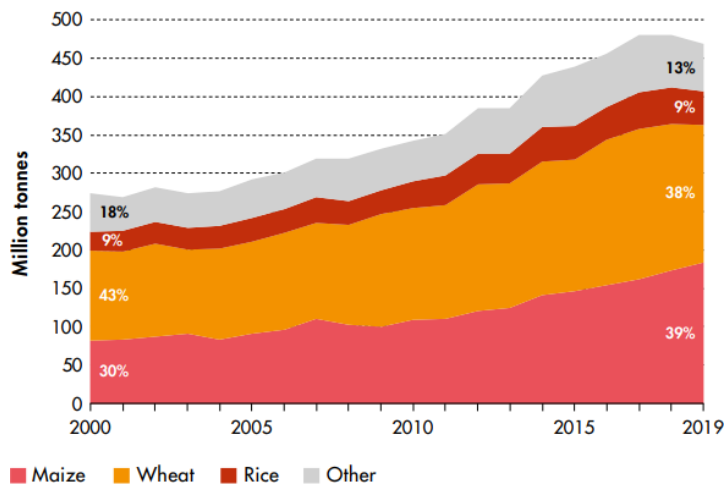
Figure 1-1: Global crop production from 2000-2019 adapted from FAO, 2021
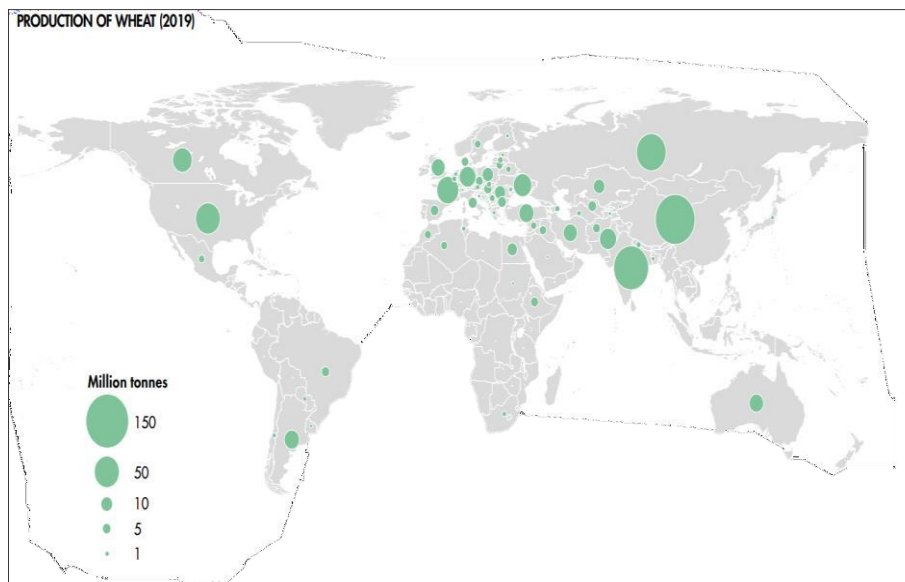
Figure 1-2: Global wheat production in 2019 by country. Adapted from FAO, 2021

1.3. Wheat, from an evolutionary viewpoint

Wheat was domesticated around 8000-10,000 years ago by farmers in what is known today as the Fertile Crescent, in the mountainous regions that surround the plains of the Tigris and Euphrates Rivers in modern-day Iran, Iraq, Turkey, Syria, Lebanon, Jordan and Israel (Charmet, 2011). The most common forms of domesticated wheat are tetraploid durum wheat (*T. turgidum* ssp. *durum L.*) and hexaploid bread wheat (*T. aestivum*) (Adamski et al., 2020). Polyploid wheat is derived from hybridisation events between different ancestral progenitor species (*Triticum* and *Aegilops*). The A and B genomes diverged around 6.5 million years ago (Mya) from a common ancestor. A hybridization occurred ~5.5 Mya between the A and B genomes giving rise to the D genome. About ~0.8 Mya the A and B genome hybridised giving rise to tetraploid durum wheat (AABB) or pasta wheat. Finally, around ~0.4 Mya the AA

and the BB genome hybridised with the DD genome from *Ae. tauschii* giving rise to the hexaploid bread wheat (AABBDD) (Figure 1.3) (Marcussen et al., 2014). These closely related genomes, known as homoeologous genomes, are on average >95% similar across their coding regions and usually have a highly conserved gene structure (Adamski et al., 2020). Tetraploid and hexaploid wheat have large genomes, 12 and 16 Giga base pair (Gbp) respectively, which consist mostly of (>85%) repetitive elements (Adamski et al., 2020). The present work focuses on bread wheat although some of the germplasm we used is derived from crosses with tetraploid wheat Kronos.
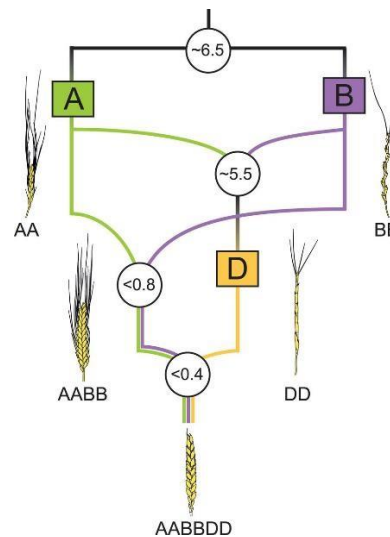
Figure 1-3: Model of the phylogenetic history of bread wheat (Triticum aestivum; AABBDD).Approximate dates for divergence and the hybridization events are given in white circles in units of million years ago adapted from (Marcussen et al., 2014).

1.4. Available genomic resources in wheat

A comprehensive list of wheat genomic resources can be found in Adamski et al. (2020). In this section, we discuss the genomic resources relevant for this thesis.

1.4.1. Wheat genome assemblies

As we previously mentioned, bread wheat consists of three genomes (A, B and D), each composed of seven chromosomes, that share >95% similarity in the coding regions. In total, they add up to 16 Gbp and over 85% of the genome are highly repetitive sequences (Adamski et al., 2020). The study of wheat used to be challenging due to the lack of available genomic resources. However, a turning point in the study of wheat came when the most comprehensive wheat genome assembly, called RefSeqv1.0, was released (Appels et al.,2018). This assembly was based on the landrace 'Chinese Spring' which has been used to develop extensive cytogenetic stocks for wheat genetic research.

1.4.2. Comparing plant orthologs and wheat homologues in Ensembl Plants

Another useful tool for the present work was the Ensembl Plants website (https://plants.ensembl.org/index.html). In this portal, over 128 genomes (RefSeqv1.0) are available, including *Arabidopsis thaliana, Oryza sativa, Triticum aestivum, Hordeum vulgare* and *Zea mays,* allowing users to quickly compare between plant genomes (Howe et al., 2020). For example, orthologous genes can be identified through predefined phylogenetic trees defined by the Plants Compara pipeline (Howe et al., 2020). The Ensembl Plant website also allows user to download these sequences for further examination and has a catalogue of single nucleotide polymorphisms (SNPs) including the sequenced mutant populations of wheat (described below). In 2020, an additional 14 wheat genomes from commercial cultivars were added to the browser. This was particularly useful as most of the thesis work was conducted in cv Paragon which was part of this newly added set of genome assemblies (Walkowiak et al., 2020).

1.4.3. TILLING wheat population

The Targeting Induced Local Lesions in Genomes (TILLING) populations were developed in durum wheat cv Kronos and bread wheat cv Cadenza by inducing random mutations in the genome using ethyl methanesulphonate (EMS) as a chemical mutagen. This method can be used to generate novel variations for both breeding and research purposes (Uauy et al., 2017). However, screening for desired mutations on each of the EMS individual lines can be extremely time consuming as it requires the design of genome specific primers followed by PCR, screening and sequencing of individual lines or pools. To overcome this hurdle, the *in silico* wheat TILLING resource was generated to search for alleles of interest across the genome with a ~90% coverage (Krasileva et al., 2017). Exome capture and Illumina sequencing were conducted across 2,735 mutant lines from both Kronos and Cadenza EMS populations. This resource allows the rapid identification of novel mutations in specific genes for functional characterisation. In the present work, all the mutations in the *GW2* genes to generate the Paragon *gw2* triple mutants originated from either the Kronos or Cadenza TILLING mutants (see more details in chapter 2). The mutations in the A and B copies were previously identified using the PCR-based method Uauy et al. (2009), whereas the mutation in the *gw2* D genome was found using the *in silico* approach (Krasileva et al., 2017, Wang et al., 2018).

1.4.4. CerealsDB

Many genotyping arrays have been developed for wheat over the past 10 years. Access to this data and cross-comparisons are often difficult due to the data being available in a wide range of databases. CerealsDB is a website that allows us to compare similarities between wheat varieties, as it includes a database which contains over 100,000 putative varietal SNPs Wilkinson et al. (2020) across over 6,000 genotypes. We used this online resource to compare SNP's between cultivars Reedling and Recital in Chapter 3.

1.4.5. Wheat Haplotypes

The wheat pangenome project was a global effort to assemble 14 bread wheat genomes at chromosome-scale level to complement the previously published Chinese Spring reference (Walkowiak et al., 2020). Using pairwise chromosome-based alignments, Brinton et al (2020) identified regions with very high sequence identity (median over 99.99% identity) which they defined as identical-by-state or that shared a common haplotype. This analysis was done in a pairwise manner for all chromosome scale assemblies and scaffold level assemblies of UK cultivars (Cadenza, Paragon, Claire and Robigus) and the CIMMYT cultivar Weebill-1(Brinton et al., 2020). This data was organised and visualised in the crop haplotype website (http://www.crop-haplotypes.com) which allows users an interactive way of visualizing the shared haplotypes between the wheat genomes. This resource was useful when comparing the 6A chromosome haplotypes in Chapter 3.

These resources opened new opportunities for wheat research, and the present work has drawn extensively from them.

1.5. Wheat developmental stages

Wheat development is a succession of changes in the growth of different plant organs describing the life cycle from sowing to the harvesting of mature grains. The life cycle can be divided in vegetative, reproductive and grain filling phase which are influenced by environmental conditions and external events alongside the physiological life cycle of a plant. Final grain yield is therefore the outcome of this developmental process to which most, if not all, genes will contribute in one way or another (Figure 4) (Slafer, 2003).
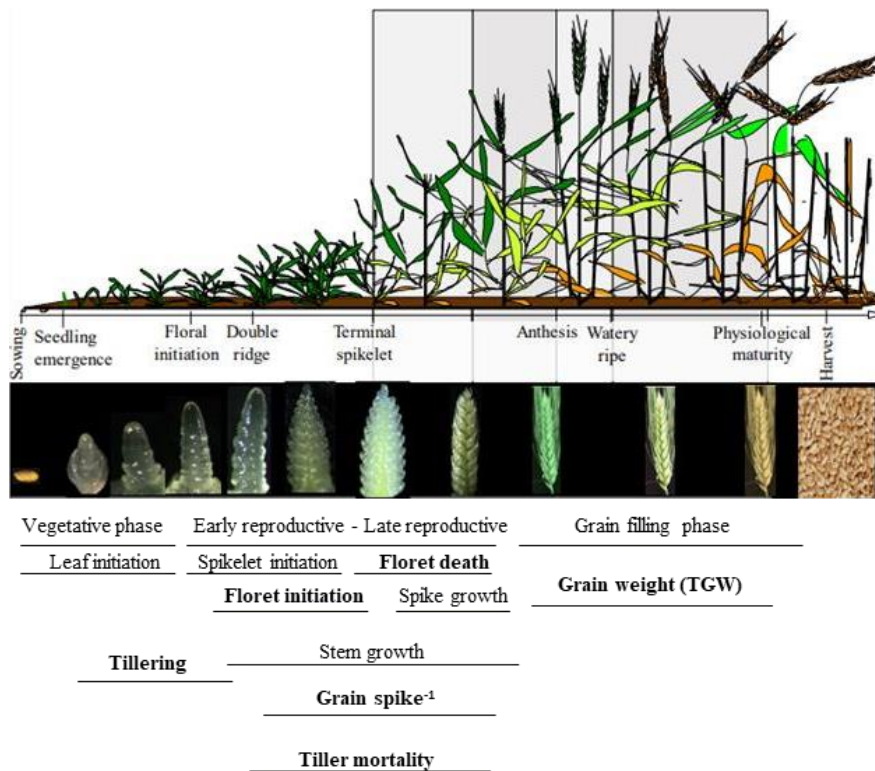
Figure 1-4: Schematic diagram of wheat growth and development including the main growth stages. Bars at the bottom of the figure represent stages which define the establishment of individual yield components or sub-components. Adapted from Slafer et al., 2022.

1.5.1. Vegetative phase

The vegetative phase starts at sowing time where leaf emergence and tiller initiation take place. Lateral shoots located in the axils of leaves differentiate to produce tillers (branches) sequentially. Each tiller has the potential to produce secondary tillers and wheat inflorescences contributing to the number of spikes per plant (spikes plant^{-1}) (Hyles et al., 2017). Tiller survival and tiller fertility are tightly affected by environmental conditions like temperature, day length, nitrogen and plant density (Hyles et al., 2020). Depending on whether the wheat variety is a "winter" or "spring" type, the vegetative phase's length can change. Winter wheat have a long vegetative phase because of the need of a cold spell, to initiate flowering known as vernalization. Conversely, spring wheats flowers without the requirement for a vernalization period, growing more quickly through the vegetative phase (Ordon, 2019). The transition from vegetative phase to reproductive phase is defined by the initiation of the floral primordial (Waddington. et al., 1983).

1.5.2. *Reproductive phase*

The reproductive phase can be divided in two main stages: the early reproductive stage is when floral initiation occurs followed by double ridge stage and ending with the terminal spikelet stage. The terminal spikelet stage determines the total spikelet number and is the first yield component to be fixed. During the early reproductive stage, tiller numbers reach its peak. The late reproductive phase is marked by the transition of the terminal spikelet stage to anthesis. During this phase, tiller numbers drop by about 25% while only 3-5 florets out of 10-20 florets per spike, will survive and set grains. Thus, the total amount of spikes per area (spikes m^{-2}) and grains per spike is fixed during the reproductive phase (Slafer et al., 2022). Simultaneously, stem elongation and spike growth occur. Both are considered critical for yield formation as the total number of fertile florets that potentially can become grains depends on the duration of both (Kronenberg et al., 2017). The floret survival/mortality is thought to be determined by the competition for resources between the spike and the stem Kirby (1988) and will ultimately define grain number per spike.

1.5.3. *Grain filling phase*

The grain filling phase occurs when the grain first develops endosperm cells growing to its final weight and size mainly by accumulating starch, proteins and minerals. The grain filling rate peaks from 14 to 28 days post anthesis (dpa). During this period, the dry weight doubles while the grain size and volume continue to increase. Grain length and total water content also reaches it maximal during this phase (~ 40 dpa), while final width and weight reach their peak at physiological maturity when the grain reaches maximum dry weight. Finally, in the desiccation and maturation period, water is lost from the grain and grain volume changes slightly due to decreases in length, width and final grain area (Brinton and Uauy, 2019).

1.5.4. *Grain development*

Around 2-3 dpa, the grain begins to develop as a result of a double fertilisation in which one pollen reproductive nucleus fuses with two female polar nuclei inside the embryo sac to produce a triploid (3n) endosperm nucleus, and the second pollen reproductive nucleus fuses with the egg nucleus to produce a diploid zygote (2n). The maternally derived tissues (nucellus, nucellar epidermis, inner integument, outer integument, tube cells, cross cells, and maternal pericarp) surround the endosperm nucleus and the diploid zygote embryo (Bechtel et al., 2009). After fertilisation, the process of mitosis begins, resulting in the development of a single multinucleate cell called the endosperm, which has a large central vacuole and a peripheral zone of cytoplasm. (Shewry et al., 2012). At the beginning of the cellularization stage, the endosperm cells begin to differentiate, producing the aleurone layer and the starchy endosperm. Under UK growing conditions, the beginning of grain filling is marked by the development of both the starchy endosperm and aleurone layer, which is followed by a phase of grain maturation and desiccation. The mature

aleurone accounts for about 6.5% of the grain dry weight and the starchy endosperm for about 80% (Barron et al., 2007). Once the seed is completely mature, it consists mainly of the endosperm and the embryo surrounded by the pericarp, which is the maternal outer layer composed by the epicarp, mesocarp and endocarp (Figure 1.5). Pericarp cells go through a phase of cell division shortly after fertilization (~2 dpa) followed by cell expansion and a rapid programmed cell death. At maturity, the pericarp tissue is dry and together comprise about 7–8% of the grain dry weight (Brinton and Uauy, 2019; Shewry et al., 2012).

Different stages or aspects of grain development or grain filling phase can be genetically altered to boost grain yields. To list some examples, the *TaTGW6-A1* allele located on chromosome 4AL was found to increase TGW and grain morphometrics by accumulating more carbohydrates in the grain than the wild type (Hu et al., 2016). The *GNI-A1* allele was found to contribute to floret survival increasing grain number probably due to more resources being allocated to more distal florets and hence allowing them to remain fertile and set grain (Golan et al., 2019a). While the *TaExpA6* α-expansin transgene increases TGW and yield by 12% and 11%, respectively, without a trade-off on grain number (Calderini et al., 2021). These three studies exemplify how grain weight, size and number can be manipulated at different growth stages and via different mode of actions to achieve grain and yield increases.
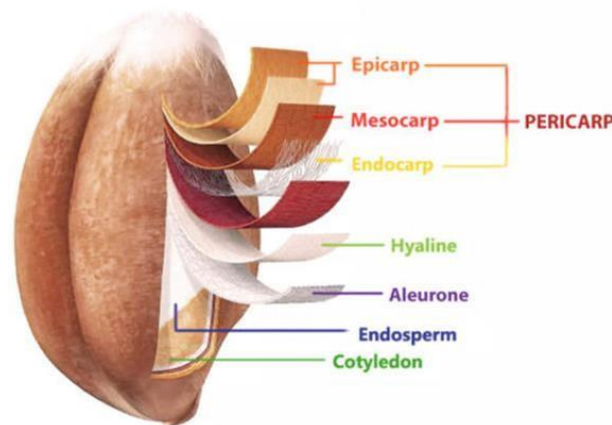
Figure 1-5: Illustration of a mature grain with each of its layers. From: https://theartofmilling.com/

1.5.5. *Wheat yield components*

Final yield is a complex trait, that can be broken down into what are known as yield components to facilitate their study. Each of the components will contribute towards final yield:

- Grain weight, expressed in thousand kernel weight (TKW): Which can be complemented by grain morphometric parameters: grain area, length and width.

- Grain number per spike: grains / spikes
- Number of spikes per area: Spikes m^{-2}

All yield components interact during plant development. Therefore, when trying to manipulate one of the components to boost yield, other components can be affected, leading to undesirable pleiotropic effects. For example, the 'classical' trade-off between grain number and grain weight is probably due to competition for resources between individual grains across the spike (Kuchel et al., 2007). The number of spikes per area is established very early in development, reaching its maximal capacity shortly after terminal spikelet (Figure 4). Around that same time, the maximal number of potential grains per spike begins to be established peaking at booting time, followed by a drastic drop in the number of fertile florets between booting and anthesis, in a process known as floret abortion. Around grain filling, the maximal number of grains per spike is fixed. Finally, grain weight is the last of the yield components to be established, starting pre-anthesis as carpel development sets the limit for grain growth until physiological maturity, when the grain reaches its maximal weight (Reynolds et al., 2022) (Brinton and Uauy, 2019). In Chapters 2 and 3, we introduce each yield component in more detail and discuss their contribution towards final grain yield.

Furthermore, the effect of genes affecting yield components and final grain yield can also be influenced by their interaction with the environment (GxE). This makes it difficult to predict how certain alleles will influence yield components when tested in different environments (Slafer 2003) (Parent et al., 2017). For that reason, Near Isogenic Lines (NILs) are a useful resource when investigating the effect of a certain gene in each phenotype. For example, the NILs carrying different alleles of the *PHOTOPERIOD-D1* (*PPD-D1*) gene located on chromosome 2D were found to differ greatly in heading and flowering time when compared to the insensitive *ppd* allele in cultivar Triple Dirk (Kitagawa et al., 2012). Another set of NILs broadly used in agriculture, are those carrying alternative alleles at the *REDUCED HEIGHT 1* (*RHT1*) locus giving either a tall or a semi-dwarf phenotype. In cv Fortuna, the semi-dwarf *Rht-B1b* allele reduces grain protein content and grain weight by 12% and 15.2% when compared to the tall *Rht-B1a* NIL (Jobson et al., 2021). Thus, the detrimental effect on protein content and grain size can be attributed to a single gene (*Rht-B1*). NILs can be also useful when elucidating how a certain gene will interact with a given environment for example, a major QTL was found in chromosome 5A NILs associated to grain weight in a double haploid line CB53x CB89. Across 12 different environments, they found that yield increases were only significant in one of the five growing seasons and that the full potential of grain length can only be seen under certain environments (Brinton et al., 2017). In chapter 3, we conducted field trials in three contrasting environments using NILs to understand how lines carrying mutant alleles affecting grain weight and size interact with the environment in different genetic backgrounds.

1.6. The genetic control of yield components in wheat

Genetic studies are helpful when elucidating how genes affect individual yield components. Several genetic associations with yield components have been reported, but very few have been validated and little mechanistic insight has been provided (Kuchel, 2007). Current developments in wheat genomics, sequencing and assembly methods, have allowed the identification of genes for increases in grain weight or grain number per spike in wheat (Uauy, 2018). Mapping studies for grain yield components have identified quantitative trait loci (QTL) on all 21 wheat chromosomes using either linkage mapping in biparental populations and marker-trait associations in genome wide association studies (GWAS) (Mangini et al., 2018). Major QTL associated to thousand grain weight have been detected on chromosomes 1B, 2A, 2D, 3A, 3B, 4B, 4D, 5A, 5B, 6A, 7B and 7D Zhang et al. (2017) and QTL for grain number per spike on chromosomes 2B, 3B, 4A, 4B, 4D, 5A, 5D, 7A and 7B (Cui et al., 2014). Most of the identified associations, however, have not been validated nor has the underlying gene cloned. To date, 36 genes(homeologs included) have been associated with grain number and 28 with grain size. Among them are the *GRAIN NUMBER INCREASE 1* (*GNI1*, see discussion chapter 2), the *REDUCED HEIGHT* genes (*RHT*, see chapter 4 and general discussion) and the RING E3 ubiquitin ligase gene *GRAIN WEIGHT 2* (*GW2)* broadly discussed in the present work. For a complete list of genes associated with grain number and grain size see table (S5 and S6 Supplementary file1 (XLSX 33 KB)) (Xie and Sparkes, 2021b).

1.6.1. Growth regulators in plants

As already stated above, seed weight and size constitute an important agricultural trait coordinated by the growth of the embryo, endosperm, and maternal tissue. Proteins with ubiquitin, peptidase or binding activities have been identified to either restrict growth or enhance seed size (Xia et al., 2013). In *Arabidopsis thaliana*, proteins which restrict growth in several plant organs have been discovered and characterized. For example, the RING-type E3 ligase Big Brother (BB) and DA1 a ubiquitin receptor, acts co-ordinately with BB to repress growth. Double knockout *da1-1 bb* mutant plants resulted in organ overgrowth, particularly in flowers, due to an extended phase of cell proliferation (Zhang and Lenhard, 2017). Following that discovery, three more members of the DA family were found and characterized. Firstly, an E3 ubiquitin ligase like protein DA2 was found to affect maternal tissue to restrict seed growth. DA2 protein shares similarities with GW2 proteins in wheat, maize and rice all associated with seed size control (Li and Li, 2016). The mutant *da2-1* seeds were larger and heavier than the wild-type seeds. Two other DA1-related proteins, DAR1 and DAR2, act redundantly with DA1 to regulate endoreduplication during plant development. The triple mutant *da1-dar1-1 dar2-1* Arabidopsis plants formed larger flowers and seeds than the wild type (Xia et al.,2013). All BB, DA1, DA2, DAR2 and DAR1 proteins act co-ordinately to restrict growth as described below (Figure 1.6).
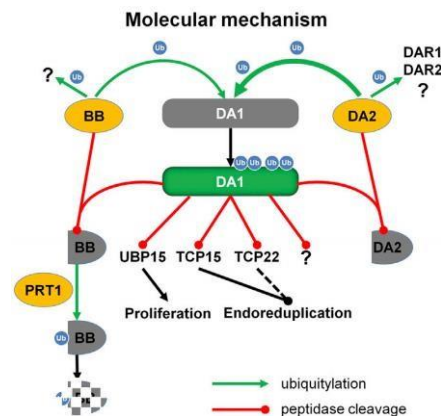
Figure 1-6: Developmental and Molecular Action of BB, DA1, and DA2 in Arabidopsis. The RING-type E3 ligases BB and DA2 activate DA1 peptidase activity by ubiquitylation. DA1 peptidase activity then cleaves the deubiquitylase UBP15 and the transcription factors TCP15 and TCP22 to arrest cell proliferation and promote endoreduplication, respectively. In addition, activated DA1 cleaves BB and DA2. From Zhang and Lenhard, 2017.

The DA1 and DAR protein families, instead of having ubiquitin properties, regulate growth by inducing peptidase cleavage, thereby inactivating key proteins, including transcription factors, for cell proliferation and endoreduplication. In wheat, the RNAi lines targeting the *DA1-A1* and *GW2* genes increased TGW synergistically when compared to single RNAi lines targeting only one of the genes (Liu et al., 2020). This confirmed that the DA2 in Arabidopsis, and the GW2 protein in wheat, act consistently as growth repressors.

Transcription factors of the TCP family (maize *TEOSINTE BRANCHED 1* (*TB1*), snapdragon *CYCLOIDEA* (*CYC*) and *PROLIFERATING CELL FACTORS 1/2* (*PCF1/2*)) are genes involved in plant growth, development, and stress responses (Zhao et al., 2018). The Class I TCPs interact with different hormone pathways such as auxins and gibberellins (GA). In Arabidopsis, TCP8, TCP14, TCP15 and TCP22 are considered the "master" regulators of endoreduplication (Peng et al., 2015). A yeast two-hybrid assay was conducted proving a physical interaction between the three DAR proteins with the transcription factors TCP15 and TCP14 (Peng et al., 2015, Ferrero et al., 2019b). The redundant role of these four TCP transcription factors on plant height has further been confirmed in genetic analysis using quadruple mutants (Davière et al., 2014). In wheat, little is known about the effect of the TCPs on agronomical important traits. Recently, it was demonstrated that TCP21 and TCP18 interact in a yeast two hybrid assay and that a TILLING Kronos knockout mutant targeting TCP9 increased spike and grain length and spikelet number when compared to Kronos WT (Zhao et al., 2018).

In *Arabidopsis*, five DELLAs proteins have been identified (GA1, RGA, RGL1, RGL2, RGL3) as negative regulator of growth and have been reported to interact with TCP family proteins. A yeast two-hybrid assay demonstrated that the five DELLAs proteins in Arabidopsis interact with TCP8, TCP14, TCP15, and TCP22 by binding to their DNA-recognition domain, causing inactivation. To "unlock" DELLA repression, GAs targets DELLA for ubiquitination. Firstly, active GA_4 binds to the GID1 protein forming a GA-GID1 complex that will bind to DELLA and the E3 ubiquitin ligase SCF resulting in DELLA being targeted for ubiquitination and degraded (see chapter 4) (Thomas, 2017). Once DELLA has been ubiquitinated, the now active TCPs induce the expression of GA biosynthesis genes *GA3ox1* and *GA20ox1* and the mitotic related gene *PRE6*. The TCPs and GAs act concomitantly to enhance grain growth, but do not interact or bind together (Ferrero et al., 2019b).Collating information from several authors, and the fact that the *DA2* gene and *GW2* gene act consistently as growth repressors across species, we propose a model on how the GW2 protein represses growth and how this is relieved in the case of the triple *gw2* mutants. This model is shown only for the wildtype and the *gw2* triple mutants (Figure 1.7).
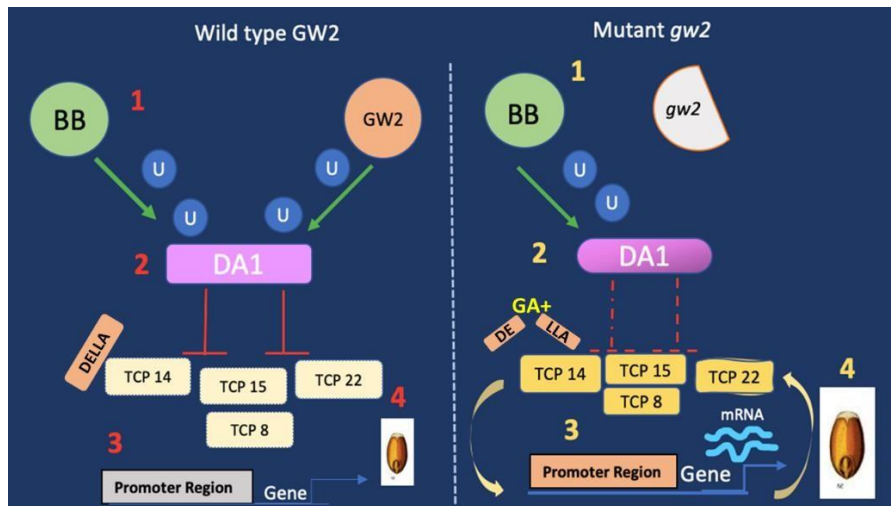
Figure 1-7: Left, wild type GW2: 1) GW2 and Big Brother (BB) ubiquitinates DA1 triggering a cascade. 2) DA1 cleaves the TCP14, TCP15, TCP8, TCP22 inactivating them. Alternatively, DELLA protein binds to the DNA recognition domain of the TCP causing inactivation.3) Inactivated TCPs do not bind to the promoter region of growth-related genes.4) Grain growth is constrained. Right, mutant gw2: 1) gw2 is truncated, BB partially ubiquitinates DA1, 2) DA1 does not cleaves the TCPs. DELLA is targeted for ubiquitination by GAs.3) TCPs bind to the promoter region of growth-related genes like GA3ox. 4) Grain growth is enhanced.

1.6.2. *The role of plant hormones on grain growth*

Plant hormones are molecules regulating key plant growth stages and signalling networks involved in responses to diverse biotic and abiotic stresses. They function as part of a complex network that finely regulates gene expression and growth in response to environmental cues. Major plant hormones affect a variety of biological processes. Auxin, gibberellin (GA) and brassinosteroids (BR) affect cell growth; abscisic acid (ABA) and strigolactones have an impact on apical dominance; cytokinin (CK) and ethylene (ET) affect root and hypocotyl elongation; while salicylic acid (SA) and jasmonic acid (JA) are involved in biotic response (Müller and Munné-Bosch, 2011). In Arabidopsis and rice, BR insensitive mutants produce smaller seeds while the overexpression causes larger seeds. The *AUXIN RESPONSE FACTOR 2* (*ARF2*) controls seed size in Arabidopsis, by regulating cell proliferation in the maternal layers (Li and Li, 2016). While hormonal signalling and cross talk has been broadly investigated in plants such as Arabidopsis and rice, in wheat our understanding is still limited specially under field conditions. This is despite hormones playing key roles in important agronomical traits in wheat, such as final grain size, germination and disease resistance (Qi et al., 2019). The introduction in 1960 of the semi-dwarfing alleles of the *RHT1* genes substantially increased grain yields by manipulating the GA signalling pathway in wheat and rice. We will further introduce the GA pathway in chapter 4. Other GA responsive alleles have the potential to increase yield by manipulating the biosynthesis of the gibberellins pathway (Qi et al., 2019). To date, the mode of action of the *RH12, RHT14, RHT18, and RHT24* alleles had been characterized an increased expression of *GA2oxidaseA13* genes caused decreases in the biosynthesis of GA_{12} resulting in low concentrations of the bioactive GA_1 (see chapter 5, section 5.1.9) (Agarwal et al., 2020). Recently, a new *Rht13* allele that encodes a nucleotide-binding site leucine-rich repeat (NBS-LRR) gene, not related to the GA signalling or metabolism, reduces plant height by interfering with cell wall properties constraining cell expansion and cell growth. The reduction in plant height is comparable to the conventional *Rht-B1b and Rht-D1b* dwarfing genes. This novel allele might be of beneficial used in the field as the height-reducing effect of the *Rht*-13 dwarfism gene is

mostly related with a reduction in peduncle growth and is not correlated with decreased seedling growth or coleoptile length (Borill et al., 2022).

1.1.1. The GW2 gene for grain weight and size in wheat

In chapter 2, we describe the *GRAIN WIDTH 2 (GW2)* gene and its effect on grain size and weight in detail. However, given that *GW2* is a central component of this thesis, we will briefly introduce it here. The *GW2* gene was first discovered and described in rice. It was found to negatively affect grain weight and size and to encode for a novel RING-type protein with a E3 ubiquitin ligase activity (Song et al., 2007). In bread wheat, it was discovered based on its homology to rice, and it was demonstrated that all three homoeologous copies are expressed (Su et al., 2011a). Simmonds et al. (2016) generated a set of Paragon NILs where the *gw2-A1* mutant allele increased TGW by 6% and grain morphometrics by ~2.3%, compared to the wildtype NIL. Consistent with that, Geng et al. (2017) found that in cv Chinese Spring, the increases on grain size was due to increases on cell number and cell size in the endosperm of the single *gw2-A1* mutant. Moreover, it was discovered that the *gw2* mutant alleles have an additive effect on grain size, and as the number of mutant copies increase, so does the effect on grain weight: single genome mutants increase TGW by 5%, double mutants by 10.5% and triple mutants by 21% when compared to the controls (Wang et al., 2018). Furthermore, it was demonstrated in wheat that *TaDA1-A1* and *TaGW2-B1* (orthologous to Arabidopsis *DA2*) genes physically interact and that the RNAi mutants of both genes, act synergistically enhancing TGW (Liu et al., 2020). A triple *da1* mutant in cv Trappe (EMS population) resulted in 8% increases on TGW, and ~2% increase on grain morphometrics (Mora-Ramirez et al., 2021). These results provide strong evidence that the mechanistic understanding of the *DA1-DA2* pathway from Arabidopsis can be transferred to wheat.

1.2. Creating NILs for grain weight and size: the *gw2* alleles

To understand how the *GW2* genes work in different wheat cultivars, the Kronos and Cadenza TILLING populations were screened to identify *GW2* mutants, first on chromosome 6A, and then followed by mutants on chromosomes 6B and 6D Simmonds et al. (2016) and Wang et al. (2018). Briefly, the mutations and the NILs were developed as followed:

- The *GW2-A1 single* mutant with a guanine (G) to adenine (A) transition was identified in *Kronos* mutant line T4-2235 in the splice acceptor site of exon 5 of the 6A genome copy of *GW2*. This leads to a mis-splicing of *GW2-A1* and results in two types of mutant proteins: one which has a premature termination codon and results in a truncated gw2 protein, and a second type which is missing three amino acids but is rare (Figure 1.8). Once identified, Kronos mutant line T4-2235 was crossed to cv Paragon, and further backcrossed four times to generate the A genome single mutant *gw2* NILs (Simmonds et al., 2016).

- The *GW2-B1* TILLING mutant was identified in Kronos341, carrying the heterozygous C2504T mutation causing a truncated protein due to a premature stop codon (Figure 1.8). Once identified, Kronos341 was crossed to cv Paragon and NILs differing for the presence of the wildtype and mutant *GW2-B1* allele were generated (Wang et al., 2018).

- Finally, the *GW2- D1* TILLING mutant was identified in Cadenza using an *in silico* approach (Krasileva et al., 2017). Cadenza mutant line 1441 carries a homozygous mutation G7139A with a G to A mutation causing a truncated protein due to a premature stop codon (Figure 1.8). The Cadenza mutant line 1441, was crossed to Paragon and NILs were again developed for the *GW2-D1* single mutant.

- Based on the individual Paragon single mutants, the Paragon *gw2* triple mutant NILs (and the associated single and double mutant lines) were generated (Wang et al., 2018). This germplasm will be used extensively in the thesis.
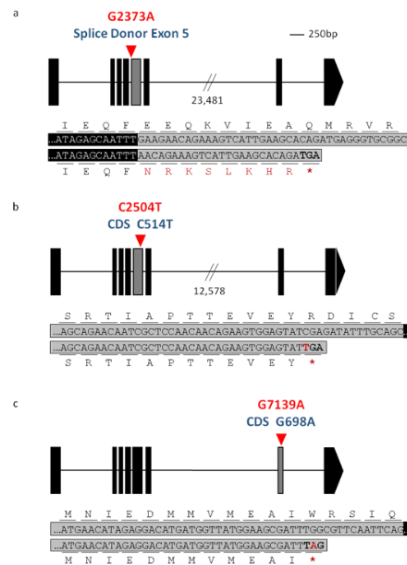
Figure 1-8: Mutations in the wheat *GW2* gene a) *GW2-A1* where a G>A transition causing missplicing of exon 5. b) *GW2-B1* where a C>T transition causes a premature stop codon in exon 5. c) *GW2-D1* a G698A substitution causes a premature stop codon in exon 7. Premature stop codons are marked by the red asterisk. Figure from (Wang et al., 2018).

1.3. Thesis aims

The overall aim of this thesis is to understand whether the *gw2* alleles increase grain weight and grain morphometrics in different bread wheat cultivars tested under different environments. In addition, we want to understand if these increases are mediated by the plant hormones gibberellins. We combined phenotypic characterisation, chemical assays, analytical chemistry and genetics to answer the following questions:

- Do the *gw2* knockout alleles increase grain weight and size across years, environments and different wheat cultivars? For this purpose:
  - We tested the *gw2* single, double and triple mutant Paragon NILs across three different years (2019, 2020, 2021) and environments in the UK.
  - We evaluated single *gw2-A1* and *gw2* triple mutants NILs in two CIMMYT cultivars under irrigation, drought and heat stress in 2019 and 2022 in CIMMYT, Ciudad Obregon, Mexico.
- Is there any alteration in the gibberellin pathway leading to increases on grain weight and size in Paragon NILs? We first addressed this by conducting glasshouse experiments using bioactive GA and a gibberellin antagonist, paclobutrazol. We also wanted to understand if *gw2* interacts with the semi dwarf *Rht-B1b* allele. To address this, we generated crosses between Paragon *gw2* triple mutant x Paragon *Rht-B1b* NILs and evaluated them in the field.

1.4. References

1. Gibberellin biosynthesis in higher plants. *Annual Plant Reviews, Volume 49.*
2. ADAMSKI, N. M., BORRILL, P., BRINTON, J., HARRINGTON, S. A., MARCHAL, C., BENTLEY, A. R., BOVILL, W. D., CATTIVELLI, L., COCKRAM, J., CONTRERAS-MOREIRA, B., FORD, B., GHOSH, S., HARWOOD, W., HASSANI-PAK, K., HAYTA, S., HICKEY, L. T., KANYUKA, K., KING, J., MACCAFERRRI, M., NAAMATI, G., POZNIAK, C. J., RAMIREZ-GONZALEZ, R. H., SANSALONI, C., TREVASKIS, B., WINGEN, L. U., WULFF, B. B. & UAUY, C. 2020. A roadmap for gene functional characterisation in crops with large genomes: Lessons from polyploid wheat. *Elife,* 9.
3. BARRON, C., SURGET, A. & ROUAU, X. 2007. Relative amounts of tissues in mature wheat (*Triticum aestivum L.*) grain and their carbohydrate and phenolic acid composition. *Journal of Cereal Science,* 45**,** 88-96.
4. BECHTEL, D., ABECASSIS, J., SHEWRY, P. & EVERS, A. 2009. CHAPTER 3: Development, Structure, and Mechanical Properties of the Wheat Grain.
5. BORRILL, P., MAGO, R., XU, T., FORD, B., WILLIAMS, S. J., DERKX, A., BOVILL, W. D., HYLES, J., BHATT, D., XIA, X., MACMILLAN, C., WHITE, R., BUSS, W., MOLNÁR, I., WALKOWIAK, S., OLSEN, O.-A., DOLEŽEL, J., POZNIAK, C. J. & SPIELMEYER, W. 2022. An autoactive NB-LRR gene causes *Rht13* dwarfism in wheat. Proceedings of the National Academy of Sciences, 119, e2209875119.
6. BRINTON, J., RAMIREZ-GONZALEZ, R. H., SIMMONDS, J., WINGEN, L., ORFORD, S., GRIFFITHS, S., HABERER, G., SPANNAGL, M., WALKOWIAK, S., POZNIAK, C., UAUY, C. & WHEAT GENOME, P. 2020. A haplotype-led approach to increase the precision of wheat breeding. *Communications Biology,* 3**,** 712.
7. BRINTON, J., SIMMONDS, J., MINTER, F., LEVERINGTON-WAITE, M., SNAPE, J. & UAUY, C. 2017. Increased pericarp cell length underlies a major quantitative trait locus for grain weight in hexaploid wheat. *New Phytol,* 215**,** 1026-1038.
8. BRINTON, J. & UAUY, C. 2019. A reductionist approach to dissecting grain weight and yield in wheat. *Journal of Integrative Plant Biology,* 61**,** 337-358.
9. CALDERINI, D. F., CASTILLO, F. M., ARENAS-M, A., MOLERO, G., REYNOLDS, M. P., CRAZE, M., BOWDEN, S., MILNER, M. J., WALLINGTON, E. J., DOWLE, A., GOMEZ, L. D. & MCQUEEN-MASON, S. J. 2021. Overcoming the trade-off between grain weight and number in wheat by the ectopic expression of expansin in developing seeds leads to increased yield potential. *New Phytologist,* 230**,** 629-640.
10. CHARMET, G. 2011. Wheat domestication: Lessons for the future. *Comptes Rendus Biologies,* 334**,** 212-220.
11. CUI, F., ZHAO, C., DING, A., LI, J., WANG, L., LI, X., BAO, Y., LI, J. & WANG, H. 2014. Construction of an integrative linkage map and QTL mapping of grain yield-related traits using three related wheat RIL populations. *Theoretical and Applied Genetics,* 127**,** 659-675.
12. DAVIÈRE, J.-M., WILD, M., REGNAULT, T., BAUMBERGER, N., EISLER, H., GENSCHIK, P. & ACHARD, P. 2014. Class I TCP-DELLA Interactions in Inflorescence Shoot Apex Determine Plant Height. *Current Biology,* 24**,** 1923-1928.
13. FAO 2021. *World Food and Agriculture – Statistical Yearbook 2021. Rome.*
14. FERRERO, V., VIOLA, I. L., ARIEL, F. D. & GONZALEZ, D. H. 2019. Class I TCP Transcription Factors Target the Gibberellin Biosynthesis Gene *GA20ox1* and the Growth-Promoting Genes *HBI1* and *PRE6* during Thermomorphogenic Growth in Arabidopsis. *Plant Cell Physiol,* 60**,** 1633-1645.
15. GENG, J., LI, L., LV, Q., ZHAO, Y., LIU, Y., ZHANG, L. & LI, X. 2017. *TaGW2-6A* allelic variation contributes to grain size possibly by regulating the expression of cytokinins and starch-related genes in wheat. *Planta,* 246**,** 1153-1163.
16. GOLAN, G., AYALON, I., PERRY, A., ZIMRAN, G., ADE-AJAYI, T., MOSQUNA, A., DISTELFELD, A. & PELEG, Z. 2019. *GNI-A1* mediates trade-off between grain number and

grain weight in tetraploid wheat. *Theor Appl Genet,* 132**,** 2353-2365.

17. HOWE, K. L., CONTRERAS-MOREIRA, B., DE SILVA, N., MASLEN, G., AKANNI, W., ALLEN, J., ALVAREZ-JARRETA, J., BARBA, M., BOLSER, D. M., CAMBELL, L., CARBAJO, M., CHAKIACHVILI, M., CHRISTENSEN, M., CUMMINS, C., CUZICK, A., DAVIS, P., FEXOVA, S., GALL, A., GEORGE, N., GIL, L., GUPTA, P., HAMMOND-KOSACK, K. E., HASKELL, E., HUNT, S. E., JAISWAL, P., JANACEK, S. H., KERSEY, P. J., LANGRIDGE, N., MAHESWARI, U., MAUREL, T., MCDOWALL, M. D., MOORE, B., MUFFATO, M., NAAMATI, G., NAITHANI, S., OLSON, A., PAPATHEODOROU, I., PATRICIO, M., PAULINI, M., PEDRO, H., PERRY, E., PREECE, J., ROSELLO, M., RUSSELL, M., SITNIK, V., STAINES, D. M., STEIN, J., TELLO-RUIZ, M. K., TREVANION, S. J., URBAN, M., WEI, S., WARE, D., WILLIAMS, G., YATES, A. D. & FLICEK, P. 2020. Ensembl Genomes 2020-enabling non-vertebrate genomic research. *Nucleic Acids Res,* 48**,** D689-d695.

18. HU, M.-J., ZHANG, H.-P., CAO, J.-J., ZHU, X.-F., WANG, S.-X., JIANG, H., WU, Z. Y., LU, J., CHANG, C., SUN, G.-L. & MA, C.-X. 2016. Characterization of an IAA-glucose hydrolase gene *TaTGW6* associated with grain weight in common wheat (Triticum aestivum L.). *Molecular Breeding,* 36**,** 25.

19. HYLES, J., BLOOMFIELD, M. T., HUNT, J. R., TRETHOWAN, R. M. & TREVASKIS, B. 2020. Phenology and related traits for wheat adaptation. *Heredity,* 125**,** 417-430.

20. HYLES, J., VAUTRIN, S., PETTOLINO, F., MACMILLAN, C., STACHURSKI, Z., BREEN, J., BERGES, H., WICKER, T. & SPIELMEYER, W. 2017. Repeat-length variation in a wheat cellulose synthase-like gene is associated with altered tiller number and stem cell wall composition. *J Exp Bot,* 68**,** 1519-1529.

21. International Wheat Genome Sequencing Consortium (IWGSC).2018. Shifting the limits in wheat research and breeding using a fully annotated reference genome. *Science (New York, N.Y.),* 361(6403), eaar7191.

22. JOBSON, E. M., OHM, J.-B., MARTIN, J. M. & GIROUX, M. J. 2021. *Rht-1* semi-dwarfing alleles increase the abundance of high molecular weight glutenin subunits. *Cereal Chemistry,* 98**,** 337-345.

23. KIRBY, E. J. M. 1988. Analysis of leaf, stem and ear growth in wheat from terminal spikelet stage to anthesis. *Field Crops Research,* 18**,** 127-140.

24. KITAGAWA, S., SHIMADA, S. & MURAI, K. 2012. Effect of *Ppd-1* on the expression of flowering-time genes in vegetative and reproductive growth stages of wheat. *Genes & Genetic Systems,* 87**,** 161-168.

25. KRASILEVA, K. V., VASQUEZ-GROSS, H. A., HOWELL, T., BAILEY, P., PARAISO, F., CLISSOLD, L., SIMMONDS, J., RAMIREZ-GONZALEZ, R. H., WANG, X., BORRILL, P., FOSKER, C., AYLING, S., PHILLIPS, A. L., UAUY, C. & DUBCOVSKY, J. 2017. Uncovering hidden variation in polyploid wheat. *Proceedings of the National Academy of Sciences,* 114**,** E913-E921.

26. KRONENBERG, L., YU, K., WALTER, A. & HUND, A. 2017. Monitoring the dynamics of wheat stem elongation: genotypes differ at critical stages. *Euphytica,* 213**,** 157.

27. KUCHEL, H., WILLIAMS, K. J., LANGRIDGE, P., EAGLES, H. A. & JEFFERIES, S. P. 2007. Genetic dissection of grain yield in bread wheat. I. QTL analysis. *Theor Appl Genet,* 115**,** 1029-41.

28. LI, N. & LI, Y. 2016. Signaling pathways of seed size control in plants. *Current Opinion in Plant Biology,* 33**,** 23-32.

29. LIU, H., LI, H., HAO, C., WANG, K., WANG, Y., QIN, L., AN, D., LI, T. & ZHANG, X. 2020. *TaDA1*, a conserved negative regulator of kernel size, has an additive effect with *TaGW2* in common wheat (*Triticum aestivum L.*). *Plant Biotechnology Journal,* 18**,** 1330-1342.

30. MANGINI, G., GADALETA, A., COLASUONNO, P., MARCOTULI, I., SIGNORILE, A. M., SIMEONE, R., DE VITA, P., MASTRANGELO, A. M., LAIDÒ, G., PECCHIONI, N. & BLANCO, A. 2018. Genetic dissection of the relationships between grain yield components by genome-wide association mapping in a collection of tetraploid wheats. *PLoS One,* 13**,** e0190162.

31. MARCUSSEN, T., SANDVE, S. R., HEIER, L., SPANNAGL, M., PFEIFER, M., JAKOBSEN, K. S., WULFF, B. B. H., STEUERNAGEL, B., MAYER, K. F. X., OLSEN, O.-

A., ROGERS, J., DOLEŽEL, J., POZNIAK, C., EVERSOLE, K., FEUILLET, C., GILL, B., FRIEBE, B., LUKASZEWSKI, A. J., SOURDILLE, P., ENDO, T. R., KUBALÁKOVÁ, M., ČÍHALÍKOVÁ, J., DUBSKÁ, Z., VRÁNA, J., ŠPERKOVÁ, R., ŠIMKOVÁ, H., FEBRER, M., CLISSOLD, L., MCLAY, K., SINGH, K., CHHUNEJA, P., SINGH, N. K., KHURANA, J., AKHUNOV, E., CHOULET, F., ALBERTI, A., BARBE, V., WINCKER, P., KANAMORI, H., KOBAYASHI, F., ITOH, T., MATSUMOTO, T., SAKAI, H., TANAKA, T., WU, J., OGIHARA, Y., HANDA, H., MACLACHLAN, P. R., SHARPE, A., KLASSEN, D., EDWARDS, D., BATLEY, J., LIEN, S., CACCAMO, M., AYLING, S., RAMIREZ-GONZALEZ, R. H., CLAVIJO, B. J., WRIGHT, J., MARTIS, M. M., MASCHER, M., CHAPMAN, J., POLAND, J. A., SCHOLZ, U., BARRY, K., WAUGH, R., ROKHSAR, D. S., MUEHLBAUER, G. J., STEIN, N., GUNDLACH, H., ZYTNICKI, M., JAMILLOUX, V., QUESNEVILLE, H., WICKER, T., FACCIOLI, P., COLAIACOVO, M., STANCA, A. M., BUDAK, H., CATTIVELLI, L., GLOVER, N., PINGAULT, L., PAUX, E., SHARMA, S., APPELS, R., BELLGARD, M., CHAPMAN, B., NUSSBAUMER, T., BADER, K. C., RIMBERT, H., WANG, S., KNOX, R., KILIAN, A., ALAUX, M., ALFAMA, F., COUDERC, L., GUILHOT, N., VISEUX, C., LOAEC, M., KELLER, B. & PRAUD, S. 2014. Ancient hybridizations among the ancestral genomes of bread wheat. *Science,* 345**,** 1250092.

32. MORA-RAMIREZ, I., WEICHERT, H., VON WIRÉN, N., FROHBERG, C., DE BODT, S., SCHMIDT, R.-C. & WEBER, H. 2021. The *da1* mutation in wheat increases grain size under ambient and elevated CO2 but not grain yield due to trade-off between grain size and grain number. *Plant-Environment Interactions,* 2**,** 61-73.

33. MÜLLER, M. & MUNNÉ-BOSCH, S. 2011. Rapid and sensitive hormonal profiling of complex plant samples by liquid chromatography coupled to electrospray ionization tandem mass spectrometry. *Plant Methods,* 7**,** 37.

34. ORDON, F., & FRIEDT, W. (EDS.). 2019. *Advances in breeding techniques for cereal crops (1st ed.).*

35. PARENT, B., BONNEAU, J., MAPHOSA, L., KOVALCHUK, A., LANGRIDGE, P. & FLEURY, D. 2017. Quantifying wheat sensitivities to environmental constraints to dissect genotype× environment interactions in the field. *Plant Physiology,* 174**,** 1669-1682.

36. PENG, Y., CHEN, L., LU, Y., WU, Y., DUMENIL, J., ZHU, Z., BEVAN, M. W. & LI, Y. 2015. The ubiquitin receptors DA1, DAR1, and DAR2 redundantly regulate endoreduplication by modulating the stability of TCP14/15 in Arabidopsis. *Plant Cell,* 27**,** 649-62.

37. QI, P.-F., JIANG, Y.-F., GUO, Z.-R., CHEN, Q., OUELLET, T., ZONG, L.-J., WEI, Z.-Z., WANG, Y., ZHANG, Y.-Z., XU, B.-J., KONG, L., DENG, M., WANG, J.-R., CHEN, G.-Y., JIANG, Q.-T., LAN, X.-J., LI, W., WEI, Y.-M. & ZHENG, Y.-L. 2019. Transcriptional reference map of hormone responses in wheat spikes. *BMC Genomics,* 20**,** 390.

38. RAY, D. K., MUELLER, N. D., WEST, P. C. & FOLEY, J. A. 2013. Yield Trends Are Insufficient to Double Global Crop Production by 2050. *PLoS One,* 8**,** e66428.

39. REYNOLDS, M., MANES, Y., IZANLOO, A. & LANGRIDGE, P. 2009. Phenotyping approaches for physiological breeding and gene discovery in wheat. *Annals of Applied Biology,* 155**,** 309-320.

40. REYNOLDS, M. P., SLAFER, G. A., FOULKES, J. M., GRIFFITHS, S., MURCHIE, E. H., CARMO-SILVA, E., ASSENG, S., CHAPMAN, S. C., SAWKINS, M., GWYN, J. & FLAVELL, R. B. 2022. A wiring diagram to integrate physiological traits of wheat yield potential. *Nature Food,* 3**,** 318-324.

41. ROSEGRANT, M. W., RINGLER, C., ZHU, T., TOKGOZ, S. & BHANDARY, P. 2013. Water and food in the bioeconomy: challenges and opportunities for development. *Agricultural Economics,* 44**,** 139-150.

42. SHEWRY, P. R., MITCHELL, R. A. C., TOSI, P., WAN, Y., UNDERWOOD, C., LOVEGROVE, A., FREEMAN, J., TOOLE, G. A., MILLS, E. N. C. & WARD, J. L. 2012. An integrated study of grain development of wheat (cv. Hereward). *Journal of Cereal Science,*56**,** 21-30.

43. SIMMONDS, J., SCOTT, P., BRINTON, J., MESTRE, T. C., BUSH, M., DEL BLANCO, A., DUBCOVSKY, J. & UAUY, C. 2016. A splice acceptor site mutation in *TaGW2-A1* increases thousand grain weight in tetraploid and hexaploid wheat through wider and longer grains. *Theor Appl Genet,* 129**,** 1099-112.

44. SLAFER, G. A. 2003. Genetic basis of yield as viewed from a crop physiologist's perspective. *Annals of Applied Biology,* 142**,** 117-128.

45. SLAFER, G. A., FOULKES, M. J., REYNOLDS, M. P., MURCHIE, E., CARMO-SILVA, E., FLAVELL, R., GWYN, J., SAWKINS, M. & GRIFFITHS, S. 2022. A 'Wiring Diagram' for sink-strength traits impacting wheat yield potential. *Journal of Experimental Botany***,** erac410.

46. SONG, X.-J., HUANG, W., SHI, M., ZHU, M.-Z. & LIN, H.-X. 2007. A QTL for rice grain width and weight encodes a previously unknown RING-type E3 ubiquitin ligase. *Nature Genetics,* 39**,** 623-630.

47. STEWART, B. A. & LAL, R. 2018. Increasing World Average Yields of Cereal Crops: It's All About Water.

48. SU, Z., HAO, C., WANG, L., DONG, Y. & ZHANG, X. 2011. Identification and development of a functional marker of *TaGW2* associated with grain weight in bread wheat (Triticum aestivum L.). *Theor Appl Genet,* 122**,** 211-23.

49. THOMAS, S. G. 2017. Novel *Rht-1* dwarfing genes: tools for wheat breeding and dissecting the function of DELLA proteins. *Journal of Experimental Botany,* 68**,** 354-358.

50. UAUY, C., PARAISO, F., COLASUONNO, P., TRAN, R. K., TSAI, H., BERARDI, S., COMAI, L. & DUBCOVSKY, J. 2009. A modified TILLING approach to detect induced mutations in tetraploid and hexaploid wheat. *BMC Plant Biology,* 9**,** 115.

51. WADDINGTON., S. R., CARTWRIGHT, P. M. & WALL, P. C. 1983. A Quantitative Scale of Spike Initial and Pistil Development in Barley and Wheat. *Annals of Botany,* 51**,** 119-130.

52. WALKOWIAK, S., GAO, L., MONAT, C., HABERER, G., KASSA, M. T., BRINTON, J., RAMIREZ-GONZALEZ, R. H., KOLODZIEJ, M. C., DELOREAN, E., THAMBUGALA, D., KLYMIUK, V., BYRNS, B., GUNDLACH, H., BANDI, V., SIRI, J. N., NILSEN, K., AQUINO, C., HIMMELBACH, A., COPETTI, D., BAN, T., VENTURINI, L., BEVAN, M., CLAVIJO, B., KOO, D.-H., ENS, J., WIEBE, K., N'DIAYE, A., FRITZ, A. K., GUTWIN, C., FIEBIG, A., FOSKER, C., FU, B. X., ACCINELLI, G. G., GARDNER, K. A., FRADGLEY, N., GUTIERREZ-GONZALEZ, J., HALSTEAD-NUSSLOCH, G., HATAKEYAMA, M., KOH, C. S., DEEK, J., COSTAMAGNA, A. C., FOBERT, P., HEAVENS, D., KANAMORI, H., KAWAURA, K., KOBAYASHI, F., KRASILEVA, K., KUO, T., MCKENZIE, N., MURATA, K., NABEKA, Y., PAAPE, T., PADMARASU, S., PERCIVAL-ALWYN, L., KAGALE, S., SCHOLZ, U., SESE, J., JULIANA, P., SINGH, R., SHIMIZU-INATSUGI, R., SWARBRECK, D., COCKRAM, J., BUDAK, H., TAMESHIGE, T., TANAKA, T., TSUJI, H., WRIGHT, J., WU, J., STEUERNAGEL, B., SMALL, I., CLOUTIER, S., KEEBLE-GAGNÈRE, G., MUEHLBAUER, G., TIBBETS, J., NASUDA, S., MELONEK, J., HUCL, P. J., SHARPE, A. G., CLARK, M., LEGG, E., BHARTI, A., LANGRIDGE, P., HALL, A., UAUY, C., MASCHER, M., KRATTINGER, S. G., HANDA, H., SHIMIZU, K. K., DISTELFELD, A., CHALMERS, K., KELLER, B., MAYER, K. F. X., POLAND, J., STEIN, N., MCCARTNEY, C. A., SPANNAGL, M., WICKER, T. & POZNIAK, C. J. 2020. Multiple wheat genomes reveal global variation in modern breeding. *Nature,* 588**,** 277-283.

53. WANG, W., SIMMONDS, J., PAN, Q., DAVIDSON, D., HE, F., BATTAL, A., AKHUNOVA, A., TRICK, H. N., UAUY, C. & AKHUNOV, E. 2018. Gene editing and mutagenesis reveal inter-cultivar differences and additivity in the contribution of *TaGW2* homoeologues to grain size and weight in wheat. *Theoretical and Applied Genetics,* 131**,** 2463-2475.

54. WILKINSON, P. A., ALLEN, A. M., TYRRELL, S., WINGEN, L. U., BIAN, X., WINFIELD, M. O., BURRIDGE, A., SHAW, D. S., ZAUCHA, J., GRIFFITHS, S., DAVEY, R. P., EDWARDS, K. J. & BARKER, G. L. A. 2020. CerealsDB-new tools for the analysis of the wheat genome: update 2020. *Database (Oxford),* 2020.

55. XIA, T., LI, N., DUMENIL, J., LI, J., KAMENSKI, A., BEVAN, M. W., GAO, F. & LI, Y. 2013. The Ubiquitin Receptor DA1 Interacts with the E3 Ubiquitin Ligase DA2 to Regulate Seed and Organ Size in Arabidopsis *The Plant Cell,* 25**,** 3347-3359.

56. XIE, Q. & SPARKES, D. L. 2021. Dissecting the trade-off of grain number and size in wheat. *Planta,* 254**,** 3.

57. ZHANG, N., FAN, X., CUI, F., ZHAO, C., ZHANG, W., ZHAO, X., YANG, L., PAN, R., CHEN, M., HAN, J., JI, J., LIU, D., ZHAO, Z., TONG, Y., ZHANG, A., WANG, T. & LI, J. 2017. Characterization of the temporal and spatial expression of wheat (*Triticum aestivum L.*)

plant height at the QTL level and their influence on yield-related traits. *Theoretical and Applied Genetics,* 130**,** 1235-1252.

58. ZHANG, Y. & LENHARD, M. 2017. Exiting Already? Molecular Control of Cell-Proliferation Arrest in Leaves: Cutting Edge. *Mol Plant,* 10**,** 909-911.
59. ZHAO, J., ZHAI, Z., LI, Y., GENG, S., SONG, G., GUAN, J., JIA, M., WANG, F., SUN, G., FENG, N., KONG, X., CHEN, L., MAO, L. & LI, A. 2018. Genome-Wide Identification and Expression Profiling of the TCP Family Genes in Spike and Grain Development of Wheat (*Triticum aestivum L.*). *Front Plant Sci,* 9**,** 1282.

2. The effect of the *TaGW2* mutants NILs on grain weight and yield in cultivar Paragon

2.1. Chapter summary

In this chapter, a detailed characterisation of the *TaGW2* single, double and triple mutant NILs, alongside the WT in cultivar Paragon, was conducted across three growing seasons of field trials. Phenology and yield components were evaluated and discussed in detail. Overall, we found that thousand grain weight increased consistently as the number of *GW2* copies were mutated mainly due to increases in grain width. We found that yield does not increase in the single and double mutants, but a significant decrease was found in the triple mutants. Furthermore, we found that tiller number decreases alongside seed number per spike and final seed set, most likely offsetting the increases in grain weight.

2.2. Introduction

Cereal crops belonging to the grass (Poaceae) family, such as wheat (*Triticum* sp.), maize (*Zea mays*) and rice (*Oryza sativa*), are staple foods worldwide accounting for 32% (2.7 billion tonnes) of the world food production in 2019. Wheat accounts for 8% of the world food production with 0.8 billion tonnes produced yearly. In 2020, the Food and Agriculture Organization of the United Nations (FAO) stated that between 720-811 million people in the world faced hunger and that cropland area per capita decreased in all regions between 2000 and 2019 as population increased faster than cropland areas (FAO, 2021). Moreover, the demand for wheat from farmers, consumers and food industry is currently increasing due to its high protein content and broad growing range (Reynolds et al., 2022). To keep up with the demand for cereals and achieve sustainable productivity and yield, the development of new varieties with improved grain yield potential is needed (Sakuma and Schnurbusch, 2020).

In the past century, improvements on grain yield have been achieved by increasing the number of grains per spike and spikelet as grain number determines yield (Sanchez-Garcia et al., 2013). A comprehensive study summarizing 20 years of data found that yield is positively associated to what are known as yield components such as grains per spike, spikes per unit area and individual grain weight (Xie and Sparkes, 2021a). To understand the contribution of each of the yield components towards final yield, a reductionist approach has been adopted, for example, focusing on the role of final grain weight and grain morphometrics (width, length) Brinton and Uauy (2019) as a strategy to improve yield and end use quality (Zhang et al., 2018). One of the genes that has been identified is the *GRAIN WIDTH2* (*GW2*) gene that negatively regulates grain weight and size. *GW2* was discovered in rice and encodes a previously unknown RING-type protein with E3 ubiquitin ligase activity, involved in the degradation pathway of the ubiquitin-proteasome (Song et al., 2007).

There have been multiple studies in wheat investigating the effect of *GW2* on yield. The *GW2* gene was first described and cloned by Su et al. (2011b) based on its homology to rice. Furthermore, they found that all *GW2* homoeologues copies (A, B and D located on group 6 chromosomes) are expressed. Yang et al. (2012) sequenced the complete *GW2-A1* gene and found that in the wheat cultivar 'Lankaodali', a single T base insertion in the eighth exon led to a frameshift mutation that reduces the coding protein sequence from 424 amino acids in the WT to 328 amino acids (-96 amino acids); this mutation was associated with higher grain weight. Following this discovery, a segregating population for grain size and width was created by crossing Lankaodali x Chinese Spring (CS); the $F_{2:3}$ families with the mutant *gw2-A1* allele significantly increased seed width and thousand grain weight (TGW). In contrast, RNA interference (RNAi) transgenic lines suppressing the three *GW2* copies resulted in an unexpected significant reduction in grain weight and size (Bednarek et al., 2012). Qin et al. (2014) found that the *GW2-A1* has two main haplotypes: Hap-6A-A which was more frequent in Australian, Chinese, and Russian cultivars whereas Hap-6A-G was predominant in US, CIMMYT and European accessions. *GW2-B1* forms four haplotypes related to TGW and heading date: Hap-6B-1 and Hap-6B-2 were more frequent in all regions followed by Hap-6B-3, while Hap-6B-4 is virtually absent. An additive effect between *GW2-A1* and *GW2-B1* (Hap-6A-A/Hap-6B-1) was correlated positively with TGW and width in modern cultivars. Simmonds et al. (2016) generated a set of near isogenic lines (NILs; lines that differ for only a small segment of the genome allowing the study of phenotypic effect of a single gene/genomic interval in the same genetic background Brinton et al. (2017) using mutants identified by screening the Kronos TILLING population (Uauy et al., 2009). The *gw2-A1* single mutants carried a G to A transition in exon five causing missplicing of exons and resulting in a truncated protein of 134 amino acids. The single mutant allele was backcrossed in both tetraploid and hexaploid wheat and evaluated in glasshouse and field experiments. It was found that BC4 NILs with the *gw2-A1* mutant allele showed a 6% increase in TGW whereas grain width and length were increased by 2.8% and 2.1%, respectively. Geng et al. (2017) reported that the increase in width and TGW in a Chinese Spring (CS) NIL31 single *gw2-A1* mutant (generated between a cross of Chinese winter wheat cultivar Lankaodali and CS), was due to an increase in cell number and cell size in the endosperm based on histological observations through the developing seed. Moreover, it was found that both cytokinin and AGPase (starch biosynthesis) genes are positively regulated in the single *gw2-A1* mutant lines when compared with the controls. Zhai et al. (2018) generated single *gw2-A1* NILs after evaluating 191 recombinant inbred lines (RIL) between two Chinese hexaploid winter wheat cultivars Yumai 8679 (Y8679) and Jing 411 (J411). The allele coming from the cultivar Yumai 8679 increased TGW by 8.3% but decreased seed number by 3%. In 2018, Wang and Simmonds Wang et al. (2018) generated CRISPR-Cas9 genome edited alleles of *GW2* in cultivar Bobwhite and NILs carrying different EMS-mutant alleles in cultivar Paragon. Using these two complementary approaches, each homoeologous gene copy was knocked out (KO), generating single, double, and triple homozygous mutants. It was demonstrated that *GW2* has an additive effect on grain size and weight in glasshouse trails. Single copy lines increased TGW by 5%, double mutants by 10.5% and triple mutants by 21% when compared to the controls (Figure 2.1). Taking together all the results cited above, with one exception (RNAi by Bednarek et al. 2012), agreed on the positive and additive effect of the *gw2* alleles on TGW and grain morphometrics that is consistent across cultivars and growing conditions.
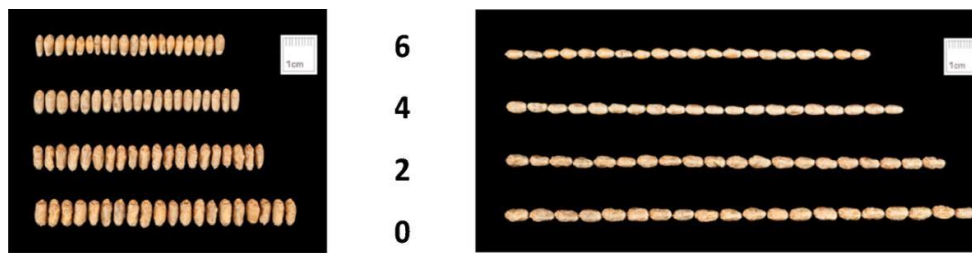
Figure 2-1: Increase in grain width (left) and length (right) in Paragon NILs with decreasing number of functional *GW2* copies (indicated by numbers). The Paragon WT NIL is shown with six functional copies whereas the Paragon *gw2* triple mutant has zero functional copies. Adapted from Wang and Simmonds et al 2018.

In addition to its effect on grain size, *GW2* has been also found to influence grain protein content, grain storage and starch biosynthesis which might explain the increases on both TGW and grain morphometrics. Zhang et al. (2018) investigated the grain protein content (GPC) and grain storage proteins (GSP) of the *GW2* mutants in cultivar Kenong 199. They found that the GPC was elevated in the single B copy mutants by 18.8% while GSP by 17.2%. In the double B and D *gw2* mutants, the GPC increased by 15.4% and the GSP by 3.2% when compared to the wildtype. In a recent study, it was found that the CS WT (GW2) binds to the starch synthesis *TaAGPS* gene targeting it for ubiquitination. In contrast, the CS *gw2* single mutant (NIL31) does not target *TaAGPS* for destruction. As a result, the average number and average area of the starch granules increases in the NIL31 endosperm when compared with the WT. The *TaAGPS* positively regulates seed size in transgenic *Arabidopsis* lines (Lv et al., 2022).

Although advances in the understanding of how *GW2* works and interacts with other genes has been made, many questions remain unanswered with respect to its effect on yield. Most of the experiments have been conducted in the glasshouse or across one or two field growing seasons, and have focused on TGW, grain morphometrics and spike yield. However, there are few reports on additional important yield components such as grain number and final grain yield, especially in the double and triple mutants as most of the studies have a focus on the single mutants. We wanted to understand if significant increases in TGW would be closely associated with increases in grain yield and the trade-offs among yield components. Here we present field studies of Paragon NILs carrying a single, double, and triple mutant combination of the *GW2* gene conducted across three growing seasons (2019, 2020, 2021) in a UK rainfed environment. We also performed analyses on the grain protein content of the triple mutants for the first time.

2.3. Material and methods

2.3.1. Plant material and growing conditions

The Paragon NILs used in this chapter were generated by James Simmonds and are fully described in Wang and Simmonds et. al (2018). Briefly, the *gw2-A1* mutant allele carrying a homozygous G to A mutation at exon 5 (G2373A) was discovered through screening of the Kronos TILLING population Uauy et al. (2009) as reported in Simmonds *et al* (2016). For *GW2-B1,* a heterozygous C to T transition at position 514 of the *GW2-B1* gene coding sequence (CDS) in exon 5 (position 2504 in gDNA) was found, leading to a premature stop codon in TILLING line Kronos0341. The D genome mutation was discovered through the in-silico wheat TILLING database (wheat-tilling.com,Krasileva et al. (2017)) using a BLASTN-based comparison of the *GW2-D1* sequence. TILLING line Cadenza1441 was identified as containing a G to A transition at position 698 of CDS in exon 7 (position 7139 in gDNA) causing a premature termination codon.

All NILs were evaluated in Church Farm in Norfolk, UK (52.628 N, 1.171 E). All lines were grown following the experimental design conducted by Brinton et al. (2017) in rainfed, large-scale yield plot (1.1 x 6 m) as a randomised complete block design with five replicates during 2019, 2020,2021. We use five blocks instead of three, to maximize data output and to ensure there is enough statistical power to uncover yield variation in the field. All the generated NILs had sister lines that were all merged and analysed as single, double, or triple mutants (see Supplementary Materials 6 for the complete list of NILs).

2.3.2. Grain morphometrics, spike yield components and phenotyping

Thousand grain weight and grain morphometrics (grain width and grain length) were taken using a Marvin grain analyser (GTA Sensorik GmbH, Germany) connected to a digital scale (Precisa BJ 610C). The grain samples were taken from harvested field trials from each plot. Spike yield components were taken from ten main spikes coming from each 6.6 m^2 plot in the field. Both spike yield components and developmental traits (phenology) were measured as follow:

- Spikelet number per spike: Ten randomly selected main spikes per plot were collected and the total number of all spikelets across the spike were counted.
- Viable spikelets: all spikelets containing at least one grain
- Seed number per spike: total number of grains coming from a single spike
- Spike yield: total seed weight per individual spike
- Seeds per spikelet: ratio between seed number and viable number
- Days to heading days from sowing until 75% of the plot had visible spikes
- Days to maturity: days from sowing until 75% of the plot reaches maturity (complete yellowing of the spike)
- Total tiller number in 2019-2020 and 2021: Two 1 m² quadrats were placed in the inner rows, main tillers with fertile spikes were counted within the quadrat at dough development (GS83, early dough development).
- Total tiller number in 2022: Two 1 m² quadrats were placed in the inner rows, main tillers with fertile spikes were counted within the quadrat at booting stage (GS45, flag leaf swollen or Waddington scale ~ 8) and at dough development (GS83, early dough development).
- Crop height: total length of individual culms from the soil surface to the tip of the spike excluding awns taken 14 days after anthesis.

2.3.3. Grain Protein Content

The grain protein content was measured with Perten DA7250 Near Infrared Reflectance (NIR) device. Paragon *gw2* triple mutants and Paragon WT seeds were analysed by placing them under the infrared reader making sure that the seeds were evenly distributed in the plate reader. All the seeds were coming from field trials from the 2020-2021 growing seasons.

2.3.4. Statistical analyses

The statistical analyses were carried out with R studio 1.4.11 and the package lme4 1.1. A mixed effects model was fitted for each of the response variables (e.g., TGW, seed width, seed length, yield, spike yield and phenology) with, genotype, and the Year/Block interaction as a nested effect in response to genotype. The P values for explanatory variables in individual models refer to the P values computed by the ANOVA. Percentage difference data refer to the estimated marginal means deriving from the same models. The statistical analyses for tiller number were performed as a two ways ANOVA considering Genotype* (Paragon NILs WT and *gw2* triple mutants plus and extra Paragon WT control which is not display in the table) and Trial Name (different lines were coming from different crosses and/ or sister lines so we consider it as a factorial trial).

2.4. Results

We assessed the effect of the GW2 KO mutants in single, double, and triple homoeolog combinations in cultivar Paragon. Grain weight, grain morphometrics, spike yield components, phenology, and final yield across three years of field trial were analysed and discussed. Paragon WT will be referred to as WT, while Paragon single mutants (A, B or D), double (AB, BD or DA) and triple (ABD) mutants will be denoted as single, double, and triple mutants.

2.4.1. Thousand grain weight (TGW) increases in a dose-dependent manner as copy numbers are mutated

A three-way ANOVA (year*genotype*block/year) was conducted (Table 2.1) highlighting a borderline (P < 0.05) interaction between year and genotype for TGW. However, given the consistency of the data and the fact that the interaction is due to the magnitude of the effect, we discuss the data across all years (Figure 2.2). Overall, we found that TGW increased in a step wise manner as the number of *GW2* gene copies were mutated when compared to the controls (WT). Albeit not significant (except for 2020), TGW increased in the single mutants by 2.8% whereas in the double mutants TGW increased significantly by 9.6 % (P < 0.0005) and by 21.4% (P < 0.0001) in the triple mutants, when compared to the WT. A Tukey post hoc analysis showed that in 2019 the difference between the single and double mutants was border lines significant (P<0.05) while in 2020 and 2021 a significant increase of

8.7% (P < 0.001) in weight was found. Finally, a significant increase of 9.6% (P < 0.0001) in weight was recorded between the double and triple mutants across all years. These results demonstrate the additive effect of the *gw2* mutant alleles on grain weight. Previously, Wang and Simmonds 2018 demonstrated the same effect in Paragon and Bobwhite lines in glasshouse/single plant experiments.
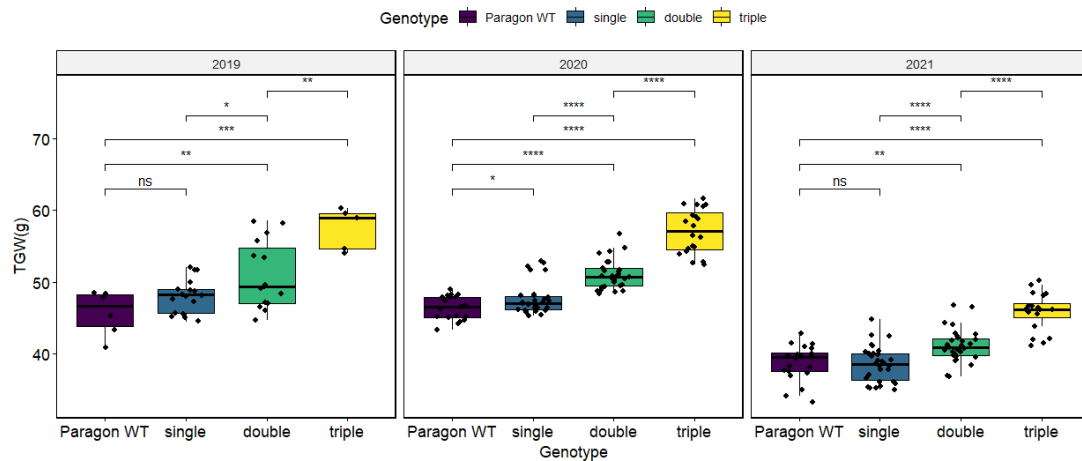
Figure 2-2: TGW in Paragon WT, single, double and triple *gw2* mutants across 2019, 2020, and 2021. The box represents the middle 50% of data with the borders of the box representing the 25th and 75th percentile. The horizontal line in the middle of the box represents the median. Whiskers represent the minimum and maximum values, unless a point exceeds 1.5 times the interquartile range in which case the whisker represents this value and values beyond this are plotted as single points (outliers). Statistical classifications are based on Tukey's HSD tests. ns:P>0.05;*P<0.05;**P<0.01;***P<0.001;**** P<0.0001.

2.4.2. Grain width underlies the increase in weight in Paragon double and triple gw2 mutants

Previously, Simmonds et al, 2016 identified that the *GW2* single mutants increase TGW by both wider and longer grains. We wanted to understand if the same increase in TGW was due to an increase in width or length in the double and triple mutants across different years of field trials. We found that in the single mutants, width did not significantly increase which is consistent with the effects seen for TGW. In the double and triple mutants, width increased consistently across year by 3.7% (P< 0.0001) and 7.6% (P< 0.0001), respectively, when compared to the WT. Following the same trend as TGW, width increased significantly and consistently by 1.91% (P < 0.0001) between the single and the double mutants (except in 2019), same was found for the double and the triple mutants where a significant 3.6% (P < 0.0001) increase was found following a step wise pattern (Figure 2.3) (Table 2.1).
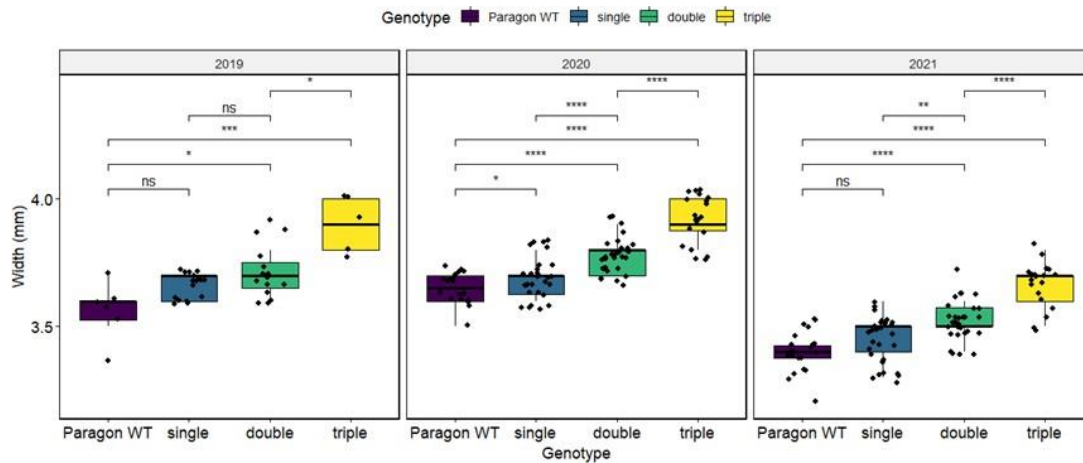
Figure 2-3: Grain width in Paragon WT, single, double and *gw2* triple mutants across 2019, 2020 and 2011.The box represents the middle 50% of data with the borders of the box representing the 25th and 75th percentile. Statistical classifications are based on Tukey's HSD tests. ns: *P* > 0.05; * *P* < 0.05; ** *P* < 0.01; ***P<0.001; **** P<0.0001.

2.4.3. Grain length increases in a dose-dependent manner between the double and triple gw2 mutants

We analysed the contribution of the *gw2* alleles on grain length across all years. A three-way ANOVA was performed, showing a borderline non-significant interaction between year and genotype (P< 0.07). We found that in the single mutants, length was non-significant (P> 0.05) across all years, while for the double and the triple mutants, length significantly increased (P< 0.001) by 3.1% and 7.2%, respectively, when compared to the WT. Between the single and the double mutants, a 1.67% (P< 0.01) increase was found and once more grain length increased significantly by 3.8% (P < 0.0001) between the double and triple mutants. These results are consistent with the increases in TGW and grain width demonstrating that the effect of the *gw2* allele on grain length is additive and consistent across years (Figure 2.4, Table 2.1).
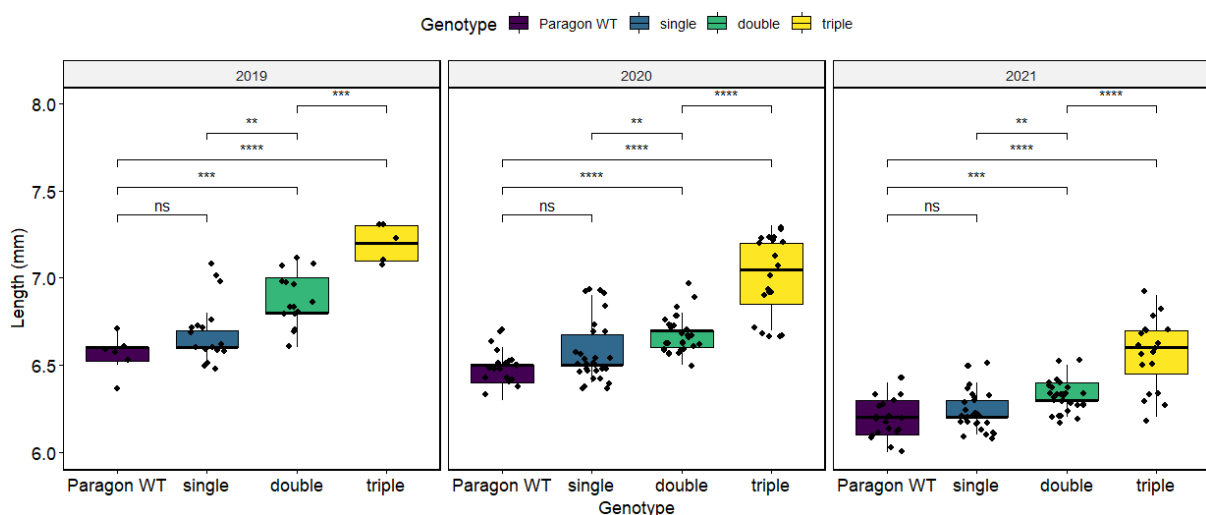
Figure 2-4: Grain length in Paragon WT, single, double and gw2 triple mutants across 2019, 2020 and 2011.The box represents the middle 50% of data with the borders of the box representing the 25th and 75th percentile. Statistical classifications are based on Tukey's HSD tests. ns: *P* > 0.05; ** *P* < 0.01; ***P<0.001; **** P<0.0001.

In summary, we found that the effect of the single mutations are very subtle under field conditions with non-significant increases on TGW, width and length. On the other hand, significant increases on grain weight and grain morphometrics were found in the double and triple mutants when compared with the WT across all years.

2.4.4. Final yield decreases in the triple mutants in 2020 and 2021

We hypothesized that bigger and heavier grains would lead to an increase in yield. For that reason, we grew the NILs in yield plots (1.1 m x 6 m) and evaluated them for final yield. Overall, we found that yield did not increase across three years in the single, double and triple mutants when compared to the WT. On the contrary, a significant decrease of 5.8% ($P < 0.01$) and 3.6% ($P < 0.18$) was measured in 2020 and 2021, respectively, in the triple mutants when compared to the WT (Figure 2.5, Table 2.1). These results were unexpected as we hypothesize that the >20 % increase in TGW would lead to yield gains in field conditions.
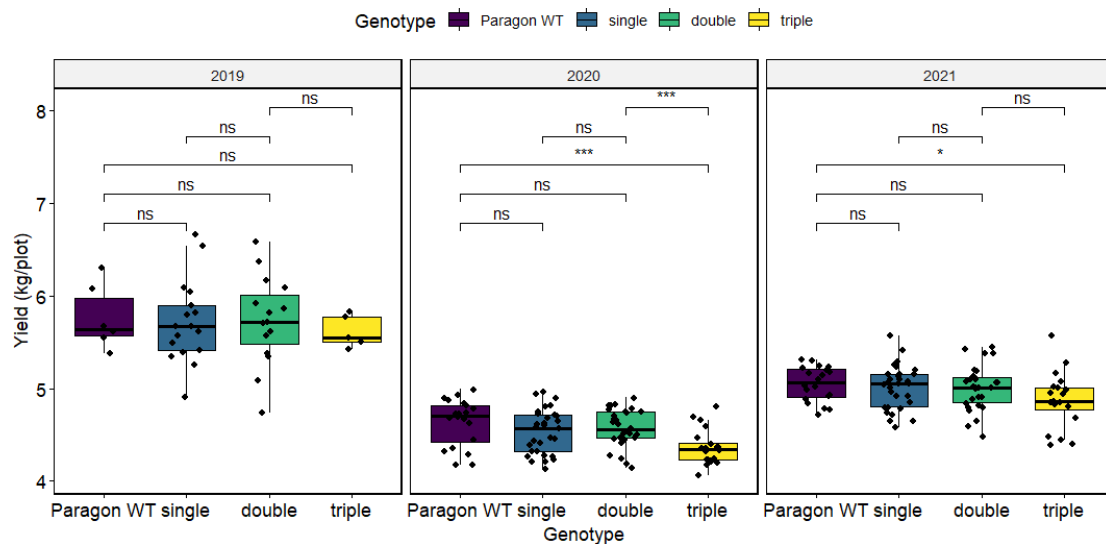
Figure 2-5: Plot yield in Paragon WT, single, double and *gw2* triple mutants across 2019, 2020 and 2011.The box represents the middle 50% of data with the borders of the box representing the 25th and 75th percentile. ns: *P* > 0.05; * *P* < 0.05; * *P*<0.001.**

Table 2-1: Mean thousand grain weight (TGW), grain morphometric and yield parameters of Paragon WT, single, double, and triple gw2 mutants. Means are from biological replicates per year (N varies per year), Delta values (%) vs WT. For TGW, width and length across all years, the triple mutants were significantly higher than the double mutants. Similarly, the double mutants were also significantly higher than the single mutants. Opposite, yield decreased as the number of mutations increased. Significant P values in bold.

Year	Genotype	TGW (g)		Delta (%)	Tukey p values (vs WT)	Grain Width (mm)		Delta (%)	Tukey p values (vs WT)	Grain Length (mm)		Delta (%)	Tukey p values (vs WT)	Yield (kg/plot)		Delta (%)	Tukey p values (vs WT)
2019	WT (N=6)	45.8	±1.07	....	....	3.50	±0.03	....	....	6.57	±0.05	....	....	5.78	±0.11	....	....
	Single (N=15)	48.2	±0.65	5.2	0.2	3.67	±0.01	4.9	**0.03**	6.69	±0.03	1.8	0.25	5.74	±0.06	-0.7	0.99
	Double (N=15)	51.1	±0.69	11.6	**0.0002**	3.73	±0.02	6.6	**0.0004**	6.88	±0.03	4.7	**0.0001**	5.76	±0.07	-0.3	0.99
	Triple (N=5)	57.6	±1.13	25.8	**0.0001**	3.91	±0.03	11.7	**0.0001**	7.20	±0.06	9.6	**0.0001**	5.64	±0.12	-2.4	0.82
2020	WT (N=20)	46.4	±0.5	....	....	3.64	±0.01	....	....	6.50	±0.03	....	....	4.63	±0.06	....	....
	Single (N=30)	47.7	±0.4	2.8	0.33	3.69	±0.01	1.4	0.19	6.57	±0.02	1.1	0.28	4.53	±0.05	-2.2	0.57
	Double (N=30)	51.1	±0.4	10.1	**0.0001**	3.78	±0.01	3.8	**0.0001**	6.68	±0.02	2.8	**0.0001**	4.57	±0.05	-1.3	0.85
	Triple (N=20)	57.1	±0.5	23.1	**0.0001**	3.92	±0.01	7.7	**0.0001**	7	±0.06	7.7	**0.0001**	4.36	±0.06	-5.8	**0.01**
2021	WT (N=20)	38.7	±0.5	....	....	3.40	±0.01	....	....	6.20	±0.03	....	....	5.05	±0.06	....	....
	Single (N=30)	38.6	±0.4	-0.3	0.99	3.44	±0.01	1.2	0.14	6.24	±0.02	0.6	0.7	5.01	±0.05	-0.8	0.97
	Double (N=30)	41.2	±0.4	6.5	**0.007**	3.52	±0.01	3.5	**0.0001**	6.32	±0.02	1.9	**0.021**	5	±0.05	-1.0	0.95
	Triple (N=20)	45.9	±0.5	18.6	**0.0001**	3.92	±0.01	15.3	**0.0001**	6.57	±0.03	6.0	**0.0001**	4.87	±0.06	-3.6	0.18
Overall	WT	42.9	±0.7	....	....	3.53	±0.02	....	....	6.37	±0.03	....	....	4.95	±0.07	....	....
	Single	44.1	±0.6	2.8	0.63	3.59	±0.01	1.7	0.1	6.46	±0.02	1.4	0.21	4.96	±0.05	0.2	0.99
	Double	47.0	±0.6	9.6	**0.0005**	3.66	±0.01	3.7	**0.0001**	6.57	±0.02	3.1	**0.0002**	4.96	±0.05	0.2	0.99
	Triple	52.1	±0.8	21.4	**0.0001**	3.80	±0.02	7.6	**0.0001**	6.83	±0.03	7.2	**0.0001**	4.72	±0.07	-4.6	**0.1**
Anova	Year				**0.0001**				**0.0001**				**0.0001**				**0.0001**
	Genotype				**0.0001**				**0.0001**				**0.0001**				**0.001**
	Year:Block				1				1				1				**0.06**
	Year:Genotype				**0.05**				1				**0.07**				1
	Year:Block: Genotype				1				1				1				1

2.4.5. *Dissecting spike yield components to understand the compensatory effects of gw2 on final yield*

To understand and identify pleiotropic effects of the *GW2* allele affecting final yield, ten main spikes per plot/year of Paragon WT, single, double, and triple mutants were evaluated for a series of spike yield components These included spikelet number, viable spikelets, seed number, yield per spike and tiller number (Table 2.2).

2.4.6. *Spikelet number remains largely stable across years and genotypes*

We found no effect on final spikelet number in 2019-2020 however, in 2021 we found a slight decrease in spikelet number ($P > 0.09$) in the double mutant, (2.3%, 0.5 spikelet) and a significant decrease ($P < 0.001$) in the triple mutants (4.1%, 1 spikelet) when compared to the WT (Table 2.2). These results suggests that the difference across years is related to changes in the environment rather than the presence of *GW2*.

2.4.7. *Viable spikelets are not affected by the presence of the GW2 allele*

Consistent with spikelet number, the viability of the spikelets was not affected across years and genotypes, except in 2021 were we found a decrease in viable spikelets ($P < 0.0001$) in the triple mutants (4.8%, 21 vs 20, Table 2.2) versus the WT. Overall, the data suggests that *GW2* does not affect viable spikelet number in the field.

2.4.8. *Seed number per spike decreased significantly in 2020-2021 in the triple mutants*

When analysing the total seed number (coming from ten main spikes), a non-significant effect was found when comparing the single and double mutants with the WT, except for 2021 where a significant decrease of 4.7% ($P > 0.01$, 77.1 vs 73.5) was observed for the double mutant. Moreover, we found a significant decrease ($P < 0.0001$) in the seed numbers in the triple mutants when compared to the WT across all three years (Figure 2.6), with the strongest effect observed in 2021. When comparing the single and double mutants, we did not observe any significant effect. Finally, when comparing the single and double mutants with the triple mutants, we found a significant effect ($P > 0.0001$) in 2020 and 2021 were the seed number dropped (60<59<55 and 76<73<67, respectively, Figure 2.6, Table 2.2). This suggests a stepwise effect of increasing GW2 mutant copies and decreasing seed number per spike. Taken together, we see a significant decline in seed number per 10 spikes in the triple mutants across all years. This effect is not driven, however, by fewer viable spikelets as in 2019 and 2020 there were no effects on the spikelet number but there were significant decreases in seed number per spike in the triple mutants.
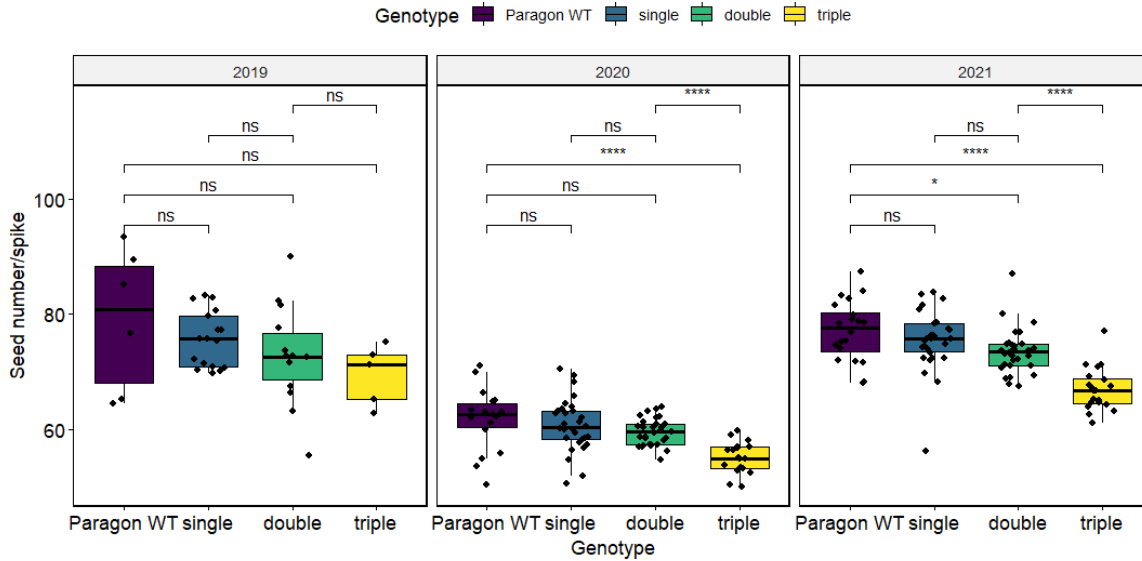
Figure 2-6: Seed number per ten main spikes in Paragon WT, single, double and *gw2* triple mutants across 2019, 2020 and 2011.The box represents the middle 50% of data with the borders of the box representing the 25th and 75th percentile. Statistical classifications are based on Tukey's HSD tests. ns: *P* > 0.05; * *P* < 0.05; ** *P* < 0.0001.**

2.4.9. *Yield per spike increases but not in a significant manner*

Consistent with the increases in TGW, individual yield per spike increased across all years in the single (2.4%), double (4.6%), and triple mutants (5.2%) when compared to the WT NILs. Although this effect was not significant, we can see it follows the same trend when the number of mutations increases (Table 2.2).

2.4.10. *Tiller number decreases significantly across years in the triple mutants*

Previously, we documented a slight decrease in yield (Table 1, Figure 5), but an increase in individual yield per spike (Table 2.2). We therefore counted the total tiller number to investigate if yield was affected not only by a decrease in seed number but also by the number of tillers per square meter. Across all years, we observed a significant (P>0.0001) decrease in tiller numbers when comparing the *gw2* triple mutants to the WT NILs (77 vs 70 tillers/m^2). Single and double mutants showed intermediate phenotypes consistent with a cumulative negative effect of *gw2* mutations on tiller number (Table 2.2).

Table 2-2: Spike yield components of ten representative single ears per plot from Paragon WT, single, double and triple mutants

Year	Genotype	Spikelet number		Spikelet #	Tukey p values (vs WT)	Viable Spikelets		Viable Spk (#)	Tukey p values (vs WT)	Seed number/Spike		Decreases in seed number	Tukey p values (vs WT)
2019	WT (N=6)	24.2	±0.2	....	....	22.8	±0.3	....	....	79.6	±2.0	....	....
	Single (N=15)	24.7	±0.1	+0.5	0.34	23.6	±0.1	3.5	**0.08**	76.0	±1.2	-3.6	0.42
	Double (N=15)	24.4	±0.1	+0.2	0.86	23	±0.2	0.9	0.87	73.1	±1.3	-6.5	**0.04**
	Triple (N=5)	23.8	±0.2	-0.4	0.8	22.3	±0.3	-2.2	0.75	69.9	±2.2	-9.7	**0.008**
2020	WT (N=20)	19.8	±0.1	....	....	18.4	±0.1	....	....	61.8	±1.1	....	....
	Single (N=30)	19.7	±0.1	-0.1	0.96	18.4	±0.1	0.0	0.99	60.7	±0.9	-1.1	0.86
	Double (N=30)	19.5	±0.1	-0.3	0.31	18.0	±0.1	-2.2	0.41	59.5	±0.9	-1.3	0.38
	Triple (N=20)	19.4	±0.1	-0.4	0.28	17.9	±0.1	-2.7	0.16	54.9	±1.1	-6.9	**0.0002**
2021	WT (N=20)	21.8	±0.1	....	....	21.0	±0.1	....	....	77.1	±1.1	....	....
	Single (N=30)	21.7	±0.1	-0.1	0.95	21.0	±0.1	0.0	1	75.8	±0.9	-1.7	0.79
	Double (N=30)	21.3	±0.1	-0.5	**0.09**	20.5	±0.1	-0.5	**0.07**	73.5	±0.9	-4.7	**0.05**
	Triple (N=20)	20.9	±0.1	-1.1	**0.0002**	20	±0.1	-1.0	**0.0001**	66.9	±1.1	-13.2	**0.0001**
All years	WT	21.2	±0.2	....	....	20.1	±0.2	....	....	71.1	±1.3	....	....
	Single	21.5	±0.2	+0.3	0.8	20.5	±0.2	+0.4	0.94	69.8	±0.9	-0.3	0.86
	Double	21.1	±0.2	-0.1	0.9	19.9	±0.2	-0.2	0.16	67.6	±1.0	-3.5	0.15
	Triple	20.5	±0.2	-0.7	0.2	19.3	±0.2	-0.7	0.28	62.2	±1.3	-8.9	**0.0001**
Anova	Year				**0.0001**				**0.0001**				**0.0001**
	Genotype				**0.0001**				**0.0001**				**0.0001**
	Year:Block				**0.05**				1				**0.001**
	Year:Genotype				0.1				0.1				0.5
	Year: Block :Genotype				0.1				0.1				1

Table 2-2 (continued): Spike yield components of ten representative single ears per plot from Paragon WT, single, double and triple mutant

Year	Genotype	Yield per Spike		Delta (%)	Tukey p values (vs WT)	Seeds/ Spikelet		Delta (%)	Tukey P values (vs WT)	Tiller Number		Delta (%)	Tukey p values (vs WT)	HLW*		Delta (%)	Tukey p values (vs WT)
2019	WT (N=6)	**3.98**	±0.11	....	....	**3.47**	±0.10	....	....	**80.3**	±1.32	....	....	**73.9**	±0.63	....	....
	Single (N=15)	**4.01**	±0.06	0.8	0.98	**3.20**	±0.06	-7.78	0.13	**79.6**	±1.11	-0.9	0.92	**75.3**	±0.36	1.89	0.21
	Double (N=15)	**4.10**	±0.07	3.0	0.79	**3.15**	±0.06	-9.27	0.06	**77.6**	±1.13	-3.4	0.1	**74.5**	±0.38	0.81	0.81
	Triple (N=5)	**4.29**	±0.12	7.8	0.24	**3.10**	±0.11	-10.66	0.09	**73.5**	±1.34	-8.5	**0.0001**	**72.5**	±0.62	-1.89	0.42
2020	WT (N=20)	**3.10**	±0.06	....	....	**3.35**	±0.04	....	....	**71.3**	±1.43	....	....	**75.9**	±0.30	....	....
	Single (N=30)	**3.13**	±0.04	1.0	0.98	**3.30**	±0.03	-1.43	0.82	**70.8**	±1.17	-0.7	0.98	**75.8**	±0.24	0	0.99
	Double (N=30)	**3.25**	±0.04	4.8	0.25	**3.29**	±0.03	-1.60	0.72	**68.3**	±1.17	-4.2	0.34	**75.6**	±0.24	0	0.88
	Triple (N=20)	**3.31**	±0.06	6.8	0.1	**3.09**	±0.04	-7.75	**0.0002**	**66.6**	±1.43	-6.6	**0.09**	**75.4**	±0.30	0	0.68
2021	WT (N=20)	**3.27**	±0.06	....	....	**3.66**	±0.04	....	....	**79.2**	±1.43	....	....	**68.9**	±0.30	....	....
	Single (N=30)	**3.25**	±0.04	-0.6	0.99	**3.59**	±0.03	-1.64	0.66	**77.4**	±1.17	-2.3	0.78	**67.4**	±0.24	-2.17	**0.001**
	Double (N=30)	**3.33**	±0.04	1.8	0.85	**3.58**	±0.03	6.88	0.44	**76.6**	±1.17	-3.4	0.51	**67.5**	±0.24	-2.18	**0.001**
	Triple (N=20)	**3.39**	±0.06	3.7	0.47	**3.34**	±0.04	-9.58	.0001	**69.8**	±1.43	-12.1	**0.0001**	**66.6**	±0.24	-3.33	**0.0001**
Overall	WT	**3.28**	±0.06	....	....	**3.52**	±0.03	....	....	**76.8**	±0.96	....	....	**72.6**	±0.62	....	....
	Single	**3.36**	±0.04	2.4	0.79	**3.41**	±0.02	**-3.12**	0.08	**76.1**	±0.7	-0.9	0.99	**72.3**	±0.49	**0**	0.98
	Double	**3.43**	±0.04	4.6	0.25	**3.40**	±0.02	**-3.40**	0.05	**74.1**	±0.7	-3.5	0.28	**72.1**	±0.49	**-0.5**	0.90
	Triple	**3.45**	±0.06	5.2	0.23	**3.21**	±0.03	**-8.82**	0.0001	**70**	±0.9	-8.9	**0.0001**	**71.2**	±0.63	**-1.92**	0.36
Anova	**Year**				**0.0001**				**0.0001**				**0.0001**				**0.0001**
	Genotype				**0.001**				**0.0001**				**0.0001**				**0.001**
	Year:Block				**0.01**				**0.0001**				0.1				0.5
	Year:Genotype				1				0.20				0.1				**0.0001**
	Year:Block:Genotype				0.5				1				0.1				1

Table 2-3: Developmental traits of Paragon WT, single, double and triple mutants.

Year	Genotype	Height (cm)		Days	Tukey p values (vs WT)	Days to Heading		Days	Tukey p values (vs WT)	Days to Maturity		Days	Tukey p values (vs WT)	GFD[a]		Delta (%)	Tukey p values (vs WT)
2019	**WT**	91.4	±1.4	....	....	244	±0.4	....	....	298	±0.3	....	....	53	±0.4	....	....
	single	93.0	±0.9	+1.6	0.8	242	±0.4	-2	**≤0.001**	297	±0.1	-1	0.32	55	±0.2	3.8	**0.09**
	double	93.2	±0.9	+1.8	0.7	243	±0.5	-1	**0.04**	297	±0.2	-1	0.61	54	±0.2	1.9	0.56
	triple	94.5	±1.6	+3.1	0.5	242	±0.3	-2	**0.01**	297	±0.3	-1	0.87	55	±0.5	3.8	0.17
2020	**WT**	72.8	±0.8	....	....	125	±0.2	....	....	172	±0.1	....	....	47	±0.2	....	....
	single	73.4	±0.6	+0.8	0.9	125	±0.2	0.0	0.94	172	±0.1	0.0	0.39	47	±0.2	0.0	0.90
	double	73.3	±0.6	+0.7	0.9	125	±0.2	0.0	0.99	172	±0.1	0.0	0.47	47	±0.2	0.0	0.81
	triple	72.3	±0.8	-0.5	0.9	125	±0.2	0.0	0.63	172	±0.1	0.0	0.93	47	±0.2	0.0	0.94
2021	**WT**	95.3	±0.8	....	....	216	±0.2	....	....	264	±0.1	....	....	47	±0.2	....	....
	single	94.6	±0.6	-0.7	0.9	216	±0.2	0.0	0.67	264	±0.1	0.0	1	48	±0.2	2.1	0.84
	double	94.3	±0.6	-1.0	0.7	216	±0.2	0.0	0.67	263	±0.1	-1	0.82	47	±0.2	0.0	0.98
	triple	94.8	±0.8	-0.5	0.9	216	±0.2	0.0	0.9	263	±0.1	-1	0.98	47	±0.2	0.0	0.99
Overall	**WT**	84.9	±1.6	....	....	180	±7.3	....	....	228	±7.5	....	....	48	±0.4	....	....
	single	85.8	±1.2	+1.1	0.9	185	±5.6	+5	0.99	234	±5.8	+6	0.99	49	±0.3	2.1	0.49
	double	85.5	±1.2	+0.7	0.9	184	±5.7	+4	0.99	233	±5.9	+5	0.99	48	±0.3	0.0	0.85
	triple	84.7	±1.6	-0.2	0.9	178	±7.3	-2	0.99	226	±7.6	-2	0.99	48	±0.4	0.0	0.99
Anova	**Year**				**0.0001**				**0.0001**				**0.0001**				**0.0001**
	Genotype				1.00				**0.01**				0.5				0.1
	Year:Block				**0.01**				1.00				**0.0001**				**0.5**
	Year:Genotype				0.5				1.00				1.00				0.1
	Year:Blo:Genotype				1.00				1.00				1.00				0.1

2.4.11. The mutated A allele increases TGW and width in the single and double mutants

We wanted to investigate how the mutations across the single *aa*BBDD, AA*bb*DD, AABB*dd* copies compared among them with respect to yield, grain weight, and grain morphometrics. Previously, Wang and Simmonds (2016) found that the highest single genome increases were obtained in the A and B genome mutants in glasshouse experiments. We found that the A mutant allele increased TGW, width and length in 2020 and 2021 but we see no effect on final yield when compared to the B and D mutants (Figure 2.7).
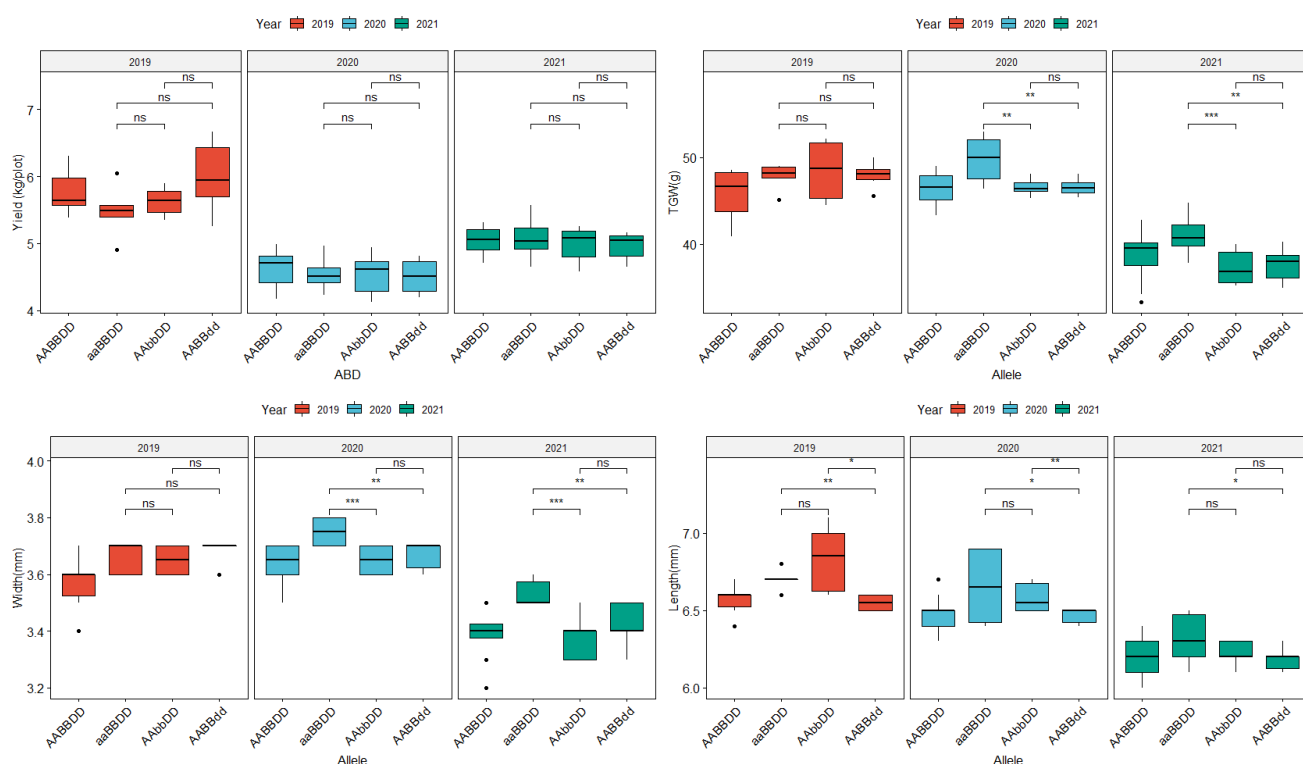
Figure 2-7: Yield, TGW, grain width and length in the WT AABBDD and single mutants *aa*BBDD, AA*bb*DD, AABB*dd* across 2019, 2020 and 2021. The box represents the middle 50% of data with the borders of the box representing the 25th and 75th percentile. ns: P > 0.05; * P < 0.05; **P<0.01, ***P<0.001. The WT boxplots were placed only as a reference to the reader.

Based on the data from the single mutants, we hypothesised that the double mutants carrying the A genome mutation in combination with either the B or D genome (*AB* or *AD*, respectively) would show increases in TGW and width. We found that, the *AD* combination increased TGW when compared to the double *BD* mutants. Regarding grain width, we found a favourable in the double *AD* mutants. Finally, length was found to be not uniform across years and mutations except for 2020 where the double *AB* mutants had an increased grain size (P<0.01, 6.69 mm vs 6.63 mm).

Our results agree with what was previously reported by Wang and Simmonds (2018) in Paragon NILs where the A genome mutant allele increased TGW and grain width consistently with respect to the other alleles and WT. In the double mutants, the trait is less clear as most of the evaluated parameters were found to be non-significant. As

expected, final yield remains non-significant across all growing season except in year 2020 were we found that the AB mutants yield significantly (P < 0.01) more than the double AD copies (Figure 2.8).
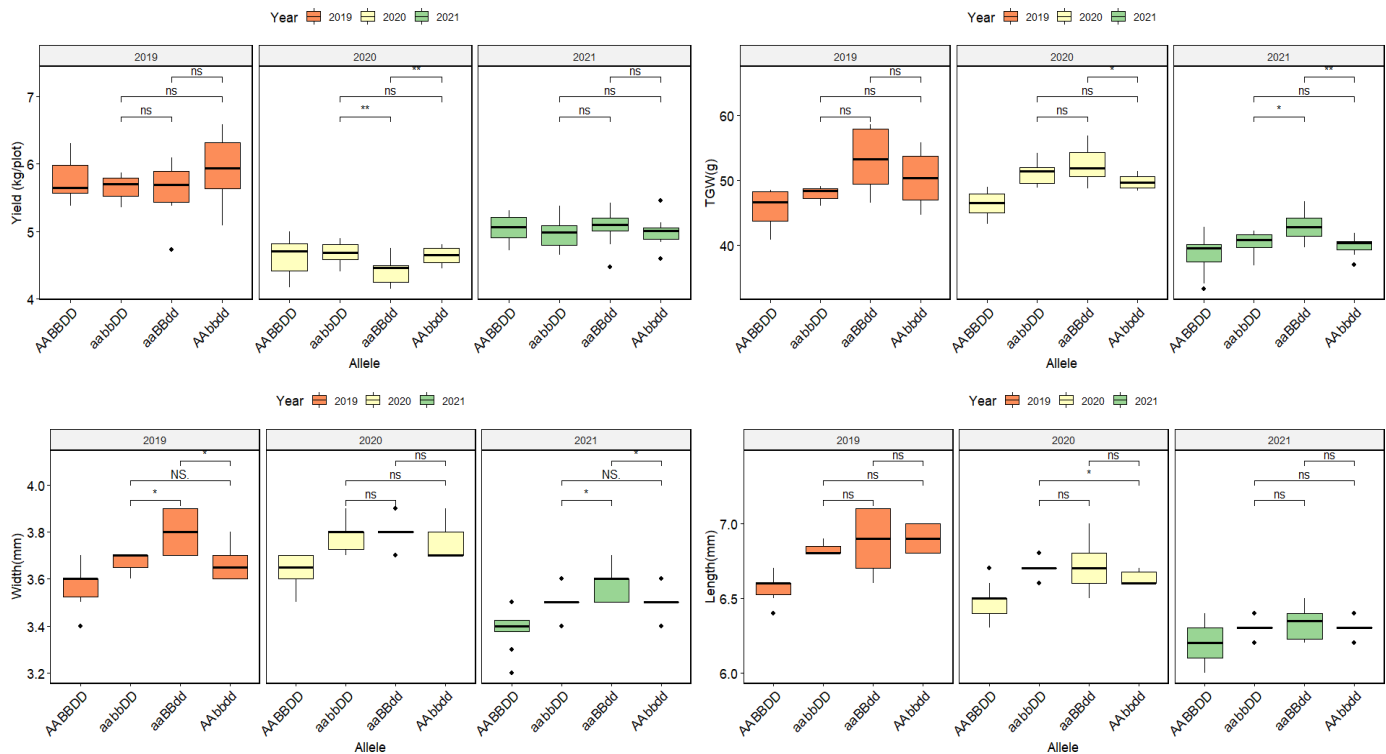
Figure 2-8: Yield (g), TGW (g), width and length in the WT AABBDD and double mutants aabbDD, aaBBdd, AAbbdd, across 2019,2020 and 2021.The box represents the middle 50% of data with the borders of the box representing the 25th and 75th percentile. ns: P > 0.05; * P < 0.05; **P<0.01. The WT boxplots were placed only as a reference to the reader.

2.4.12 Phenological traits

Finally, we measured phenology traits in the field to measure if the *gw2* alleles had any effect on them. We found no significant effects of the *gw2* mutations on height across the three years. In days to heading, again we found no significant effects although there were contrasting effects between mutants: Single and double mutants headed five days later than the control, whereas the triple mutants headed two days earlier than the wildtype controls but none of them were significant. In days to maturity, the trend mirrors that of heading date, with the triple mutants maturing earlier than the controls by two days while the single and double mutants had a delay in final maturity by five and six days, respectively, no differences were observed in grain filling duration (GFD) (Table 3).

2.4.13 Tiller number decreases at the same rate in two growing stages in both WT and triple mutants

In the 2019-2021 growing seasons we found that tiller number was negatively affected by the presence of the *gw2* allele in a dose-dependent manner (Table 2.2). For that reason, we counted tiller number in the two most contrasting genotypes (WT and triple mutants) at two different growth stages if a fourth growing season in 2022. The first tiller counting was made at stage GS45 or early booting, as it is expected that the number of shoots per square meter will reach its maximum number here. We also measured at stage GS83 where tiller number should be lower due to tiller mortality and should remain unaltered until maturity. We found that the triple mutants had significantly less tillers 14.4% (100 vs 85) than the WT at stage GS45 and that the differences in tiller number was maintained at stage GS38 where a significant decrease of 15% (75 vs 65) was found between the triple mutants and the WT. The tiller abortion rate was calculated ([tiller number at GS45 - tiller number at GS83]/tiller number at GS45) and was found to be non-significant when compared to the WT (Table 2.4)

Table 2-4: Tiller abortion rate between WT and triple mutants

Year	Genotype	Tiller number GS45	Delta (%)	Tukey	Tiller number GS83	Delta (%)	Tukey	Tiller Abortion (%)	Delta (%)	Tukey
2022	WT (36)	101 ± 3.16	-14.40%	A	76.22±1.58	-15.40%	A	23.6±2.05	3.00%	A
	triple mutants (37)	85.64 ± 1.41		B	64.5±1.40		B	24.3±1.16		A

2.4.14 Grain protein content increase consistently in the triple mutants across years

We found increases in grain protein content (GPC) in the double and triple mutants by 2.52% (P <0.05) and by 7.49% (P ≤0.001) respectively, in 2020 while in 2021, GPC only increased in the triple mutants by 5.3% (P ≤0.001). Our results agree with what was previously reported by Zhang et al. (2018), they found a significant increase in GPC in the single and double mutants. We will talk about the implications of these findings in the discussion.

Table 2-5: Grain protein content across NILs

Year	Genotype	GPC	SE	Delta (%)	Tukey P.values
2020	**WT**	14.68	±0.11	....	....
	single	14.81	±0.09	0.89	0.83
	double	15.05	±0.09	2.52	0.05
	triple	15.78	±0.11	7.49	≤0.001
2021	**WT**	13.79	±0.11	....	....
	single	14.04	±0.09	1.81	0.3
	double	13.85	±0.09	0.44	0.96
	triple	14.58	±0.11	5.73	≤0.001
ANOVA	**Year**				**0.0001**
	Genotype				**0.0001**
	Year:Block				0.30
	Year:Genotype				0 .06
	Year:Block: Genotype				0.91

2.5 Discussion

The *gw2* allele has been characterised across different plant species and wheat cultivars and found to have a role in negatively regulating grain weight and size. In this chapter, we analysed field data from three growing seasons in Paragon *gw2* NILs carrying mutations in single homoeologs, or in combinations of double and triple mutants. We identified trade-offs between yield, TGW, seed number per spike and tiller number which we discuss below.

2.5.1 Increases in TGW do not consistently translate into increases in final yield

In this chapter, we found a consistent increase in TGW (2.8% single, 9.6% double and 21.4% triple mutant *gw2* NILs) and grain morphometrics conferred by mutations in individual or combinations of *gw2* mutant alleles. Yield, however, did not increase in the single and double mutants while in the triple mutants, yield decreased significantly by 4.6%. To investigate further into yield losses, we conducted a Spearman correlation test across twelve yield and phenological parameters (Figure 2.9). We found among other variables, that TGW was positively correlated with grain area, width, and length while it was negatively correlated with tiller number and seed number per spike (traits that are highly correlated between each other). Additionally, we found that in our field experiments, yield was positively linked to seed number and tiller number but not to grain weight and grain morphometrics.
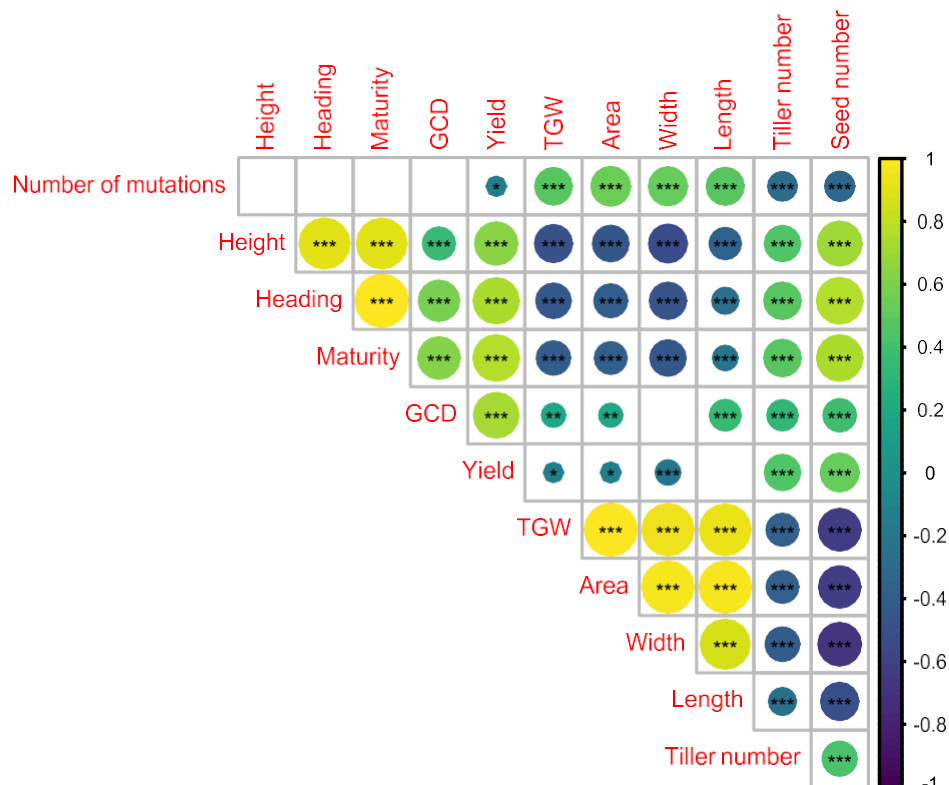
Figure 2-9: Spearman's correlation among twelve parameters, across all three growing seasons and mutations. In yellow and green significant correlations are depicted while blue purple colours negative correlations. Bigger circles represent stronger correlations while smaller circles weak correlations.

Several studies support our results of a trade-off between grain weight with seed and tiller number. Wiersma et al. (2001) conducted an experiment across eight growing seasons of recurrent selection for TGW in three Minnesota environments. He reported that increases of 31% in TGW did not translate into yield mainly due to a decrease in tiller number and grains per spike. Zhai et al. (2018), reported that in a set of four NILs coming from Yumai 8679 and Jing 411 although TGW increased by 8%, seed number decreased by 3% in the lines carrying the Yumai 8679 allele on chromosome 6A. Würschum et al. (2018) studied a panel with 407 European winter wheat accessions, sown in three sites across Germany. They observed that the number of grains per spike and spikelet fertility were positively correlated while, both traits showed a significant negative correlation with TGW. Thus, despite the isogenic nature of the lines and the large effect on grain size in the triple mutants, our results are consistent with previous studies and show that there is a very tight negative correlation between grain size and seed number as these two processes overlap in space and time making it impossible for the plant to compensate for seed number (Figure 2.10).
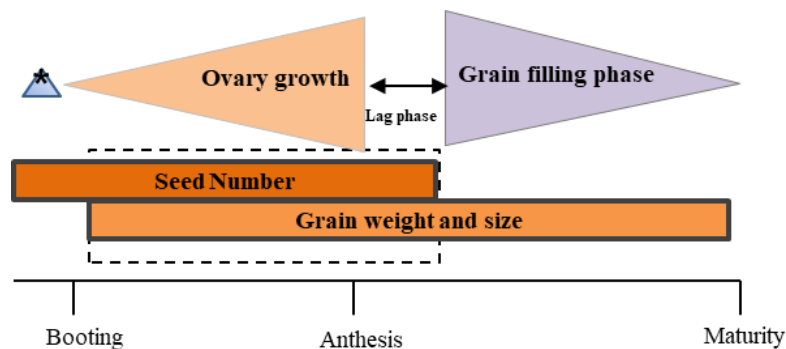
Figure 2-10: Growth dynamic of seed number and grain weight in wheat from booting to maturity. The blue triangle* represents the early effect of *GW2* on ovary growth, follow by lag phase and grain filling. The overlap between seed number and grain weight from booting to the end of the lag phase is highlighted. Figure adapted from Calderini et al. (2021)

In a ground-breaking study Calderini et al. (2021) proved that this trade-off can be overcome. They overexpress a *TaExpA6* α-expansin transgene in young developing grains which results in significant increase in TGW and yield by 12.3% and 11% respectively, without affecting grain number. Suggesting that the increase of GW without a negative impact on GN was due to the expression of the expansin transgene after the overlapping period of GW and GN determination, avoiding the trade-off between these yield components.

Brinton et al. (2020) conducted a haplotype-based approach across chromosome 6A where the *GW2-A1* gene is located and has been hypothesized to be at least partially responsible for heavier and wider grains. Across 15 sequenced cultivars (Paragon included), the authors identified seven different haplotypes across a conserved 258 Mbp centromeric region of chromosome 6A, where multiple QTL and GWAS hits for productivity-related traits have been localised. Breeders have historically selected for this 258 Mbp interval on chromosome 6A due to its positive effects on yield. This region has relatively low recombination rates and contains over 2000 genes (Brinton et al., 2020). This study showed that disruption of the interval led to intermediate effects on grain size and yield and the

authors argue that breeders have selected for the complete interval to maintain allelic combinations which maximise yield effects. Therefore, it is likely that there will be other genes beyond *GW2* with small size effects on grain size or genes that might take part in other developmental process that affect yield. Thus, when generating the NILs we might have disrupted the Paragon recurrent parent haplotypes by introducing the *gw2* mutations from Kronos (A and B genomes) and Cadenza (D-genome) mutants. Using the available wheat haplotype browser (http://www.crop-haplotypes.com/) we conducted a comparison between Cadenza (*gw2-D1* allele donor) and Paragon across chromosome 6D and found that the D genome of both cultivars are identical by state. The A and B genomes were not analysed with this tool because cultivar Kronos (donor of the *gw2-A1* and *-B1* mutant alleles) is not yet assembled. Nevertheless, it is well documented that tetraploid and hexaploid wheat have distinct genetic diversity, including across chromosome 6A. In our lab, James Simmonds run 17 KASP markers diagnostic of the seven 6A haplotypes confirming that Kronos and Paragon belong to different haplotypes (personal communication). Until the exact genes that causes the positive effect on grain size on chromosome 6A are not cloned, it will be challenging even with NILs to identify pleiotropic effects like the reduction in tiller number and seed number found in this chapter. New precise gene editing technologies like CRISPR can help us to target only the gene of interest avoiding the potential pleiotropic effects of introducing hundreds of novel genes from Kronos into Paragon. Such lines were generated in cultivar Bobwhite by Wang et al. (2018) using CRISPR-Cas9 but there is only glasshouse data from them. Further field trials are needed to evaluate phenology, spike yield, final yield and potential pleiotropic effects to determine if the *gw2* mutations *per se* are causing the reduction in tiller and seed number, or if there are additional genes along the 6A and 6B Kronos haplotypes which could be responsible.

2.5.2   *Advantages of breeding for heavier and bigger grain size*

For all NILs assessed in this chapter and across all growing seasons, we found that increases in grain size are mainly driven by grain width in the double and triple Paragon *gw2* mutants. The effect is very robust and is independent from final yield (Figure 2.9). Bigger grains are suitable for deep planting of wheat under drought conditions in Mediterranean-like climates where low precipitations are common (< 300 mm annual). Deeper sowing allows these larger seeds to reach adequate soil moisture needed for germination (Rebetzke et al., 2005). The lack of moisture in the upper soil layers can cause the seedlings to dehydrate leading to poor emergence and establishment which translates into yield losses. Moreover, deep sowing can prevent seed removal from predators and provide protection against herbicide waste in the upper soil layers (Mohan et al., 2013). With the introduction of the semi-dwarf, gibberellin insensitive, *Rht-B1b* and *Rht-D1b* alleles, coleoptile length has decreased by 20% causing a poor seedling establishment if these cultivars are sown too deep (Rebetzke et al., 2007). Increasing seed size can affect positively coleoptile early emergence; Moore and Rebetzke (2015) studied a population of 150 double haploid lines with different embryo sizes and found that early vigour was positively correlated with TGW and embryo width, length and area, the effect nevertheless, was not always consistent across populations. In contrast, long coleoptiles that are gibberellin sensitive had significantly better emergence, positively correlating with an increase in spikes per plant, spikelets per spike and yield (Amram et al., 2015). However, selecting for TGW, does not necessarily translate into

increases in GPC, Guzmán et al. (2017) analysed data coming from 50 years of breeding for grain quality in CIMMYT semi-dwarf spring wheat lines, they found that TGW and GPC were not significant despite yield increases over the years. Laidig et al. (2017b) found that GPC decreased by 7.9% between 1983-2014 while grain yield increased by 24% in German winter wheat lines. In contrast, Wiersma et al. (2001) found that selecting for grain weight and grain morphometrics increases GPC by 0.16% per year, across eight growing cycles in Montana, United States. Here and against popular belief, we found that GPC increased across two years 2020 -2021 in Paragon *gw2* triple mutants by 7.4% and 5.7%, respectively, when compared to the WT (Table 2.5). Zhang et al. (2018) reported that GPC increased in cv Kenong by 18.9% and 15.5% in the single mutants and in the double mutants respectively, increases in GPC were correlated with increases on cell number and cell length of the outer pericarp cells in developing grains. In rice Achary and Reddy (2021) found that the *GW2* KO seeds accumulate substantially more (12–14%) total grain protein content when compared to the WT seeds related to a thickening of the endosperm. From these studies, we learn that the trade-offs between TGW and GPC can be overcome with the incorporation of novel alleles in wheat germplasm. Lastly, shifting grain size towards bigger kernels can be advantageous during combine harvesting as larger seeds are less likely to be blown away alongside the chaff causing yield losses. To date, we haven't sown Paragon NILs at different soil depths to assess for emergence and the other traits mentioned above, but these would be important studies to understand the value of the larger grain weight in the absence of improved yield.
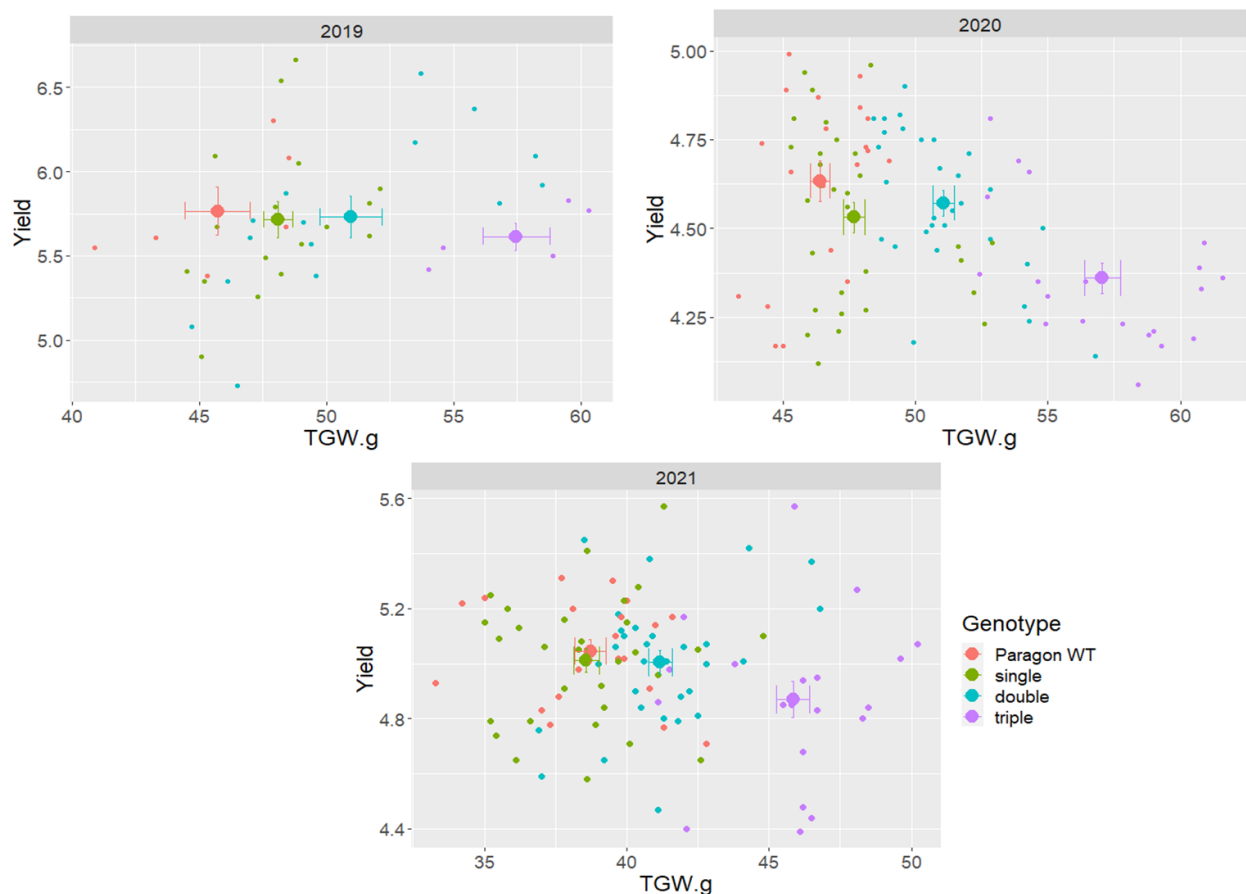
Figure 2-11: Scatter plots, yield plotted against TGW(g). Centroids of distribution with their relative standard error bars and individual data points shown by genotype and year.

To visualise a way to select for bigger grain without yield penalties, we plotted yield vs TGW independently across three growing seasons (Figure 2.11). The scatter plots show that the increases on TGW are not significant among the WT and single mutants but that the significant increases in the double (9%) and triple mutants (20%) causes a yield decreased only the triple mutants across 2020 and 2021. Following these results, we propose the use of the double mutants in breeding programs as they balance the increase in grain weight yet circumvent the loss of yield observed in the triple mutants. It is important to acknowledge, however, that these results are in a single genetic background (cv. Paragon) grown in a single UK growing environment (Morley UK).

2.5.3 *Understanding the trade-offs between tiller number and grain number per spike and their effect on yield.*

In the introduction (see section 1.5.1 and 1.5.2) we discuss that the final tillers number (spikes per m²) and final grains per spike are determined pre anthesis and that both are classified as sink related yield traits (Dreisigacker et al., 2021). The consistent and additive negative effect on tiller number and seed number per spike found in the NILs allows us to hypothesize that the *GW2* gene has an effect not only on final grain weight and grain size but in the already mentioned phenological traits. Our results display that both traits are positively correlated meaning that, when the tiller number goes down so does the seed per spike. Moreover, the number of mutations in *GW2* are negatively correlated with both traits (Figure 2.9). We verify the expression levels of the *GW2* genes in different tissues using the https://bar.utoronto.ca tool. We found that *GW2* had its higher expression of ~20-21 transcript per million (TPM) in both the embryo and the grain at ripening stage, followed by an expression of ~ 8.9 TPM in ovaries while, at tillering stage in roots, shoots and first leaf sheath, the expression values were ~ 5.5 TPM in cv. Azhurnaya which is wild type for *GW2* (Ramirez- Gonzales et al., 2018 ; Winter et al., 2007). The high expression levels of the genes in ovary, embryo and grain are consistent with the literature and with *GW2* being a seed growth repressor however, at tillering stages, we were not able to link our results based only on the expression profile. Furthermore, we need to consider that there is none or marginal expression of the *gw2* alleles in Paragon *gw2* triple mutants so we will expect these values to be lower than in cv Azhurnaya.

Previously, it was reported that the effect of *GW2* was first visible in developing carpels leading to increases in width and length from heading onwards (Brinton et al 2017). Here, we found that the triple mutants have less initial and final tiller number than the WT (-15%) across two different developmental stages, but that the tiller abortion ratio was similar between WT and triple mutants (both abort ~24% between stages). Taken together, the decreases in tiller number across seasons might indicate that the mutations in the *GW2* homoeologs have a direct effect on tiller number, and perhaps floret survival, before anthesis. The question is how does the tiller dynamics work in the mutant lines? We hypothesize three case scenarios:
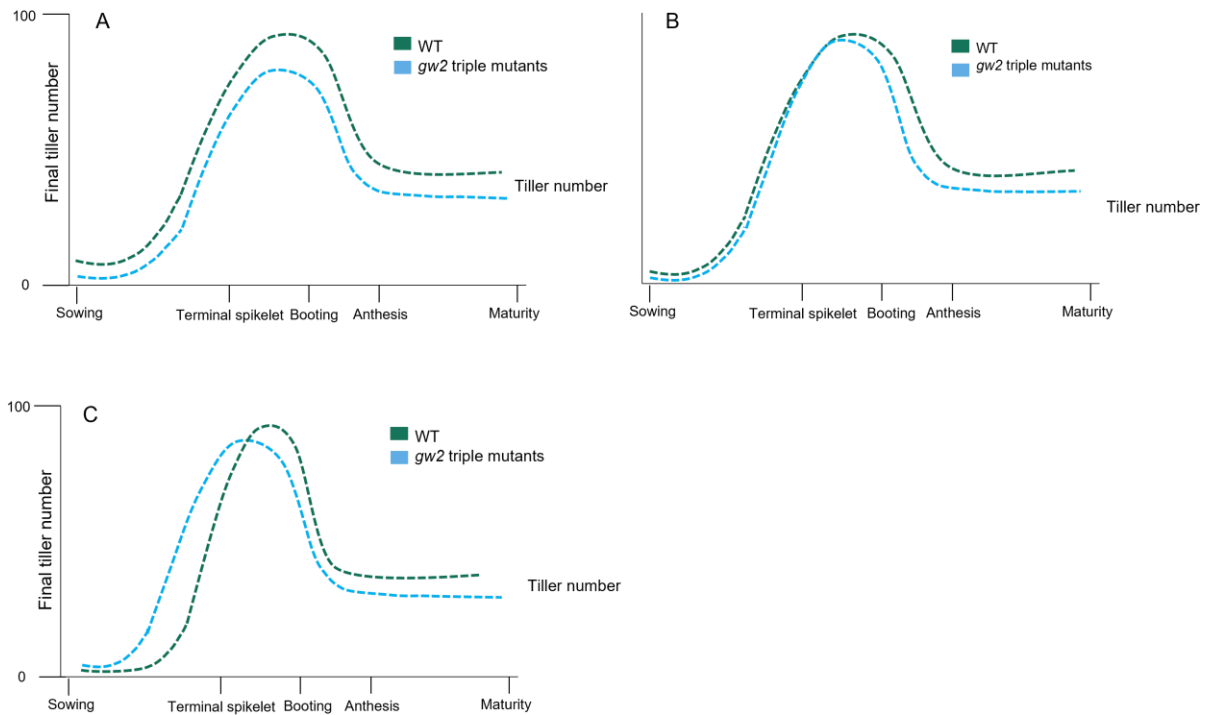
Figure 2-12: Panel A) shows that the WT has more tillers since the beginning of the growing season and that both NILs had the same abortion rate. Panel B) shows how the two NILs start with the same number of tillers but during development the triple mutants lose more tillers that the WT. Panel C) shows that *gw2* triple mutant produces more tillers but loses more at booting stage.

Our data supports hypothesis A or C, as we demonstrated that at two growing stages, the mutants have less tiller when compared to the WT (Table 2.2) which makes hypothesis B unlikely (Figure 2.12). Nevertheless, we lack an earlier measurement at terminal spikelet stage. As a followed up, on the next growing season, we are going to count tiller number per unit area at terminal spike and booting followed by shoot and spike number at anthesis and at seven-ten days after anthesis. In that way, we can monitor the whole growth tiller dynamic of both NILs. Further field studies are needed to understand if *GW2* affects the ratio between floret abortion at anthesis and floret survival (grains). To do so, we will follow the method described by Prieto et al. (2018), Reynolds et al. (2022) as we hypothesize that floret survival might be lower in the triple mutants which then leads to a reduction on final seed number per spike. From stem elongation onwards, five plants from each genotype are going to be sampled once a week. The spikes from the main tillers are going to be dissected under a microscope and then within central spikelets floret primordia are going to be counted and classified from 1 to n from the closest to the most distal positions with respect to the rachis, the stage of development of each primordium is going to be determine following the Waddington scale Waddington. et al. (1983) until W10 (or anthesis).

2.5.4 Possible genes and pathways to achieved yield increases via increases in tiller number and grain number per spike

As already stated in the introduction, in the past century, breeding efforts have focused on increasing the number of grains per spike Sanchez-Garcia et al. (2013), while increases in tiller number have great variation between cultivars and sowing densities. To date, 36 genes have been identified to affect grain number but only 13 of these genes have been analysed for yield related traits and trade-offs (Xie and Sparkes, 2021a). One of them is the *Grain Number Increase 1* (*GNI1*) gene that is related to floret survival due to alternation in assimilate distribution. A significant fraction of the florets will degenerate after the beginning of floret primordia through a genetically controlled environment-responsive mechanism called floret abortion (Golan et al., 2019b). In a recent study, a *GNI-A1* allele was found to contribute to the increases in the number of both fertile florets and grain set. Moreover, it was found that the allelic variation coming from cultivar Kitahonami which encodes a Y105N substitution increases grain number without adverse effects on spike yield and with yield increases of 10% and 30% across two growing sites in Japan (Sakuma et al., 2019). Alternatively, tiller number can be modified to boost final yield, a tiller related gene *TaPIN1-6A* was identified in wheat (cv. CB037) which is ortholog to *Arabidopsis* and rice. RNAi mutant lines were developed (*TaPIN1-RNAi*) and planted in the field. Overall, the three mutant lines increased significantly final tiller number by 25% suggesting that *TaPIN1-6A* plays a role in the regulation of tiller number (Yao et al., 2021). However, plants were sown at a very low density of 40 plants/m² vs 300 plants/m² on a conventional field which might explained the increases in tiller number. Another gene linked to tiller production was recently discovered, *TaD27* (cv. Kenong199). *TaD27-RNAi* wheat plants had ~ 50% more tillers than the WT at maturity (Zhao et al., 2020). But once more, the plant density was very low in comparison with lines sown for a commercial setting. The question here is how these two tiller related genes will behave in normal density plots. Interestingly, both studies linked tillers production with plant hormones, the first one with auxins for branch production and the second study with strigolactones which inhibits axillary bud outgrowth. In our lab James Simmonds is currently developing a set of NILs to investigate the gw2 triple mutants in both the *GNI-A1* positive allele (Paragon) and WT *GNI-A1* (Cadenza) backgrounds. Soon, the lines are going to be evaluated in field experiments for floret survival, seed set and total grain number.

References

1. ACHARY, V. M. M. & REDDY, M. K. 2021. CRISPR-Cas9 mediated mutation in GRAIN WIDTH and WEIGHT2 (*GW2*) locus improves aleurone layer and grain nutritional quality in rice. *Scientific Reports,* 11**,** 21941.
2. AMRAM, A., FADIDA-MYERS, A., GOLAN, G., NASHEF, K., BEN-DAVID, R. & PELEG, Z. 2015. Effect of GA-sensitivity on wheat early vigor and yield components under deep sowing. *Frontiers in Plant Science,* 6.
3. BEDNAREK, J., BOULAFLOUS, A., GIROUSSE, C., RAVEL, C., TASSY, C., BARRET, P., BOUZIDI, M. F. & MOUZEYAR, S. 2012. Down-regulation of the *TaGW2* gene by RNA interference results in decreased grain size and weight in wheat. *Journal of Experimental Botany,* 63**,** 5945-5955.
4. BRINTON, J., RAMIREZ-GONZALEZ, R. H., SIMMONDS, J., WINGEN, L., ORFORD, S., GRIFFITHS, S., HABERER, G., SPANNAGL, M., WALKOWIAK, S., POZNIAK, C., UAUY, C. & WHEAT GENOME, P. 2020. A haplotype-led approach to increase the precision of wheat breeding. *Communications Biology,* 3**,** 712.
5. BRINTON, J., SIMMONDS, J., MINTER, F., LEVERINGTON-WAITE, M., SNAPE, J. & UAUY, C. 2017. Increased pericarp cell length underlies a major quantitative trait locus for grain weight in hexaploid wheat. *New Phytol,* 215**,** 1026-1038.
6. BRINTON, J. & UAUY, C. 2019. A reductionist approach to dissecting grain weight and yield in wheat. *Journal of Integrative Plant Biology,* 61**,** 337-358.
7. CALDERINI, D. F., CASTILLO, F. M., ARENAS-M, A., MOLERO, G., REYNOLDS, M. P., CRAZE, M., BOWDEN, S., MILNER, M. J., WALLINGTON, E. J., DOWLE, A., GOMEZ, L. D. & MCQUEEN-MASON, S. J. 2021. Overcoming the trade-off between grain weight and number in wheat by the ectopic expression of expansin in developing seeds leads to increased yield potential. *New Phytologist,* 230**,** 629-640.
8. DREISIGACKER, S., BURGUEÑO, J., PACHECO, A., MOLERO, G., SUKUMARAN, S., RIVERA-AMADO, C., REYNOLDS, M. & GRIFFITHS, S. 2021. Effect of Flowering Time-Related Genes on Biomass, Harvest Index, and Grain Yield in CIMMYT Elite Spring Bread Wheat. *Biology,* 10**,** 855.
9. FAO 2021. *World Food and Agriculture – Statistical Yearbook 2021. Rome.*
10. GENG, J., LI, L., LV, Q., ZHAO, Y., LIU, Y., ZHANG, L. & LI, X. 2017. *TaGW2-6A* allelic variation contributes to grain size possibly by regulating the expression of cytokinins and starch-related genes in wheat. *Planta,* 246**,** 1153-1163.
11. GOLAN, G., AYALON, I., PERRY, A., ZIMRAN, G., ADE-AJAYI, T., MOSQUNA, A., DISTELFELD, A. & PELEG, Z. 2019. *GNI-A1* mediates trade-off between grain number and grain weight in tetraploid wheat. *Theoretical and Applied Genetics,* 132**,** 2353-2365.
12. GUZMÁN, C., AUTRIQUE, E., MONDAL, S., HUERTA-ESPINO, J., SINGH, R. P., VARGAS, M., CROSSA, J., AMAYA, A. & PEÑA, R. J. 2017. Genetic improvement of grain quality traits for CIMMYT semi-dwarf spring bread wheat varieties developed during 1965–2015: 50 years of breeding. *Field Crops Research,* 210**,** 192-196.
13. KRASILEVA, K. V., VASQUEZ-GROSS, H. A., HOWELL, T., BAILEY, P., PARAISO, F., CLISSOLD, L., SIMMONDS, J., RAMIREZ-GONZALEZ, R. H., WANG, X., BORRILL, P., FOSKER, C., AYLING, S., PHILLIPS, A. L., UAUY, C. & DUBCOVSKY, J. 2017. Uncovering hidden variation in polyploid wheat. *Proceedings of the National Academy of Sciences,* 114**,** E913-E921.
14. LAIDIG, F., PIEPHO, H.-P., RENTEL, D., DROBEK, T., MEYER, U. & HUESKEN, A. 2017. Breeding progress, environmental variation and correlation of winter wheat yield and quality traits in German official variety trials and on-farm during 1983–2014. *Theoretical and Applied Genetics,* 130**,** 223-245.
15. LV, Q., LI, L., MENG, Y., SUN, H., CHEN, L., WANG, B. & LI, X. 2022. Wheat E3 ubiquitin ligase *TaGW2-6A* degrades *TaAGPS* to affect seed size. *Plant Science,* 320**,** 111274.

16. MOHAN, A., SCHILLINGER, W. F. & GILL, K. S. 2013. Wheat seedling emergence from deep planting depths and its relationship with coleoptile length. *PloS one,* 8**,** e73314-e73314.

17. MOORE, C. & REBETZKE, G. 2015. Genomic Regions for Embryo Size and Early Vigour in Multiple Wheat (*Triticum aestivum L.*) Populations. *Agronomy,* 5**,** 152-179.

18. PRIETO, P., OCHAGAVÍA, H., SAVIN, R., GRIFFITHS, S. & SLAFER, G. A. 2018. Dynamics of floret initiation/death determining spike fertility in wheat as affected by *Ppd* genes under field conditions. *J Exp Bot,* 69**,** 2633-2645.

19. QIN, L., HAO, C., HOU, J., WANG, Y., LI, T., WANG, L., MA, Z. & ZHANG, X. 2014. Homologous haplotypes, expression, genetic effects and geographic distribution of the wheat yield gene *TaGW2*. *BMC Plant Biology,* 14**,** 107.

20. RAMÍREZ-GONZÁLEZ, R. H.,BORRILL, P., LANG, D.,HARRINGTON, S. A., BRINTON, J., VENTURINI, L., DAVEY, M., JACOBS, J., VAN EX, F., PASHA, A., KHEDIKAR, Y., ROBINSON, S. J., CORY, A. T., FLORIO, T., CONCIA, L., JUERY, C., SCHOONBEEK, H., STEUERNAGEL, B., XIANG, D., RIDOUT, C. J.,UAUY,C. 2018.The transcriptional landscape of polyploid wheat. *Science (New York, N.Y.), 361*(6403), eaar6089.

21. REBETZKE, G. J., BRUCE, S. E. & KIRKEGAARD, J. A. 2005. Longer coleoptiles improve emergence through crop residues to increase seedling number and biomass in wheat (*Triticum aestivum L.*). *Plant and Soil,* 272**,** 87-100.

22. REBETZKE, G. J., RICHARDS, R. A., FETTELL, N. A., LONG, M., CONDON, A. G., FORRESTER, R. I. & BOTWRIGHT, T. L. 2007. Genotypic increases in coleoptile length improves stand establishment, vigour and grain yield of deep-sown wheat. *Field Crops Research,* 100**,** 10-23.

23. REYNOLDS, M. P., SLAFER, G. A., FOULKES, J. M., GRIFFITHS, S., MURCHIE, E. H., CARMO-SILVA, E., ASSENG, S., CHAPMAN, S. C., SAWKINS, M., GWYN, J. & FLAVELL, R. B. 2022. A wiring diagram to integrate physiological traits of wheat yield potential. *Nature Food,* 3**,** 318-324.

24. SAKUMA, S., GOLAN, G., GUO, Z., OGAWA, T., TAGIRI, A., SUGIMOTO, K., BERNHARDT, N., BRASSAC, J., MASCHER, M., HENSEL, G., OHNISHI, S., JINNO, H., YAMASHITA, Y., AYALON, I., PELEG, Z., SCHNURBUSCH, T. & KOMATSUDA, T. 2019. Unleashing floret fertility in wheat through the mutation of a homeobox gene. *Proceedings of the National Academy of Sciences,* 116**,** 5182-5187.

25. SAKUMA, S. & SCHNURBUSCH, T. 2020. Of floral fortune: tinkering with the grain yield potential of cereal crops. *New Phytologist,* 225**,** 1873-1882.

26. SANCHEZ-GARCIA, M., ROYO, C., APARICIO, N., MARTÍN-SÁNCHEZ, J. A. & ÁLVARO, F. 2013. Genetic improvement of bread wheat yield and associated traits in Spain during the 20th century. *The Journal of Agricultural Science,* 151**,** 105-118.

27. SIMMONDS, J., SCOTT, P., BRINTON, J., MESTRE, T. C., BUSH, M., DEL BLANCO, A., DUBCOVSKY, J. & UAUY, C. 2016. A splice acceptor site mutation in *TaGW2-A1* increases thousand grain weight in tetraploid and hexaploid wheat through wider and longer grains. *Theor Appl Genet,* 129**,** 1099-112.

28. SONG, X.-J., HUANG, W., SHI, M., ZHU, M.-Z. & LIN, H.-X. 2007. A QTL for rice grain width and weight encodes a previously unknown RING-type E3 ubiquitin ligase. *Nature Genetics,* 39**,** 623-630.

29. SU, Z., HAO, C., WANG, L., DONG, Y. & ZHANG, X. 2011. Identification and development of a functional marker of *TaGW2* associated with grain weight in bread wheat (Triticum aestivum L.). *Theoretical and Applied Genetics,* 122**,** 211-223.

30. UAUY, C., PARAISO, F., COLASUONNO, P., TRAN, R. K., TSAI, H., BERARDI, S., COMAI, L. & DUBCOVSKY, J. 2009. A modified TILLING approach to detect induced mutations in tetraploid and hexaploid wheat. *BMC Plant Biology,* 9**,** 115.

31. WADDINGTON., S. R., CARTWRIGHT, P. M. & WALL, P. C. 1983. A Quantitative Scale of Spike Initial and Pistil Development in Barley and Wheat. *Annals of Botany,* 51**,** 119-130.

32. WANG, W., SIMMONDS, J., PAN, Q., DAVIDSON, D., HE, F., BATTAL, A., AKHUNOVA, A., TRICK, H. N., UAUY, C. & AKHUNOV, E. 2018. Gene editing and mutagenesis reveal inter-cultivar differences and additivity in the contribution of TaGW2 homoeologues to grain size and weight in wheat. *Theoretical and Applied Genetics,* 131**,** 2463-2475.

33. WIERSMA, J. J., BUSCH, R. H., FULCHER, G. G. & HARELAND, G. A. 2001. Recurrent selection for kernel weight in spring wheat. *Crop Science,* 41**,** 999-1005.

34. WINTER D, VINEGAR B, NAHAL H, AMMAR R, WILSON GV & PROVART NJ .2007. An "Electronic Fluorescent Pictograph" Browser for Exploring and Analyzing Large-Scale Biological Data Sets. PLoS ONE 2(8): e718.

35. WÜRSCHUM, T., LEISER, W. L., LANGER, S. M., TUCKER, M. R. & LONGIN, C. F. H. 2018. Phenotypic and genetic analysis of spike and kernel characteristics in wheat reveals long term genetic trends of grain yield components. *Theoretical and Applied Genetics,* 131**,** 2071-2084.

36. XIE, Q. & SPARKES, D. 2021. Dissecting the trade-off of grain number and size in wheat. *Planta,* 254.

37. YANG, Z., BAI, Z., LI, X., WANG, P., WU, Q., YANG, L., LI, L. & LI, X. 2012. SNP identification and allelic-specific PCR markers development for *TaGW2*, a gene linked to wheat kernel weight. *Theoretical and Applied Genetics,* 125**,** 1057-1068.

38. YAO, F. Q., LI, X. H., WANG, H., SONG, Y. N., LI, Z. Q., LI, X. G., GAO, X.-Q., ZHANG, X. S. & BIE, X. M. 2021. Down-expression of *TaPIN1*s Increases the Tiller Number and Grain Yield in Wheat. *BMC Plant Biology,* 21**,** 443.

39. ZHAI, H., FENG, Z., DU, X., SONG, Y., LIU, X., QI, Z., SONG, L., LI, J., LI, L., PENG, H., HU, Z., YAO, Y., XIN, M., XIAO, S., SUN, Q. & NI, Z. 2018. A novel allele of *TaGW2-A1* is located in a finely mapped QTL that increases grain weight but decreases grain number in wheat (Triticum aestivum L.). *Theoretical and Applied Genetics,* 131**,** 539-553.

40. ZHANG, Y., LI, D., ZHANG, D., ZHAO, X., CAO, X., DONG, L., LIU, J., CHEN, K., ZHANG, H., GAO, C. & WANG, D. 2018. Analysis of the functions of *TaGW2* homoeologs in wheat grain weight and protein content traits. *The Plant Journal,* 94**,** 857-866.

41. ZHAO, B., WU, T. T., MA, S. S., JIANG, D. J., BIE, X. M., SUI, N., ZHANG, X. S. & WANG, F. 2020. *TaD27-B* gene controls the tiller number in hexaploid wheat. *Plant Biotechnology Journal,* 18**,** 513-525.

3. The effect of the *GW2* mutations on TGW and yield in wheat cultivars Reedling and Kingbird across contrasting environments.

3.1. Chapter summary

In this chapter, we compared the effect of the *gw2* mutant alleles in two wheat cultivars with contrasting grain size (Reedling, large grain size; Kingbird, small grain size), in contrasting field environments (Irrigation, Heat Stress and Drought) grown in CIMMYT's Norman E. Borlaug Experimental Station in the Yaqui Valley, in Mexico. We found contrasting effects, with the *gw2* mutant alleles having a positive effect on TGW, yield and spike yield components in Kingbird, while in Reedling the effect was either non-significant or detrimental. This suggests that the *gw2*-mediated mechanism for increased grain size is genotype dependant. Furthermore, we found that Heat Stress and Drought reduced yield by an average of 50 % and 72%, respectively, when compared to irrigation.

3.2. Introduction

In chapter 2, we described the contribution of the *gw2* mutant alleles on increasing grain weight and size in cv. Paragon NILs across three growing seasons in a fully irrigated environment in the United Kingdom. In this chapter, we investigated whether the introduction of the mutant alleles would also be beneficial in the two CIMMYT spring wheat cultivars (Kingbird and Reedling), with contrasting grain size phenotypes across different environments. The reasoning behind this is that wheat is a crop that is grown worldwide in a plethora of different environments. Therefore, it is exposed to different abiotic stresses and diseases that can cause final yield production to drop, and the phenology of the plant can vary largely dependent on the target environment. Optimal temperatures for wheat growth and development have been defined between 17 °C to 23 °C , while above 30 °C floret sterility occurs and grain filling and starch deposition are seriously compromised (Altenbach, 2012).

Climate change, which refers to shifts in temperatures and novel weather patterns, are challenging the adaptability of wheat across many growing regions. According to the NOAA National Centres for Environmental Information (NOAA, 2020), temperatures have been constantly increasing since preindustrial times, while the IPCC (Intergovernmental Panel on Climate Change) predicted that average world temperatures will rise by 1.5 °C degrees in the next two decades (Reynolds et al., 2021b). For wheat, the average global yield is predicted to drop by $6.0 \pm 2.9\%$ for every 1 °C increase in temperature (Zhao et al., 2017). Sukumaran et al. (2018) found that yield dropped 11% for every 1 °C increase in temperature in a durum panel grown under heat stress in CIMMYT experimental field in Mexico. Ortiz-Monasterio R et al. (1994), found that yield, thousand grain weight (TGW) and seed per m² are compromised when mean temperatures rise between 20 days before heading and 10 days after heading. The timing and type of stress will also have an impact on the damage to the crop, e.g., if drought occurs at sowing time, poor emergence is expected. It was found that flowering time is the most susceptible stage while terminal drought

can lead to low harvest index and yield losses (Langridge and Reynolds, 2021). Moreover, extreme climatological conditions like extreme heat and flood can happen simultaneously across the Northern Hemisphere in areas known as breadbasket regions causing up to 11% reductions of crop output (Kornhuber et al., 2020). Overall, major yield losses are due to drought and heat at critical developmental points during wheat life cycle (Snowdon et al., 2021). In the latest FAO report, climate change was listed as one of the main factors that will cause food insecurity (FAO, 2021).

Despite the changing temperatures and rain regimens, wheat has the genetic potential to tolerate drought, heat stress or the combination of both (Langridge and Reynolds, 2021). Furthermore, advances in phenotyping, data analysis, bioinformatics and genome editing technologies can accelerate genetic gains (Langridge et al., 2021). Breeding for wheat varieties capable of adapting to extreme weather conditions like drought can be achieved by selecting for lines with higher yields in a water-limited context as it is assumed that this will combine the most favorable traits (Richards et al., 2010). Likewise, testing cultivars in multi- environments trials can help identify those cultivars which combine traits which make them resilient. As in the foreseeable future severe drought and heat will be more common and not the exception Lobell et al. (2011), urgent actions must be taken to tackle yield loses due to the reasons mentioned above.

The desert conditions in Obregon with almost no rainfall during the cropping season enables screening for future extreme weather scenarios. These include complete drought stress, drought stress in specific growth stages (achieved using controlled drip irrigation), early or terminal heat stress by an alternation of planting dates and fully irrigated plots. Moreover, the setting allows to verify whether water saving technologies like drip irrigation can be applied to agriculture as a strategy to address the problem of water scarcity due to climate change (Patra et al., 2021). Our aim for this chapter was to understand if the *gw2* alleles increase grain weight and grain morphometrics not only in different cultivars but also in different environments than that of the UK rainfed environment. Here we presented field studies where final yield, TGW and yield components were measured from cv Kingbird and cv Reedling NILs across two seasons 2019 -2022 grown under irrigation, drought and heat stress environments.

3.3. Material and Methods
3.3.1. Plant material and growing conditions

gw2-A1 single mutants
In 2014, two sets of *gw2-A1* single mutant NILs in CIMMYT cultivars Reedling and Kingbird were developed by James Simmonds. Each pair or NILs (wildtype and *gw2-A1* allele) comprised of four sister lines. The *gw2-A1* mutant allele came from durum wheat cv Kronos (described in chapter 2) and the cultivars were tested with specific KASP markers (Simmonds et al., 2016) to confirm the presence of the *gw2-A1* mutant allele in the NILs. After three backcrosses, the BC$_3$ NILs were sent to CIMMYT's Norman E. Borlaug Experimental Station (CENEB) in the Yaqui Valley, Ciudad Obregon, Sonora, Mexico (27°24′ N, 109°56′ W, 38 masl). In 2018, the lines were grown

under four different treatments in randomized complete block designs, each comprising six replicates per genotype giving a total of 48 plots (24 plots per genotype) in 2m x 1m plots.

The treatments were as follows:

- **Irrigation**: Surface irrigation with water distributed evenly by gravity across the terrain. Plants were sown on 30th of November 2018 and harvested on the 26th of April in 2019. Irrigation was conducted for 11 hours every 30 days until maturity giving a total of five irrigation events across the cycle. The average temperature was 20 °C during daytime and 17°C during night-time.

- **Drought**: Seeds were sown on the 3rd of December of 2018 and irrigation was carried out twice, once before sowing on the 17th of November of 2018 and after sowing on the 5th of February of 2019. Surface irrigation is performed by gravity flow to the surface of the field. The average temperature was 20 °C /17 °C during night-time

- **Drip irrigation**: Water drips to the base of the plants from above the soil through a system of tubes. Seeds were sown and harvested on the same dates as drought. Irrigation was conducted twice after sowing on the 8th of December and on the 5th of February. The average temperature was 20 °C /17 °C during night-time.

- **Heat Stress**: High temperatures were achieved by a late sowing on the 28th of January 2019 and a harvest date of 30th of May 2019. The average temperatures in the heat stress treatment were 23 °C max and 15 °C min and water was applied all along the life cycle of the crop every 30 days (for 11 hours) until harvest. Note that grain morphometrics from this environment are not available for either cultivar.

gw2 triple mutants

In 2017, *gw2* triple mutants NILs were developed by James Simmonds at the John Innes Centre in both cultivars as follows:

- The Reedling *gw2* triple mutant NILs were developed by crossing Reedling GW2 wildtype plants with a Paragon (BC$_3$F$_1$) heterozygous for all three alleles. F$_1$ plants heterozygous (*GW2/gw2*) for all three homoeologs were backcrossed to Reedling and this backcrossing cycle was repeated two more times. At the BC$_3$F$_1$ stage, plants were self-pollinated to generate BC$_3$F$_2$ seeds which were sown to select for the BC$_3$F$_2$ Reedling triple *GW2* wildtype NIL and the Reedling triple *gw2* mutant NIL.

- The Kingbird NILs *gw2* triple mutant were generated as above but by crossing and backcrossing to cultivar Kingbird.

Seeds from both pairs of NILs, were sent in 2020 to the CIMMYT experimental field where they were sown in irrigation plots only for seed bulking.

In 2021, the two sets of triple mutant and triple wildtype NILs (Reedling and Kingbird background) were sown in the same four contrasting environments described above. Briefly, eight genotypes (2 *GW2* alleles * 4 sister lines) with two replicates in Kingbird were grown (16 plots per environment), while in Reedling six genotypes (2 *GW2*

alleles * 3 sister lines) with two replicates were sown (twelve plots per environment). The field was managed as followed:

- **Irrigation**: Plants were sown on the 24th of November 2021 and harvested on the 4th of May of 2022. During the growing season, the plots were irrigated seven times for 11 hours, at 15 days intervals.

- **Drought**: Plants were sown on the 16th of December of 2021 and harvested on the 24th of May of 2022. The field was irrigated three times at 30 days intervals. The data for Kingbird is not available for this environment due to damage suffered by accidental herbicide spraying of the plots.

- **Heat Stress:** Plants were sown on the 3rd of March of 2022 and harvested on the 16th of June of 2022. The field was irrigated six times for 11 hours at 15 days intervals until maturity.

3.3.2. *Phenotyping measurements*

Thousand grain weight and grain morphometrics (grain width and grain length) were taken using a SeedCount - Model SC5000 (Next Instruments, Australia), measuring the harvested grain samples from each of the plots. Developmental traits (phenology) were measured as follow:

- *Days to heading*: days from sowing until 75% of the plot had visible spikes

- *Days to flowering*: days from sowing until the 75% of the plot had visible yellow anthers

- *Days to maturity*: days from sowing until 75% of the plot reaches maturity (complete yellowing of the spike)

- *Crop height*: total length of individual culms from the soil surface to the tip of the spike excluding awns taken 14 days after anthesis.

- *Harvest Index*: Thirty randomly selected culms were cut at maturity at the base of the stem, each spike was removed at the spike collar from the stem and separately stored in labelled paper bags (30 stems and 30 spikes per plot). The samples were dried at constant heat (75 °C) overnight to remove most of the water content. After 24 hours all the samples were weighed, and the spikes were threshed. The grains were stored in small paper bags and left to dry for 24 hours at (75 °C) and weighed for thousand-grain weight (TGW). Harvest Index (HI) was calculated as:

$$HI = \left(\frac{Grain\ weight}{Weight\ of\ total\ biomass} \right) * 100$$

Spike yield components

Spike yield components were taken from ten main spikes coming from the field plots and were measured as follows:

- *Spikelet number per spike*: Ten randomly selected main spikes per plot were collected and the total number of spikelets were counted.

- *Viable spikelets*: the number of spikelets containing grains across the spike

- *Seed number per spike*: total number of grains coming from a single spike

- *Spike yield:* total seed weight per individual spike

- *Seeds per spikelet:* ratio between seed number and spikelet number

- *Height:* total length of individual culms from the soil surface to the tip of the spike excluding awns taken 14 days after anthesis.

DNA extraction and KASP genotyping

DNA extraction and Kompetitive Allele Specific Polymerase Chain Reaction (KASP) genotyping were performed as previously described (Pallotta et al., 2003b, Trick et al., 2012). Briefly, leaf samples from 14 days old seedlings were collected and carefully placed on a 96 DNA tray and stored at -4 °C until the DNA extraction was conducted. Once extracted, KASP markers were tested for the *gw2* homoeologs (Wang et al., 2018; Table 3.1) assays were performed in a 384 well plate , 2.5 µL of DNA, 2.5 µL of KASP master mix (LGC, UK) and 0.07 µL of primer mix to a total volume of 5.07 µL. PCR was performed on an Eppendorf Mastercycler pro 384 using the following protocol: Hotstart at 95 °C for 5 min, ten touchdown cycles (95 °C for 20 s; touchdown 65 °C, −1 °C per cycle, 25 s) followed by 40 cycles of amplification (95 °C 10 s; 57 °C 60 s). Plates were read using PHERAstar FSX and genotype data was visualized with the KlusterCaller™ genotyping software (LGC, UK).

Table 3-1: KASP *gw2* primers sequence used in this study The black letters are target specific primers, the blue and red letters are common tails for FAM and HEX fluorescent signal respectively.

Allele	Amplified region	Primer Name	Primer Sequence (5'-3')
KASPar-*TaGW2-A*	G2373A SNP	TaGW2_A_WT_FAM	GAAGGTGACCAAGTTCATGCTGCTTCAATGACTTTCTGTTCTTCc
		TaGW2_A_M_HEX	GAAGGTCGGAGTCAACGGATTGCTTCAATGACTTTCTGTTCTTCt
		TaGW2_A_C	AGAGCAATTTGTAAGTCTTATTCC
KASPar-*TaGW2-B*	C2504T SNP	TaGW2_B_WT_FAM	GAAGGTGACCAAGTTCATGCTCTCCAACAACAGAAGTGGAGTAc
		TaGW2_B_M_HEX	GAAGGTCGGAGTCAACGGATTCTCCAACAACAGAAGTGGAGTTt
		TaGW2_B_C	GTAAGTTATCAGATTAAGCTACAGG
KASPar-*TaGW2-D*	G7139A SNP	TaGW2_D_WT_FAM	GAAGGTGACCAAGTTCATGCTCATGATGGTTATGGAAGCGATTg
		TaGW2_D_M_HEX	GAAGGTCGGAGTCAACGGATTCATGATGGTTATGGAAGCGATTa
		TaGW2_D_C	GAAAACAATTTGATCCAACAAGTCA

3.3.3. Statistical analyses

The statistical analyses were carried out with R studio 1.4.11 and the package lme4 1.1. A mixed effects model was fitted for each of the response variables (e.g., TGW, seed width, seed length, yield, and phenology) with mutation and genotype as fixed effects. The P values for explanatory variables in individual models refer to those computed by the ANOVA. Percentage difference data refer to the estimated marginal means deriving from the same models. Each environment was analysed separately in both 2019 and 2022. Field data from 2020 is missing due to the COVID-19 pandemic, which made both the sowing and data collection challenging, while in 2021 the *gw2* triple mutants were sent only for seed bulking. Data from Kingbird in drought is not available for 2022, while the irrigated plots both in Kingbird and Reedling were damaged by herbicide application.

3.4. Results

In this section, we will present the field results from 2019 of the *gw2-A1* single mutant NILs (*aaBBDD*) and the 2022 results from the *gw2* triple mutant NILs (*aabbdd*) in three contrasting environments grown at the CIMMYT Experimental Station, Norman E. Borlaug (CENEB) in the Yaqui Valley, Ciudad Obregon, Sonora, Mexico.

3.4.1. Thousand grain weight and yield do not increase in the single gw2-A1 mutants across environments and genotypes

We hypothesize that the introgression of the *gw2-A1* allele in both Reedling and Kingbird will increase TGW. Furthermore, we wanted to test the effect of the mutant allele under four contrasting environments: irrigation, drip, drought and heat stress. We conducted a two-way ANOVA considering the interaction between genotype and mutation for each environment. We found that the introgression of the *gw2-A1* single mutant did not translate into increases in TGW in Irrigation, DRIP and drought (Figure 3.1, Figure 3.2, Figure 3.3) except for Kingbird NILs in Heat Stress where a 3.46% increase was found (Figure 3.4). Concerning yield, across all environments a non-significant effect was found except in Reedling NILs in drought where yield dropped significantly by 29% ($P < 0.05$) (Figure 3.3). These results were unexpected based on what was previously reported by (Wang et al., 2018, Simmonds et al., 2016) who found TGW increases of 6% under glasshouse and field experiments for both Kronos and Paragon single mutant NILs.

These findings agree with the results from Chapter 2, where the single mutant Paragon NIL only increased TGW in 2019 by 5.2%, and without any effect on final yield. We can hypothesise that the contribution of the single *aa* mutant allele is background dependent and environmentally unstable. (Simmonds et al., 2016) found increases in TGW in both Kronos and Paragon single mutants in UK and California under irrigated conditions and in glasshouse experiments. Glasshouse experiments however do not necessarily reflect how a cultivar and an allele will interact in field conditions. As TGW and grain morphometrics were found to be non-significantly affected in the single mutants and in order to test the contribution of the triple *gw2* mutants on both cultivars across different environments, in the next section, we will analyse the data from the *gw2* triple mutant in 2022.
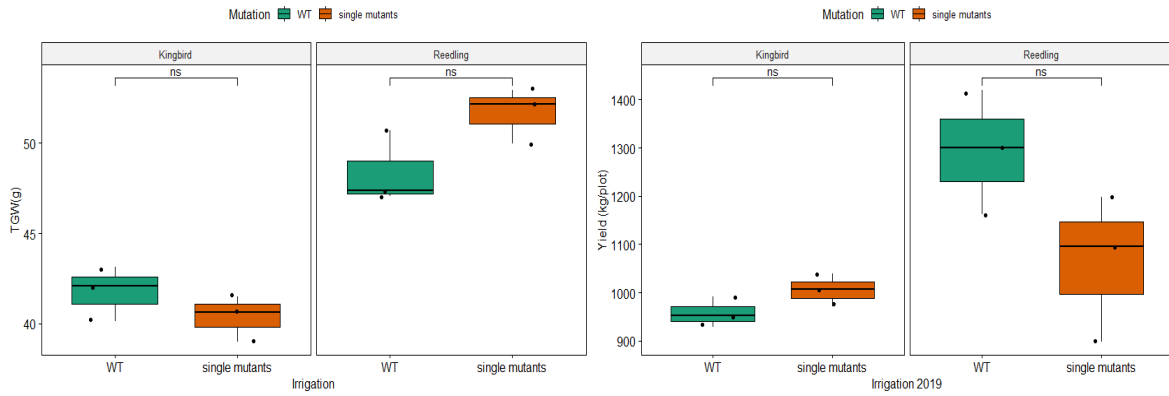
Figure 3-1: TGW and yield in WT and single mutants Kingbird and Reedling under irrigation in 2019. The box represents the middle 50% of data with the borders of the box representing the 25th and 75th percentile. The horizontal line in the middle of the box represents the median. Whiskers represent the minimun and maximum values, unles a point exceeds 1.5 times the interquartile range in which case the whisker represents this value and values beyond this are plotted as single points (outliers). Statistical classifications are based on Tukey's HSD tests. ns:P>0.05
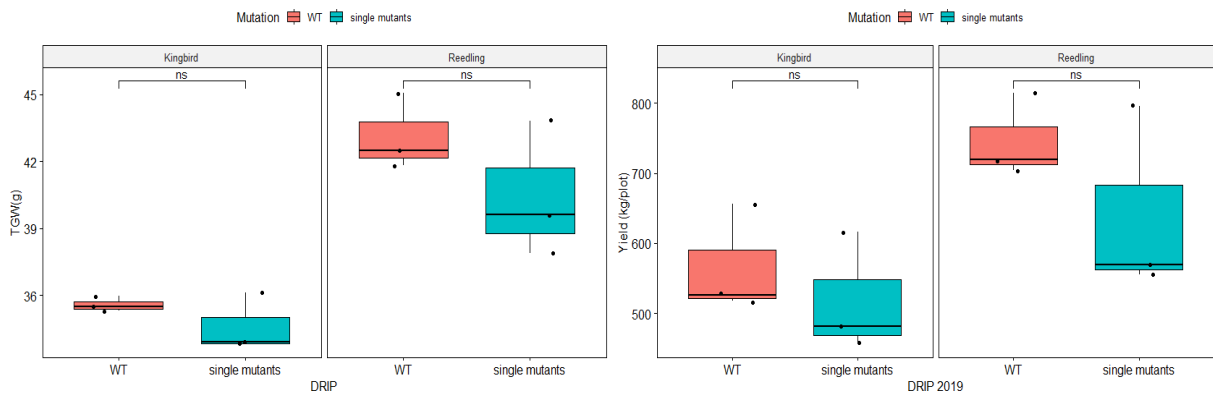
Figure 3-2: TGW and yield in WT and single mutants Kingbird and Reedling at DRIP in 2019. The box represents the middle 50% of data with the borders of the box representing the 25th and 75th percentile. Statistical classifications are based on Tukey's HSD tests. ns: *P* > 0.05.
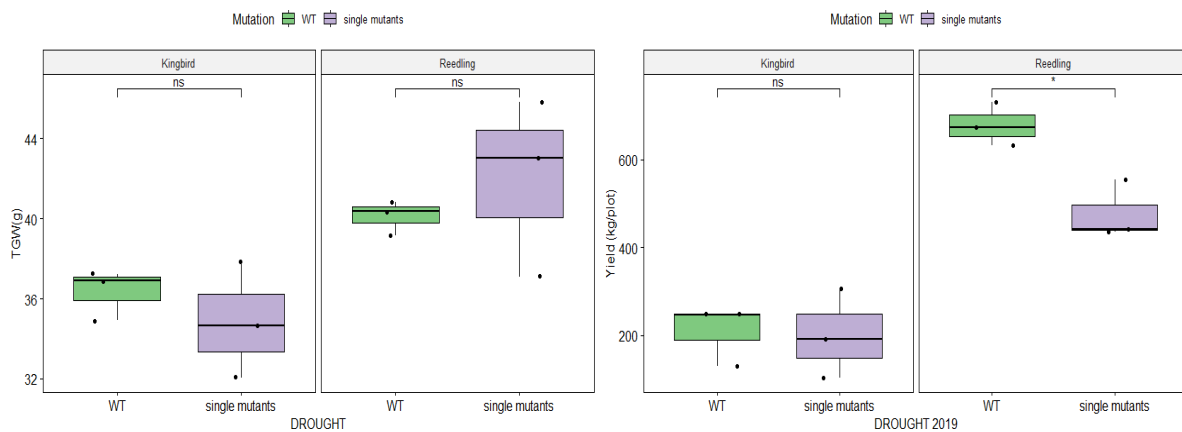
Figure 3-3: TGW and yield in WT and single mutants Kingbird and Reedling in drought during 2019. The box represents the middle 50% of data with the borders of the box representing the 25th and 75th percentile. Statistical classifications are based on Tukey's HSD tests. ns: P > 0.05; * P < 0.05.
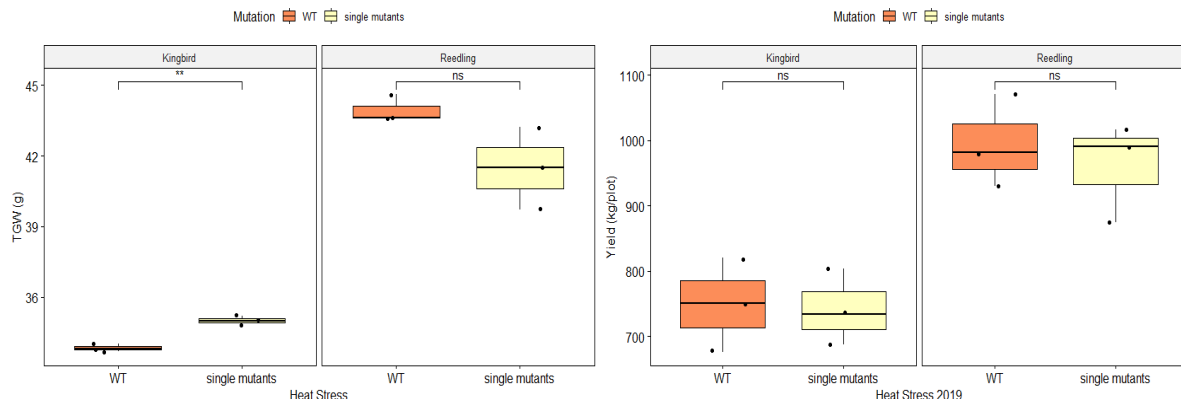
Figure 3-4: TGW and yield in WT and single mutants Kingbird and Reedling in heat stress during 2019. The box represents the middle 50% of data with the borders of the box representing the 25th and 75th percentile. Statistical classifications are based on Tukey's HSD tests. ns: P > 0.05; ** *P* < 0.01.

Table 3-2: Mean of phenology, thousand grain weight (TGW), grain morphometrics and Yield of Kingbird NILs in Irrigation, DRIP, drought and Heat Stress. Means are from biological replicates per year (N=24), Delta values (%) vs WT. DTH: Days to Heading, DTA: Days to anthesis, DTM: Days to maturity, HI: Harvest Index, TGW: Thousand Grain Weight.

KINGBIRD 2019

	Irrigation				DRIP				Drought				Heat Stress			
Trait	WT	single mutants	Delta (%)	Tukey P values (vs WT)	WT	single mutants	Delta (%)	Tukey P values (vs WT)	WT	single mutants	Delta (%)	Tukey P values (vs WT)	WT	single mutants	Delta (%)	Tukey P values (vs WT)
DTH	68±1.73	60.66±0.33	-10.78	0.001	63±0.57	55.6±0.33	-11.65	<0.001	67.33±0.33	59±0.00	-12.38	<0.001	64.33±0.66	66.33±1.33	3.11	0.07
DTA	72±1	66±0.0	-8.33	0.001	66.33±0.3	60±1.0	-9.54	<0.001	70.66±0.33	65±0.00	-8.02	<0.001	69.66±0.33	71.66±1.76	2.87	0.157
DTM	121±1	120.33±0.88	-0.55	0.56	104±1.15	102.33±0.3	-1.61	0.46	108.66±2.18	106±0	-2.45	0.130	NA	NA	NA	NA
Height (cm)	91±1.25	84.5±0.88	-7.14	0.03	77.16±1.09	77.5±1.75	0.44	0.94	63.33±4.70	64.66±2.84	2.11	0.6812	91±1	82.33±3.17	-9.52	NA
HI	0.485±0.01	0.519±0.0	6.89	0.049	0.518±0.03	0.500±0.01	-3.53	0.48	0.501±0.3	0.531±0.6	4.59	0.0140	0.483±0.009	0.51±0.01	7.56	NA
Grain Length (mm)	6.14±0.02	6.13±0.05	-0.05	0.10	6.05±0.02	6.18±0.02	2.2	0.59	6.08±0.01	6.19±0.03	1.81	0.580	NA	NA	NA	NA
Grain width (mm)	3.36±0.02	3.32±0.02	-0.99	0.58	3.14±0.01	3.15±0.02	0.32	0.56	3.14±0.02	3.14±0.06	0	0.874	NA	NA	NA	NA
TGW (g)	41.77±0.8	40.38±0.7	-3.33	0.93	35.58±0.19	34.61±0.75	-2.73	0.02	36.35±0.71	34.84±1.6	-4.14	0.150	33.83±0.6	35±0.9	3.46	0.01
Yield (kg/plot)	957.36±18.14	1005.73±19.8	5.05	0.07	566.66±44.72	518±49.5	-8.59	0.88	209.3±39.6	200.6±58.47	-4.14	1	748.66±41.5	742±33.72	-0.89	0.5

Table 3-3: Mean of phenology, thousand grain weight (TGW), grain morphometrics and Yield of Reedling NILs in Irrigation, DRIP, drought and Heat Stress. Means are from biological replicates per year (N=24), Delta values (%) vs WT. DTH: Days to Heading, DTA: Days to anthesis, DTM: Days to maturity, HI: Harvest Index, TGW: Thousand Grain Weigh

REEDLING 2019

Trait	Irrigation				DRIP				Drought				Heat Stress			
	WT	single mutants	Delta (%)	Tukey P values (vs WT)	WT	Single mutants	Delta (%)	Tukey P values (vs WT)	WT	single mutants	Delta (%)	Tukey P values (vs WT)	WT	single mutants	Delta (%)	Tukey P values (vs WT)
DTH	78.33±0.66	70.33±0.33	-10.21	**<0.001**	73.33±0.33	64±0	-12.73	<0.001	75.66±0.33	68.33±0.33	-9.692	<0.001	76.33±0.66	63.66±0.88	-16.59	<0.001
DTA	83.66±1.33	74±0.57	-11.54	**<0.001**	76±0.5	67±0	-11.84	<0.001	79.33±0.33	71.33±0.33	-10.084	<0.001	81.33±1.21	69±0.57	15.16	<0.001
DTM	123±1	120.33±0.88	-2.16	0.05	114.66±1.33	112.66±2.02	-1.74	0.37	116.33±0.33	114±0.5	-2.0	0.17	NA	NA	NA	NA
Height	122.16±2.16	102.33±1.45	-16.23	<0.001	97.5±3.8	82.33±4.6	-15.56	0.01	83.33±1.85	78.33±0.33	-6	0.15	106.33±2.18	105.33±3.17	-0.94	0.2
HI	0.454±1.45	0.473±2.16	4.11	0.21	0.471±0.01	0.511±0.03	8.57	0.14	0.468±0.06	0.492±0.07	5.22	0.01	0.489±0.09	0.503±0.03	2.99	0.5
Grain Length (mm)	6.45±0.04	6.51±0.09	0.82	0.008	6.40±0.01	6.43±0.03	0.47	0.17	6.28±0.05	6.44±0.05	2.54	0.05	NA	NA	NA	NA
Grain width (mm)	3.58±0.02	3.65±0.02	2.047	0.033	3.40±0.04	3.28±0.06	-3.53	0.22	3.33±0.02	3.31±0.07	-0.60	0.81	NA	NA	NA	NA
TGW (g)	48.363±1.16	51.67±0.88	6.837	0.17	43.12±1.75	40.44±0.9	-6.22	0.50	40.113±0.49	41.96±2.51	4.61	0.49	41.6	43.9	5.52	0.6
Yield (kg/plot)	1293.6±74.26	1063.8±87.98	-17.759	0.003	746±34.31	640.66±77.77	-14.12	0.11	678.66±28.38	477.33±38.37	-29.666	0.008	994±40.85	960±43.65	-3.42	0.8

3.4.2. Heading, flowering time and height are significantly different in the single *aa* mutants without yield gains.

We hypothesize that the statistically significant differences in heading and flowering time on the single *aa* mutants in both cultivars and across all environments (apart from Kingbird in heat stress) will result in increases in TGW and yield (Table 3.2 and Table 3.3; (Arjona et al., 2020). Although the grain filling period is extended by ~ 8 to 10 days in the mutants, that does not translate into yield gains. The WT plants flowers on an average of 8-15 days later (except for heat stress), but both genotypes reach maturity around the same days. Lastly, we found that the NILs carrying the single allele were significantly shorter than the WT mainly in irrigation and Heat Stress (Table 3.4 and Table 3.5). In contrast, in cv. Paragon which carries WT *RHT1* alleles, we found no significant differences in height across years and mutations. This raises the question as to whether the *gw2* mutants and the semi-dwarf *RHT-B1b* allele (present in Kingbird and Reedling) have a significant genetic interaction which causes a significant reduction on height when combined. We are going to explore this idea in Chapter 4.

3.4.3. Thousand grain weight, grain morphometrics and yield increases in Kingbird gw2 triple mutants but not in Reedling across all environments

In the next section, we are going to analyse the *gw2* triple mutants lines from both Kingbird and Reedling NILs. Each environment irrigation, heat stress and drought were analysed separately as the effect of the triple mutants was found to be significant in most of the evaluated parameters.

Irrigated trials

To understand the effect of the *gw2* triple mutants on TGW across both cultivars, firstly, we conducted irrigated trials as our control environment. Using a three-way ANOVA, we found that the interaction between Mutation and Genotype was significant ($P < 0.0001$) for the response variables TGW, grain width and yield (Figure 3.5). We found that TGW increased by 9.8% ($P < 0.001$, 34.2 vs 31.1), width by 7.49% ($P < 0.0001$, 3 mm vs 3.35 mm) and final yield by 37.94% ($P < 0.0001$; 444 kg/plot vs 322 kg/plot) in Kingbird triple mutants under irrigation plots (Figure 3.5 and Table 3.4). On the other hand, TGW and grain morphometrics were found to be non-significant in Reedling triple mutants when compared to the controls. These results were unexpected, based on what we found in Paragon triple mutants – where we saw significant increases in grain size with minor negative effects on yield (Chapter 2). We found a significant yield decrease of 15.3% ($P < 0.01$; 786 kg/plot vs 666 kg/plot) in Reedling *gw2* triple mutants but, neither TGW nor grain width/length increased. These contrasting results indicate that the effect of the *gw2* mutant alleles is perhaps dependent of the genetic background, or that it could be affected by environmental conditions. To further assess this, we examined the other tested environments (heat stress and drought) to see if our results are consistent with what we found in this section.
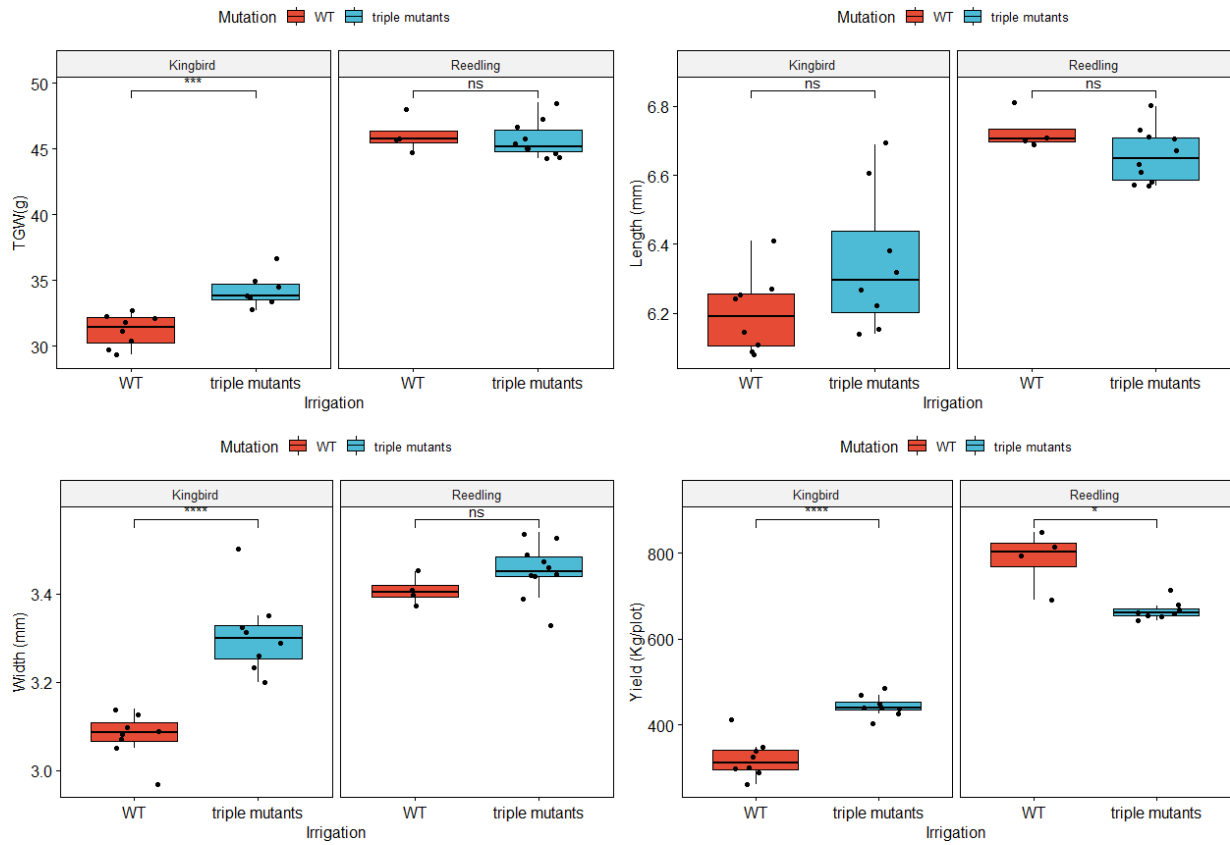
Figure 3-5: TGW, length, width and yield in Kingbird and Reedling in irrigation, the box represents the middle 50% of data with the borders of the box representing the 25th and 75th percentile. Statistical classifications are based on Tukey's HSD tests. ns: P>0.05; *P<0.05; ***P<0.001; **** P<0.0001.

Heat Stress trials

Consistent with what we found in irrigation; Kingbird responded differently to Reedling. In Kingbird, TGW increased significantly by 11% (P < 0.006), grain length by 2.3% (P < 0.023) and grain width by 8.2% (P < 0.04), which translated into increases in yield of 24.3% (P < 0.006) in the *gw2* triple mutants (Figure 3.6, Table 3.4). In Reedling, consistent with what we found under irrigation (Figure 3.5) and in the single *aa* mutants under heat stress (Figure 3.4), TGW and length did not increase, while width increased significantly (P <0.021) by 4.8% and yield decreased significantly (P <0.003) by 17.2%. The primary effect of *GW2* is on grain width, which was significantly increased in Reedling. However, the magnitude of the effect was subtle (4.8 %) when compared to the increases in Paragon (20%,Wang et al. (2018)) and Kingbird (8.2%). This could explain the non-significant effects on TGW, and grain length observed under heat stress and the irrigation trials.
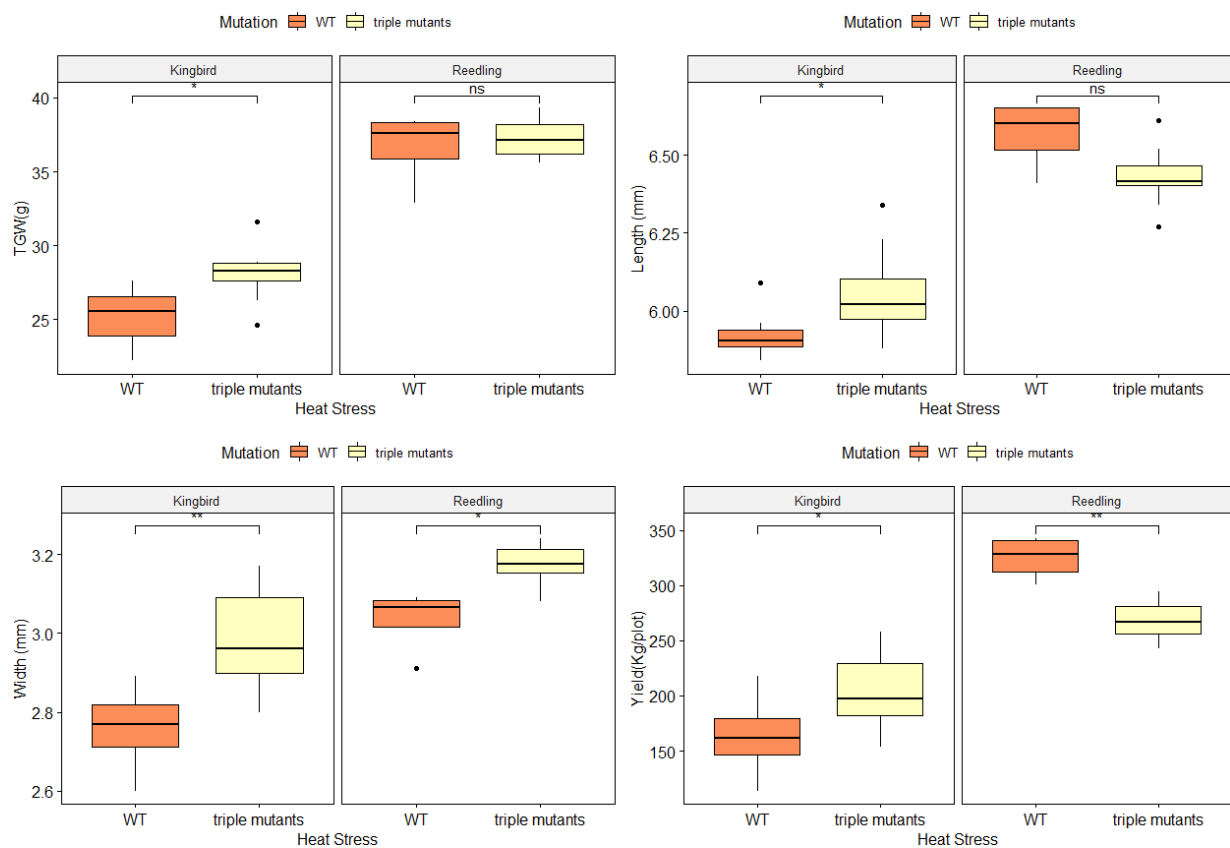
Figure 3-6: TGW, length, width and yield in Kingbird and Reedling in heat stress plots, the box represents the middle 50% of data with the borders of the box representing the 25th and 75th percentile. Statistical classifications are based on Tukey's HSD tests. ns: P>0.05; *P<0.05; **P<0.01.

Drought trials

We will only analyse Reedling data in this section due to herbicide damage to the Kingbird trials. In drought trials, we found once more that the *gw2* allele had no effect on TGW or length, but increased grain width significantly by 4.4% (P < 0.004) in a Reedling background. As seen earlier, the positive effect of width did not translate into yield gains in drought trials in cv Reedling. Next, we investigated spike yield components hoping to understand why the introgressions of the *gw2* mutant alleles are not beneficial in Reedling.
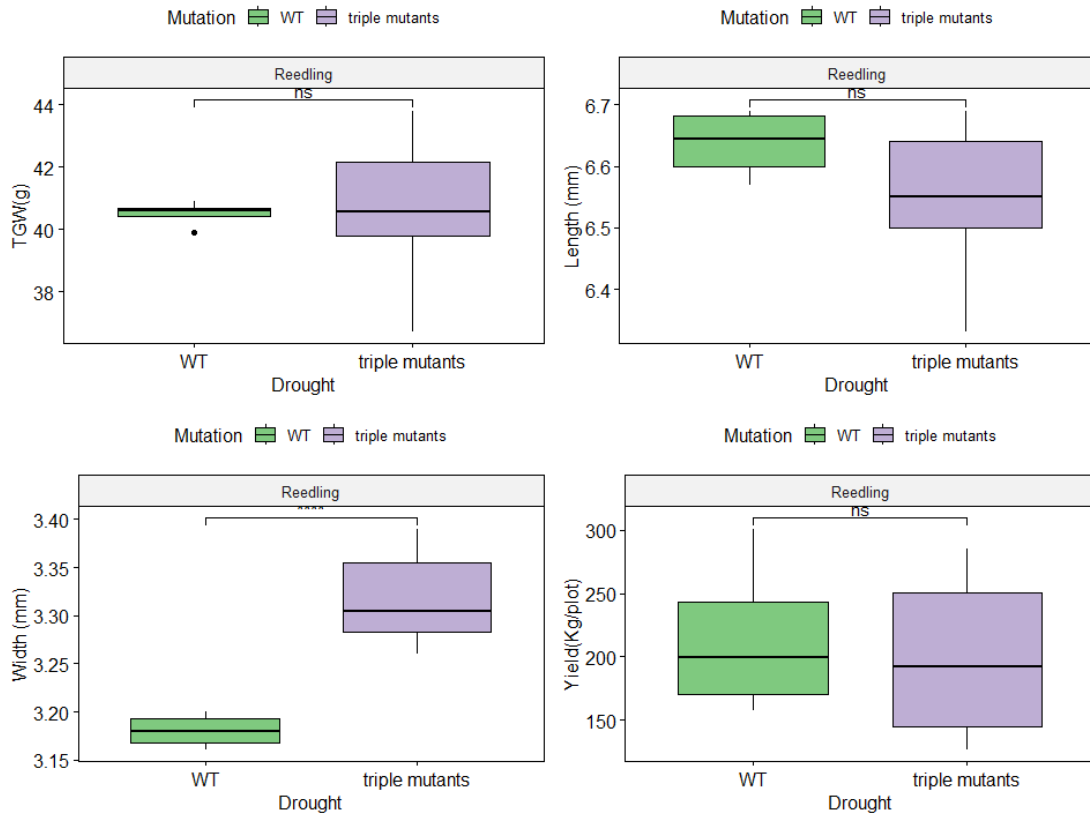
Figure 3-7: TGW, length, width and yield in Reedling in drought field trials, the box represents the middle 50% of data with the borders of the box representing the 25th and 75th percentile. Statistical classifications are based on Tukey's HSD tests. ns: P>0.05; **** P<0.0001.

Table 3-4: Mean of phenology, thousand grain weight (TGW), grain morphometrics and yield of Kingbird NILs in Irrigation and Heat Stress. Means are from biological replicates per year (N varies per year), Delta values (%) vs WT.

Kingbird 2022

Trait	Irrigation (damaged by herbicide)				Heat Stress			
	WT	triple mutants	Delta (%)	Tukey P values (vs WT)	WT	triple mutants	Delta (%)	Tukey P values (vs WT)
Yield	321.875±0.44	444±0.49	37.94	<0.001	163.83±0.8	203.56±0.71	24.25	0.009
Seed length	6.195±0.04	6.345±0.07	2.42	0.035	5.92±0.02	6.06±0.05	2.36	0.023
Seed width	3.075±0.01	3.35±0.03	7.49	<0.001	2.75±0.03	2.98±0.04	8.17	0.04
TGW	31.175±0.44	34.22±0.49	9.79	<0.001	25.27±0.68	28.11±0.71	11.22	0.006
HI	0.275±0.01	0.368±0.0	33.33	<0.001	0.434±0.00	0.435±0.00	0	0.928
Biomass	1210.55±77.25	1210.37±32.53	-0.01	0.99	375.33±20.66	465.12±2.46	23.92	0.002
Grain Number/m^2	10305.12±439	12548.55±526	21.77	0.006	6476.54±383	7211.02±329.8	11.34	0.099
Tiller Number	321.62±26.73	297.12±14.30	-7.62	0.29	213.33±9.6	234.63±6.8	9.98	0.16
Grain Per Spike	33.25±2.34	42.55±1.38	27.82	<0.001	30.36±1.2	30.71±0.9	1.15	0.87
Grain Weight Spike	1.03±0.06	1.535±0.06	48.19	<0.001	0.76±0.04	0.86±0.04	13.82	0.24
Days To Heading	74.5±0.32	70.875±0.22	-4.87	<0.001	52.625±0.77	50.375±0.53	-4.28	0.01
Days To Anthesis	79.5±0.32	75.875±0.22	-4.56	<0.001	55.625±	53.375±	-4.04	0.01
Days To Maturity	NA	NA	NA	NA	78.5±0.94	75.87±0.39	-3.35	0.01
Height	103±1.25	91.125±1.25	-11.52	<0.001	65.25±1.10	58.6±1.10	-10.19	0.008
Spikelet number	21.52±0.32	20.95±0.29	-2.64	0.15	17.08±0.33	17.6±0.24	-2.95	0.22
Viable Spikelets	20.06±0.24	19.18±0.24	-4.38	0.02	16.06±0.32	16.02±0.24	-0.25	0.93

Table 3-5: Mean of phenology, thousand grain weight (TGW), grain morphometrics and yield of Reedling NILs in Irrigation, Heat Stress and Drought. Means are from biological replicates per year (N varies per year), Delta values (%) vs WT.

	Reedling 2022											
	Irrigation (damage by herbicide)				**Heat Stress**				**Drought**			
Trait	**WT**	**triple mutants**	**Delta (%)**	**Tukey P values (vs WT)**	**WT**	**triple mutants**	**Delta (%)**	**Tukey P values (vs WT)**	**WT**	**triple mutants**	**Delta (%)**	**Tukey P values (vs WT)**
Yield	786±0.69	666±0.43	-15.27	1.05E-05	325.1±1.28	269.24±0.38	-17.18	0.003	214±0.21	197.4±0.62	-7.76	0.639
Seed length	6.72±0.02	6.65±0.02	-1.04	0.3879	6.56±0.05	6.43±0.02	-1.98	0.054	6.63±0.02	6.55±0.03	-1.21	0.215
Seed width	3.40±0.01	3.45±0.01	1.34	0.2588	3.03±0.04	3.173±0.016	4.72	0.021	3.18±0.00	3.318±0.01	4.34	0
TGW	46.05±0.69	45.70±0.43	-0.76	0.5751	36.625±1.28	37.23±0.38	1.65	0.592	40.5±0.21	40.76±0.62	0.64	0.804
HI	0.46±0.00	0.43±0.00	-5.53	0.1328	0.457±0.00	0.439±0.00	-3.94	0.186	0.306±0.02	0.290±0.01	-5.03	0.564
Biomass	1687.25±56.03	1415.6±71.09	-16.1	0.0082	709.77±10.83	612.52±11.11	-13.7	0.003	691.25±59.10	672.2±42.7	-2.76	0.812
Grain Number/m²	17048.5±548	13589.4±631	-20.29	0.0007	8889.95±227.05	7245.34±199.04	-18.5	0.003	5283.5±791	4863.9±245	-7.94	0.631
Tiller Number	306.5±16.02	271.5±14.54	-11.42	0.213	273.26±13.92	257.89±11.45	-5.62	0.389	273.25±31.75	245.2±17.54	-10.27	0.44
Grain Per Spike	56±2.91	50.3±0.81	-10.18	0.0429	32.88±2.38	28.73±1.74	-12.62	0.123	19.5±2.72	20.2±1.89	3.59	0.845
Grain Weight Spike	2.57±0.13	2.29±0.03	-11.07	0.0115	1.204±0.09	1.06±0.06	-11.26	0.175	0.8±0.10	0.83±0.07	3.75	0.838
Days To Heading	66.75±0.75	64.5±0.26	-3.37	0.0004	47±0.86	47.6±0.68	1.28	0.578	70.25±0.47	68.6±0.26	-2.35	0.009
Days To Anthesis	71.75±0.75	69.5±0.26	-3.14	0.0004	50±0.86	50.6±0.68	1.2	0.578	73.25±0.47	71.6±0.26	-2.25	0.009
Days To Maturity	NA	NA	NA	NA	75.5±0.64	79.5±0.60	5.2	0.002	101.5±0.63	101.5±0.40	0	1
Height	103.5±0.5	88.2±0.69	-14.78	5.95E-10	59.9±3.24	56.65±1.31	-5.43	0.246	61.25±1.31	57±0.86	-6.94	0.022
Spikelet number	21.08±0.27	20.39±0.18	-3.24	0.146	17.66±0.45	17.38±0.36	-1.6	0.571	16.75±0.53	17.56±0.33	4.88	0.235
Viable Spikelets	19.79±0.51	18.75±0.16	-5.26	0.019	16.58±0.47	15.55±0.34	-6.23	0.079	14.45±0.58	15.16±0.33	4.9	0.299

3.4.4. Dissecting spike yield components and HI by environment to understand the conflicting results between Kingbird and Reedling NILs.

In order to understand the positive effect of the *gw2* allele on TGW, grain morphometrics and yield in cv Kingbird and the trade-off in cv Reedling, we dissected spikes into yield components. Under irrigation, we found that HI despite the herbicide damage increased significantly (P <0.0001, 0.275 vs 0.368) in Kingbird triple mutants (Table 3.4 and Figure 3.8). HI increased in the single mutants in season 2019 consistently with 2022 (Table 3.2). We found that grain number per spike increased significantly in the triple mutants by 27.8% (P <0.1, 42 vs 33) but not spikelet number (ns); moreover, viable spikelets decreased by 4.3% (P > 0.05, 20.95 vs 21.52) when compared to the WT. We then divided seeds per spike by viable spikelet number to find out that the triple mutant had a seed set of 2.1 seeds per spikelet while the WT 1.6 seeds per spikelet, which might explain the increases in HI and yield (Table 3.4, Figure 3.8). The opposite effect was found in Reedling, were the HI decreased significantly in the triple mutants (P <0.01, 0.437 vs 0.460; Table 3.5 and Figure 3.8). This HI result was not consistent with what we found in the single mutants during season 2019 where HI increased in each of the tested environments (Table 3.3). However, it did correlate with all the spike yield components (grain number per spike, spikelet number, viable spikelet), which all decreased albeit not always significantly in the triple mutants when compared to the WT (Figure 3.8, Table 3.5).
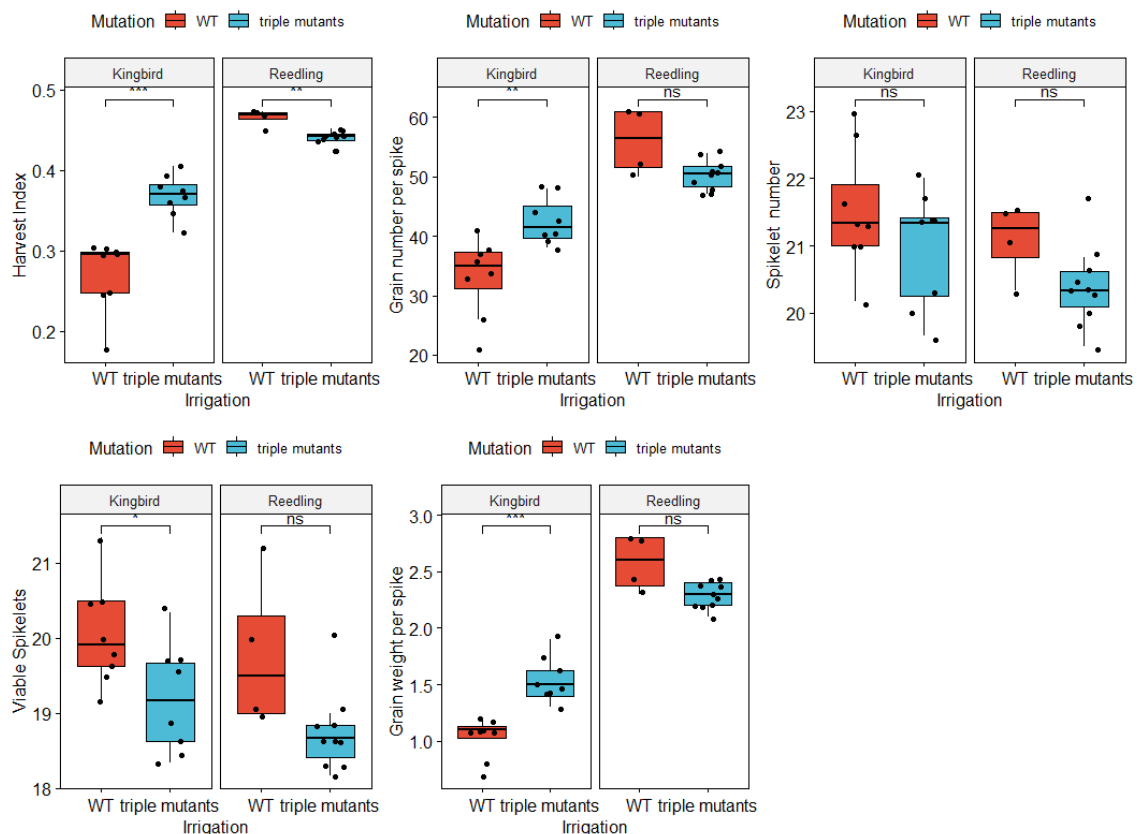
Figure 3-8: Spike yield components, HI and height in Kingbird and Reedling on irrigation plots. The box represents the middle 50% of data with the borders of the box representing the 25th and 75th percentile. Statistical classifications are based on Tukey's HSD tests. ns: P > 0.05; * P<0.05; **P<0.01; ***P<0.001.

To our surprise we found that in both genotypes, the *gw2* mutant effects on HI and spike yield components were non-significant in heat stress when compared to their respective WT (Figure 3.9), which might indicate that increases in yield and TGW in Kingbird can be explained by increases in tiller number by 10% (234/m^2 vs 213/m^2) and grain number per area by 11.4% (7211 vs 6476; Table 3). In Reedling, we observed the opposite effect: fewer tillers and grains per area, that can be correlated with yield loses (Table 3.5). Once more, we see contrasting effects on Kingbird and Reedling NILs and the way the *gw2* alleles contributed to each of the tested parameters.
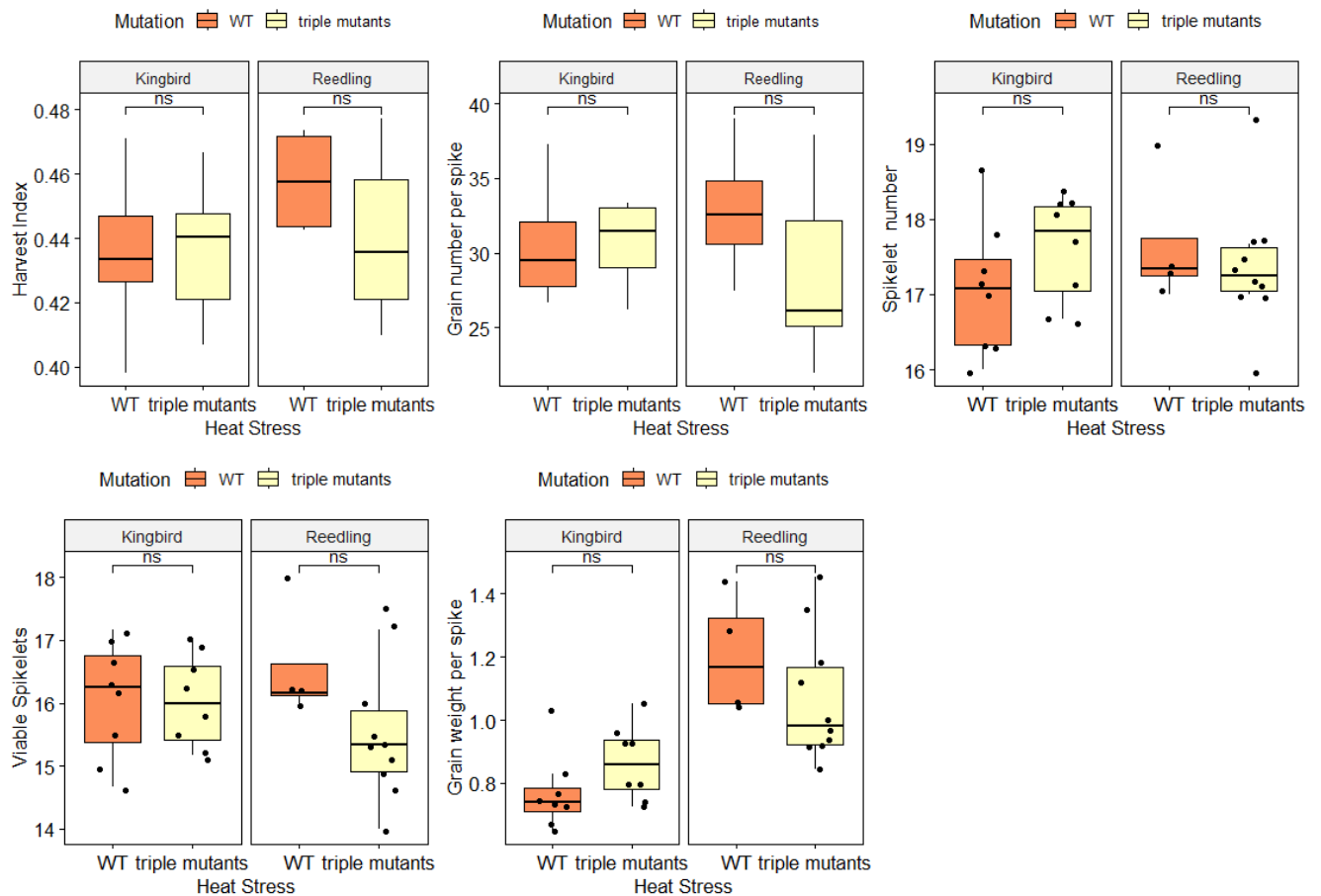
Figure 3-9: Spike yield components, HI and height in Kingbird and Reedling on heat stress plots. The box represents the middle 50% of data with the borders of the box representing the 25th and 75th percentile. Statistical classifications are based on Tukey's HSD tests. ns: P > 0.05.

In drought, consistently with what we found in Heat Stress, HI and spike yield components were found to be non-significant in Reedling (Figure 3.10; data from Kingbird not available). As all the spike yield components were found to be non-significantly affected across all environments, we then analysed tiller number and grain per m² as a possible explanation for yield loses in Reedling.
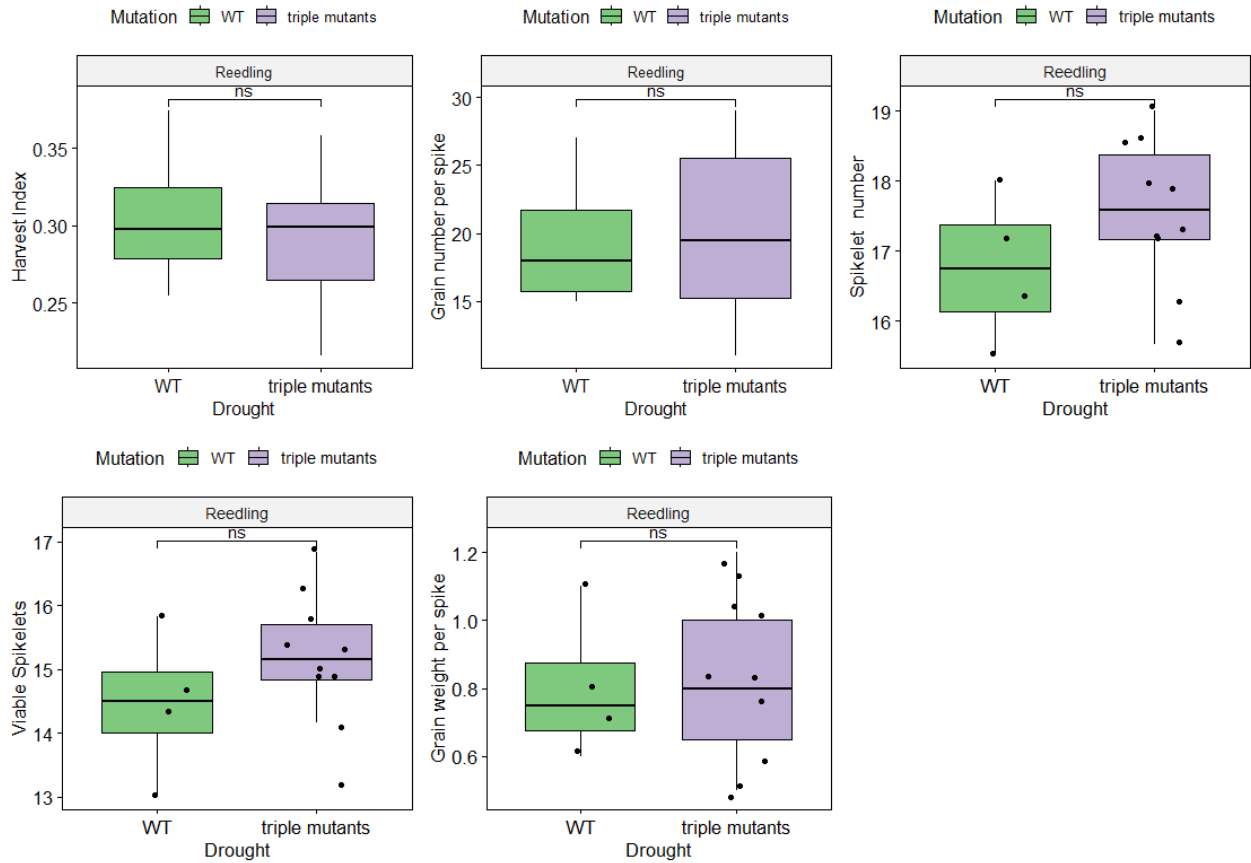
Figure 3-10: Spike yield components, HI and height in Reedling on drought plots. The box represents the middle 50% of data with the borders of the box representing the 25th and 75th percentile. Statistical classifications are based on Tukey's HSD tests. ns: P > 0.05.

### 3.4.5. Grains per m^2 and tiller number decreased consistently across environments in Reedling but not in Kingbird under Heat Stress.

In chapter 2, we identified decreases (not significant both consistent across environments and genotypes) in tiller number and significant decreases in grain per m^2 in the WT and in the *gw2* triple mutants in cv Reedling across all environments (Table 3.5), which is consistent with what we found in Paragon triple mutants (chapter 2). In Reedling, albeit not significantly, tiller number decreased consistently, while grain number per m^2 decreased significantly and consistently under Irrigation and Heat Stress (Table 3.5). Under irrigation, tiller number decreased by 11.42% (P > 0.213, 271 vs 306) and grain number by 20.3% (P < 0.0007, 13,589 vs 17,048), while under Heat Stress tiller number decreased by 5.62% (P > 0.389, 257 vs 273) and grain number by 18.5% (P < 0.003, 8889 vs 7245). Lastly, under drought, we found that tiller number dropped by 10% (P > 0.5, 245 vs 273) and grain number by 8% (P > 0.6, 4863 vs 5283). Despite being the lowest yielding environment, yield losses remained non-significant when compared to the WT. On the other hand, in Kingbird *gw2* triple mutants in irrigated plots, tiller number decreased by 7.62% (P > 0.299, 297 vs 321 tiller/m^2) but not under heat stress, where tiller number increased by 9.98% (P > 0.163, 234 vs 213 tiller/m^2) and grain number per m^2 by 11.35% (P < 0.09, 7211 vs 6476). Surprisingly, these increases also translate into yield, TGW and grain morphometrics gains (Figure 3.6). Although the findings are very promising, we need to conduct at least one more year of field experiments to be confident about these results.

3.4.6. Raising temperatures can cause severe yield losses.

We plotted maximum and minimum temperatures across the wheat growing season under Irrigation and Heat Stress combined with the key growing stages of development (heading, anthesis and maturity) in both genotypes. We found that between anthesis and maturity, which is known to be a critical period for grain filling and starch deposition Altenbach (2012), average temperatures were higher by 4.4 °C in the heat stress environment (late sowing) with respect to the irrigation plots (see material and methods). Similarly, under heat stress, the maximum daily temperature from anthesis to maturity exceeded 30 °C in 22 out of 24 days, with an average of 34 °C, above the temperature threshold identified by Altenbach (2012) for proper grain filling. The heat stress environment caused an average yield loss of 50% in both genotypes when compared to their irrigation pairs despite the herbicide damage. We found that on average, increases of temperature by 1°C can cause up to 11% yield losses (35 kg/plot per degree in Kingbird) when compared to irrigation. We also calculated the cumulative degree days (thermal time in °Cd), that is another way of quantifying the amount of temperature needed for the plant to shift to the next developmental stage. Every phase of development requires a minimum accumulation of temperature (optimal temperature) before that stage can be complete and the plant can move to the next one. Speeding the life cycle of the crop due to heat stress will result in yield loses. The critical grain filling phase, from anthesis to maturity, was reduced by 30%, while final yield decreased by 41% (Figure 3.11). These results revealed the urgency to breed for climate resilience cultivars capable of overcoming increases in temperatures for yield stability.
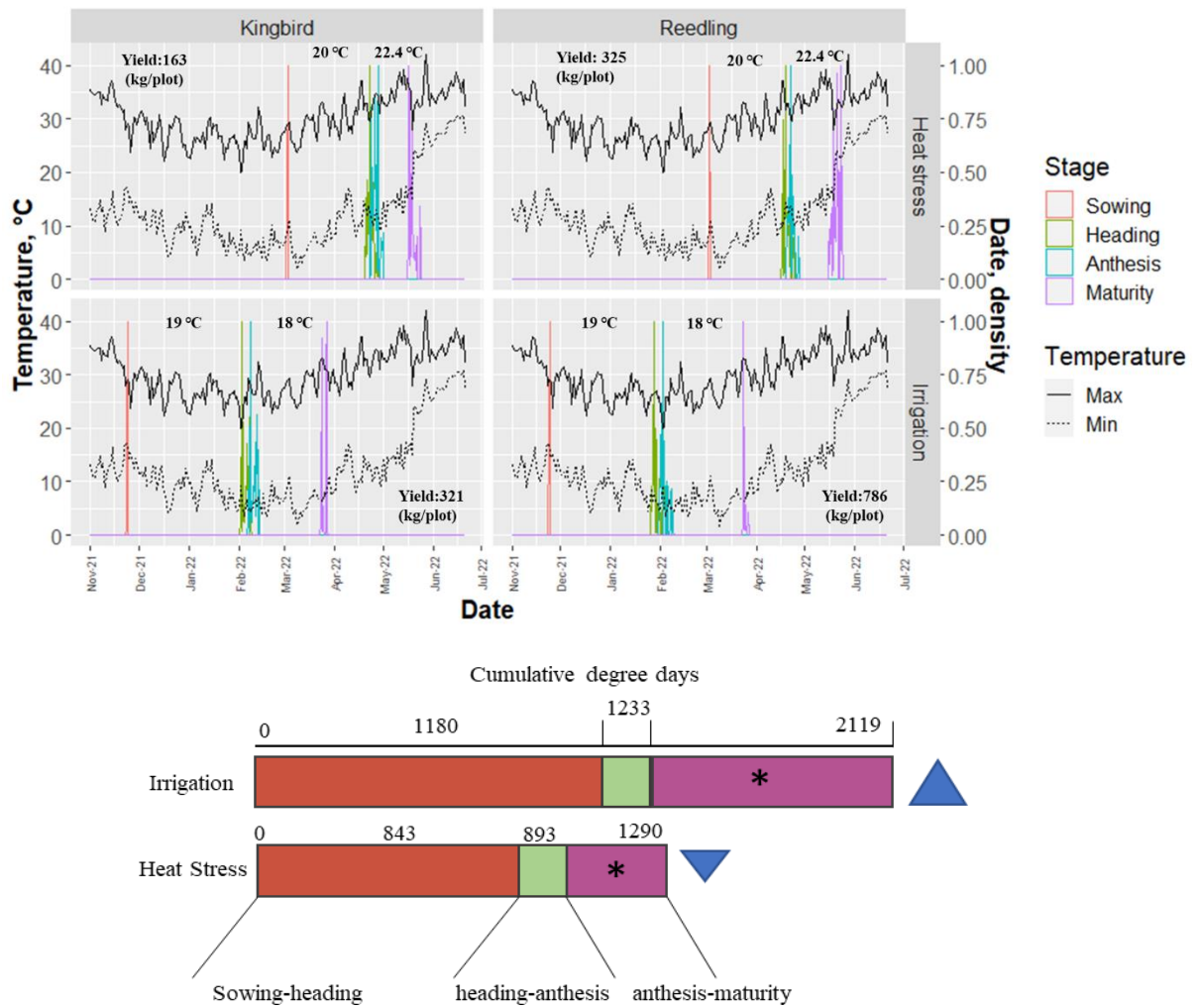
Figure 3-11: A) Average temperatures (max and min) during the crop life cycle at Irrigation and Heat Stress, key stages of development on the right. Temperature depicts the average °C at which the crop was growing between sowing and heading, heading-anthesis and anthesis-maturity. Yield data is coming from the WT during the growing season 2022. B) Cumulative degree days in Irrigation and Heat Stress, * represents the critical grain filling period while the blue triangle represents total yield.

3.4.7. *Double checking DNA and KASP markers in Reedling triple mutants*

We sought to identify potential explanations for the lack of effect of the triple *gw2* mutations on TGW in Reedling. Given the unexpected nature of these results, each plot (86) was re-genotyped to rule out possible errors in the experimental process. We confirmed that there was no mix up in seeds and that all 86 genotypes were correct, disproving the idea that a technical/mislabeling error had occurred along the way.

In the discussion section of Chapter 2, we examine the possible trade-offs in yield, TGW and spike yield components when novel alleles are introgressed into different wheat cultivars. In both the Kingbird and Reedling NILs, the *gw2-A1* mutant allele was coming from durum wheat cv Kronos. Based on the 17 haplotype-informed SNP markers from Brinton et al (2020) we could classify Kingbird as Haplotype 7 (H7) whereas Reedling (aka Borlaug) carries haplotype H5. Kronos on the other hand was classified as a durum-specific haplotype H8. Hence the introduction of

70

the *gw2-A1* mutation, along with chromosome 6A of Kronos, removes the original Kingbird (H7) or Reedling (H5) haplotypes and substitutes it for haplotype H8 (Figure 3.13). Interestingly, analysis of Reedling/Borlaug haplotype H5 shows that the region between 240 and 470 Mbp (which is tightly linked to *GW2-A1* at 237 Mbp) likely originated from a wild wheat relative as comparisons to Cadenza (haplotype H2) and Chinese Spring (haplotype H1) show a large degree of variation between Reedling/Borlaug and the two other hexaploid accessions (Figure 3.12a and 3.12b). This same analysis shows that Reedling/Borlaug is identical by state to Weebill-1 as predicted by the SNP markers (Figure 3.12c; blue dots represent variations within 50 kbp windows). Hence the introduction of the *gw2-A1* mutation (within durum Haplotype H8) into Reedling chromosome 6A, most likely removed the wild wheat haplotype H5 present in Reedling. The same introduction of *gw2-A1* into Kingbird, exchanged a hexaploid wheat haplotype (H7) for a durum haplotype (H8) and perhaps was less detrimental to overall plant performance and allowed the effect of the *gw2-A1* allele to be more evident in the presence of the mutant *gw2* homoeologs.
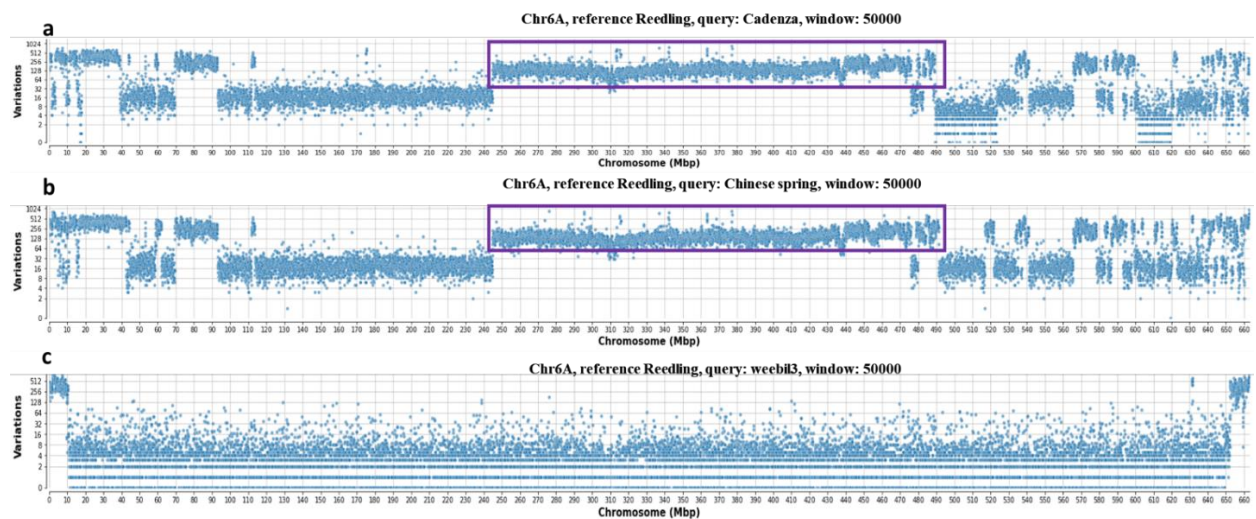
Figure 3-12: Scatter plots showing in the X axis, the whole 6A chromosome in mega base pairs (Mbp) a comparison between a) Reedling vs Cadenza, b) Reedling vs Chinese Spring and c) Reedling vs Weebill-1 that are identical by state. The Y axis is in (Log scale) each blue dot represents the number of variations (equivalent to SNPs) in 50,000 bp. The higher the dot is in the Y axis, thehigher the number of variations between cultivars. The 230 Mbp alien introgression is highlighted in purple representing high variability in that specific region of cv Borlaug.
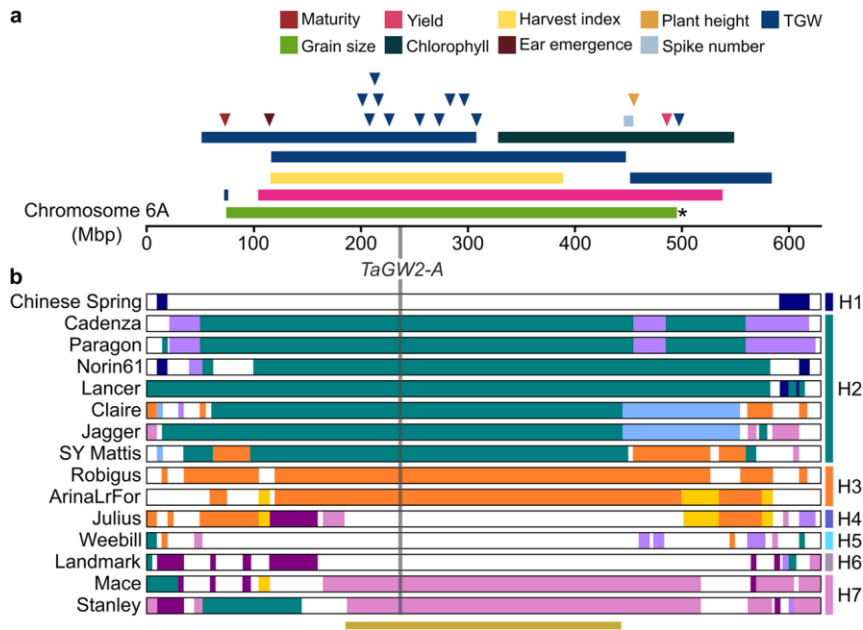
Figure 3-13: a) Physical position of productivity-related QTL (rectangles) and GWAS hits (triangles) mapped to the highly conserved region on chromosome 6A. b) Diagrammatic representation of all haplotype blocks on chromosome 6A in the 15 sequenced cultivars (based on 5-Mbp bin haplotypes; scaled to the longest chromosome 6A). Regions with the same colour at the same position share common haplotypes (except for white regions which are not contained within haplotype blocks). Vertical grey line indicates the position of *TaGW2-A* (237 Mbp). Labels H1–H7 indicate haplotype groups based on the minimum haplotype block (beige bar; 187–445 Mbp) taken from (Brinton et al., 2020).

3.5. Discussion

In this chapter, we analysed the effect of the *gw2* alleles in two spring wheat cultivars Reedling and Kingbird grown in four environments in 2019 (single *gw2-A1* mutants) and three environments in 2022 (triple *gw2* mutants). We identified contrasting yield and grain size phenotypes across environments and genotypes.

3.5.1. *TGW, grain morphometrics and yield increases in Kingbird gw2 triple mutants in heat stress trials*

We found that in the Kingbird *gw2* triple mutants, yield, TGW and grain morphometrics increased in both irrigation and heat stress in 2022, whereas we saw no significant effect in the Reedling NILs. These results tell us that increases in yield can be achieved by introgressing the *gw2* alleles but that the outcome will be strongly related to the genetic background. In the case of the triple mutants tested under heat stress, we found that yield increases by 24% when compared to its isogenic pair. These results are consistent with previous studies exploring the effect of heat on yield components. Studies conducted in growth chamber to simulate heat stress Vijayalakshmi et al. (2010) mapped two QTLs in chromosomes 6A and 6B in recombinant inbred lines (RIL) from a cross between Ventnor (heat-tolerant cultivar) and Karl 92. The study found that delaying senescence confers increased tolerance to heat stress when temperatures were artificially set to 30/25 °C (day/night) after flowering. The authors, however, did not report final yield or TGW. Mohammadi et al. (2008) mapped heat tolerance traits into chromosomes 1B, 5B, and 7B in a RIL population coming from a cross between Kauz (Heat tolerant coming from CIMMYT) and MTRWA166 (heat sensitive). In their study, plants were moved to a chamber that was set to 35/30 °C (day/night) at seven days after anthesis (DAA) for three days. They found that this short period of time was sufficient to reduce TGW by 38%. Mason et al. (2010) identified five QTL regions on chromosomes 1A, 2A, 2B and 3B in RILs coming from Halberd (heat tolerant) and Cutter. Only three days of heat stress at 38/18°C (day/night) 10 days after anthesis caused a 28% reduction in grain yield per spike on susceptible RIL lines. Esten Mason et al. (2011) found that three QTLs located on chromosomes 1B, 5A and 6D can be potentially beneficial when selecting for multiple heat tolerance alleles in RIL lines coming from Halberd (heat tolerant), Cutter and Karl92. Recently, Schmidt et al. (2020) developed NILs targeting a QTL on chromosome 6B associated with both drought and heat stress tolerance from a population screening of 73 exotic Australian donors and two modern cv. Gladius and cv. Scout. Plants were artificially heated in glasshouse experiments three DAA at 35/25 °C. The NILs carrying the exotic haplotypes increased grain weight in the primary tiller and the whole plant significantly by ($P \leq 0.011$). Finally, Lu et al. (2020) developed NILs for a major 7A QTL related to heat tolerance from two populations Cascades $\times$ Tevere and Cascades $\times$ W156, with the latter overperforming in yield and chlorophyll content after heat stress. All the studies mentioned above provide evidence that there is genetic variability in wheat to overcome heat stress related yield losses. Nevertheless, there are few studies using NILs under field conditions, highlighting the importance of this study as yield components originating from controlled environment experiments can vary greatly when compared to the field (Poorter et al., 2016). To make sure our results are consistent across years, we are going to repeat the field experiments in the 2023 growing season in Obregon.

3.5.2. The gw2 allele does not universally increase TGW and yield in wheat

In the results section, we observed that Reedling (a cultivar with relatively big grains) has a chromosome 6A haplotype that was disrupted by the introgression of *gw2-A1* coming from Kronos, leading to a decrease in grain size and yield. Previously, Bednarek et al. (2012) reported that in RNAi transgenic lines in hexaploid cultivar Récital, down-regulating all three *GW2* homoeologs led to a significant reduction in grain size and endosperm cell number when compared to the controls. They concluded that *GW2* is a positive regulator of grain size-related traits, contrary to several other studies in rice and wheat. The RNAi constructs were designed targeting the full length of the *GW2* sequence which might have generated off-target effects leading to silencing of other related genes and potentially smaller grain size. Furthermore, this study was conducted in 2012 when neither a fully annotated wheat genome (2018) nor the pangenome wheat sequence (2020) were available. Similarly, we found that in the triple *gw2* mutant Reedling lines, *gw2* did not affect grain size and TGW, but led to significant yield losses across all environments. A possible explanation for this could be that the downregulation or knockout of *GW2* homoeologs does not affect TGW in certain genetic backgrounds. We can conclude that, although different methods were deployed to create the triple *gw2* mutants (Reedling by cross breeding and Recital by RNAi), both resulted either in no effect or in significant grain size reductions. In the case of Reedling, chromosome 6 haplotypes were disrupted by the introduction of the EMS mutations, but in the case of Récital, the RNAi would not have affected the wider genomic haplotypes. Hence, these results suggest that there may be genetic background effects outside the chromosome 6A region which mask or compensate the *gw2* effect on grain size.

3.5.3. Reedling carries a wild wheat segment in the 6A region where the GW2 gene is located

We wanted to understand the detrimental effect of the introgression of the *gw2* allele in Reedling. Reedling haplotype H5 carries a 230 Mbp segment originating from a wild wheat hybridisation. It is tempting to speculate that this haplotype H5 of Reedling confers bigger grain size and is disrupted by the introgression of the *gw2-A1* mutation originating from Kronos (haplotype H8) (Figure 3.12 and Figure 3.13). Hence the beneficial effect of the *gw2-A1* mutation would be cancelled out by the replacement of the original positive effect haplotype H5. This suggests that the introduction of the *gw2-A1* mutation in a Kronos background (haplotype H8) might have different effects if introduced into different haplotypes given that we see beneficial effects on TGW in Paragon (haplotype H2) and Kingbird (haplotype H7), but not in Reedling/Borlaug (haplotype H5). In chapter 2 and the paragraphs above, we talked about the results obtained by Bednarek et al. (2012). They found that RNAi transgenic lines suppressing the three *GW2* copies resulted in a significant reduction in grain weight and size in cv Recital. Using the 17 SNP markers from Brinton et al (2020) we recently found that Recital carries haplotype H3, the same as Arina (Figure 3.13). Hence it might be that the *gw2-A1* mutation will yield a positive effect on TGW when it replaces certain haplotypes (H2 of Paragon, H7 of Kingbird), but not others (H3 of Recital, H5 of Reedling). We hypothesize that I) the haplotype linkage effect can be overcome with new genome editing technologies (see general discussion, section 5.1.7, for a broader discussion on this topic) and II) that introgression of the *gw2-A1* mutation from Kronos might be beneficial

only when introduced into specific chromosome 6A haplotypes. Hence a haplotype based approach could be useful when introgressing novel alleles into different genetic backgrounds.

3.5.4. *Drought severely reduces yield, followed by heat Stress across years and cultivars*

In this chapter, we compared three contrasting environments: irrigation and (drip irrigation), drought and heat stress, in two different wheat cultivars Kingbird and Reedling, and two different allelic combinations (either the single mutants or the triple *gw2* mutants) across different field seasons. We did so to (I) mimic the future changes in temperature and rain patterns, and (II) assess the effect of the *gw2* mutant alleles in different environments and cultivars. Our results show that irrespective of the *GW2* allelic status, mean yield was reduced by 79% in drought followed by a 21% reduction under HS in Kingbird when compared to irrigation. In Reedling, mean yield was reduced by 52% under drought and by 23% under HS when compared to irrigation (means from 2019). The same traits were observed in 2022, although data from Kingbird is missing. In a similar study, Sukumaran et al. (2018) found that the heat stress environment reduces yield by 72% and by 60% under drought, with HS more damaging that drought by 30%. We observed the opposite trend; with drought reducing yield by 24% in Kingbird and 31% in Reedling when compared to HS. However, Sukumaran et al. (2018) evaluated a durum wheat panel adapted to Mediterranean climates, while we used spring wheat cultivars adapted to irrigated environments. Furthermore, they found that in the heat stress treatment, a 1°C increase in temperature, will cause yield to drop by 11% (0.6 t/ha per degree) in durum wheat. We found that 1°C raise in temperature will cause a 11% decrease in yield in bread wheat. Finally, we observed how drip irrigation can increase yield by 63% in Kingbird (566 kg/plot vs 209 kg/plot) and by 10% in Reedling (746 kg/plot vs 678 kg/plot) when compared with drought WT (Table 3.2 and Table 3.3) proving that delivering water directly to the base of the plant and minimizing evaporation can significantly increase yield (both environments were irrigated twice). This result is valuable as drought is a recurring feature in different parts of the world where wheat is grown. Up to 45% of the earth surface sown with wheat has low to moderate rainfall while the high rainfall and irrigated regions are predicted to have sub-optimal rainfall in the upcoming years (Fischer et al., 2014).

3.6. References

1. ALTENBACH, S. B. 2012. New insights into the effects of high temperature, drought and post-anthesis fertilizer on wheat grain development. Journal of Cereal Science, 56, 39-50.
2. ARJONA, J. M., VILLEGAS, D., AMMAR, K., DREISIGACKER, S., ALFARO, C. & ROYO, C. 2020. The Effect of Photoperiod Genes and Flowering Time on Yield and Yield Stability in Durum Wheat. Plants (Basel), 9.
3. BEDNAREK, J., BOULAFLOUS, A., GIROUSSE, C., RAVEL, C., TASSY, C., BARRET, P., BOUZIDI, M. F. & MOUZEYAR, S. 2012. Down-regulation of the *TaGW2* gene by RNA interference results in decreased grain size and weight in wheat. Journal of Experimental Botany, 63, 5945-5955.
4. BRINTON, J., RAMIREZ-GONZALEZ, R. H., SIMMONDS, J., WINGEN, L., ORFORD, S., GRIFFITHS, S., HABERER, G., SPANNAGL, M., WALKOWIAK, S., POZNIAK, C., UAUY, C. & WHEAT GENOME, P. 2020. A haplotype-led approach to increase the precision of wheat breeding. Communications Biology, 3, 712.
5. ESTEN MASON, R., MONDAL, S., BEECHER, F. W. & HAYS, D. B. 2011. Genetic loci linking improved heat tolerance in wheat (Triticum aestivum L.) to lower leaf and spike temperatures under controlled conditions. Euphytica, 180, 181-194.
6. FAO 2021. World Food and Agriculture – Statistical Yearbook 2021. Rome.
7. FISCHER, R. A., BYERLEE, D. & EDMEADES, G. 2014. Crop yields and global food security: will yield increase continue to feed the world? ACIAR Monograph No. 158. Australian Centre for International Agricultural Research. Canberra.
8. KORNHUBER, K., COUMOU, D., VOGEL, E., LESK, C., DONGES, J. F., LEHMANN, J. & HORTON, R. M. 2020. Amplified Rossby waves enhance risk of concurrent heatwaves in major breadbasket regions. Nature Climate Change, 10, 48-53.
9. LANGRIDGE, P., BRAUN, H., HULKE, B., OBER, E. & PRASANNA, B. M. 2021. Breeding crops for climate resilience. Theoretical and Applied Genetics, 134, 1607-1611.
10. LANGRIDGE, P. & REYNOLDS, M. 2021. Breeding for drought and heat tolerance in wheat. Theoretical and Applied Genetics, 134, 1753-1769.
11. LOBELL, D. B., SCHLENKER, W. & COSTA-ROBERTS, J. 2011. Climate Trends and Global Crop Production Since 1980. Science, 333, 616-620.
12. LU, L., LIU, H., WU, Y. & YAN, G. 2020. Development and Characterization of Near-Isogenic Lines Revealing Candidate Genes for a Major 7AL QTL Responsible for Heat Tolerance in Wheat. Frontiers in Plant Science, 11.
13. MASON, R. E., MONDAL, S., BEECHER, F. W., PACHECO, A., JAMPALA, B., IBRAHIM, A. M. H. & HAYS, D. B. 2010. QTL associated with heat susceptibility index in wheat (*Triticum aestivum L.*) under short-term reproductive stage heat stress. *Euphytica*, 174, 423-436.
14. MOHAMMADI, V., ZALI, A. & BIHAMTA, M. 2008. Mapping QTLs for heat tolerance in wheat.
15. ORTIZ-MONASTERIO R, J. I., DHILLON, S. S. & FISCHER, R. A. 1994. Date of sowing effects on grain yield and yield components of irrigated spring wheat cultivars and relationships with radiation and temperature in Ludhiana, India. Field Crops Research, 37, 169-184.
16. PALLOTTA, M., WARNER, P., FOX, R., KUCHEL, H., JEFFERIES, S. & LANGRIDGE, P. 2003. Proceedings of the 10th international wheat genetics symposium.
17. PATRA, K., PARIHAR, C. M., NAYAK, H. S., RANA, B., SINGH, V. K., JAT, S. L., PANWAR, S., PARIHAR, M. D., SINGH, L. K., SIDHU, H. S., GERARD, B. & JAT, M. L. 2021. Water budgeting in conservation agriculture-based sub-surface drip irrigation in tropical maize using HYDRUS-2D in South Asia. Sci Rep, 11, 16770.
18. POORTER, H., FIORANI, F., PIERUSCHKA, R., WOJCIECHOWSKI, T., VAN DER PUTTEN, W. H., KLEYER, M., SCHURR, U. & POSTMA, J. 2016. Pampered inside, pestered outside? Differences and similarities between plants growing in controlled conditions and in the field. New Phytologist, 212, 838-855.

19. REYNOLDS, M. P., LEWIS, J. M., AMMAR, K., BASNET, B. R., CRESPO-HERRERA, L., CROSSA, J., DHUGGA, K. S., DREISIGACKER, S., JULIANA, P., KARWAT, H., KISHII, M., KRAUSE, M. R., LANGRIDGE, P., LASHKARI, A., MONDAL, S., PAYNE, T., PEQUENO, D., PINTO, F., SANSALONI, C., SCHULTHESS, U., SINGH, R. P., SONDER, K., SUKUMARAN, S., XIONG, W. & BRAUN, H. J. 2021. Harnessing translational research in wheat for climate resilience. Journal of Experimental Botany, 72, 5134-5157.

20. RICHARDS, R., REBETZKE, G., WATT, M., SPIELMEYER, W. & DOLFERUS, R. 2010. Breeding for improved water productivity in temperate cereals: Phenotyping, quantitative trait loci, markers and the selection environment. Functional Plant Biology - FUNCT PLANT BIOL, 37.

21. SCHMIDT, J., GARCIA, M., BRIEN, C., KALAMBETTU, P., GARNETT, T., FLEURY, D. & TRICKER, P. J. 2020. Transcripts of wheat at a target locus on chromosome 6B associated with increased yield, leaf mass and chlorophyll index under combined drought and heat stress. PLoS One, 15, e0241966.

22. SIMMONDS, J., SCOTT, P., BRINTON, J., MESTRE, T. C., BUSH, M., DEL BLANCO, A., DUBCOVSKY, J. & UAUY, C. 2016. A splice acceptor site mutation in *TaGW2-A1* increases thousand grain weight in tetraploid and hexaploid wheat through wider and longer grains. Theor Appl Genet, 129, 1099-112.

23. SNOWDON, R. J., WITTKOP, B., CHEN, T.-W. & STAHL, A. 2021. Crop adaptation to climate change as a consequence of long-term breeding. Theoretical and Applied Genetics, 134, 1613-1623.

24. SUKUMARAN, S., REYNOLDS, M. P. & SANSALONI, C. 2018. Genome-Wide Association Analyses Identify QTL Hotspots for Yield and Component Traits in Durum Wheat Grown under Yield Potential, Drought, and Heat Stress Environments. Front Plant Sci, 9, 81.

25. TRICK, M., ADAMSKI, N. M., MUGFORD, S. G., JIANG, C.-C., FEBRER, M. & UAUY, C. 2012. Combining SNP discovery from next-generation sequencing data with bulked segregant analysis (BSA) to fine-map genes in polyploid wheat. BMC Plant Biology, 12, 14.

26. VIJAYALAKSHMI, K., FRITZ, A. K., PAULSEN, G. M., BAI, G., PANDRAVADA, S. & GILL, B. S. 2010. Modeling and mapping QTL for senescence-related traits in winter wheat under high temperature. Molecular Breeding, 26, 163-175.

27. WANG, W., SIMMONDS, J., PAN, Q., DAVIDSON, D., HE, F., BATTAL, A., AKHUNOVA, A., TRICK, H. N., UAUY, C. & AKHUNOV, E. 2018. Gene editing and mutagenesis reveal inter-cultivar differences and additivity in the contribution of *TaGW2* homoeologues to grain size and weight in wheat. Theoretical and Applied Genetics, 131, 2463-2475.

28. ZHAO, C., LIU, B., PIAO, S., WANG, X., LOBELL, D. B., HUANG, Y., HUANG, M., YAO, Y., BASSU, S., CIAIS, P., DURAND, J.-L., ELLIOTT, J., EWERT, F., JANSSENS, I. A., LI, T., LIN, E., LIU, Q., MARTRE, P., MÜLLER, C., PENG, S., PEÑUELAS, J., RUANE, A. C., WALLACH, D., WANG, T., WU, D., LIU, Z., ZHU, Y., ZHU, Z. & ASSENG, S. 2017. Temperature increase reduces global yields of major crops in four independent estimates. Proceedings of the National Academy of Sciences, 114, 9326-9331.

4. Are gibberellins involved in the increases of grain weight and size in the Paragon *gw2* triple mutant NILs?

4.1. Chapter summary

We performed glasshouse (GH) experiments to determine the effect of bioactive gibberellins (GA_3) and paclobutrazol (PAC) applications on final seed weight, length, and width in the Paragon *gw2* triple mutants and Paragon WT NILs. In this experiment, we applied PAC (1 uM) at booting, GA_3 (10 uM) at flowering, and a combined treatment applied PAC at booting and GA at flowering (PAC+GA). The experiment also included a no-treatment control. We found that PAC significantly decreased the final TGW of Paragon *gw2* triple mutants in both years when compared with the controls. The GA_3 treatment increased grain morphometrics in the Paragon WT while no effects were found in the *gw2* triple mutants. Furthermore, the combined PAC+GA treatment partially restored the TGW in the triple mutants. We hypothesize that GAs are involved in the *gw2* mediated increase in grain size. We therefore analysed GAs concentration in carpels but found no differences between the genotypes. Moreover, we measured pericarp cell length and width, we found significant increases on pericarp cell in the *gw2* triple mutant when compared to the control. Finally, we generated a set of NILs to assess the effect of the *REDUCED HEIGHT1 Rht-B1b* semi-dwarf allele in combination with the *gw2* triple mutants in a Paragon background and found that increases in grain weight and grain size are independent from the allelic status at *RHT-B1*.

4.2. Introduction

In the previous chapters, we discuss how the *GW2* gene negatively regulates growth, grain size and thousand grain weight primarily by constraining cell division in different cereal species (Song et al., 2007). In rice *OsGW2* RNAi lines, Verma et al. (2021) found that decreased expression levels of *OsGW2* contributed to higher grain width by affecting cell division and cell expansion. The two paralogous copies of *GW2* in maize have been associated with variation in both the width and weight of the kernels (Li et al., 2010).

The knockdown of *GW2* has been associated with expression changes in genes encoding starch biosynthesis. In wheat RNAi lines, the gene encoding the large subunit of AGPase (an enzyme which catalyses the conversion of glucose-1-phosphate and ATP to pyrophosphate and ADP-glucose Jeon et al. (2010), was strongly up-regulated. Consistent with an enhancement to AGPase activity, Sestili et al. (2019a) found that in *GW2* RNAi durum lines, the starch content of the mutant lines were 10 - 40 % higher than that of the wild type grains. In addition, it was also reported that final grain width increased 4-13% when compared with the controls.

Similarly, expression of gibberellin biosynthesis genes has been reported to be affected in lines with mutations in *GW2*. Gibberellins (GAs) are plant hormones that control fundamental processes of plant development including

seed germination, stem elongation, leaf expansion, flower and seed development by promoting growth by cell expansion and cell division (Hedden and Sponsel, 2015). GA biosynthesis is initiated in the plastids, proceeds through the endoplasmic reticulum and finishes in the cytoplasm. GA biosynthesis is modulated by the activity of a series of enzymes, which results in the conversion between different forms of GA, resulting in the bioactive forms GA_1, GA_4 and GA_3. The biosynthesis of GA is regulated mainly by the enzymes GA20-oxidase (GA_{20ox}) and GA3-oxidase (GA_{3ox}), while its inactivation is controlled primarily by GA2-oxidase (GA_{2ox}) (Figure 4.1) (Tuan et al., 2018). The GA3ox enzymes catalyse the conversion of several precursors to bioactive forms of GA. Finally, the GA2ox enzymes convert bioactive and precursor GAs to inactive forms reducing bioactive GA levels (Figure 4.1). The rate of GA biosynthesis is controlled by feedback regulatory mechanisms among the genes encoding these biosynthetic enzymes (Zhang et al., 2018). There have been contrasting results on the effect of *gw2* down-regulation on GA biosynthesis genes in wheat. Li et al. (2017) reported that *GW2* negatively controls the synthesis of the GAs. They found that the expression of the gene which encodes for *GA3ox* is up-regulated in the *gw2-A1* single mutant in the Chinese Spring genetic background. Furthermore, when GA_3 was applied to the single mutants, the grain decreased in length when compared with the WT. However, interpretation of these results are difficult as there was no information on the concentrations that were used to conduct this experiment. In contrast, Sestili et al (2018) reported that GA_3ox was not upregulated in the *GW2* RNAi lines when compared to the WT controls.
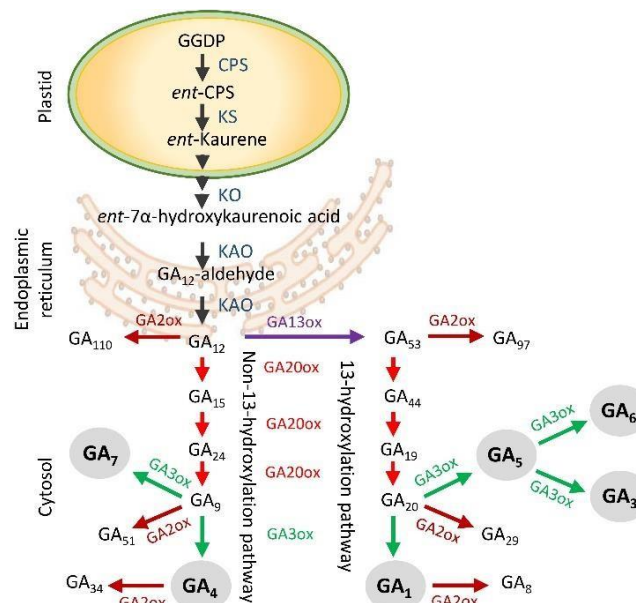
Figure 4-1: Principal reactions of the GA biosynthetic pathway in plants. 2ODDs class enzymes are in red and green whereas the bioactive GAs are at the bottom of the diagram in grey circles. Adapted from Katyayini et al. (2020).

Once synthesized, bioactive GA_4 promotes growth by targeting for degradation the nucleus localised DELLA proteins, well-known growth and developmental suppressors (Van De Velde et al., 2017). In WT plants (*Rht-A1a, Rht-B1a* and *Rht-D1a* alleles), DELLA proteins physically interact with transcription factors (TFs) involved in the regulation of GA responsive genes, thereby constraining growth Thomas (2017) (Figure 4.2). The first step to release the TFs starts when GA_4 (bioactive forms) binds to GID1 in the cytoplasm forming a GID1-GA_4 complex that travels to the nucleus where it binds to DELLA. Here, the GID1–GA–DELLA complex enhances the interaction

between DELLA and the E3 ubiquitin ligase SCF, resulting in DELLA being targeted for degradation through the 26S proteasome pathway. Once DELLA is degraded, the TFs are released leading to expression of the GA-responsive genes. Additionally, the DELLA–PFD (prefoldin complex) interaction stops, allowing the PFD to migrate to the cytoplasm leading to microtubules polymerization inducing cell expansion (Figure 4.2) (Xu et al., 2014).

The GA mediated degradation of DELLA is the centerpiece of a discovery that led to substantial increases on wheat yields through the introgression of the semi-dwarfing GA-insensitive mutant alleles known as *RHT-B1b* and *RHT-D1b*. These mutant alleles had an altered response to GAs which causes an overall reduction of stem and organ elongation resulting in improved resistance to lodging, yield benefits through increases on grain number per square meter and by increasing the number of grains per spike Pearce et al. (2011), (Boeven et al., 2016). Nevertheless, *RHT-B1b* and *RHT-D1b* significantly decreased grain weight and size by up to 15% (Jobson et al., 2019).
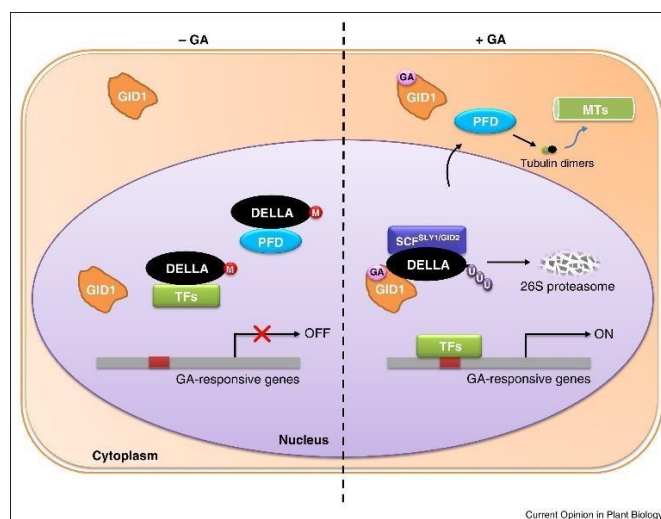
Figure 4-2: Schematic representation of the DELLA-mediated GA signalling de-repression regulatory model adapted from (Xu, Liu et al. 2014).

In the semi-dwarf mutants, there is an altered response caused by mutations in the homoeologous DELLA genes *RHT-B1 and RHT-D1* which have nucleotide substitutions that create premature stop codons. In the *RHT-B1b* allele, a T-C substitution converts the Q64 codon (CGA) to a translational stop codon. In the *RHT-D1b* allele, a T-G substitution affects the E61 codon (GGA) causing a premature stop codon (Figure 4.3) affecting the GID1-GA-mediated degradation of DELLA. (Peng et al., 1999, Thomas, 2017). The DELLA protein domain is needed for the binding of the GIDI-GA complex and recently it was discovered that the semi-dwarf alleles encode N-terminal truncated DELLA proteins with low protein abundance due to a reduction on efficiency of translation reinitiation. Thus, taken together, the lower protein abundance and the GA insensitivity of the protein can explain reductions on height and organ size in wheat (Van De Velde et al., 2021).

```
Rht-B1a  GEEVDELLAALGYKVRASDMADVAQKLEQLEMAMGMGGVGAGAAPDDSFATHLATDTVHYNPTDLSSWVESMLS
Rht-B1b  GEEVDELLAALGYKVRASDMADVAQKLE◦ MAMGMGGVGAGAAPDDSFATHLATDTVHYNPTDLSSWVESMLS
Rht-D1b  GEEVDELLAALGYKVRASDMADVAQKL◦  MAMGMGGVGAGAAPDDSFATHLATDTVHYNPTDLSSWVESMLS
Rht-D1a  GEEVDELLAALGYKVRASDMADVAQKLEQLEMAMGMGGVGAGAAPDDSFATHLATDTVHYNPTDLSSWVESMLS
```

Figure 4-3: Differences between wild-type *Rht-B1a* and *Rht-D1a* and mutant sequences *Rht- B1b* and *Rht-D1b* (deletions and substitutions) are highlighted in white, the position of translational stop codons is represented by an asterisk adapted from Peng et al. (1999).

In the General Introduction we proposed a model of how the GW2 protein might interact with different proteins promoting or suppressing the expression of GAs genes resulting in growth constraints (grain size as an example). We hypothesize that once the GW2 protein is truncated and non-functional (e.g., in the *gw2* mutants), GAs genes can be transcribed enhancing grain growth. Furthermore, we propose that DELLA proteins bind to inactivate key transcription factors of the TCPs class which are considered the "master" regulators of endoreduplication by interacting with different growth and elongation hormones pathways (like auxins and GA) Ferrero et al. (2019a) (Zhang and Lenhard, 2017). Due to the conflicting results reported by Li (2017) and Sestili (2018), we conducted an experiment using a GA biosynthesis inhibitor to understand physiologically how GAs are involved in final grain size and TGW in Paragon *gw2* triple mutants. Paclobutrazol (PAC) is antagonistic to gibberellins and auxins, reducing cell elongation and cell division. The growth-retarding property of PAC is largely attributed to interference with the gibberellin precursor ent-Kaurenoic acid (Figure 4.1). PAC-induced growth inhibition can be reversed by exogenous application of gibberellins which makes PAC a good compound for studying how the depletion of GAs can influence final tissue growth in plants (Desta and Amare, 2021). Additionally, we decided to use analytic chemistry to determine the relative concentration of GAs between the NILs. We hypothesize that the enzymes GA20-oxidase (GA20ox) and/or GA3-oxidase (GA3ox) will be more abundant in the triple mutants resulting in increases of the bioactive forms GA_1 and/or GA_4 when compared to the WT. By employing these two different methods, we hope to gain insights into the behavior and quantification of the GAs in the NILs that might explain the 20% increases in weight and the 6% in width and length in Paragon *gw2* triple mutant grains. Furthermore, we generated a set of NILs with contrasting *Rht-B1* alleles and *GW2* allelic status to test if GW2 and DELLA proteins genetically interact to affect grain weight and size.

4.3. Material and methods

4.3.1. Ovary/ grain developmental time course

We performed an ovary time-course development experiment where final ovary length and width from Paragon WT and Paragon *gw2* triple mutants were sampled from the middle spike at different time points starting from heading and until the embryo was 20 days old. Five spikes per genotype were sampled at six time-points: heading (-5 days post anthesis (dpa)), anthesis (0 dpa), 5, 10, 15, and 20 dpa. From these spikes, eight carpels/grains were sub-sampled from the two outer florets (floret positions F1 and F2, Figure 4.4) of the five spikelets located in the middle of the spike. The carpels/grains were then weighed (fresh weight) and analysed for grain morphometric using a MARVIN seed analyser.

4.3.2. Ultra-high performance liquid chromatography tandem mass spectrometry (UHPLC-MS)

We use Ultra-high performance liquid chromatography tandem mass spectrometry (UHPLC-MS) to determine the relative concentration of GAs between the NILs. We hypothesize that the concentration of the enzymes GA 20-oxidase (GA20ox) and/or GA3-oxidase (GA3ox) will be higher in the *gw2* triple mutants resulting in increases of the bioactive forms GA_1 and/or GA_4 when compared to the WT. UHPLC-MS is a separation method in which particles smaller than 2.5 µm travel through columns and can be separated by polarity with great resolution, while mass spectrometry (MS) measures the molar mass of a compound or a complex mixture (Guillarme and Veuthey, 2017). This method is suitable for detecting compounds with very low biological concentrations or with very similar carbon skeletons like GAs that range from 10^{-9} to 10^{-15} mol g^{-1} fresh weight depending on the tissue (Urbanová et al., 2013). We collected wheat ovaries at heading time from Paragon WT and Paragon *gw2* triple mutants to quantify GAs content. The ovaries were taken from the middle part of the spike from the two outer florets (position F1 and F2, Figure 4.4) coming from the main tiller. Overall ~12 ovaries per plant were collected per genotype in triplicate. Once collected with tweezers, ovary samples were immediately stored in Eppendorf tubes (2.5 ml) and frozen in liquid nitrogen. Afterwards, the samples were weighed using an analytical balance and freeze dried (Edwards Modulyo Freeze Dryer) with the caps open for 48 hours. After that, the tubes were weighed, and dry weights were recorded. Finally, we sent them to the Laboratory of Gibberellin Research at Olomouc University, Czech Republic for UHPLC-MS analysis. Full gibberellins analysis was performed following the method reported by (Urbanová et al., 2013). This protocol allows the detection of up to 20 GAs at the same time including the biologically active GAs as well as their precursors and metabolites. GA_{12} and GA_{24} were not detected and removed from the results.
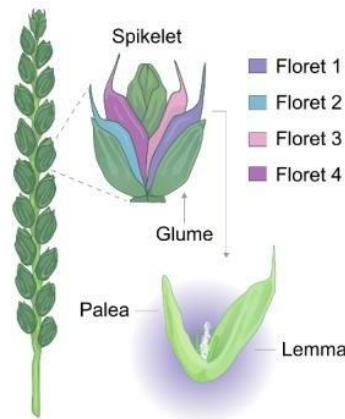
Figure 4-4: Spikelet positions within the spike (left), the florets within spikelet from those closest to the rachis (F1) to those located at increasingly distal positions. Adapted from Adamski et al 2020.

4.3.3. Gibberellin and Paclobutrazol glass house experiments 2020 and 2021

In September of 2020, a total of 160 plants coming from Paragon WT (80 plants) and Paragon *gw2* triple mutants (80 plants) were grown in a lit glasshouse under long day conditions (16-h light/8-h dark) in 1 L pots in "John Innes Cereal Mix" (65% peat, 25% loam Soil, 10% grit, 3 kg/m3 dolomitic limestone,1.3 kg/m3 PG mix and3 kg/m3 osmocote exact). Once potted, plants were randomly distributed across the glasshouse bench to avoid any block effect and randomly assigned to each of the following four treatments:

1. PAC treatment: 10 ml of Paclobutrazol (SIGMA-ALDRICH CO LTD, cat.no. 43900-50MG) mixed with water at a concentration of 1 µM was applied via root uptake at booting stage for 14 days, every second day (18-20 plants per genotype).

2. GA treatment: 10 ml of Gibberellic acid 90% (SIGMA-ALDRICH CO LTD, cat.no. G7645-1G) mixed with water and Tween 20 (THERMO FISCHER SCIENTIFIC cat.no. 85114; as a surfactant at 1% to a final concentration of 10 µM) were applied by spraying three spikes per plant at anthesis (visible yellow anthers) during five consecutive days (15 plants per genotype, ~45 spikes per genotype). Every spike was tagged individually at flowering. Afterwards, they were harvested individually to see the effect on the treatments in each individual spike.

3. Combined PAC+GA treatment: Between 18-20 plants per genotype, were subjected to PAC treatment at booting as described above followed by GA treatment at anthesis as described above.

4. Control treatment: 10 ml of water was supplied via root uptake at booting stage then, 10 ml were sprayed to spikes at anthesis.

In March 2021, a total of 100 plants from the Paragon WT (50 plants) and Paragon *gw2* triple mutants NILs (50 plants) were grown in the glasshouse under natural long day conditions in 1 L pots in "John Innes Cereal Mix". Once potted, plants were randomly distributed across the glasshouse bench plants were subjected to the following three treatments:

1. PAC treatments: 10 ml of PAC at 0.5 uM and 1 uM were applied at booting stage (Zadoks 45) for 14 days via root uptake.

2. GA treatments: 20 plants per genotype were treated with GA$_3$ (5 uM, 10 uM) at heading (Zadoks 59) or anthesis (Zadoks 61) by spraying 10 ml at three main tillers for five consecutive days.

3. Control treatment: 10 plants per genotype were used as a control group and were treated with water.

Once the plants reached maturity, treated spikes, internodes and peduncle were measured. Afterwards, spikes were harvested individually and left at 35 °C for 48 hours to reduced moisture. Once dried, spikes were threshed, and grain weight and size were obtained with a MARVIN seed analyser (GTA Sensorik GmbH, Germany).

4.3.4. *Pericarp cell size measurements with scanning electron microscope*

One representative *GW2* WT and *gw2* triple mutant BC4 NIL was used for pericarp cell size measurements. For each NIL, nine grains of average grain length were selected from the whole 2019 field sample from two different blocks; we call this group the normal distribution group (the WT is smaller than the triple mutants). For the *GW2* WT NIL, an additional nine grains were selected that had grain lengths equivalent to the average of the *gw2* triple mutants NIL sample (*GW2* WT with larger grains). For the *gw2* triple mutants NIL, nine grains were selected that had grain lengths equivalent to the average of the *GW2* WT NIL sample; we call them overlap group (*gw2* triple mutants with smaller grains). Three grains were stuck to a 12.5 mm diameter aluminum specimen stubs using 12 mm adhesive carbon tabs (both Agar Scientific), sputter-coated with gold using an Agar high resolution sputter coater and imaged using a Zeiss Supra 55 scanning electron microscope (SEM). The pericarp of each grain was imaged in the top and bottom using the embryo as a reference, two images per grain were taken in each half. All images were taken at a magnification of 500x. Cell length and width were measured manually using OMERO (University of Dundee & Open Microscopy Environment.) (Figure 4.5). Cell number was estimated for each grain using average grain length /cell length*1000. For the statistical analyses, the average cell length of each individual grain was used.
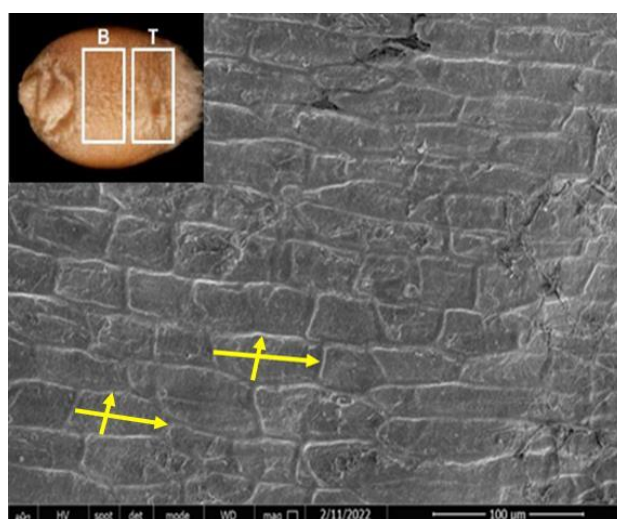
Figure 4-5: A) Top left: Wheat grain divided in bottom and top for microscopy purpose using the embryo as reference B) SEM image from pericarp cell length, the yellow arrow represents how length and width were manually measured.

4.3.5. Plant material: Generating NILs with the Rht-B1b x gw2 alleles

We wanted to understand if *gw2* genetically interacts with the *Rht-B1b* allele affecting not only plant height but also grain weight and morphometrics. In order to do so, we generate a set of NILs by crossing 'tall' Paragon *gw2* triple mutants (BC$_2$F$_3$ Paragon) plants to the semi-dwarf *Rht-B1b* Paragon NILs (BC$_2$F$_3$) (carrying the wildtype *GW2* alleles) developed by the Wheat Genetic Improvement Network (WGIN 2 - home). First, seeds were given a cold stratification inside Petri dishes with moist filter paper and left for 48 hours at 4 °C. Afterwards, the Petri dishes were left on the bench at room temperature for one day or until coleoptile emergence and transplanted to a 96 well tray filled with John Innes Cereal Mix. After 20 days, the growing plants were potted in standard 1L pots, again with John Innes Cereal Mix. Before flowering (when the spike was fully emerged and the peduncle just visible) selected main spikes were emasculated and covered with cellophane bags to avoid pollen cross-contamination. During flowering (anthers with yellow pollen visible, Zadoks 65) individual anthers were taken and carefully placed on the stigma of the recipient spike (previously emasculated). The crossed plants were covered again with cellophane bags following the protocol available at (http://www.wheat-training.com). Once the plants reached maturity, the grains were harvested. Figure 4.6 shows a crossing scheme of the generated NILs.
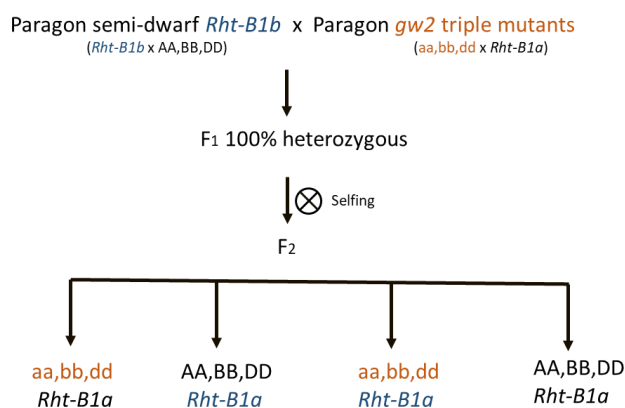
Figure 4-6: Crossing scheme for *Rht-B1b* NILs in blue and triple mutant *gw2* (aa, bb,dd) in orange. The wild type alleles (*Rht-B1a*, *GW2* AA, BB,DD) are represented in black. F$_1$ is self-pollinated. In F$_2$ the probability of having all four different alleles in homozygous state is 1/256. Crossing scheme from the semi-dwarf Paragon *Rht-D1B* and Paragon *gw2* triple mutants are not shown.

Once the plants reached maturity, spikes from the F$_1$ were harvested and threshed. A total of 51 seeds were obtained (coming from five plants). Each individual seed was grown in the glasshouse, leaf samples were taken for DNA extraction 15 days after emergence. A set of Kompetitive Allele specific PCR (KASP) markers were tested for the *GW2* homoeologs (Wang et al, 2018) and for *RHT-B1 (Ellis et al., 2002)*. In 2020, F2 seeds coming from the F1 plants were potted and a total of 1,300 plants were sampled for DNA. DNA extraction was performed following the protocol described by Pallotta et al. (2003a). Afterwards, DNA was tested for quality and quantity with the help of a Nanodrop. DNA was diluted to a final concentration of 1:10 and genotyped using the KASP markers described above following Trick et al. (2012) protocol (Table 3.1, chapter 3). Paragon wild type was used as a control. Once KASP genotyping was conducted, plants were selected as follows:

- Paragon WT for *GW2* (AA, BB, DD) and WT tall allele *RHT-B1a.*
- Paragon *gw2* triple mutants (aa,bb,dd) and the WT tall allele *RHT-B1a.*
- Paragon wild type for GW2 (AA, BB, DD) and *RHT-B1b* semi-dwarf
- Paragon *gw2* triple mutants (aa,bb,dd) and the semi-dwarf *RHT-B1b* (Figure 4.6).

Selected plants were left in the glasshouse for self-pollination. At maturity, seeds were threshed and resown in the glasshouse during autumn for seed bulking. Seeds were saved for spring sowing and planted on the 14 of April of 2021 at Morley Farm for seed bulking. Due to the low number of available seeds, yield was not measured during the 2021 growing season. Once at maturity (Zadoks 99) plants were machine harvested for TGW and grain morphometrics. Seeds from cycle 2021 were saved for the 2022 growing cycle. During 2022, two sowing dates were conducted: winter sowing and spring sowing (Table 4.1) all plots were arranged in a randomized block design with five blocks.

Table 4-1: Field plots in Paragon NILs 2022

Alleles	2022 winter (# of plots)	2022 spring (# of plots)
Tall/*GW2*	20	20
semi dwarf/*GW2*	14	20
Tall/*gw2* triple	12	20
semi dwarf/gw2 triple mutants	16	19
Total	**62**	**79**

4.4. Statistical analysis

The statistical analysis for the glasshouse experiments was carried out with R studio version 4.2.1 and the package lme 4 1.1. For both glasshouse experiments conducted in 2020 (PAC/GA) and 2021 (PAC/GA), a mixed effects model was fitted for each of the response variables (TGW, seed length and seed width) with treatment, genotype, plant ID and the genotype/treatment interaction as fixed effects and plant ID as random effect. The *P* values for explanatory variables in individual models refer to the *P* values computed by the ANOVA; each experiment (year) was analysed individually. Percentage difference data refer to the estimated marginal means deriving from the same models. Plants with values lower or higher than the mean ± 2 standard deviations (SD) were considered outliers and were removed from the datasets. For the ovary-grain development time course, a two-way ANOVA including genotype and block was conducted for each timepoint. Similarly, a two-way ANOVA including genotype and distribution was conducted for cell size measurements. For Paragon *Rht-B1b* x *gw2* triple mutants crosses, a three-ways ANOVA was fitted to the response variables (e.g., TGW, seed width, seed length, yield and height) with the Year/Block interaction as a nested effect in response to mutations. The *P* values for explanatory variables in individual models refer to the *P* values computed by the ANOVA. For the Tukey values, a two ways ANOVA was fitted for each variable in response to *RHT* GW2* alleles, and each year was analysed independently.

4.5. Results

4.5.1. Carpel/grain width and length increase significantly during development in the triple gw2 mutants when compared to the Paragon WT.

A developmental time course of carpel/ grain size was conducted using Paragon *GW2-A1* and Paragon single gw2-*A1* NILs which showed significant differences on grain width and length since heading (Simmonds et al., 2016). Since increases on grain morphometrics are more subtle in the single mutants when compared to the *gw2* triple mutans and to determine when differences on grain morphometrics are first established in the Paragon WT and Paragon *gw2* triple mutants NILs, we conducted a glasshouse experiment. Developing ovaries from central spikelets were taken at six different time points: heading (-5), anthesis (0 dpa), 5, 10, 15 and 20 dpa. We found non-significant differences at the first sampling point (heading -5) in both grain length and width (Figure 4.7).
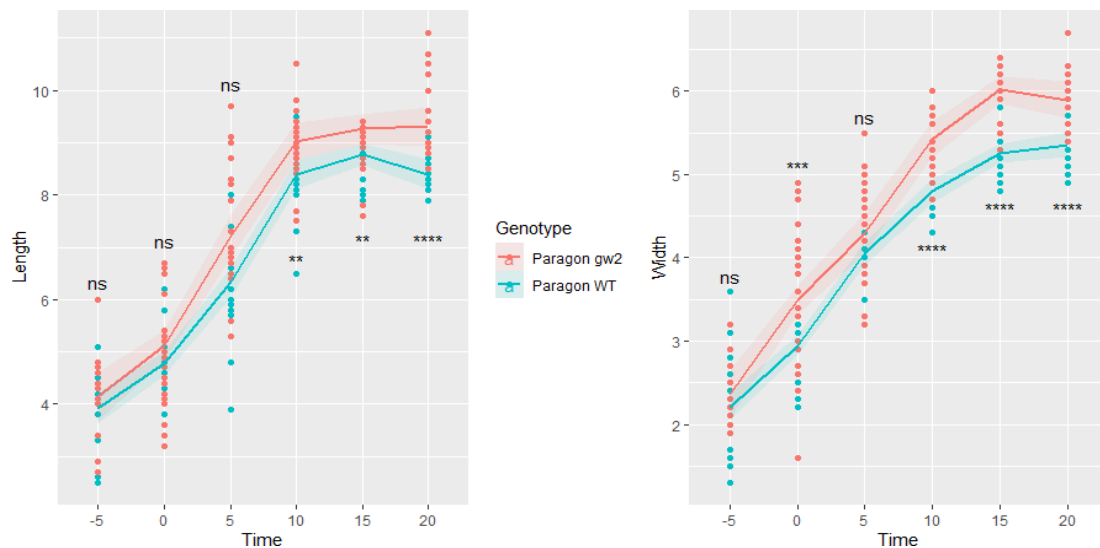
Figure 4-7: (A) Ovary/grain length (mm) in Paragon WT and Paragon *gw2* triple mutants at different developmental stages. Each data point represents the mean of twenty ovaries/grains coming from five different plants. (B) Ovary/grain width (mm) in Paragon WT and Paragon *gw2* triple mutants at different developmental stages. The lines connect the mean values of eachgenotype. Time (-5 heading, 0 anthesis, 5,10,15 and 20 days post anthesis). ns: P > 0.05; ** P < 0.01, *** P < 0.001, ****P<0.0001.

The same non-significant trait was found on grain length for the two following time points (0 and 5 dpa), until day 10, 15 and 20 after anthesis where significantly longer grains were found (*P < 0.01*, Figure 4.7). In width, we found a stronger effect from anthesis onwards (expect 5 dpa) with significant increases (*P < 0.001*, Figure 4.7) in the *gw2* triplemutant when compared to the WT NILs. These results demonstrate the robust effect on grain increases due to widergrains followed by increases on grain length in the presence of the *gw2* alleles which is consistent with what was previously reported by (Wang et al., 2018).

4.5.2. UHPLC-MS displayed significant differences on GAs content across genotypes.

We hypothesize that the abundance of the enzymes GA20-oxidase (GA20ox) and/or GA3-oxidase (GA3ox) will be higher in developing carpels at heading stage in the *gw2* triple mutants resulting in increases on bioactive forms GA$_1$ and/or GA$_4$ when compared to the WT. To test this, we conducted a UHPLC-MS analysis where 18 out of 20 GAs catabolites were quantified (Table 4.2). Most of the GAs were found to be significantly higher in the WT (10 out of 18) (Table 4.2). Both the bioactive GA$_4$ and GA$_3$ increased by 135% and 7.1% respectively, in the triple mutant (Table 4.2). Despite the increases, the concentrations of GAs in both lines are extremely low, almost beyond detection as it is measured in picogram (pg) making the interpretation and the attribution of a biologically significant effect challenging. From this experiment, we can conclude that although there are statistical differences in GAs concentrations at heading time, it may be difficult to attribute increases in ovary size in the tested NILs to GA concentrations alone.

Table 4-2: Gibberellin content (pg/mg DW) from Paragon NILs in developing carpels at heading stage. The bioactive Gas are highlighted in bold.

Pathway	Gibberellins	Paragon WT	Paragon triple *gw2* mutants	Delta (%)	*P* values (t-test)
Non-13-H Hydroxylation	**GA$_3$**	**2.45±0.27**	**2.63±0.38**	**7.14**	**0.50**
13-H	GA$_{54}$	0.46±0.02	1.40±0.06	203.38	0.006
13-H	GA$_{12}$ald	51.64±3.32	44.89±5.7	-13.08	0.47
13-H	GA$_{15}$	3.31±0.14	4.83±0.63	45.65	0.007
13-H	GA$_9$	0.27±0.0	0.19±0.0	-28.52	0.23
13-H	GA$_4$	**0.23±0.0**	**0.54±0.0**	**135.49**	**0.01**
13-H	GA$_{34}$	0.40±0.0	0.35±0.0	-11.22	0.50
13-H	GA$_{51}$	1.04±0.0	0.87±0.09	-16.37	0.12
13-OH Hydroxylation	GA$_{53}$	8.87±0.28	6.38±0.5	-28.09	0.008
13-OH	GA$_{44}$	5.45±0.22	3.44±0.09	-36.92	0.05
13-OH	GA$_{19}$	5.84±0.19	3.75±0.13	-35.783	0.04
13-OH	GA$_{20}$	1.17±0.12	0.87±0.12	-25.04	0.19
13-OH	**GA$_1$**	**1.24±0.05**	**1.21±0.01**	**-2.88**	**0.70**
13-OH	GA$_{29}$	1.69±0.12	1.05±0.03	-37.84	0.02
13-OH	GA$_8$	9.84±0.89	9.87±0.5	0.32	0.63
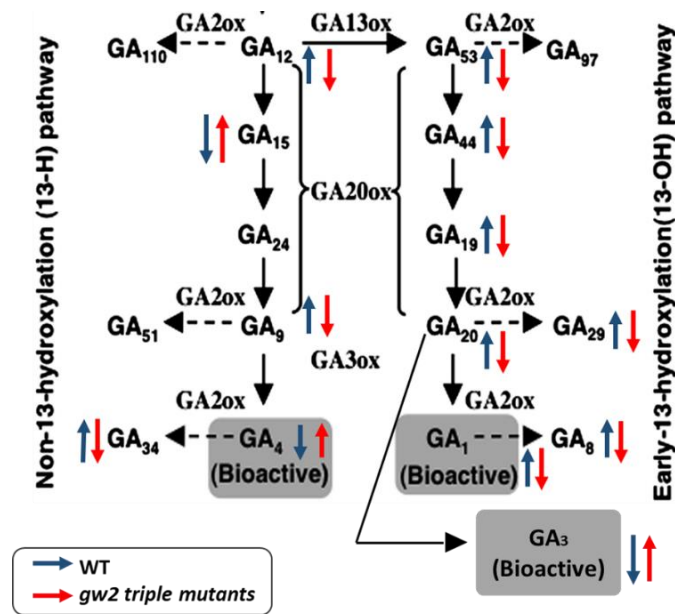
Figure 4-8: Simplified gibberellin pathway with the non-13-H (left) and 13-OH (right), the arrows indicate if each of the GA metabolites increased or decreased with the absence WT (in blue) or the presence of the *gw2* triple mutant allele (in red) in a Paragon backgroud. Values comes from UHPLC-MS analysis in table 4.2. Adapted from Magome *et al.* (2013).

The data in table 4.2 and figure 4.8 suggests that the proportion of the Non-13-H (left) and 13-OH (right) GA metabolites change between Paragon NILs. In the WT, the levels of GA_{53}, GA_{44}, GA_{19}, GA_{20}, GA_{29} increases when compared to the *gw2* triple mutants leading to higher concentrations of bioactive GA_1 but not GA_3 that was found to be more concentrated in the *gw2* triple mutants. While in the Non-13-H pathway (left) the pattern is not so clear, we found that only the GA_{15} catabolite concentration was higher in the *gw2* triple mutants leading to a higher concentration of bioactive GA_4 when compared to the WT. We hypothesize that this shift in GAs concentrations between the non-13-H and 13-OH pathways in developing carpels is somehow related to the effect of the *gw2* alleles (Table 4.2, Figure 4.8).

4.5.3. TGW was significantly reduced in the gw2 triple mutants treated with PAC in 2020

In 2020 we conducted a GH experiment where we applied contrasting treatments; GA_3 was directly sprayed onto spikes at a concentration of 10 μM at flowering time, other plants were treated with PAC 1 μM at booting stage and a different set of plants were first treated with PAC at booting followed by GA_3 spraying at flowering time (Figure 4.9).
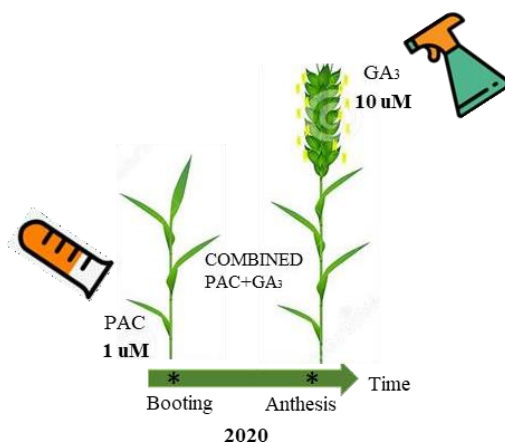
Figure 4-9: Glasshouse 2020 treatments, PAC was applied at booting via root uptake, while GA_3 was sprayed at anthesis.

This experiment was conducted in order to investigate the effect of GA on grain size in the triple mutants as conflicting results were reported by (Li et al., 2017) and (Sestili et al., 2019b) in *gw2-A1* single mutants and *GW2* RNAi lines, respectively. The first authors reported an overexpression of the *GA3ox* gene while the others a very low expression. Furthermore, we applied PAC to study how the depletion of GAs might influence final grain size. The combined treatment (PAC+GA) was conducted first to deplete the plant from GAs and then, to try to rescue the bigger grain size phenotype in the triple mutants.

We found that in the WT, TGW was not affected with the application of GA_3 at anthesis. In Paragon *gw2* triple mutants a borderline effect was found ($P < 0.05$) where a 3.8% reduction in weight was observed when compared to the control (Figure 4.10). PAC 1 μM does not affect final grain weight in Paragon WT; on the other hand, PAC 1 μM decreases significantly ($P < 0.0001$) final grain weight by 18.3% (reducing it from 55.1 g to 45.0 g) in triple mutants. The combined PAC+GA treatment affected grain weight in both genotypes in contrasting ways. In Paragon WT, final weight increased significantly ($P < 0.01$) by 5.4% (42 g vs 40 g, Table 4.3) when compared to the control. In contrast, in Paragon *gw2* NILs we see a significant reduction ($P < 0.0001$) of 15.4% on grain weight (46.6 g vs 55.5 g) when compared to the control (Figure 4.10, Table 4.3). Taken all together, we see no effect in Paragon WT (except combined treatment), while PAC induces significant reductions in grain weight only in Paragon *gw2*, which might indicate that GAs are involved in the bigger grain size phenotype. In the combined PAC+GA treatment, TGW slightly increases when compared to the PAC 1 μM treatment in both genotypes, albeit not significantly.
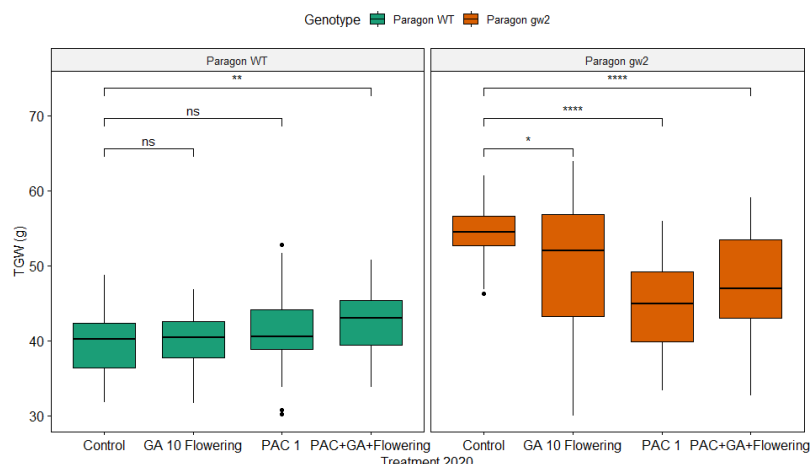
Figure 4-10: TGW (g) in Paragon WT and *gw2* triple mutants in response to GA, PAC and PAC+GA treatments at different time points. The box represents the middle 50% of data with the borders of the box representing the 25th and 75th percentile. The horizontal line in the middle of the box represents the median. Whiskers represent the minimum and maximum values, unless a point exceeds 1.5 times the interquartile range in which case the whisker represents this value and values beyond this are plotted as single points (outliers). Statistical classifications are based on Tukey's HSD tests. ns: $P > 0.05$; *$P < 0.05$; ** $P < 0.01$; **** $P < 0.0001$.

Table 4-3: TGW in response to PAC, GA and PAC+GA treatments

Genotypes	Control	GA 10 Flowering	PAC 1	PAC+GA
Paragon WT	40.1 ± 2.0	40.0 ± 1.6	42.0 ± 1.65	43 ± 0.92
Paragon gw2	55.1 ± 1.5	53.0 ± 1.8	45.0 ± 1.83	46.6 ± 1.02
%	37	32.5	7.1	8.3

4.5.4. Width and length are significantly reduced in Paragon gw2 treated with PAC in 2020

Grain width was not affected by any of the treatments in Paragon WT, including the combined treatment which resulted in a statistically significant difference for TGW. On the contrary, in Paragon *gw2*, PAC 1 μM reduced width significantly ($P < 0.0001$) by 7.5% (4 mm vs 3.7 mm, Figure 4.11, Table 4.4). In the combined treatment width was significantly reduced ($P < 0.01$) by 5% (4 mm vs 3.8 mm). Regarding length, GA treatments were found to be non-significant in both genotypes. The PAC 1 μM treatments have contrasting effects: in Paragon WT length increased slightly ($P < 0.01$) by 1.5% (6.4 mm vs 6.3 mm) while in Paragon *gw2* we found a significant decreased in length ($P < 0.01$) by 2.98% (6.5 mm vs 6.7 mm). Finally, in the combined treatment, a borderline ($P < 0.05$) reduction by 6.4% in length was found in Paragon WT and a non-significant effect was found in Paragon *gw2* (Table 4.5).

In sum, we did not observe any effect of the GA$_3$ treatment on grainweight (except for a slight decrease in TGW in the triples) and size in both genotypes, while in the PAC treatments, the only detrimental effect was found in the triple mutants. In the combined treatment, we found contrasting effects as length increase in the WT while width decrease in the triple mutants. We hypothesize that the effect of GAs was marginal because of the application time (flowering), furthermore we wanted to try with a different GA dose. The detrimental effect on PAC only in the triple mutants caught our attention, hence we decided to repeat the experiment this time testing two different doses. In our next experiment, we are going to test different GA$_3$ and PAC doses applied at different time points.
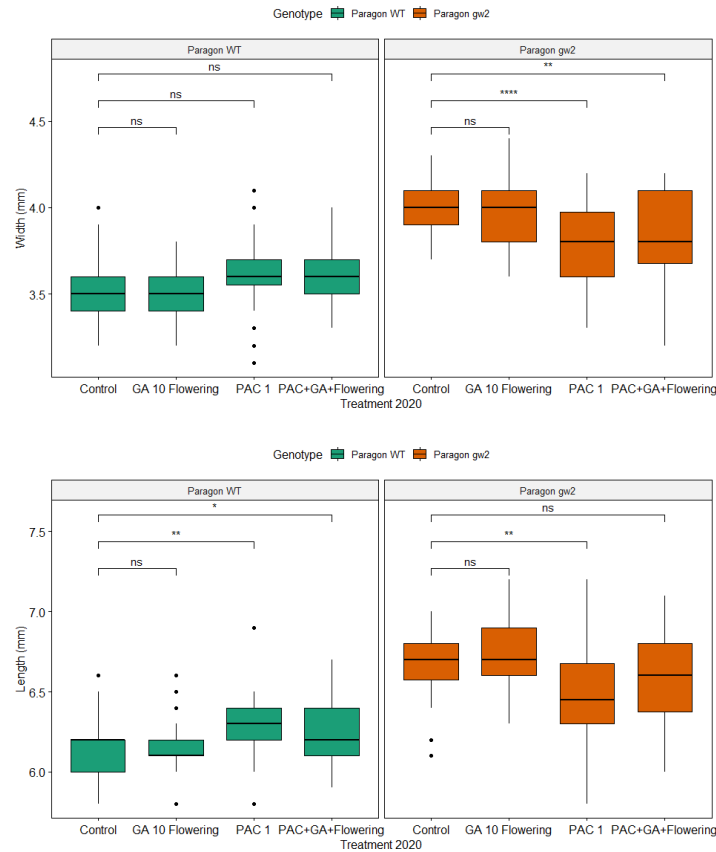
Figure 4-11: Width and Length (mm) in Paragon WT and gw2 triple mutants in response to GA, PAC and PAC+GA treatments at different time points. The box represents the middle 50% of data with the borders of the box representing the 25th and 75th percentile. Statistical classifications are based on Tukey's HSD tests. ns: $P > 0.05$; $*P < 0.05$; $** P < 0.01$; $**** P < 0.0001$.

Table 4-4: Grain width in response to PAC, GA and PAC+ GA treatments

Genotypes	Control	GA 10 Flowering	PAC 1	PAC+GA
Paragon WT	3.5 ±0.05	3.5 ±0.03	3.6±0.05	3.5±0.03
Paragon *gw2*	4.0±0.04	3.9±0.03	3.7 ±0.06	3.8±0.03
%	14	11.5	2.7	8.5

Table 4-5: Grain length in response to PAC, GA and PAC+ GA treatments

Genotypes	Control	GA 10 Flowering	PAC 1	PAC+GA
Paragon WT	6.3±0.07	6.1 ±0.07	6.4 ±0.05	6.2±0.03
Paragon *gw2*	6.7 ±0.06	6.7 ±0.05	6.5 ±0.09	6.6±0.04
%	6.34	9.8	1.5	6.4

4.5.5. *PAC reduces TGW significantly in the gw2 triple mutants in 2021*

In the 2020 results, we observed a significant reduction on final grain weight in the *gw2* triple mutants treated with PAC. To corroborate these results and to see if there was an effect at lower concentrations of PAC, we grew plants from Paragon WT and Paragon *gw2* triple mutants and we treated them with two different PAC doses (0.5 µM and 1 µM) at booting stage for 14 days, in addition to the control treated with water. We found a significant interaction between PAC treatment and genotype ($P < 0.05$), and therefore we examined the simple effects. In the WT, we found that the PAC treatment did not affect final grain weight at a lower concentration, but that TGW increased in the highest PAC 1 µM concentration by 7.14% (44.8 g vs 41.6 g, Figure 4.12, Table 4.6). On the other hand, in the *gw2* triple mutants, PAC decreased TGW significantly in a dose dependant manner by 13% (43.2 g vs 50.2g) and by 16.5% (41.9g vs 50.2g) in the PAC 0.5 uM and PAC 1 uM treatments respectively (Figure 4.12, Table 4.6). These findings are consistent with what was observed in 2020, when the *gw2* triple mutant plants treated with PAC 1 uM resulted in 25% lighter grains than the untreated *gw2* triple mutants plants. In both years, PAC eliminated the effect of the *gw2* triple mutant on final TGW. These results support our hypothesis that if the GA pathway is blocked at booting stage, the Paragon *gw2* triple mutant loses the heavier grain size phenotype and produces grains with a final grain weight matching those of Paragon WT plants.
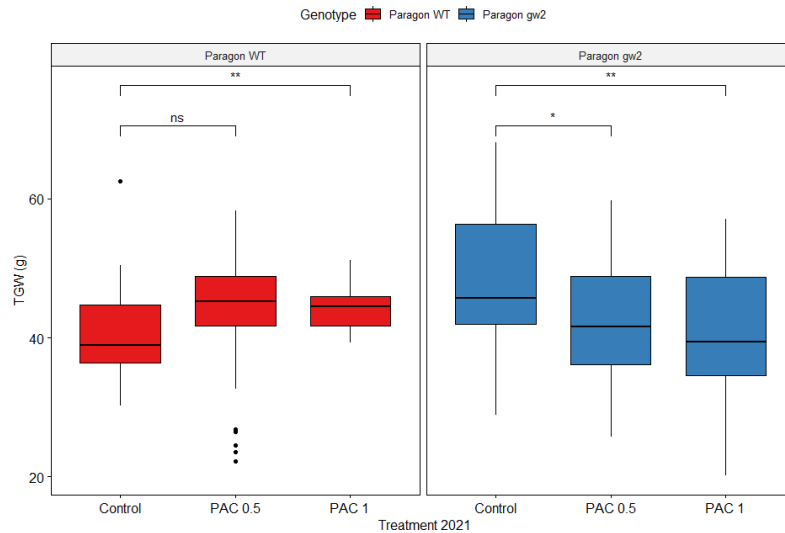
Figure 4-12: TGW (g) in Paragon WT and *gw2* triple mutants in response to PAC treatments at booting. The box represents the middle 50% of data with the borders of the box representing the 25th and 75th percentile. The horizontal line in the middle of the box represents the median. Whiskers represent the minimum and maximum values, unless a point exceeds 1.5 times the interquartile range in which case the whisker represents this value and values beyond this are plotted as single points (outliers). Statistical classifications are based on Tukey's HSD tests. ns: $P > 0.05$; *$P < 0.05$; ** $P < 0.01$.

Table 4-6: Average TGW (g) of Paragon WT and *gw2* triple mutants in response to PAC treatments at booting. Values represent the means of ten plants. Percentage (%) values at the bottom refer to the difference between genotypes the wild type and the mutant lines.

Genotypes	TGW in response to PAC treatments		
	PAC 0 (control)	PAC 0.5μM	PAC 1μM
Paragon WT	41.6 ± 1.8	44.3 ± 1.8	44.8 ± 1.8
Paragon *gw2*	50.2 ± 2.0	43.2 ± 1.6	41.9 ± 1.6
%	20.6	-2.4	-6.4

4.5.6. GAs increases on grain weight are time dependant rather than dose dependant

In the experiment carried out in 2020, no effect was found on TGW when GA 10 μM was applied at flowering time. We hypothesised that applying GAs at heading time (~5 days before flowering) and at flowering time at two different doses (5 μM and 10 μM) would induce ovary growth that would translate in heavier and bigger final grain size. We used the same Paragon WT and *gw2* triple mutant NILs to measure the effect of gibberellins on final grain weight. We tagged primary spikes and treated them with GA$_3$ at 5 μM and 10 μM starting at heading or anthesis for five consecutive days (Figure 4.13).
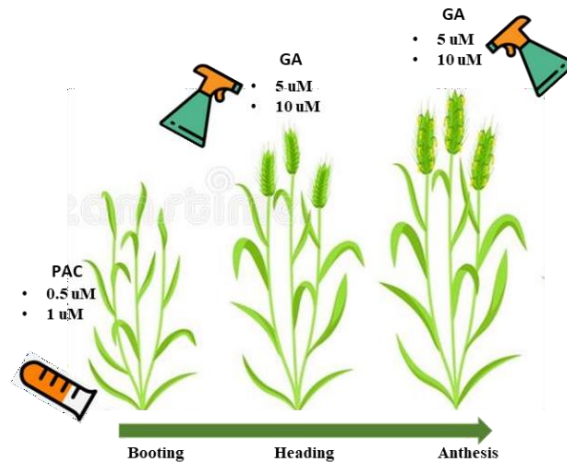
Figure 4-13: Glasshouse experiments 2021. PAC was added at booting stage at different concentrations, while GA₃ was sprayed at heading and anthesis at different concentrations.

Mature spikes were harvested and threshed. We first compared the effect of GA within each genotype (Figure 4.14); we found that the only significant difference ($P < 0.01$) was in the WT NILs, where the GA treatments both at heading and flowering increased the grain weight (Table 4.7). Firstly, in Paragon WT plants, TGW increased by 12% when GA 5 μM was applied at heading with respect to non-treated control plants, but this effect was not significant. However, a highly significant effect was seen for GA application at flowering time ($P < 0.0001$; Figure 4.14). In the MT genotype, a more variable effect was observed with non-significant reductions on final gran weight regardless of the dose and application time (except for GA10 μM at heading which reduced TGW) (Figure 4.14, Table 4.7). In summary, we found that GAs increased TGW only in the WT, especially when the plant hormone was applied at flowering time, and that the highest concentration (GA10 μM) almost approaches the TGW of the triple mutants, in contrast to the triple mutants which were not responsive to GAs.
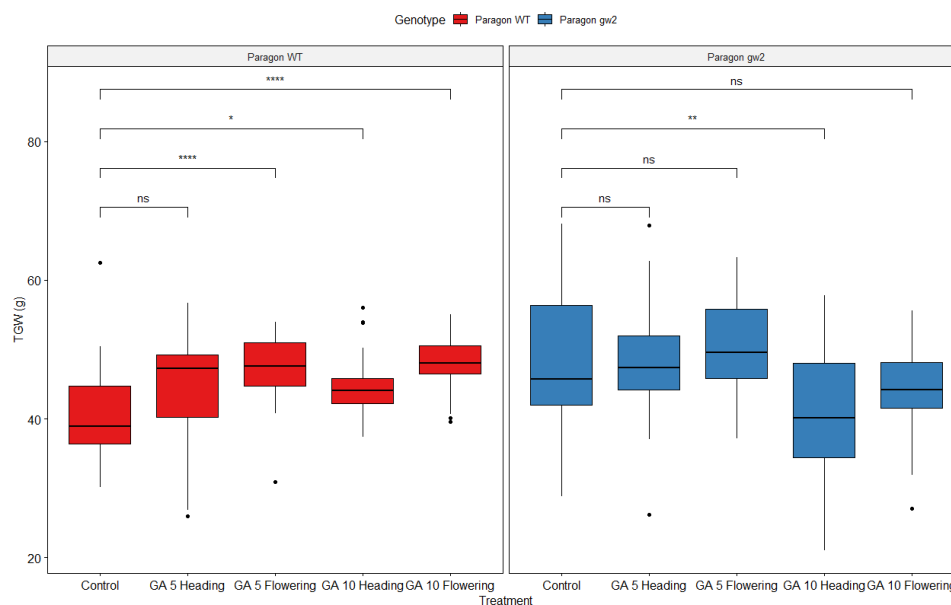
Figure 4-14: (A) TGW (g) in response to treatment GA5 µm and GA10 µM treatments. The box represents the middle 50% of data with the borders of the box representing the 25th and 75th percentile (as described above).ns: *P* > 0.05; **P < 0.01; ****P < 0.0001.

Table 4-7: Average TGW (g) of Paragon WT and gw2 triple mutants in response to GA treatments at heading (H) and flowering (F). Values represent the means from 10 plants. Percentage (%) values at the bottom refer to the difference between genotypes the wild type and the mutant lines.

Genotypes	control	GA 5 H	GA 5 F	GA 10 H	GA 10 F
Paragon WT	41.6 ± 1.83	45.5±1.76	47.4±1.76	45.5±1.99	48.8±1.7
Paragon gw2	50.2 ±2.00	50.0±1.76	51.9±1.67	40.9±1.87	44.3±2
%	20.6 **	9.8	9.4	-10.7	-7.4

4.5.7. *PAC has contrasting effects on grain morphometrics depending on the genotype*

In 2020 we found that PAC 1 µM treatments did not affect grain length and width in the WT while both length and width dropped significantly in the triple mutants. For that reason, we wanted to assess in the following year the consistency of the effect on final grain morphometrics at both PAC 0.5 µM and PAC 1 µM doses. We conducted a two-way ANOVA for length, we found that, the variables genotype ($P < 0.001$) and treatment ($P < 0.05$) were significant. The interaction between genotype and treatment was also significant ($P < 0.001$), and therefore simple effects were analysed. In the WT, we found that all PAC treatments were significant. Firstly, a 5.3% increase in final grain length ($P < 0.001$) was found when PAC 0.5 was applied (Figure 4.15), whereas a 4.3% increase ($P < 0.001$) was found when PAC 1 was applied in comparison with the control (Table 4.8). In contrast, in the MT genotype we see that final length tends to decrease but only as a borderline significant ($P < 0.50$) effect in the lower dose. A comparison between treatments was carried out; regardless of the PAC treatment, grain length was found to be significantly higher in the MT ($P < 0.01$). As for grain width, in the WT grain in increased significantly in both PAC

treatments (P <0.01 and P <0.001) while in the MT, grain it remained the same compared with the control (Figure 4.15) (Table 4.9). In a two-way ANOVA for width, the variable treatment resulted highly significant as well as the interaction between genotype and treatment (P <0.001). We found contrasting effects in the treatments across the two years. In 2021 grain length and width were not affected when PAC 0.5 μM or PAC 1 μM were applied at booting in the *gw2* triple mutant lines while the positive effect in the WT lines is most likely linked to variations between the plants and the tested spikes. In 2020, PAC 1 μM treatment did not affect grain morphometrics in the WT while in the *gw2* triple mutants both length and width decrease significantly.
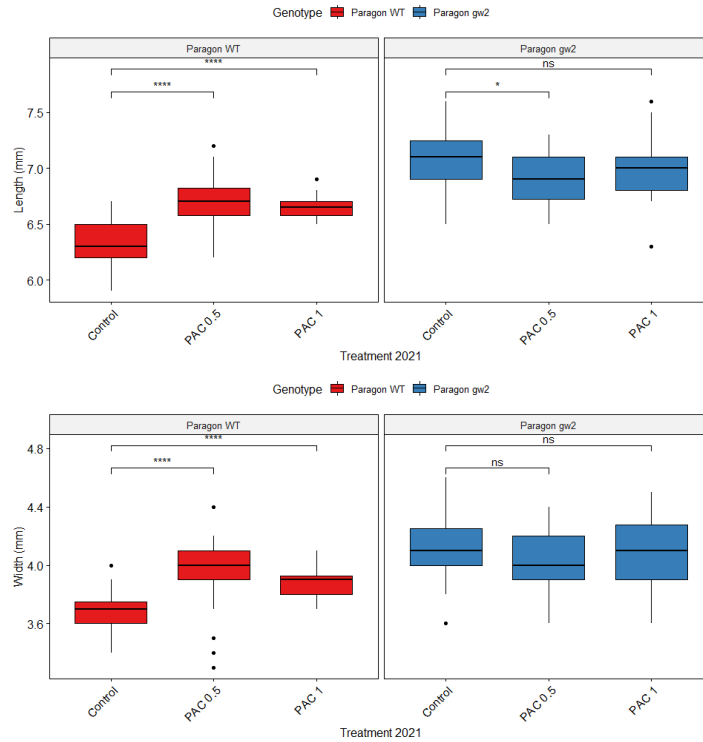
Figure 4-15: Length and width (mm) in Paragon WT and *gw2* triple mutants in response to PAC treatments at booting. The box represents the middle 50% of data with the borders of the box representing the 25th and 75th percentile. ns: $P > 0.05$; *$P < 0.5$; **$P < 0.01$; ****P<0.0001.

Table 4-8: Average length of Paragon WT and gw2 triple mutants in response to PAC treatments at booting. Values represent the means from 10 plants. Percentage (%) values at the bottom refer to the difference between the wild type and the mutant lines

Genotypes	control	PAC 0.5 μM	PAC 1 μM
Paragon WT	6.36±0.07	6.77±0.06	6.65±0.0
Paragon *gw2*	7±0.06	6.98±0.05	6.97±0.05
%	17	3.1	4.8

Table 4-9: Average width of Paragon WT and *gw2* triple mutants in response to PAC treatments at booting. Values represent the means from 10 plants. Percentage (%) values at the bottom refer to the difference between the wild type and the mutant lines.

Genotypes	control	PAC 0.5 uM	PAC1 uM
Paragon WT	3.68±0.05	3.92±0.05	3.88±0.04
Paragon *gw2*	4.14±0.05	3.94±0.04	4.04±0.04
%	12.5	0.5	4.12

4.5.8. GAs increases length and width only in Paragon WT

As stated above, we wanted to assess the effect of GAs on grain morphometrics. In Figure 4.16, we can see that in the WT, grain length increased significantly ($P < 0.001$) when GAs were applied at both heading and anthesis (Table 4.10). We conducted a two-way ANOVA, which revealed that genotype, treatment and the interaction were all significant ($P < 0.001$). Next, we conducted a post-hoc Tukey test that highlighted both GA treatments as highly significant ($P < 0.01$) when compared with the control (Figure 4.16). In the triple mutants, length in response to treatment was non-significant, with only a borderline effect on GA_{10} emerging at flowering. Despite the significant increase in grain length in the WT compared to the non-significant response in the MT, grain length is still significantly longer in the MT plants independent of the GA treatment. The same response pattern was found in width, where we found a significant interaction between GA treatments and genotype ($P < 0.001$). In the WT, we found that GAs significantly increased width ($P < 0.001$) (Table 4.11). A non-significant effect was found in the MT, suggesting that GAs do not influence final grain width or length regardless of the dose and application time. As a general conclusion, we can see that both GA treatments increased grain morphometrics in the WT, regardless of concentrations (5 µM and 10 µM) or application time points (heading and flowering). Contrary to this, we found no effect in the MT on final grain length and width when GAs were applied. These findings agree with the results from 2020, which showed that final width and length were not affected in the MT by GA spraying. In contrast, grain morphometrics was affected in 2021 by both GA treatments whereas in 2020 no effect was recorded in the WT.
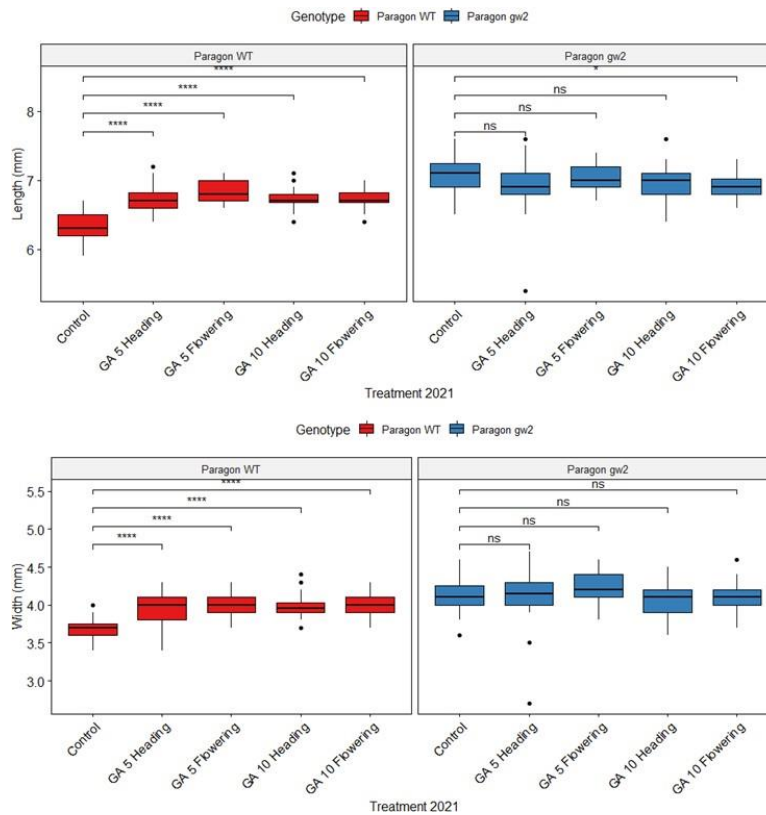
Figure 4-16: Length (mm) and width (mm) in Paragon WT and *gw2* triple mutants in response to GA5 uM and GA10 uM treatments at heading and flowering. The box represents the middle 50% of data with the borders of the box representing the 25th and 75th percentile. ns: $P > 0.05$; **** $P < 0.0001$.

Table 4-10: Average length (mm) of Paragon WT and *gw2* triple mutants in response to GA treatments at heading and flowering. Values represent the means from 10 plants. Percentage (%) values at the bottom refer to the difference between genotypes normalized for the wild type.

Genotypes	control	GA 5 H	GA 5 F	GA 10 H	GA 10 F
Paragon WT	6.36±0.07	6.80±0.06	6.86±0.06	6.77±0.06	6.78±0.06
Paragon *gw2*	7.11±0.06	6.97±0.05	7.06±0.05	6.97±0.06	6.96±0.06
%	11.7	2.5	2.9	2.9	2.8

Table 4-11: Average width (mm) of Paragon WT and *gw2* triple mutants in response to GA treatments at heading and flowering. Values represent the means from 10 plants. Percentage (%) values at the bottom refer to the difference between genotypes normalized for the wild type.

Genotypes	control	GA 5 H	GA 5 F	GA 10 H	GA 10 F
Paragon WT	3.68±0.05	3.94±0.04	3.98±0.04	3.97±0.05	4.01±0.04
Paragon *gw2*	4.14±0.05	4.15±0.04	4.25±0.04	4.02±0.05	4.09±0.05
%	12.5	5.3	6.3	1.25	1.9

4.5.9. *Height is not affected by GA nor PAC in both genotypes*

We measured internodes, peduncle and spike length at maturity to see if different treatment had an influence on final height (Figure 4.17, Table 4.12)
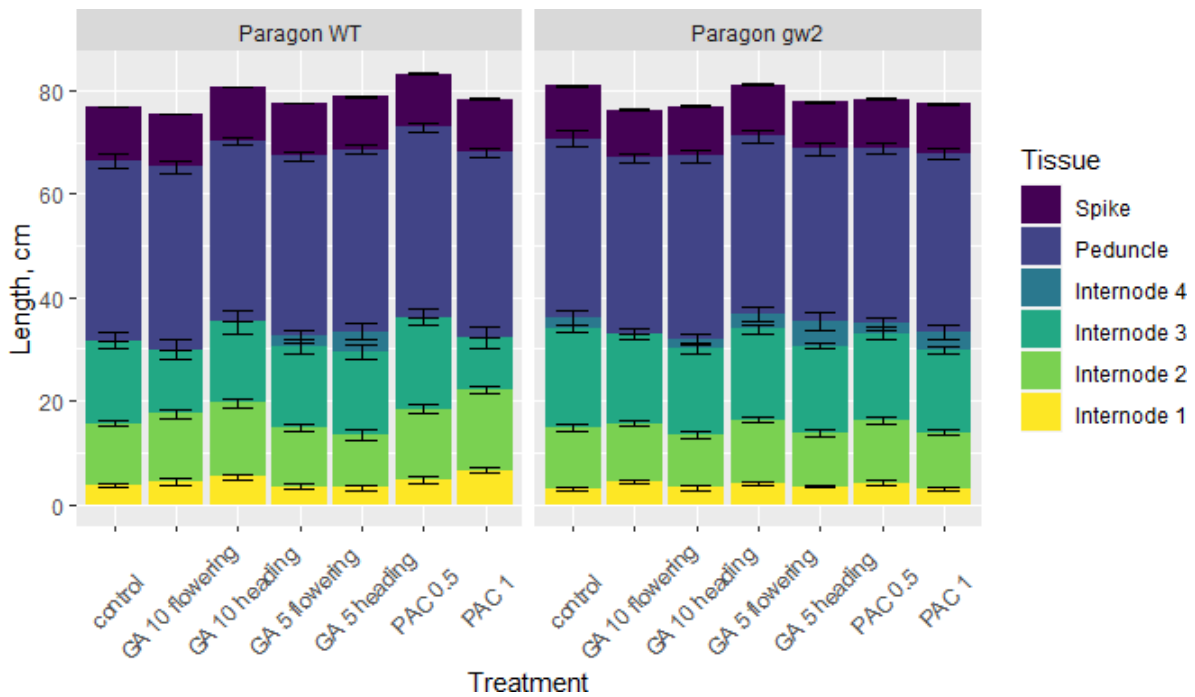
Figure 4-17: Stacked box plot of final length (cm) in Paragon WT and Paragon *gw2* triple mutants. Error bars represent the standard error of the total length per tissue.

Table 4-12: Average height (cm) of Paragon WT and *gw2* triple mutants (in cm) in response to different treatments at maturity. Values represent the means from 30 tillers per genotype and per treatment.

Genotypes	control	GA 10 F	GA 10 H	GA 5 F	GA 5 H	PAC 0.5	PAC 1
Paragon WT	76.8 ± 1.31	76.2 ± 1.31	80.2 ± 1.22	77.5 ± 1.10	78.8 ± 1.10	83.1 ± 1.10	78.3 ± 1.31
Paragon *gw2*	80.9 ± 1.22	75.4 ± 1.15	76.9 ± 1.31	81.1 ± 1.15	77.7 ± 1.15	78.3 ± 1.31	77.4 ± 1.31
%	5.3	-1.04	-4.11	4.64	-1.39	-5.77	-1.14

We found that none of the treatments affected final height ($P > 0.05$) and tissue length ($P > 0.05$) (spike, peduncle and internodes). This was unexpected in the PAC treatments as we applied it at booting time, before peduncle elongation, and Davis et al (1991) reported that PAC is a cell elongation and internode extension inhibitor. On the other hand, the GA treatments were applied at flowering time when internodes, peduncle and spike were elongated and the spike fully developed, so the overlapping measures with the controls were to be expected.

4.5.10. Increases in pericarp cell length are related to the gw2 alleles.

In order to understand whether increases in grain size were due to cell proliferation or cell expansion, we measured pericarp length and width from a set of mature grains that were imaged with SEM. Mature grains from the 2019 field season were selected from Paragon WT and *gw2* triple mutants NIL following the criteria described earlier (section 4.3.4). Briefly, in the normal distribution group (Figure 4.18, left) seeds from the WT were smaller than those of the triple mutants while in the overlap group (Figure 4.18, right) we selected seed from both NILs with similar lengths and widths. The first comparison was between the normal distribution group where on average triple mutants had a 34% significant increase in mean cell length ($P < 0.0001$) compared to average WT in the bottom of the grain. Conversely, in the top a 13% significant increase was found ($P < 0.0001$) when compared to the WT. In the overlap group, we see the opposite pattern on cell length where, a reduction of 14% and 21.3% ($P = 0.030$) was found in the bottom and in the top respectively, when compared to the WT (Figure 4.18). In figure 4.19, we found that cell width significantly increased in the normal distribution group by 14.6 % and by 4.6 % (P=0.040) in the bottom and in the top of the grain, respectively, when compared with the WT. In the overlap group, once again we found the opposite effect, with cell width decreasing by 16% and 19.8% in the bottom and in the top, respectively, in the *gw2* triple mutant compared the wildtype. Finally, we plotted and estimated cell number as follows: cell number= grain length (mm)/ mean cell length (µm) *1000. We found that Paragon WT has more cell than Paragon *gw2* in the normal distribution while in the overlap group, Paragon WT has significantly (P < 0.01) fewer cells than Paragon *gw2* (Figure 4.20). In summary, our results suggest that increases in grain length and width in Paragon *gw2* are related to increases on pericarp cell length and width.
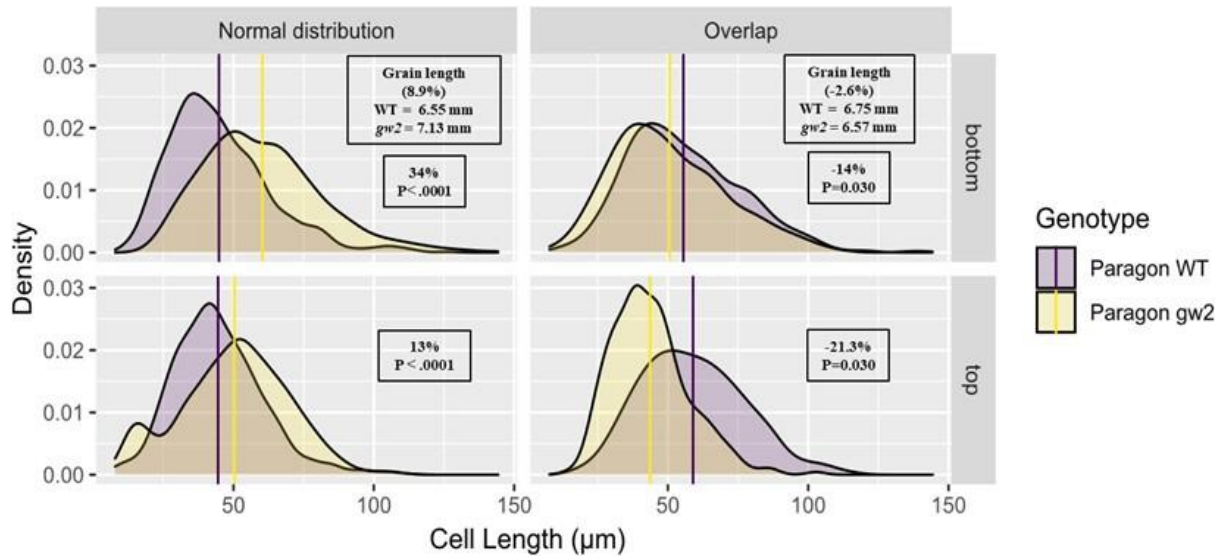
Figure 4-18: Comparison of pericarp cell length in Paragon WT and *gw2* triple mutants NILs. Density plots of cell length and width measured in 18 grains per genotype in 2019; lines represent the mean of values of cell length and width. Grain length insets at the top show the average grain length and delta (%) of each of the grains used in the study, as derived from mixed effect models having length as response variable, genotype and position as fixed effects and seed ID as a random effect. A model was fitted to each distribution. The delta values and the P values represent the differences in cell length and width in the different groups according to the same models.
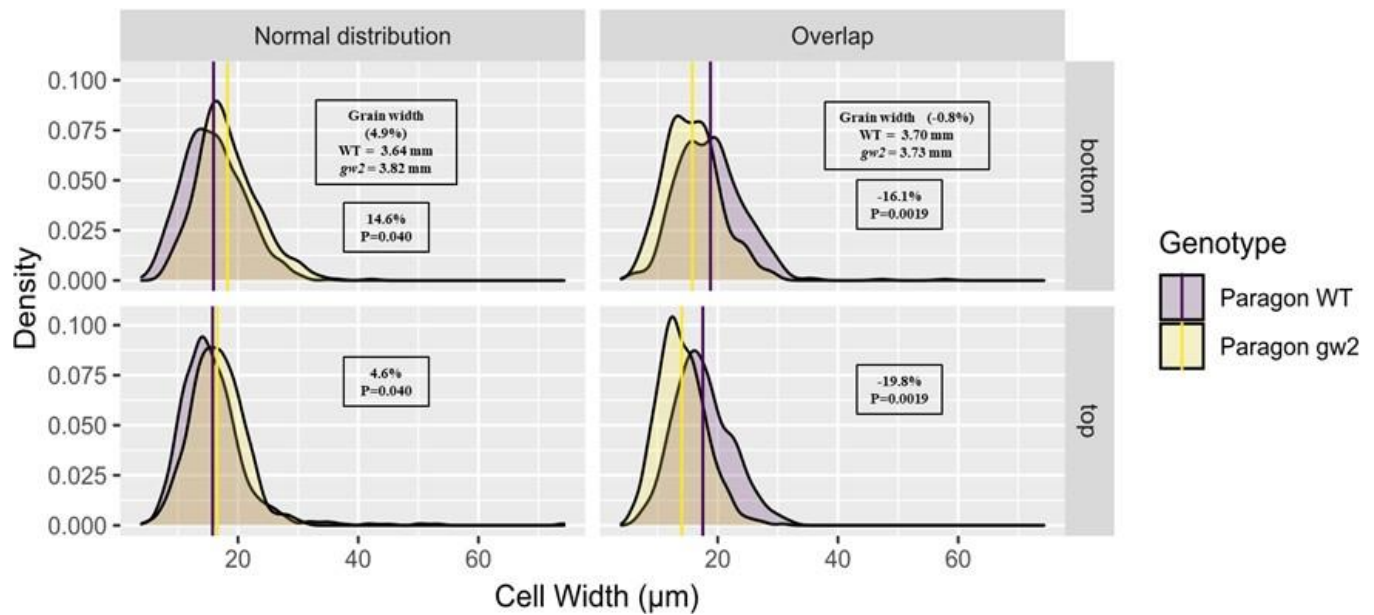
Figure 4-19: Comparison of pericarp cell width in Paragon WT and *gw2* triple mutants NILs. Density plots of cell length and width measured in 18 grains per genotype in 2019; lines represent the mean of values of cell length and width. Grain width insets at the top show the average grain width and delta (%) of each of the grains used in the study, as derived from mixed effect models having width as response variable, genotype and position as fixed effects and seed ID as a random effect. A model was fitted to each distribution. The delta values and the P values represent the differences in cell length and width in the different groups according to the same models.
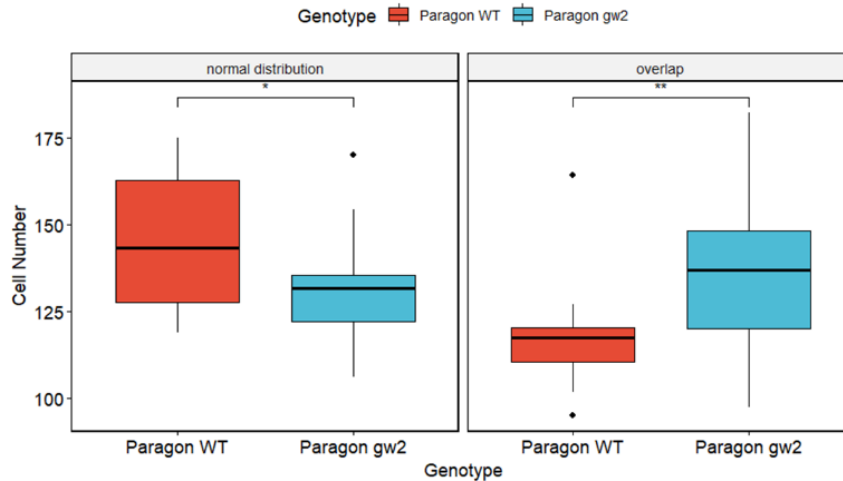
Figure 4-20: Cell number in Paragon WT and Paragon *gw2*. The box represents the middle 50% of data with the borders of the box representing the 25th and 75th percentile (as described above). * $P < 0.05$; **$P < 0.01$.

4.5.11. The gw2 mutant allele increases grain weight and size independently from the semi dwarf allele (Rht-B1b)

We hypothesized that GAs are involved in bigger grain size and weight in Paragon *gw2* triple mutants. Furthermore, we hypothesized that the *gw2* and *Rht-B1b* alleles (DELLA protein) might alter the response of the gibberellin synthesis affecting grain size. For these reasons, we crossed the "tall Rht-B1a" Paragon *gw2* triple mutants(referred to as Tall NILs) (BC_2F_3) plants to the semi-dwarf Paragon *Rht-B1b* (BC_2F_3) NILs. Across two growingseasons we measured yield, grain morphometrics and height. Firstly, we wanted to understand if the *RHT* allelesinteract with the *gw2* alleles affecting grain size, weight and yield. Secondly, in the field, we measured height to corroborate that the semi-dwarf allele was correctly introgressed. As expected, we found that final height (cm) was significantly reduced (by 10% and 20% in 2021 and 2022 respectively in the semi-dwarf lines (Table 4.13, Figure 4.21 and 4.22). This coincides with previous reports on the effect of the *Rht-B1b* allele where a 15% - 20% decrease in plant height has been measured (Jobson et al., 2019).

We then analysed TGW, seed morphometrics and yield. TGW increased significantly ($P \leq 0.001$) by 18% in 2021 and by 25% in 2022 in the Tall NILs carrying the *gw2* alleles when compared to the *GW2* (WT) controls (in green Figure 4.21 and 4.22).Grain length increased significantly ($P \leq 0.001$) by 7.9% and 4.9% in 2021 and by 9.0% and 5.6% across the two-growing season in the semi-dwarf and tall lines carrying the *gw2* alleles, respectively (Table 4.13). Following the same trend,grain width increased significantly ($P \leq 0.001$) by 7.9% and 9% in the tall/ *gw2* triple mutants, while in the semi-dwarf/*gw2* triple mutants, width increased by 1% and by 6.5% in 2021 and 2022, respectively (Table 4.13). Yielddropped significantly ($P < 0.01$) by 4.8% in the NILs carrying both the semi-dwarf allele/ *gw2* triple mutations in2021, while in 2022 a significant ($P < 0.01$) 8.2% decrease on final yield was found when compared to the Tall/*GW2* (WT/WT) (Figure 4.21 and Figure 4.22). The detrimental effect on yield caused by the triple introgression of *gw2* alleles was previouslyreported in Chapter 2 in a Paragon background. To our surprise, yield did not drop significantly in the tall mutantscarrying the *gw2* triple mutation (in green). These results are unexpected based on what we previously reported in

Chapter 2, where across two growing season yield dropped significantly by 5.8% and 3.6% in 2020 and 2021, respectively. This might indicate that yield losses are due to variation in the field across different plots rather than related to the genotypes. Finally, we found that protein content increased significantly by 4.4% and 6.4% across seasons in the Paragon *gw2* triple mutant (independently from the semi-dwarf allele) (Figure 4.21 and Figure 4.22), these results being in line with what we found in chapter 2. We also found significant protein increases in the NILs with the semi-dwarf/*gw2* triple mutants by 1.8% and 4.1% in winter and spring sowing (Table 4.13, Figure 4.21 and 4.22). This goes against what was previously reported by several authors; one of the most well documented trade-offs of the semi-dwarf alleles being the reduction of seed size and protein content by 15% and by 12% respectively (Jobson et al., 2019). Here, we found that the semi-dwarf/*gw2* triple mutants increased grain weight, size and protein content consistently across season.
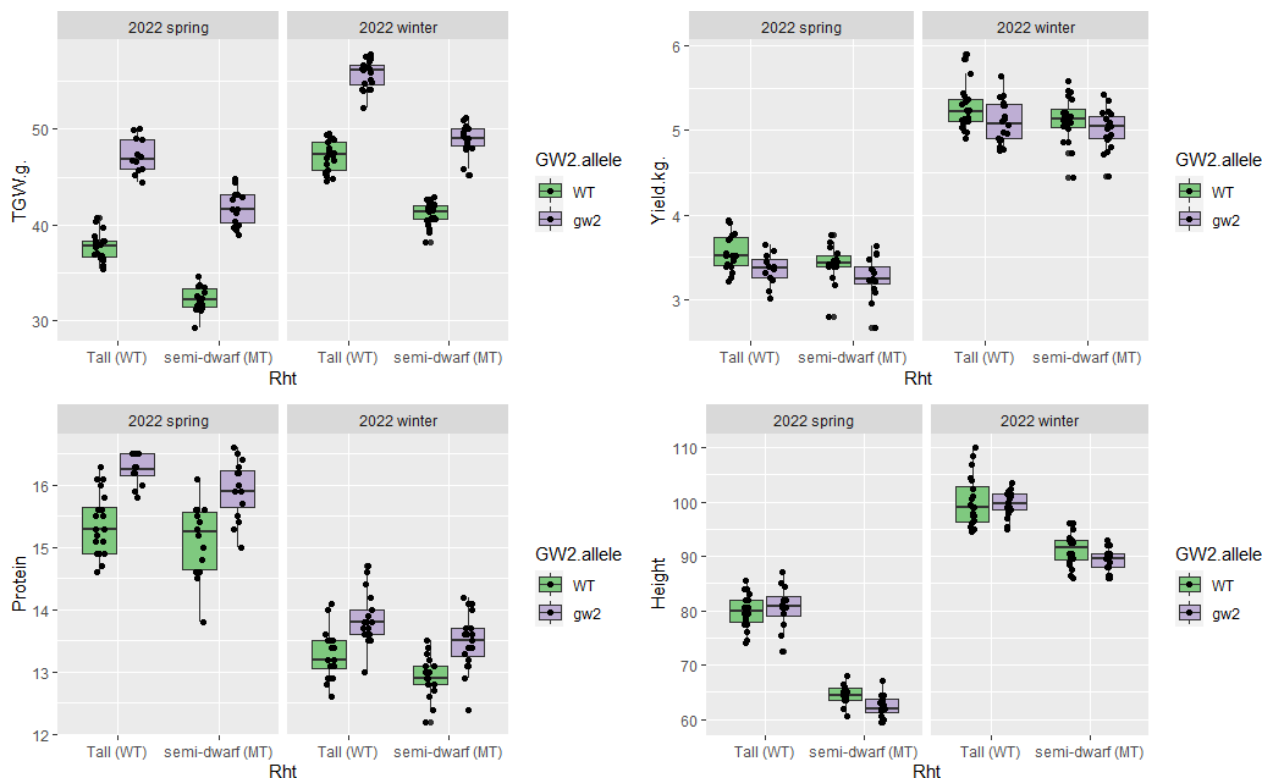
Figure 4-21: TGW, Yield, Protein content and height across two growing seasons in Paragon NILS for height and grain size. The box represents the middle 50% of data with the borders of the box representing the 25th and 75th percentile. Each dot represents a plot in the field.
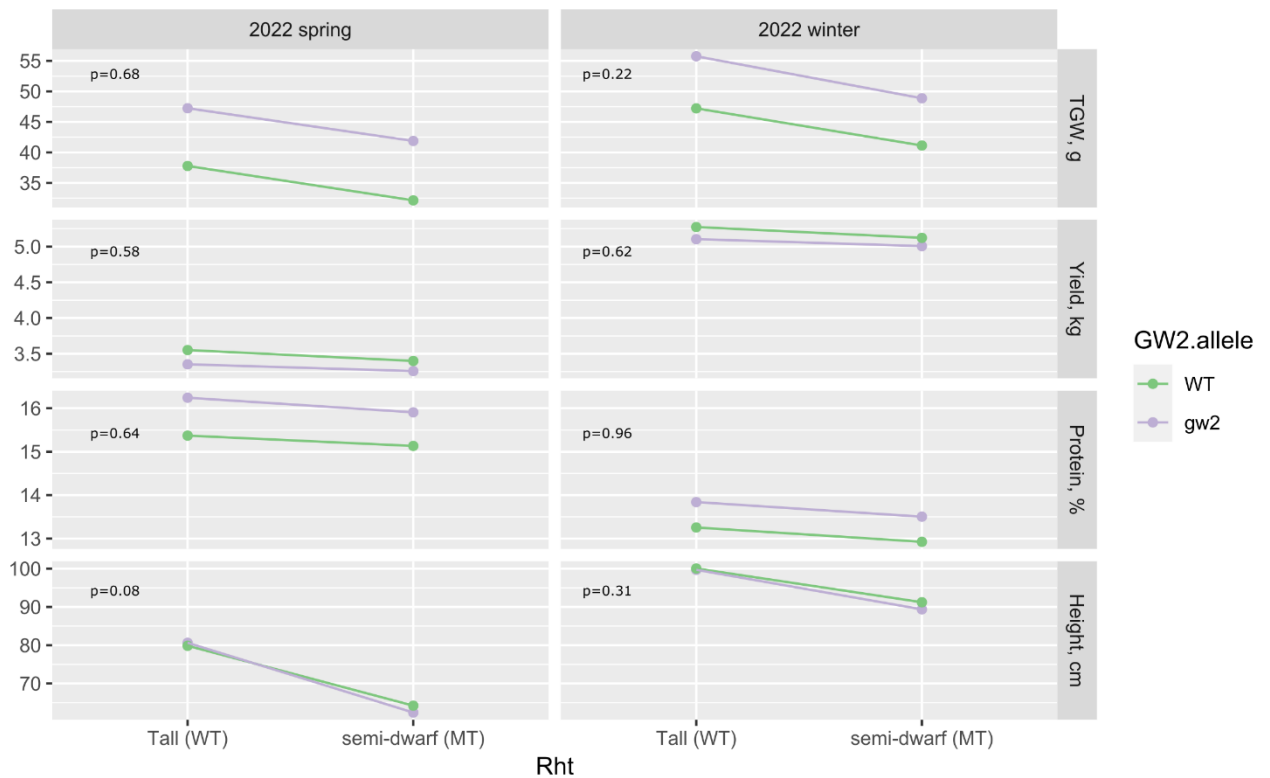
Figure 4-22: Interaction plots with P values for TGW, yield, protein content and height across two growing seasons in Paragon NILS. The dots represent marginal means derived from the model having replicate block, *Rht* and *GW2* allele plus their interaction; the p values refer to the interaction between *Rht* and *GW2* in the same model.

Lastly, we generated interaction plots to visualize if there is a significant interaction between *GW2* x *Rht* alleles and the variables under consideration: TGW, yield, protein content and height. We found no significant interactions between the alleles and the response variables. We would like to highlight that height was not affected by the presence of the *gw2* triple mutant alleles (Figure 4.22, last panel in purple) which is consistent with what we previously reported in UK trials in a Paragon background (Chapter 2, Table 2.3). In contrast, after two years of field experiments in Mexico we found that in both cv Reedling and Kingbird, height was significantly reduced in irrigated plots with the presence of the *gw2* mutant alleles. These contrasting results might be due to environmental factors (the three are spring wheat cultivars); as a follow up experiment, we could test Paragon semi-dwarf /*gw2* triple mutants in Obregon for grain morphometrics, TGW, yield and height. Adding environmental like temperature and soil moisture to models combining several locations might further elucidate the conditions under which an interaction is likely to occur. Taken together, we can conclude that the *gw2* alleles and *RHT-B1b* act independently from each other and their effects on grain weight, grain morphometrics and protein content, are antagonistic.

Table 4-13: Yield, grain morphometrics, protein content and height in Paragon NILs for height and grain size

Year	Alleles	Yield (kg/plot)	SE	Delta (%)	P values	TGW (g)	SE	Delta (%)	P values	Grain Width (mm)	SE	Delta (%)	P values	Grain Length (mm)	SE	Delta (%)	P values	ANOVA interaction
2022 Winter	Tall/*GW2*	5.274	±0.06	….	….	47.22	±0.36	….	….	3.695	±0.01	….	….	6.610	±0.02	….	….	
	semi dwarf/*GW2*	5.123	±0.06	-2.9%	0.44	41.13	±0.27	-12.9%	≤0.001	3.538	±0.01	-4.2%	≤0.001	6.414	±0.02	-3.0%	≤0.001	*Rht-B1 (semi-dwarf)*
	Tall/*gw2* triple	5.105	±0.05	-3.2%	0.57	55.75	±0.33	18.1%	≤0.001	3.894	±0.00	5.4%	≤0.001	7.135	±0.02	7.9%	≤0.001	*gw2* triple
	semi dwarf/*gw2* triple mutants	5.012	±0.05	-5.0%	0.42	48.91	±0.35	3.6%	0.2	3.730	±0.00	1.0%	0.7	6.937	±0.02	4.9%	0.49	*Rht-B1:gw2*
2022 Spring	Tall/*GW2*	3.55	±0.06	….	….	37.78	±0.37	….	….	3.40	±0.01	….	….	6.25	±0.02	….	….	
	semi dwarf/*GW2*	3.41	±0.06	-3.96	0.44	32.26	±0.32	-14.62	≤0.001	3.25	±0.01	-4.3	≤0.001	6.05	±0.01	-3.1	≤0.001	*Rht-B1 (semi-dwarf)*
	Tall/gw2 triple	3.35	±0.05	-5.62	0.57	47.24	±0.46	25.03	≤0.001	3.71	±0.01	9.1	≤0.001	6.79	±0.00	9.0	≤0.001	*gw2* triple
	semi dwarf/gw2 triple mutants	3.26	±0.05	-8.29	0.42	41.88	±0.53	10.85	0.23	3.62	±0.01	6.5	0.68	6.63	±0.02	5.6	0.49	*Rht-B1:gw2*

Year	Alleles	Grain protein content (GPC)	SE	Delta (%)	P values	Height	SE	Delta (%)	P values	ANOVA interaction
2022 Spring	Tall/*GW2*	13.3	±0.08	….	….	100.05	±1.04	….	….	
	semi dwarf/*GW2*	12.9	±0.06	-2.5%	0.2	91.2	±0.65	-8.84	≤0.001	*Rht-B1 (semi-dwarf)*
	Tall/*gw2* triple	13.8	±0.10	4.4%	0.004	99.7	±0.50	-0.3	0.9	*gw2* triple
	semi dwarf/*gw2* triple mutants	13.5	±0.08	1.8%	0.4	89.4	±0.48	-10.6	≤0.001	*Rht-B1:gw2*
2022 Winter	Tall/*GW2*	15.3	±0.16	….	….	79.85	±0.57	….	….	
	semi dwarf/*GW2*	15.11	±0.11	-1.20%	0.16	64.25	±0.69	-19.53	≤0.001	*Rht-B1 (semi-dwarf)*
	Tall/*gw2* triple	16.29	±0.12	6.40%	0.03	80.625	±0.51	0.97	0.9	*gw2* triple
	semi dwarf/*gw2* triple mutants	15.93	±0.09	4.10%	0.4	62.4063	±1.17	-21.84	0.1	*Rht-B1:gw2*

*Delta values were obtained by (*gw2* triple mutant alleles – the WT allele/ WT allele) *100

4.6. Discussion

4.6.1. GAs concentrations in developing carpels in Paragon NILs

We hypothesized that Paragon *gw2* triple mutants will have higher concentrations of bioactive GAs (GA_4, GA_3, GA_1) that explain increases in ovary and grain size. To test this idea, we analysed ovaries at heading stage from Paragon NILs using UHPLC-MS. We found that there were significant differences in GAs concentrations across genotypes and that the proportion of 13-OH and 13-H GA metabolites shifted greatly in the WT and the *gw2* triple mutants (Table 4.2, Figure 4.8). Can we hypothesize that the *gw2* alleles are changing the proportions of bioactive GA, impacting seed size? The control of final seed size is known to be a balance between endosperm expansion and maternal seed coat extension, in Arabidopsis and rice, *ELA1* gene a negative regulator of growth, participates in the deactivation of bioactive GAs. Furthermore, *ELA1* breaks down bioactive gibberellins of the non-hydroxylated-13-H pathway changing the proportions of the 13-OH pathway (Figure 4-8, left, section 4.5.2) (Yamaguchi et al., 2014; Creff et al., 2015). The data suggests that the presence of the *gw2* allele in wheat shifts the balance of bioactive GAs however, we still do not understand the consequences on grain morphometrics. In a different study, Ford et al. (2018) collected developing internodes from two wheat varieties, one Icaro with a severely dwarf phenotype and one tall variety M24. They found that a delta of 33 % and 53 % in GA_{19} and GA_{20} respectively, resulted in a 200% increase in bioactive GA_1 in the tall variety M24, when compared to Icaro, linking the increases on plant height to increases in the bioactive GA_1. In this study, GAs were measured in nanograms (ng)/g in fresh weight. In our results, GAs are expressed in picograms (pg)/mg in dry weight. In contrast, Liu et al. (2019) compared GAs concentration in wheat, rice and maize in growing coleoptiles (in fmol/mg fresh weight) and found that high concentrations of GAs precursors do not necessarily translate into higher concentrations of bioactive GAs. This publication was not trying to link GAs concentrations with a certain phenotype. Instead, the authors wanted to generate a spatial distribution of GAs in single shoots. In a similar study, Mares et al. (2022) found that none of the biologically active gibberellins (GA_1, GA_3 or GA_4) were detected in grains at any stage between 15 and 50 DPA in cv. Spica and cv. Maringa. The authors were trying to link higher levels of α-Amylase synthesis in wheat aleurone during grain development. They conclude that it must be independent from GAs. Our results suggest the same line of thinking as we did not see significant increases in GAs concentration at the time the ovaries were sampled. We were not able to link increases in ovary size with GAs content. However, in our time course (Figure 4.7) we did not observe increases in length and width at heading time (-5 heading), consistent with the GAs results. In the future, it will be interesting to sample ovaries at flowering time and the early stages of grain development to test them for GAs concentrations.

4.6.2. Paclobutrazol decreases final grain weight consistently across two years in Paragon gw2 triple mutants

We found that across two years, PAC significantly decreased final TGW while for grain morphometrics, we see a decrease too however the effect was not as strong as that of TGW in Paragon *gw2* triple mutant when applied at

booting. In contrast, conflicting and unexpected results were found on final TGW and grain morphometrics in Paragon WT. We found increases on TGW, length and width when PAC was applied. The regulatory effects of PAC on plant growth have been broadly documented, despite few studies focusing on grain size and weight (Desta and Amare, 2021). Kutzner and Buchenauer (1986) reported that seeds treated with PAC (at 250 mg per 1 kg seeds) showed diminished germination rate, reduced seedling growth and retarded elongation of leaves in wheat, barley, oat, and rye. In wheat, Berova et al. (2002) found that final shoot length was reduced by 50% when seedlings were imbibed in PAC, but after a cold treatment, the same PAC treated seedlings gave bigger and heavier shoot length, fresh and dry weight. Hajihashemi et al. (2007) found in wheat plants that total height, area, and root length decreased significantly in two leaf stage plants in the presence of PAC. The effect of PAC in reducing organ size has been broadly documented in several plant species therefore, we expected that grain size and weight will decrease in the presence of PAC. In our 2021 experiment, PAC increased both grain length and width (Table 4.15 and Table 4.16) in Paragon WT. This was unexpected, given the general negative effect on other growth traits observed in previous studies. In 2020, we found that the TGW of Paragon WT control behaved very similar to the following season (40.5 g vs 41.6 g in controls, Table 4.14), while final length increased by 2.5% (6.3 vs 6.36 mm, Table 4.15) and width increased by 4.8%, from 3.50 to 3.68 mm (Table 4.16). In the experiment carried out in 2020, PAC did not influence final grain size and morphometrics in Paragon WT while in 2021 PAC increased final grain size. The trials were conducted in two different seasons: while the first experiment was conducted in winter, the second started in early spring. Can we speculate that these contrasting results are due to differences in temperature and light intensity? In maize, Kamran et al. (2018) found that PAC improved the ear characteristics and grain yield, during summer trials mainly by increasing root density and length. In wheat (cv. Sakha 93), Manal Mohamed Emam Hassan (2013) found that plants treated with PAC at normal sowing, early sowing and late sowing yielded more than the controls mainly due to an enhanced photosynthetic capacity. Kraus and Fletcher (1994) reported that PAC (2 µM) protected wheat seedlings (cv. Frederick) after being exposed to a heat treatment (50°C for 2.5 hours) mainly through an enhanced detoxification of reactive oxygen species. PAC was found to stimulate the activity of superoxide dismutase, ascorbate peroxidase and glutathione reductase by 16%, 32% and 21% respectively when compared with the seedlings imbibed in water (controls). These results suggest that PAC can also protect plants from heat or cold stress. We can speculate that these conflicting results in Paragon WT are due to the experiments being conducted in different season. In 2021, the treatments were applied at booting time around May and the plants were harvested at the end of July. Our hypothesis is that PAC somehow protected the seeds from heat stress in the WT. In contrast, PAC decreasing final grain weight and grain morphometrics (Table 4.14, Table 4.15 and Table 4.16) in Paragon *gw2* triple mutants consistently across years and concentrations. The heavier and larger grain phenotype in Paragon *gw2* triple mutants was significantly lost when PAC was applied. This suggests that by blocking the gibberellin pathway (with PAC), the heavier and bigger grain size effect of the *gw2* alleles is almost lost when compared to the WT. This allows us to think that there is a link between the GAs and increases in grain size in the triple mutants.

Table 4-14: Summary of TGW (g) across two years with PAC treatments

Genotypes	2020 winter		2021 spring		
	PAC 0	PAC 1uM	PAC 0	PAC 0.5 uM	PAC 1 uM
Paragon WT	40.1 ± 2.0	40.0 ± 1.6	41.6 ± 1.8	44.3 ± 1.8	44.8 ± 1.8
Paragon *gw2*	55.1 ± 1.5	45.0 ± 1.8	50.2 ± 2.0	43.2 ± 1.6	41.9 ± 1.6

Table 4-15: Summary of length across two years with PAC treatments

Genotypes	2020 winter		2021 spring		
	PAC 0	PAC 1 uM	PAC 0	PAC 0.5 uM	PAC 1 uM
Paragon WT	6.3±0.07	6.4 ±0.05	6.36±0.07	6.77±0.06	6.65±0.0
Paragon *gw2*	6.7 ±0.05	6.5 ±0.09	7±0.06	6.98±0.05	6.97±0.05

Table 4-16: Summary of width (mm) across two years with PAC treatments

Genotypes	2020 winter		2021 spring		
	PAC 0	PAC 1 uM	PAC 0	PAC 0.5 uM	PAC1 uM
Paragon WT	3.5 ±0.05	3.6±0.05	3.68±0.05	3.92±0.05	3.88±0.04
Paragon *gw2*	4.0±0.04	3.7 ±0.06	4.14±0.05	3.94±0.04	4.04±0.04

4.6.3. *Exogenous gibberellin treatments increase final grain weight and grain morphometrics in Paragon WT but not in the Paragon gw2 triple mutants*

In 2021, we found that GA$_3$ treatments increased final weight (Table 4.17) and grain morphometrics (Table 4.18 and Table 4.19) in the WT NILs. This is consistent with examples in the literature where gibberellins induce growth in cereals (Hedden, 2020). GAs promote growth in wheat and barley, and it was demonstrated that the application of exogenous GA accelerates spike development under short days breaking the vernalization period Pearce et al. (2013) (Boden et al., 2014b). Probably the best studied effect of GAs involves the *Rht-1* semi-dwarfing alleles, which reduce stem extension by causing partial insensitivity to GAs. This altered response is caused by mutations in either of the homoeologous DELLA genes *Rht-B1* and *Rht-D1*, which have nucleotide substitutions that create premature stop codons (Thomas, 2017). Given the multiple examples cited above where GAs induce growth, we hypothesize that the application of GAs at different time points (heading and flowering) and concentrations will result in bigger grain size due to the action of the hormone. Thus, in accordance with literature, we found that Paragon WT increased in final grain weight (Table 4.17), length and width (Table 4.18, Table 4.19) when GAs were applied at both heading and flowering. In Paragon *gw2* triple mutants, we observed a decrease, albeit not significant, in grain weight (Table 4.17) and grain morphometrics (Table 4.18, Table 4.19), especially at the highest GA dose (10 µM). Interestingly, we found the interaction between GA10 µM and the *gw2* allele to be significant as the MT loses its heavier grain size at both application time points (Table 4.17). Li et al. (2017) reported similar results, with final weight, length and width of the WT increased when GA was applied but when GA was injected in the peduncle of the *gw2-A1* single mutants, final weight and grain morphometrics decreased. Furthermore, they report that when seeds were imbibed in a GA solution, germination and coleoptile length decreased, although it was not reported at which GA dose these effects were observed. The detrimental effect on growth at higher hormone doses had been previously reported. Wright (1961) reported that gibberellins and indole-3-acetic acid when applied at high doses (1000 µM)

constrain wheat coleoptile from growing. However, they use a dose 100 times higher than the one we used for our experiments. Matsuura et al. (2019) reported that the hormone ABA decreases the germination rate of seven different cultivars in wheat when applied at high doses in a dose-dependent manner. In the future, it will be interesting to apply GA_3 at different doses in a scale of 10 units (10 µM, 20 µM, 30 µM): firstly, to see if the results obtained in 2021 are reproducible; second, to test our hypothesis that final grain size and grain morphometrics are going to be negatively affected in the *gw2* triple mutant while in the wildtype, the grain will increase its size in a dose-dependent manner.

Table 4-17: Summary of TGW across two years and GA treatments at heading (H) and flowering (F)

Genotypes	2020		2021				
	control	GA 10 F	control	GA 5 H	GA 5 F	GA 10 H	GA 10 F
Paragon WT	40.1 ± 1.73	43.0 ± 1.65	41.6 ± 1.83	45.5±1.76	47.4±1.76	45.5±1.99	48.8±1.7
Paragon *gw2*	55.1 ± 1.80	53.0 ± 1.83	50.2 ±2.00	50.0±1.76	51.9±1.67	40.9±1.87	44.3±2

Table 4-18: Summary of length across two years of GA treatments at heading (H) and flowering (F)

Genotypes	2020		2021				
	control	GA 10 F	control	GA 5 H	GA 5 F	GA 10 H	GA 10 F
Paragon WT	6.3±0.07	6.1 ±0.07	6.36±0.07	6.80±0.06	6.86±0.06	6.77±0.06	6.78±0.06
Paragon *gw2*	6.7 ±0.06	6.7 ±0.05	7.11±0.06	6.97±0.05	7.06±0.05	6.97±0.06	6.96±0.06

Table 4-19: Summary of width across two years of GA treatments at heading (H) and flowering (F)

Genotypes	2020		2021				
	control	GA 10 F	control	GA 5 H	GA 5 F	GA 10 H	GA 10 F
Paragon WT	3.5±0.05	3.5 ±0.05	3.68±0.05	3.94±0.04	3.98±0.04	3.97±0.05	4.01±0.04
Paragon *gw2*	4.0±0.05	4.0±0.05	4.14±0.05	4.15±0.04	4.25±0.04	4.02±0.05	4.09±0.05

4.6.4. Gibberellins respond to environmental changes like temperature and light intensity.

In 2020, the experiment was conducted in the glasshouse from September to December. We found that gibberellins did not affect grain weight and size in any of the tested genotypes, in contrast to what we found in 2021 spring experiment (Tables 4.17,4.18,4.19). These contrasting effects may be due to differences in growing seasons. GA biosynthesis and inactivation responds to environmental changes like temperature, intensity, and quality of light. These responses have all been shown to affect GA synthesis expression by the 2-ODD genes (Hedden 2020). In Arabidopsis, Ferrero et al. (2019a) reported that transcription factors (TCPs) also participate in a positive feedback loop linked to GA action through the induction of GA biosynthesis genes in response to high temperature. Petiole, hypocotyl, and epidermal cell length growth increased when plants were exposed at 29°C compared to 23°C. In wheat, Pinthus et al. (1989) found that the lamina lengths of the first leaf treated with GA and grown at different temperatures increased by 110% and 170% in the 18°C and 25°C treatments when compared with the 11°C treatment. In order to clarify the effect of GAs on grain size and dissipate doubts about the contrasting results obtained in the two years, the following experiments could be planned, based on current findings and literature. First, an iteration of the GA experiment where three different gibberellin doses are to be applied, to test the hypothesis that the final grain size is going to be affected in a dose-responsive manner. Temperature should be monitored alongside the growing cycle of the plants. Second, a separate batch of plants are to be grown in two different controlled environmental room (CER) at different temperatures (15°C and 22°C), with GAs sprayed at flowering time, and final weight and grain morphometrics determined and analysed.

4.6.5. Increases in grain width and length are related to increases on pericarp cell size

We found that Paragon *gw2* triple mutants had longer and wider pericarp cells than the WT when bigger seeds were chosen (normal distribution group). On the contrary, Paragon WT showed longer and wider pericarp cells when WT seeds with bigger or similar morphometrics were selected (overlap group, Figure 4.16,4.17). Finally, we estimated the cell number and found that in the normal distribution group, Paragon *gw2* triple mutants had fewer cells than the WT while in the overlap group, the opposite was found (Figure 4.18). Similar studies have measured pericarp cells on mature grains. Liu et al. (2020) found that the wheat *da1* allele (which synergistically interacts with the *gw2* allele to enhance grain size) increase grains size. They generated overexpression lines (DA1-OE-1) and *DA1* RNAi plants (DA1-Ri-3) and compared pericarp cells from dissected developing grains (15 DPA) using a stereomicroscope. In a transverse section, they found that the DA1-Ri-3 plants produced more pericarp cells, forming a wider pericarp cell layer. In contrast, the outer pericarps of the DA1-OE-1 plants contained 8% fewer cells than those of the WT. Furthermore, they found that cell length was reduced in the DA1-Ri-3 lines in comparison with the WT. Although they measured pericarp cell thickness while us all pericarp cell length, this study suggests that genes related to the same ubiquitin pathway affect pericarp number and/or length. Proving that both *da1* and *gw2* alleles increase grain

size through a maternal effect. Brinton et al. (2017), measured pericarp cell lengths on 5A NILs for grain length. The authors found that regardless of the selected seed size, the lines with the positive 5A+ allele always had longer pericarp cells when compared with the 5A- allele. When estimating cell numbers, they found that both NILs had the same number of cells in 2015 but in 2016, the 5A- NILs had significantly more cells than the 5A+ NILs. They conclude that the 5A+ region from cv Badger increases the length of pericarp cells independent of absolute grain length. In rice, no significant difference in the outer pericarp layer thickness in both WT and GW2-KO lines was found (Achary and Reddy, 2021). Chen et al. (2022) measured wheat pericarp cell length from three different regions of the seed from a set of NILs associated with longer glumes and longer grains. It was found that $P2^{ISP}$ NILs had significantly longer cells at the top and the middle of the grain than $P2^{WT}$ NILs. They conclude that the $P2$-mediated increase in grain length is in part due to an increase in pericarp cell length. Our results suggest the same, that longer and wider pericarp cells are related to increases on grain morphometrics in the presence of the *gw2* alleles except in the overlapping group. Probably this result is due to our sampling method, we picked much bigger grains from the WT and rather small grains from the *gw2* triple mutants to try to fit for equivalent grain morphometrics "switching" completely the cell size distribution. In the future, it will be interesting to compare pericarp thickness (following the method reported by Liu et al. (2020)) on dissected mature grains of the single, double and triple *gw2* Paragon mutants. This will allow us to understand if there are changes in the pericarp thickness related to the *gw2* alleles.

4.6.6. The gw2 alleles act independently from the Rht-B1 allele to increase TGW, grain size and grain protein content

We hypothesized that the GW2 and the DELLA proteins interact affecting downstream expression of GAs, resulting in reductions in height, grain weight and size based on what we observed in Reedling *gw2* single mutants under field trails both in UK and Obregon (see chapter 3). Reedling carries the semi dwarf allele *RHT-B1b* while Paragon has the tall *RHT-B1a* allele. We attributed the detrimental effect of Reedling on TGW, grain morphometrics and yield to an interaction between the *gw2* and *RHT-B1b* allele. Furthermore, we found that height was significantly reduced by ~15% across 2019 and 2022 in both Reedling and Kingbird *gw2* single and *gw2* triple mutants under irrigation, when compared to the controls. To test our hypothesis, we generated the NILs as described in section 4.3.5.

We found that the *gw2* triple mutants alleles increase grain weight and size across two growing seasons independently from the presence of the *RHT-B1* allele (Figure 4.19, Tables 4.13). Furthermore, we found that protein content increased significantly in both NILs carrying the *gw2* alleles. All these findings agreed with what we previously reported in chapter 2, where TGW, grain size and protein content increased significantly and consistently in Paragon *gw2* triple mutants. Consistent with what we found, Zhang et al. (2018) reported increases in all the parameters mentioned above in cv Kenong *gw2* single mutants. We want to highlight this result as several authors reported the opposite, that the semi dwarf alleles are associated with decreases in seed size and protein content (Casebow et al. (2016); Jobson et al. (2019). Combined with having a lower concentration of micronutrients like zinc, iron, manganese and magnesium when compared to tall varieties (Velu et al., 2017). Additionally, increases in TGW do not translate into increases in GPC (Guzmán et al. 2017; Laidig et al., 2017a). Wheat varieties with improved nutritional quality, protein content, high yield and desirable processing quality in adapted genetic backgrounds can

help alleviate nutrient deficiencies (Velu et al., 2017). In the present work, we showed that increases in TGW and GPC are achievable regardless of the *RHT-B1* allele. We speculate that zinc and iron concentrations to be higher in the semi-dwarf and tall lines with the *gw2* alleles, both parameters can be measured in the future.

4.7. References

1. ACHARY, V. M. M. & REDDY, M. K. 2021. CRISPR-Cas9 mediated mutation in GRAIN WIDTH and WEIGHT2 (*GW2*) locus improves aleurone layer and grain nutritional quality inrice. *Scientific Reports,* 11**,** 21941.
2. BEROVA, M., ZLATEV, Z. & STOEVA, N. 2002. Effect of paclobutrazol on wheat seedlings under low temperature stress. *Bulg. J. Plant Physiol.,* 28.
3. BODEN, S. A., WEISS, D., ROSS, J. J., DAVIES, N. W., TREVASKIS, B., CHANDLER, P. M. & SWAIN, S. M. 2014. *EARLY FLOWERING3* Regulates Flowering in Spring Barley by Mediating Gibberellin Production and *FLOWERING LOCUS T* Expression. *The Plant Cell,* 26**,** 1557-1569.
4. BOEVEN, P. H. G., LONGIN, C. F. H., LEISER, W. L., KOLLERS, S., EBMEYER, E. & WÜRSCHUM, T. 2016. Genetic architecture of male floral traits required for hybrid wheat breeding. *Theoretical and Applied Genetics,* 129**,** 2343-2357.
5. CASEBOW, R., HADLEY, C., UPPAL, R., ADDISU, M., LODDO, S., KOWALSKI, A., GRIFFITHS, S. & GOODING, M. 2016. Reduced Height (*Rht*) Alleles Affect Wheat Grain Quality. *PLoS One,* 11**,** e0156056.
6. CHEN, Y., LIU, Y., ZHANG, J., TORRANCE, A., WATANABE, N., ADAMSKI, N. M. & UAUY, C. 2022. The *Triticum ispahanicum* elongated glume locus *P2* maps to chromosome6A and is associated with the ectopic expression of *SVP-A1*. *Theor Appl Genet,* 135**,** 2313- 2331.
7. CREFF, A., BROCARD, L. &INGRAM, G. 2015.A mechanically sensitive cell layer regulates the physical properties of the Arabidopsis seed coat.*Nat Commun.* Feb 23; 6:6382.
8. DESTA, B. & AMARE, G. 2021. Paclobutrazol as a plant growth regulator. *Chemical and Biological Technologies in Agriculture,* 8**,** 1.
9. ELLIS, H., SPIELMEYER, W., GALE, R., REBETZKE, J. & RICHARDS, A. 2002. "Perfect" markers for the *Rht-B1b* and *Rht-D1b* dwarfing genes in wheat. *Theor Appl Genet,* 105**,** 1038-1042.
10. FERRERO, L. V., VIOLA, I. L., ARIEL, F. D. & GONZALEZ, D. H. 2019. Class I TCP Transcription Factors Target the Gibberellin Biosynthesis Gene *GA20ox1* and the Growth-Promoting Genes *HBI1* and *PRE6* during Thermomorphogenic Growth in Arabidopsis. *Plantand Cell Physiology,* 60**,** 1633-1645.
11. FORD, B. A., FOO, E., SHARWOOD, R., KARAFIATOVA, M., VRÁNA, J., MACMILLAN, C., NICHOLS, D. S., STEUERNAGEL, B., UAUY, C., DOLEŽEL, J., CHANDLER, P. M. & SPIELMEYER, W. 2018. *Rht18* Semidwarfism in Wheat Is Due to Increased GA 2-oxidaseA9 Expression and Reduced GA Content. *Plant Physiology,* 177**,** 168-180.
12. GUILLARME, D. & VEUTHEY, J.-L. 2017. Chapter 1 - Theory and Practice of UHPLC and UHPLC–MS. *In:* HOLČAPEK, M. & BYRDWELL, W. C. (eds.) *Handbook of Advanced Chromatography/Mass Spectrometry Techniques.* AOCS Press.
13. GUZMÁN, C., AUTRIQUE, E., MONDAL, S., HUERTA-ESPINO, J., SINGH, R. P., VARGAS, M., CROSSA, J., AMAYA, A. & PEÑA, R. J. 2017. Genetic improvement of grainquality traits for CIMMYT semi-dwarf spring bread wheat varieties developed during 1965– 2015: 50 years of breeding. *Field Crops Research,* 210**,** 192-196.
14. HAJIHASHEMI, S., KIAROSTAMI, K., SABOORA, A. & ENTESHARI, S. 2007. Exogenously applied paclobutrazol modulates growth in salt-stressed wheat plants. *PlantGrowth Regulation,* 53**,** 117-128.
15. HEDDEN, P. & SPONSEL, V. 2015. A Century of Gibberellin Research. *Journal of PlantGrowth Regulation,* 34**,** 740-760.
16. JEON, J.-S., RYOO, N., HAHN, T.-R., WALIA, H. & NAKAMURA, Y. 2010. Starch biosynthesis in cereal endosperm. *Plant Physiology and Biochemistry,* 48**,** 383-392.
17. JOBSON, E. M., JOHNSTON, R. E., OIESTAD, A. J., MARTIN, J. M. & GIROUX, M. J.2019. The Impact of the Wheat *Rht-B1b* Semi-Dwarfing Allele on Photosynthesis and SeedDevelopment Under Field Conditions. *Frontiers in Plant Science,* 10.

18. KAMRAN, M., WENNAN, S., AHMAD, I., XIANGPING, M., WENWEN, C., XUDONG,Z., SIWEI, M., KHAN, A., QINGFANG, H. & TIENING, L. 2018. Application of paclobutrazol affect maize grain yield by regulating root morphological and physiological characteristics under a semi-arid region. *Scientific Reports,* 8**,** 4818.

19. KATYAYINI, N. U., RINNE, P. L. H., TARKOWSKÁ, D., STRNAD, M. & VAN DER SCHOOT, C. 2020. Dual Role of Gibberellin in Perennial Shoot Branching: Inhibition and Activation. *Frontiers in Plant Science,* 11.

20. KRAUS, T. E. & FLETCHER, R. A. 1994. Paclobutrazol Protects Wheat Seedlings from Heatand Paraquat Injury. Is Detoxification of Active Oxygen Involved? *Plant and Cell Physiology,* 35**,** 45-52.

21. KUTZNER, B. & BUCHENAUER, H. 1986. Effect of various triazole fungicides on growth and lipid metabolism of *Fusarium moniliforme* as well as on gibberellin contents in culture filtrates of the fungus / Wirkung verschiedener Triazolfungizide auf Wachstum und Lipidstoffwechsel von Fusarium moniliforme sowie auf die Gibberellingehalte in Kulturfiltraten des Pilzes. *Zeitschrift für Pflanzenkrankheiten und Pflanzenschutz / Journal ofPlant Diseases and Protection,* 93**,** 597-607.

22. LAIDIG, F., PIEPHO, H.-P., RENTEL, D., DROBEK, T. & MEYER, U. 2017. Breeding progress, genotypic and environmental variation and correlation of quality traits in maltingbarley in German official variety trials between 1983 and 2015. *Theoretical and Applied Genetics,* 130**,** 2411-2429.

23. LI, Q., LI, L., LIU, Y., LV, Q., ZHANG, H., ZHU, J. & LI, X. 2017. Influence of *TaGW2-6A*on seed development in wheat by negatively regulating gibberellin synthesis. *Plant Sci,* 263**,** 226-235.

24. LI, Q., LI, L., YANG, X., WARBURTON, M. L., BAI, G., DAI, J., LI, J. & YAN, J. 2010. Relationship, evolutionary fate and function of two maize co-orthologs of rice *GW2* associated with kernel size and weight. *BMC Plant Biology,* 10**,** 143.

25. LIU, C., LI, D., LI, J., GUO, Z. & CHEN, Y. 2019. One-pot sample preparation approach for profiling spatial distribution of gibberellins in a single shoot of germinating cereal seeds. *ThePlant Journal,* 99**,** 1014-1024.

26. LIU, H., LI, H., HAO, C., WANG, K., WANG, Y., QIN, L., AN, D., LI, T. & ZHANG, X.2020. *TaDA1*, a conserved negative regulator of kernel size, has an additive effect with *TaGW2* in common wheat (Triticum aestivum L.). *Plant Biotechnology Journal,* 18**,** 1330-1342.

27. MAGOME, H., NOMURA, T., HANADA, A., TAKEDA-KAMIYA, N., OHNISHI, T., SHINMA, Y., KATSUMATA, T., KAWAIDE, H., KAMIYA, Y., & YAMAGUCHI, S.2013. *CYP714B1* and *CYP714B2* encode gibberellin *13-oxidases* that reduce gibberellin activity in rice. *Proceedings of the National Academy of Sciences of the United States of America*, *110*(5).

28. MANAL MOHAMED EMAM HASSAN, S. A.-A. F. A. A.-R.2013.EFFECTS OF PACLOBUTRAZOL ON MITIGATION OF TEMPERATURE STRESS INDUCED BY MANIPULATION OF SOWING DATE IN WHEAT PLANT. *Egypt. J. Exp. Biol. (Bot.),* 9**,**125.

29. MARES, D., DERKX, A., CHEONG, J., ZAHARIA, I., ASENSTORFER, R. & MRVA, K. 2022. Gibberellins in developing wheat grains and their relationship to late maturity α-amylase(LMA). *Planta,* 255**,** 119.

30. MATSUURA, T., MORI, I. C., HIMI, E. & HIRAYAMA, T. 2019. Plant hormone profiling in developing seeds of common wheat (Triticum aestivum L.). *Breed Sci,* 69**,** 601-610.

31. PALLOTTA, M., WARNER, P., FOX, R., KUCHEL, H., JEFFERIES, S. & LANGRIDGE, P. Marker assisted wheat breeding in the southern region of Australia. Proceedings of the Tenth International Wheat Genetics Symposium, 2003. Istituto Sperimentale per la Cerealicoltura Puglia, Italy, 789-791.

32. PEARCE, S., SAVILLE, R., VAUGHAN, S. P., CHANDLER, P. M., WILHELM, E. P., SPARKS, C. A., AL-KAFF, N., KOROLEV, A., BOULTON, M. I., PHILLIPS, A. L., HEDDEN, P., NICHOLSON, P. & THOMAS, S. G. 2011. Molecular characterization of *Rht-1*dwarfing genes in hexaploid wheat. *Plant Physiol,* 157**,** 1820-31.

33. PEARCE, S., VANZETTI, L. S. & DUBCOVSKY, J. 2013. Exogenous Gibberellins InduceWheat Spike Development under Short Days Only in the Presence of VERNALIZATION1.*Plant Physiology,* 163**,** 1433-1445.

34. PENG, J., RICHARDS, D. E., HARTLEY, N. M., MURPHY, G. P., DEVOS, K. M., FLINTHAM, J. E., BEALES, J., FISH, L. J., WORLAND, A. J., PELICA, F., SUDHAKAR,

D., CHRISTOU, P., SNAPE, J. W., GALE, M. D. & HARBERD, N. P. 1999. 'Green revolution' genes encode mutant gibberellin response modulators. *Nature,* 400**,** 256-261.

35. PINTHUS, M. J., GALE, M. D., APPLEFORD, N. E. J. & LENTON, J. R. 1989. Effect of Temperature on Gibberellin (GA) Responsiveness and on Endogenous GA_1 Content of Tall and Dwarf Wheat Genotypes. *Plant Physiology,* 90**,** 854-859.

36. SESTILI, F., PAGLIARELLO, R., ZEGA, A., SALETTI, R., PUCCI, A., BOTTICELLA, E., MASCI, S., TUNDO, S., MOSCETTI, I., FOTI, S. & LAFIANDRA, D. 2019a. Enhancing grain size in durum wheat using RNAi to knockdown *GW2* genes. *Theoretical and Applied Genetics,* 132**,** 419-429.

37. SESTILI, F., PAGLIARELLO, R., ZEGA, A., SALETTI, R., PUCCI, A., BOTTICELLA, E., MASCI, S., TUNDO, S., MOSCETTI, I., FOTI, S. & LAFIANDRA, D. 2019b. Enhancing grain size in durum wheat using RNAi to knockdown *GW2* genes. *Theor Appl Genet,* 132**,** 419-429.

38. SIMMONDS, J., SCOTT, P., BRINTON, J., MESTRE, T. C., BUSH, M., DEL BLANCO, A., DUBCOVSKY, J. & UAUY, C. 2016. A splice acceptor site mutation in *TaGW2-A1* increases thousand grain weight in tetraploid and hexaploid wheat through wider and longer grains. *Theor Appl Genet,* 129**,** 1099-112.

39. SONG, X.-J., HUANG, W., SHI, M., ZHU, M.-Z. & LIN, H.-X. 2007. A QTL for rice grain width and weight encodes a previously unknown RING-type E3 ubiquitin ligase. *Nature Genetics,* 39**,** 623-630.

40. THOMAS, S. G. 2017. Novel *Rht-1* dwarfing genes: tools for wheat breeding and dissecting the function of DELLA proteins. *Journal of Experimental Botany,* 68**,** 354-358.

41. TRICK, M., ADAMSKI, N. M., MUGFORD, S. G., JIANG, C.-C., FEBRER, M. & UAUY, C. 2012. Combining SNP discovery from next-generation sequencing data with bulked segregant analysis (BSA) to fine-map genes in polyploid wheat. *BMC Plant Biology,* 12**,** 14.

42. TUAN, P. A., KUMAR, R., REHAL, P. K., TOORA, P. K. & AYELE, B. T. 2018. Molecular Mechanisms Underlying Abscisic Acid/Gibberellin Balance in the Control of Seed Dormancy and Germination in Cereals. *Frontiers in Plant Science,* 9.

43. URBANOVÁ, T., TARKOWSKÁ, D., NOVÁK, O., HEDDEN, P. & STRNAD, M. 2013. Analysis of gibberellins as free acids by ultra performance liquid chromatography-tandem mass spectrometry. *Talanta,* 112**,** 85-94.

44. VAN DE VELDE, K., RUELENS, P., GEUTEN, K., ROHDE, A. & VAN DER STRAETEN, D. 2017. Exploiting DELLA Signaling in Cereals. *Trends Plant Sci,* 22**,** 880-893.

45. VAN DE VELDE, K., THOMAS, S. G., HEYSE, F., KASPAR, R., VAN DER STRAETEN, D. & ROHDE, A. 2021. N-terminal truncated *RHT-1* proteins generated by translational reinitiation cause semi-dwarfing of wheat Green Revolution alleles. *Molecular Plant,* 14**,** 679-687.

46. VELU, G., SINGH, R. P., HUERTA, J. & GUZMÁN, C. 2017. Genetic impact of *Rht* dwarfing genes on grain micronutrients concentration in wheat. *Field Crops Research,* 214**,** 373-377.

47. VERMA, A., PRAKASH, G., RANJAN, R., TYAGI, A. K. & AGARWAL, P. 2021. Silencing of an Ubiquitin Ligase Increases Grain Width and Weight in indica Rice. *Frontiersin Genetics,* 11.

48. WANG, W., SIMMONDS, J., PAN, Q., DAVIDSON, D., HE, F., BATTAL, A., AKHUNOVA, A., TRICK, H. N., UAUY, C. & AKHUNOV, E. 2018. Gene editing and mutagenesis reveal inter-cultivar differences and additivity in the contribution of *TaGW2* homoeologues to grain size and weight in wheat. *Theoretical and Applied Genetics,* 131**,** 2463-2475.

49. WRIGHT, S. T. 1961. A sequential growth response to gibberellic acid, kinetin and indolyl-3-acetic acid in the wheat coleoptile (*Triticum vulgare L.*). *Nature,* 190**,** 699-700.

50. XU, H., LIU, Q., YAO, T. & FU, X. 2014. Shedding light on integrative GA signaling. *Curr Opin Plant Biol,* 21**,** 89-95.

51. YAMAGUCHI, N., WINTER, C. M., WU, M. F., KANNO, Y., YAMAGUCHI, A., SEO, M., & WAGNER, D. 2014. Gibberellin acts positively then negatively to control onset of flower formation in Arabidopsis. *Science*, *344*(6184), 638-641.

52. ZHANG, Y. & LENHARD, M. 2017. Exiting Already? Molecular Control of Cell Proliferation Arrest in Leaves: Cutting Edge. *Mol Plant,* 10**,** 909-911.

53. ZHANG, Y., LI, D., ZHANG, D., ZHAO, X., CAO, X., DONG, L., LIU, J., CHEN, K., ZHANG, H., GAO, C. & WANG, D. 2018. Analysis of the functions of *TaGW2* homoeologsin wheat grain weight and protein content traits. *The Plant Journal,* 94**,** 857-866.

5. General Discussion

The overall aim of this thesis was to understand if the *gw2* alleles increases grain weight and grain morphometrics in different bread wheat cultivars tested under different environments. In addition, we wanted to understand if these increases were mediated by the plant hormones gibberellins. We combined phenotypic characterisation, chemical assays, analytic chemistry and genetics to answer the following questions:

- Do the *gw2* knockout alleles increase grain weight and size across years, environments and different wheat cultivars? For this purpose, we:
    - tested the *gw2* single, double and triple mutant Paragon Near Isogenic Lines (NILs) across three different years (2019, 2020, 2021) and environments in the UK; and
    - evaluated cv Reedling and Kingbird single *gw2-A1* and *gw2* triple mutants NILs under irrigation, drought and heat stress in 2019 and 2022 in CIMMYT, Ciudad Obregon, Mexico.

- Is there any alteration in the gibberellin pathway leading to increases on grain weight and size in Paragon NILs? To address this, we
    - conducted glasshouse experiment using bioactive GA and a gibberellin antagonist paclobutrazol; and
    - explored if *gw2* interacts with the semi dwarf *Rht-B1b* allele through genetic crosses between Paragon *gw2* triple mutant x Paragon *Rht-B1b* NILs.

5.1.1. Introgressing gw2 alleles in wheat breeding programs as a strategy to increase grain protein content

Across chapters, we found that the introgression of the *gw2* alleles increased grain weight and grain morphometrics in wildtype Paragon (*Rht-A1*), semi-dwarf Paragon (*Rht-B1b*) and semi-dwarf Kingbird (*Rht-B1b*) across years and environments. We discuss the advantages of selecting for bigger grain weight and size, especially in dry environments like the CIMMYT experimental station located in Ciudad Obregon in the Northwest of Mexico. Furthermore, we found that in both tall and semi-dwarf Paragon NILs carrying at least one of the *gw2* alleles, the protein content increased significantly when compared to the wildtype.

In the past decades, the main challenge of wheat breeding programs has been to increase global yields without encroaching on natural areas. Undoubtedly this strategy worked, with yields having tripled in virtually the same cultivated global area (Stewart and Lal, 2018a). While selecting for yield, however, the mineral density and grain protein content have decreased in modern varieties despite being traits that are selected for breeding programs (Shewry et al., 2020). In UK winter wheat varieties with the semi-dwarf alleles, a well-known negative trade-off exists between seed size and mineral/protein content, while there is not a clear trade-off between increases on grain weight and protein content (Fradgley et al., 2022). Given the previous evidence, we would like to highlight our findings on increases in grain protein content. We found that increases in TGW and grain morphometrics driven by the *gw2* mutant alleles translate into increases in protein content, which is consistent with what was previous reported for single gw2 mutants in wheat Zhang et al. (2018) and in rice (Achary and Reddy, 2021). This demonstrates the robustness of this trait in *gw2* mutant lines. To date, UK breeders are incorporating the *gw2* allele across UK elite varieties aiming for increases on grain weight and size, and now also protein content. The results presented here would suggest that the introgression of the *gw2* mutant alleles can also serve to improve grain quality. Furthermore, these findings open the door into investigating in more depth the nutritional content of other micronutrients in the mutant lines (e.g., Iron and Zinc content) combined with the possible sources of nitrogen mobilization to the grain. To date, we don't know if the nitrogen source for building more proteins after anthesis is coming from increased remobilization from leaves to grain after anthesis or from increased roots uptake to the grain, or a combination of both (Kichey et al., 2007). Answering these questions will allow us to understand this mechanism and help target grain protein content in a more precise way, keeping in mind that wheat is a valuable resource of proteins and nutrients when compared to other staple cereals like maize and rice (Shiferaw et al., 2013).

5.1.2. *Dosage-dependant pleiotropic effects on yield components in Paragon NILs*

Increases in grain weight, width and length have the potential to improve wheat yield, however negative effects on other yield components such as grain number and tiller number have been reported (Quintero et al., 2018, Kuchel et al., 2007). Consistent with this, here we found that despite a robust increase of up to 20% in TGW and 7% in grain morphometrics, a neutral yield effect was detected in the single and the doubles mutants and a negative effect in the triple mutants. When analysing yield components, we found that seed number per spike and tiller number decreased in a stepwise manner linked to increases in the number of mutant *gw2* copies, being only significantly lower in the triple mutants when compared to the controls. These results exemplify how yield, TGW and tiller number are intrinsically linked. However, it has been demonstrated that these components can be separated and that increase in grain number does not necessarily mean decreases in TGW or vice versa (Brinton et al., 2017). In tetraploid wheat, a genome wide association analysis was conducted for grains per spike, individual grain per spike and TGW. Most of the QTL for TGW and grains per spike are mapped to different genetic intervals, indicating that they are genetically independent from each other (Mangini et al., 2018). In bread wheat cv Weebill, increases in TGW were not accompanied by a significant reduction in grain number, concluding that these components are not inherently linked and can be genetically separated (Griffiths et al., 2015). Thus, increases in grain weight and size do not necessarily entail decreases in seed and tiller number. In the single and double mutants, we found that decreases in both traits were not significant suggesting that a balance between yield components is achievable. Other examples of dosage-dependent effects are also present in the polyploid wheat literature. The *BGC1* genes related to starch production follow the same dosage-dependant effects as seen for the *GW2* genes. For this gene, Paragon triple *bgc1* mutants completely block the production of B-type starch granules, however they also reduce the total A-type starch granules volume by 50%. A balance is achieved in the double *bgc1* mutants where the B-type granules are also absent, but the total starch volume (A-type) remained the same as in the Paragon WT NILs (Chia et al., 2019). Hence the double mutant would have a more favourable agronomic potential than the triple mutant. Taken together, these studies suggest that a balance between traits is possible depending on the relative contributions of the different homoeologous copies and the functionality of the proteins they encode.

5.1.3. Combining genes involved in the same pathway to regulate grain weight and size

We hypothesized that introgressing the *gw2* triple mutant alleles into a semi-dwarf *Rht-B1b* allele background would result in a decrease in grain weight and size based on what we found in Reedling *gw2* single mutants (detrimental effect on grain weight, size and yield, Chapter 2) and based on the model that we generated where we hypothesized that both GW2 and DELLA (encoded by *Rht-B1b*) proteins are part of the same pathway (see section 1.6.1; General Introduction). Furthermore, in the introduction, we talked about downstream targets of the GW2 protein that act in a coordinated manner to repress growth. In Arabidopsis, rice and wheat, DA2 (GW2 in wheat and rice) and BIG BROTHER proteins, target DA1 for ubiquitination. Both act co-ordinately to negatively regulate grain size mainly by suppressing cell proliferation (Peng et al., 2015). The other case scenario is also possible, that is, knocking out genes of the same pathway can result in a positive effect on grain size. The wheat RNAi line targeting *DA1-A1* and *GW2-B1* genes were found to act synergistically to increase grain size in Chinese Spring across different environments (Liu et al., 2020). Both GW2 and DA1, are part of a ubiquitin-proteasome pathway playing a major role in controlling organ size in plants. While in Arabidopsis, several studies demonstrate that by altering proteins expression of the same ubiquitin pathway can positively fine-tune plant growth and development (Vanhaeren et al., 2020). Recently, two more proteins UBP12 and UBP13 were found to deubiquitinate DA1. Thus, limiting its peptidase activity resulting in cell proliferation (Chen et al., 2021). We hypothesize that increasing our understanding of how different genes/proteins interact in wheat will allow us to manipulate final grain size in a more targeted manner. Probably a good starting point will be to conduct *GW2* RNA-Seq studies in order to characterize differentially expressed ubiquitin related genes in both Paragon WT and Paragon *gw2* triple mutants. Likewise, given that the regulation could involve post-translational modifications, proteomic studies could shed light on differential protein abundance in the *gw2* NILs.

5.1.4. The gw2 alleles affect tiller number early in development

In chapter 2, we reported that total tiller number decreased in a dosage dependent manner as the number of mutated *gw2* copies increases. In the *gw2* triple mutants, the difference was significant when compared to the WT. Moreover, we reported that the triple mutants have fewer tillers at two different growing stages (GS45 and GS83) when compared to the WT and that the tiller abortion rate was the same across genotypes. This data suggests that the *gw2* alleles influence the tillering developmental phase (Zadoks 20-29) which happens before stem elongation (Zadoks 30 onwards). Previously, Simmonds et al. (2016) and Brinton et al. (2017) found that increases in carpel size were visible at heading time (Zadoks 55) (Zadoks et al., 1974), concluding that the *gw2* single copy mutants increased grain size through a maternal effect. Although these findings are not mutually exclusive, here we present evidence that the *gw2* alleles act much earlier in development than we previously knew, and that the effect extends beyond carpels and grains. Our results show that when tiller number reaches its peak at reproductive phase, plants with the *gw2* mutant alleles had significant less tillers than the WT. This suggests that GW2 has a role in promoting tiller outgrowth during early developmental stages, a function which is impaired in the triple mutants. This contrasts to

the growth repression role of GW2 later during carpel/grain development. This early effect has not previously been seen in other studies, perhaps as most studies have been conducted in glasshouse where it is not possible to replicate the canopy structure (and hence plant density) that is obtained in field trials and impacts on tillering. More in-depth analysis of tiller outgrowth across the plant cycle will be required to further support this single year observation. This could then open new questions as to the mode of action of *GW2* on tiller outgrowth and carpel/grain growth suppression.

5.1.5. *Wheat breeding in a changing environment (Obregon field experiments)*

In chapter 2, we tested the agronomical performance of Reedling and Kingbird single or triple *gw2* mutant NILs in three contrasting environments: irrigation, drought and heat stress. We found that water scarcity (drought), resulted in a significant yield reduction from 47%-75% across years and cultivars, followed by late sowing (heat stress) where an overall 40%-60% reduction in yield was found when compared to the irrigated controls. Moreover, in our experiments we found that for each 1 °C increase in temperature, yield dropped by 11%. This differs from the previously modelled estimates that a 1 °C increase in temperature will cause a 6% reduction on wheat yield (Asseng et al., 2015). Lastly, when analysing the drip irrigation plots (experiment only conducted in 2019), yield increased significantly by 63% in Kingbird and by 10% in Reedling when compared to the drought experiments proving that, evapotranspiration can be reduced with the correct irrigation equipment adapted for low rainfed regions. We found that Kingbird *gw2* triple mutants increased yield under heat stress by 24.5%; this finding will be the focus of further investigation in the coming years. The next big challenge for us wheat scientists will be not only to increase yield gains but also to breed varieties capable of withstanding either raising temperature, drought or the combination of both. We conclude that testing novel alleles in different cultivars at contrasting environments, is vital for successfully achieving these goals. In that way, the best traits for a given environment or for a given program can be selected and incorporated to meet the global food demands.

5.1.6. *What we learned from the introgression of the gw2 alleles in different wheat cultivars*

In chapter 2 and 4 we evaluated the effect of the *gw2* alleles on Paragon NILs under field trials while, in chapter 3 we evaluated the effect of the alleles in cultivar Reedling and Kingbird chosen for having differing grain weight and morphometrics. We found contrasting effects on yield, TGW, grain morphometrics and environments among them, thus, we learned that the *gw2* allele does not universally increase grain weight and size across cultivars. Previously, Bednarek et al. (2012) found that the down-regulation of the three copies of *GW2* by RNAi resulted in decreases on grain weight and morphometrics. Except from that single research, increases in grain weight and morphometrics were associated with the *gw2* mutants across different cultivars, techniques and mutations (Introduction Chapter 2). In this thesis, we found that the introgression of the *gw2* alleles does not necessarily translate in growth and that different traits "react" differently depending on the background. In Paragon NILs we found increases in TGW, length, and width, while tiller number and grains per spike decreased, and could potentially lead to significant yield losses in triple mutants (Figure 5.1). In Kingbird, we found that all yield related traits increased in the triple mutants except for total tiller number which was environmentally unstable (Figure 5.1). Finally, in Reedling, we found

detrimental effects in all evaluated parameters: final yield, grain size and phenological traits decrease consistently across years and environments in agreement with what was reported by (Bednarek et al., 2012) (Figure 5.1). This supports the idea that different genetic backgrounds interact with genes and environment in unique ways. Furthermore, we were able to link different cultivars with the different wheat haplotypes on chromosome 6A proposed by (Brinton et al., 2020) (See chapter 3). Our results suggest that breeders can use this approach when introgressing novel alleles into different wheat cultivars. We can conclude that *gw2* mutant alleles do not increase TGW and grain morphometrics universally as the effect is cultivar dependent, but based on Paragon data, it can be of great use when breeding for grain protein content and grain size in certain haplotypes.
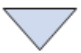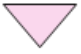
Figure 5-1: Summary of Yield, TGW, grain morphometrics, yield and haplotypes from cultivars Paragon, Kingbird and Reedling in response to the introgression of the *gw2* alleles. Triangles heading up depicts increases, pointing right non-significant effects while the triangles pointing down represent decreases. H: haplotypes based on chromosome 6A *(Brinton et al 2020)*

5.1.7. *CRISPR/Cas for precision breeding*

To date, cross breeding and mutagenesis are the main methodologies for wheat improvement (Chen et al., 2019). The cultivars used in chapter 2 and chapter 3 (Paragon, Reedling and Kingbird) were generated by cross breeding, however, the *gw2* alleles were discovered using a mutational breeding approach from an EMS-mutagenized population (General Introduction, section 1.4.3, TILLING wheat population). New genome editing technologies like CRISPR/Cas are currently being used to eliminate linkage drag or mutations in off-target genes. Many agronomic traits are conferred by single nucleotide polymorphisms which can lead to a knock-out of the gene (like the *gw2* alleles). CRISPR/Cas technology can target specific positions in the gene and induce polymorphisms to generate novel alleles, and in the case of polyploids, we can generate combinations that would be virtually impossible to happen by chance in the same plant (e.g., the triple *gw2* mutants).

In chapter 3, we hypothesize that replacing the 6A chromosomic region in Reedling for the 6A Kronos region caused TGW and yield loses. While replacing this whole block (that has virtually no recombination), we are not only introducing the gw2 mutant allele of Cadenza or Kronos but replacing a complete set of genes which have been selected by breeders in the cultivar. Furthermore, the Kronos and Cadenza TILLING lines have~ 500,000 mutations across the genome Uauy et al. (2009) adding another source of background mutations in off-target genes beyond the chromosome 6A introgression.

Luckily, in the past years, robust protocols have been developed in cereals for CRISPR/Cas genome editing eliminating or reducing both linkage drag and off-target genes(Gil-Humanes et al., 2017, Hamada et al., 2017, Hayta et al., 2019). This has allowed researchers to develop heavier and longer grains in Bobwhite (*TaGW2* triple mutants grains Wang et al. (2018), low-gluten wheat without any detectable off-target mutations in any of the 35 potential targets Sánchez-León et al. (2018), triple knock-out copies for male sterile lines in hybrid wheat Singh et al. (2018) and resistance lines to wheat powdery mildew (Wang et al., 2014). Nevertheless, transgenic approaches have limited acceptability by consumers and governments which is a mayor challenge to overcome. In January of 2022, the UK changed its legislation allowing gene editing crops to be grown in the field (as experimental plots only) and probably to launch products to the market with the new <u>Genetic Technology (Precision Breeding) Bill (Parliamentary Bills - UK Parliament)</u>. This creates an opportunity for UK based scientists to expand our research to the field. Additionally, the bottleneck of transforming only cv Fielder, has been overcome by the expression of the protein complex GROWTH-REGULATING FACTOR 4 (GRF4) and GRF-INTERACTING FACTOR 1 (GIF1) which increased both the transformation efficiency and the number of transformable wheat cultivars (and other cereals) (Debernardi et al., 2020). In the future, we will be able to transform and test different cultivars in the field, for example, Reedling *gw2* triple mutants. This should help elucidate if the detrimental effect of the triple mutant is due to the *gw2* knockout alleles per se, or if they are due to the replacement of the chromosome 6A, 6B and 6D haplotypes surrounding *GW2*.

5.1.8. Are gibberellins involved in bigger grain size in Paragon gw2 triple mutants?

One of the central questions that we wanted to answer in this thesis was if the plant hormones gibberellins are involved in bigger grain size and weight in Paragon *gw2* triple mutants. Existing literature provides contrasting evidence. First, Li et al. (2017) stated that the single *gw2-A1* mutants increase seed size via the GA hormone pathway, specifically by the overexpression of the *GA3-OXIDASE* genes. Soon afterwards, Sestili et al. (2019a) found the opposite, and that the *GA3-OXIDASE* (*GA3ox*) were downregulated in *gw2* RNAi durum lines (cv Svevo). To try and understand this contradiction, we did a BLAST analysis of the primers used in both studies against all three *GA3ox* homologous genes available at plants.ensembl.org. We found 13 identical hits to the set of primers (*Ta.32436*: gibberellin 3-oxidase 2-2) including the *GA3ox2-2* gene located in the short arm of the chromosome 3D (Figure 5.2), reported by Li et al. (2017). The lack of specificity of the primer pair raises questions into the validity of the results as the multiple amplicons would make interpretation cumbersome. The ill design of the primers was probably due to them being designed from the CS survey sequence genome and before the fully annotated genome became available in 2018. On the other hand, the primers reported by Sestili et al. (2019a) aligned to the three copies of the $GA3_{ox2}$ genes as expected (amplicon size 199).
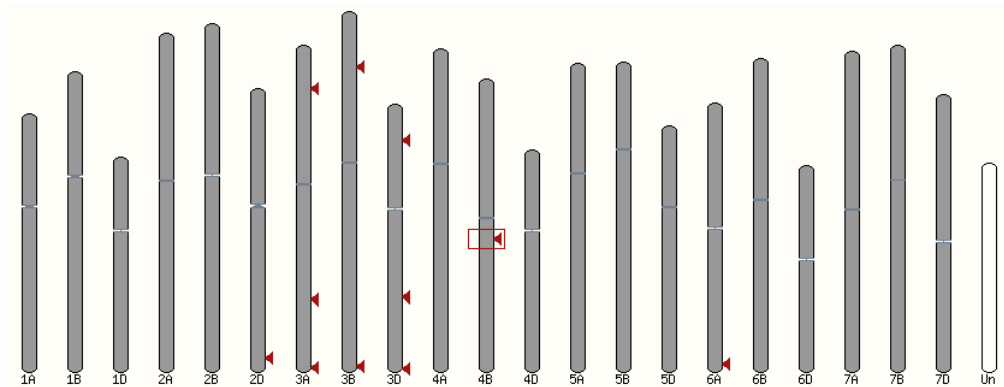
Figure 5-2: Thirteen identical matches across six chromosomes from the primers reported by Li et al 2017

As it was not clear if the GA_{3ox} genes were overexpress or downregulated, we decided to conduct a glasshouse experiment (Chapter 4) where we applied different GA_3 doses at different time points and a GA antagonist, paclobutrazol (PAC), following the method reported by (Boden et al., 2014a). After two glasshouse seasons (chapter 4), we concluded that the only robust effect was that of PAC in reducing grain weight and size, and only on in the Paragon *gw2* triple mutants. Following these findings, we decided to conduct UHPLC-MS in developing carpels of both NILs. Although, we found differences in both GAs catabolites and biological active GAs, we were not able to attribute different concentrations of GAs to increases on carpel size in the *gw2* triple mutants when compared to the WT. In parallel, we conducted qPCR experiments where we tested several GAs primers targeting $GA20_{OX4}$, $GA20_{OX1}$, $GA2_{OX7}$, and $GA3_{OX2}$ (Pearce et al. 2013; Sestili et al. 2019a) in developing carpels at different growth stages from Paragon WT, Paragon *gw2* triple mutants and Paragon semi-dwarf (*Rht-B1b*). Relative to

ACTIN, we found that although the melting curves behaved consistently, all the tested GA primers, across all genotypes, had a very low Cq value (~35 vs 23 of *ACTIN*) indicating that the GAs genes are very expressed at very low levels in developing carpels.

Additionally, to test genetically if the *gw2* alleles and the *Rht-B1b* allele interact, we generated Paragon NILs. We found that both alleles act independently from each other and that the presence of the *Rht-B1b* allele besides reducing plant height (as expected) did not decrease grain weight and size when the *gw2* alleles were introgress. While this result suggests that the effect of the gw2 triple mutant is independent of the *RHT*, we can also be critical of the experimental design. For example, we can speculate that the genetic effect of the *Rht-B1b* was not 'strong enough' to see an effect on grain weight and size as there are two more functional copies. Alternatively, a stronger *RHT1* allele, such as *Rht-B1c* or *Rht-D1c* , could be used to generate a stronger effect. Another explanation can be that the truncated DELLA protein (encoded by the *Rht-B1b* allele) is tissue specific and that it is not expressed in the carpel and grain, hence the repressive effect of both proteins due not overlap in the carpel/grain. Based on all these results, we cannot confirm that GAs are involved in bigger grain size and weight in Paragon *gw2* triple mutants.

Lastly, the detrimental effect of PAC on grain weight and size merely in the *gw2* triple mutants deserves more attention. We can speculate that PAC is interfering not only with the biosynthesis of GA but probably with the synthesis of other hormones interfering with the allocation of resources to the grain, resulting in weight and size losses. Furthermore, new evidence points out that starch related genes are overexpressed in *gw2* mutants, probably causing increases in grain weight and size (Lv et al. (2022), Geng et al. (2017)). It will be interesting to test if there is a connection between PAC and the total starch content in the *gw2* triple mutant grains. We can test this hypothesis with the use of a Coulter counter that estimates the total starch volume following the method used by our colleagues at the John Innes Centre (Chia et al., 2019).

5.1.9.   *Fine tuning gibberellins biosynthesis as a target for wheat breeding*

One central question of this thesis was to investigate the role of the GAs on grain weight and size, as already discussed. In chapter 4, we talked about the introgression of the semi-dwarf alleles into modern agriculture in 1960, exploiting a mutation in the DELLA protein to cause an altered response to the bioactive GA_4 resulting in height and organ size reduction (Pearce et al., 2011). We would now like to focus on the novel discoveries and/or altered responses to GAs that are not related to the DELLA- GA signal transduction. We believe that there is a great source of variation of the GA genes that can be incorporated into plant breeding programmes, with great potential to increase yield specially in drought areas. So far, 25 *RHT* genes have been discovered and can be divided into two categories: GA-insensitive (like the Paragon semi-dwarf NILs generated in chapter 4) and the GA-responsive dwarf genes that have no negative effect on coleoptile length and seedling vigour (discussed in chapter 2) and are responsive to exogenous GA treatments. Out of 25 *RHT* genes, ten correspond to GA-responsive genes: *RHT4*, *RHT5*, *RHT8*, *RHT9*, *RHT12*, *RHT14*, *RHT16*, *RHT18*, *RHT24, RHT25*. *RHT8* and *RHT24* are already broadly used in wheat

germplasm (Agarwal et al., 2020). While the other GA insensitive alleles have been characterized and mapped, there are some remaining questions on their mode of action and agronomic potential. To date, the mode of action of the *RHT12*, *RHT14*, *RHT18*, and *RHT24* alleles had been characterized an increased expression of *GA2oxidaseA13* genes caused decreases in the biosynthesis of GA_{12} resulting in low concentrations of the bioactive GA_1. From the other alleles, little is known but we can hypothesize that similar modes of actions are taking place. In the next paragraph, we are going to focus mainly in the *RHT* alleles that have been tested in the field for agronomical performance.

Firstly, *RHT4* was mapped to chromosome arm 2BL, reducing plant height by 11% and increasing grain number while significantly reducing TGW (Rebetzke et al., 2012). Interestingly, there was no additive effect on height in *RHT-B1B x RHT4* crosses suggesting that the two alleles act independently. *RHT5* is located on chromosome arm 3BS and was associated with a plant height reduction of 23%, delayed heading and maturity, increases in the number of fertile tillers per plant with parallel decreases in the number of spikelets and of grains per spike (Daoura et al., 2013). *RHT8* is on chromosome arm 2DS and reduces plant height via regulating bioactive GA biosynthesis without affecting coleoptile length; to date, it is used worldwide in durum wheat cultivated in dry environments (Chai et al., 2022) (Grover et al., 2018). The RHT9 allele, lies in a region with significant height effect in chromosome arm 5AL (Ellis et al., 2005). The *RHT12* dwarf allele was characterized and mapped to chromosome 5A, and it was demonstrated that an increased expression of *GA2oxidaseA13* genes triggers decreases in the biosynthesis of GA_{12}, a GA_1 precursor. The concentration of the bioactive GA_1 drops and caused a height reduction of 59%. The same authors concluded that the *RHT14* and *RHT18* decreased height by the same mechanism, both being located on the 6A chromosome (Buss et al., 2020). *RHT16* is located on chromosome arm 6AS and is among the fastest emerging genotypes both in laboratory and deep planting experiments (Mohan et al., 2021). *RHT24* encodes a gibberellin 2-oxidase (*TaGA2ox-A9*) contributing to the reduction of bioactive GA in stems (Tian et al., 2022) (Chai et al., 2022). Finally, the *RHT25B* allele was identified and mapped to chromosome arm 6AS, affecting plant height by only

11.6% when compared to the 20% reduction of the *RHT-B1b* and *RHT-D1b* alleles. This suggests that it might serve as a useful alternative dwarfing genetic source in sub-optimal environments (Mo et al., 2018). We gather all the reported yield component and final yield from the *RHT* alleles when compared with tall lines cv Vigor18 in Rebetzke et al. (2016) and the *RHT24* from (Tian et al., 2022). The different responses on plant height and the nuances on how the phenological traits are affected, are evidence of the advantages of introducing different *RHT* genes on distinct wheat cultivars and environments (Table 5.1).

Table 5-1: Summary of agronomical parameters in the *Rht* alleles

Gene	Reduced Height vs tall line	Grain number vs tall lines	Grain yield (T/Ha) vs tall line	Grain weight vs tall lines	Chromosome	Source
RHT4	-17%	19%	11%	-9.70%	2B	Rebetzke.,2012
RHT5	-55%	-66%	-70%	-18.90%	3B	Rebetzke.,2012
RHT8	-7%	-1%	0%	0.50%	2D	Rebetzke.,2012
RHT12	-45%	19%	9.30%	-11.60%	5A	Rebetzke.,2012
RHT13	-34%	27%	10%	?	7B	Rebetzke.,2012
RHT24	12.50%	0%	0%	-2%	6A	Tian., 2022

In this work, we found that the Paragon *gw2* double mutants increased TGW by 9.6% and that yield decreased in a non-significant way by 0.2%. While in chapter 3, the Kingbird *gw2* triple mutants increased yield by 24% and grain weight by 11% when compared to the controls despite growing during heat stress. Furthermore, we found that the truncated GW2 and DELLA proteins act independently on grain size in the Paragon NILs we generated (Chapter 4). These results make us hypothesize, that the introgression of the *gw2* alleles (either double or triple) in combination with the different GA sensitive *Rht* alleles (that can be planted deeper in the soil in drought areas), would be of benefit to increase grain weight without significant yield loses. Keeping in mind that, the GA enzymes are encoded by different genes and that their expression patterns vary with tissue and developmental stages (Pearce et al., 2015), it is envisaged that in the future, bespoke crops can be created for adaptation to the sub optimal conditions where these alleles prove to be more useful.

5.1.10. Sampling hormones/gibberellins in the field to account for environmental interactions

In the last decades, a great amount of work has been conducted to elucidate how plant hormones determine the fate of individual plant organ growth and development. However, fewer resources have been devoted to trying to understand how different hormones interact with each other to impact plant growth in the field (Reynolds et al., 2021a). For example, some well characterized hormone crosstalk is observed in Arabidopsis, where ethylene inhibits primary root growth by regulating auxin biosynthesis, transport, and signalling (Qin, He et al. 2019). Manipulating auxin transport regulates root architecture and decreases in auxins can enhance root vigour and rice yields (Lu et al., 2015). Another well documented example is that of the tomato and fleshy fruits, where auxins and GAs interact in fruit development. During pollination and fertilization, ethylene and abscisic acid (ABA) levels decrease in many tissues, allowing auxin and GA biosynthesis to stimulate fruit set initiation (Fenn and Giovannoni, 2021). In wheat, rice and barley, hormones affect yield-related traits. Cytokines (CKs) regulate cell division and grain filling Roitsch and Ehneß (2000), while ABA and ethylene are related to starch synthesis (Wang et al., 2015). Finally, one of the best know examples is - once more - the boost in yield due to the introduction of the semi-dwarf alleles in cereals (Khush, 1995). The last example is the best proof of concept on how manipulating hormones signaling/sensing can dramatically change agriculture. Many processes that impact on crop performance and yield are controlled by plant hormone balance, which is particular to a given organ or tissue. Understanding this balance will be vital to, "address research bottlenecks to crop productivity" (Reynolds et al., 2021a, Wilkinson et al., 2012). For example, in an uncommon field study, eight barley accessions were monitored weekly over the life span of the plant for auxins, CKs, ABA, jasmonate and salicylic acid in the leaves. The researchers found that auxins and CKs levels increase significantly in the leaves when precipitation levels increased. ABA levels followed a similar trend with the increases of temperature. This study demonstrates that the environment, and not just developmental processes, can influence hormones levels (Hirayama et al., 2020). However, they did not correlate a peak or a decrease in hormones levels with specific agronomic traits.

In the future, a more systematic hormone phenotyping platform needs to be implemented in order to advance in our knowledge on how plant hormones interact with each other to affect yield related traits. Another challenge will be quantifying hormones under field conditions rather than in lab experiments, as control conditions do not reflect soil and environment interactions (Reynolds et al., 2021a). In the field, state-of-the-art and non-destructive technology can be used to monitor the levels of different plant hormones *in situ*. Hormone biosensors can provide real-time monitoring in the field. Currently, biosensors can detect only one kind of hormone at a time, but this can be circumvented by placing several kinds of biosensors in the field (Hirayama and Mochida, 2022). With this kind of technology, we may be able to understand why different wheat or durum varieties are better adapted to drylands than others and how this reflects on TGW and grain morphometrics or yield increases.

5.2. Concluding statement

In summary, in this thesis we found that the *gw2* mutant alleles do not always prove of benefit to increase grain weight, size and yield, but rather that their effect is genotype-dependant. We did find that protein content increased in Paragon *gw2* triple mutants proving that grain size increases do not necessarily translate into decreases on grain protein content. Moreover, we found that the introgression of the *gw2* alleles might confer increased yield in Kingbird even under drought conditions while in Reedling, the introgression of the alleles had a detrimental effect possibly caused by replacement of positive haplotypes across group 6 chromosomes. These results highlight the importance of incorporating a haplotype-based approach on breeding programs combined with the relevance of testing wheat cultivars in different environments for novel trait discovery. We did not find evidence of the involvement of the plant hormone gibberellins on increasing grain weight and size either by applying chemical treatments, by deploying analytic chemistry, nor by genetic approaches. Finally, we believe that a better understanding of how these processes work will allow us to manipulate increases in grain yield in a more targeted way and help tackle food insecurity.

5.3. References

Gibberellin biosynthesis in higher plants. *Annual Plant Reviews, Volume 49.*

ACHARY, V. M. M. & REDDY, M. K. 2021. CRISPR-Cas9 mediated mutation in GRAIN WIDTH and WEIGHT2 (*GW2*) locus improves aleurone layer and grain nutritional quality in rice. *Scientific Reports,* 11**,** 21941.

ADAMSKI, N. M., BORRILL, P., BRINTON, J., HARRINGTON, S. A., MARCHAL, C., BENTLEY, A. R., BOVILL, W. D., CATTIVELLI, L., COCKRAM, J., CONTRERAS-MOREIRA, B., FORD, B., GHOSH, S., HARWOOD, W., HASSANI-PAK, K., HAYTA, S., HICKEY, L. T., KANYUKA, K., KING, J., MACCAFERRRI, M., NAAMATI, G., POZNIAK, C. J., RAMIREZ-GONZALEZ, R. H., SANSALONI, C., TREVASKIS, B., WINGEN, L. U., WULFF, B. B. & UAUY, C. 2020. A roadmap for gene functional characterisation in crops with large genomes: Lessons from polyploid wheat. *Elife,* 9.

AGARWAL, P., BALYAN, H. S. & GUPTA, P. K. 2020. Identification of modifiers of the plant height in wheat using an induced dwarf mutant controlled by *RhtB4c* allele. *Physiol Mol Biol Plants,* 26**,** 2283-2289.

ALTENBACH, S. B. 2012. New insights into the effects of high temperature, drought and post-anthesis fertilizer on wheat grain development. *Journal of Cereal Science,* 56**,** 39-50.

AMRAM, A., FADIDA-MYERS, A., GOLAN, G., NASHEF, K., BEN-DAVID, R. & PELEG, Z. 2015. Effect of GA-sensitivity on wheat early vigor and yield components under deep sowing. *Frontiers in Plant Science,* 6.

ARJONA, J. M., VILLEGAS, D., AMMAR, K., DREISIGACKER, S., ALFARO, C. & ROYO, C. 2020. The Effect of Photoperiod Genes and Flowering Time on Yield and Yield Stability in Durum Wheat. *Plants (Basel),* 9.

ASSENG, S., EWERT, F., MARTRE, P., RÖTTER, R. P., LOBELL, D. B., CAMMARANO, D., KIMBALL, B. A., OTTMAN, M. J., WALL, G. W., WHITE, J. W., REYNOLDS, M. P., ALDERMAN, P. D., PRASAD, P. V. V., AGGARWAL, P. K., ANOTHAI, J., BASSO, B., BIERNATH, C., CHALLINOR, A. J., DE SANCTIS, G., DOLTRA, J., FERERES, E., GARCIA-VILA, M., GAYLER, S., HOOGENBOOM, G., HUNT, L. A., IZAURRALDE, R. C., JABLOUN, M., JONES, C. D., KERSEBAUM, K. C., KOEHLER, A. K., MÜLLER, C., NARESH KUMAR, S., NENDEL, C., O'LEARY, G., OLESEN, J. E., PALOSUO, T., PRIESACK, E., EYSHI REZAEI, E., RUANE, A. C., SEMENOV, M. A., SHCHERBAK, I., STÖCKLE, C., STRATONOVITCH, P., STRECK, T., SUPIT, I., TAO, F., THORBURN, P. J., WAHA, K., WANG, E., WALLACH, D., WOLF, J., ZHAO, Z. & ZHU, Y. 2015. Rising temperatures reduce global wheat production. *Nature Climate Change,* 5**,** 143-147.

BARRON, C., SURGET, A. & ROUAU, X. 2007. Relative amounts of tissues in mature wheat (*Triticum aestivum L.*) grain and their carbohydrate and phenolic acid composition. *Journal of Cereal Science,* 45**,** 88-96.

BECHTEL, D., ABECASSIS, J., SHEWRY, P. & EVERS, A. 2009. CHAPTER 3: Development, Structure, and Mechanical Properties of the Wheat Grain.

BEDNAREK, J., BOULAFLOUS, A., GIROUSSE, C., RAVEL, C., TASSY, C., BARRET, P., BOUZIDI, M. F. & MOUZEYAR, S. 2012. Down-regulation of the *TaGW2* gene by RNA interference results in decreased grain size and weight in wheat. *Journal of Experimental Botany,* 63**,** 5945-5955.

BEROVA, M., ZLATEV, Z. & STOEVA, N. 2002. Effect of paclobutrazol on wheat seedlings under low temperature stress. *Bulg. J. Plant Physiol.,* 28.

BODEN, S. A., WEISS, D., ROSS, J. J., DAVIES, N. W., TREVASKIS, B., CHANDLER, P. M. & SWAIN, S. M. 2014a. *EARLY FLOWERING3* Regulates Flowering in Spring Barley by Mediating Gibberellin Production and *FLOWERING LOCUS T* Expression *The Plant Cell,* 26**,** 1557-1569.

BODEN, S. A., WEISS, D., ROSS, J. J., DAVIES, N. W., TREVASKIS, B., CHANDLER, P. M. & SWAIN, S. M. 2014b. *EARLY FLOWERING3* Regulates Flowering in Spring Barley by Mediating Gibberellin Production and *FLOWERING LOCUS T* Expression. *The Plant Cell,* 26**,** 1557-1569.

BOEVEN, P. H. G., LONGIN, C. F. H., LEISER, W. L., KOLLERS, S., EBMEYER, E. & WÜRSCHUM, T. 2016. Genetic architecture of male floral traits required for hybrid wheat breeding. *Theoretical and Applied Genetics,* 129, 2343-2357.

BRINTON, J., RAMIREZ-GONZALEZ, R. H., SIMMONDS, J., WINGEN, L., ORFORD, S., GRIFFITHS, S., HABERER, G., SPANNAGL, M., WALKOWIAK, S., POZNIAK, C., UAUY, C. & WHEAT GENOME, P. 2020. A haplotype-led approach to increase the precision of wheat breeding. *Communications Biology,* 3, 712.

BRINTON, J., SIMMONDS, J., MINTER, F., LEVERINGTON-WAITE, M., SNAPE, J. & UAUY, C. 2017. Increased pericarp cell length underlies a major quantitative trait locus for grain weight in hexaploid wheat. *New Phytol,* 215, 1026-1038.

BRINTON, J. & UAUY, C. 2019. A reductionist approach to dissecting grain weight and yield in wheat. *Journal of Integrative Plant Biology,* 61, 337-358.

BUSS, W., FORD, B. A., FOO, E., SCHNIPPENKOETTER, W., BORRILL, P., BROOKS, B., ASHTON, A. R., CHANDLER, P. M. & SPIELMEYER, W. 2020. Overgrowth mutants determine the causal role of gibberellin *GA2oxidaseA13* in *Rht12* dwarfism of wheat. *J Exp Bot,* 71, 7171-7178.

CALDERINI, D. F., CASTILLO, F. M., ARENAS-M, A., MOLERO, G., REYNOLDS, M. P., CRAZE, M., BOWDEN, S., MILNER, M. J., WALLINGTON, E. J., DOWLE, A., GOMEZ, L. D. & MCQUEEN-MASON, S. J. 2021. Overcoming the trade-off between grain weight and number in wheat by the ectopic expression of expansin in developing seeds leads to increased yield potential. *New Phytologist,* 230, 629-640.

CASEBOW, R., HADLEY, C., UPPAL, R., ADDISU, M., LODDO, S., KOWALSKI, A., GRIFFITHS, S. & GOODING, M. 2016. *Reduced Height (Rht)* Alleles Affect Wheat Grain Quality. *PLoS One,* 11, e0156056.

CHAI, L., XIN, M., DONG, C., CHEN, Z., ZHAI, H., ZHUANG, J., CHENG, X., WANG, N., GENG, J., WANG, X., BIAN, R., YAO, Y., GUO, W., HU, Z., PENG, H., BAI, G., SUN, Q., SU, Z., LIU, J. & NI, Z. 2022. A natural variation in Ribonuclease H-like gene underlies *Rht8* to confer "Green Revolution" trait in wheat. *Molecular Plant,* 15, 377-380.

CHARMET, G. 2011. Wheat domestication: Lessons for the future. *Comptes Rendus Biologies,* 334, 212-220.

CHEN, K., WANG, Y., ZHANG, R., ZHANG, H. & GAO, C. 2019. CRISPR/Cas Genome Editing and Precision Plant Breeding in Agriculture. *Annual Review of Plant Biology,* 70, 667-697.

CHEN, Y., INZÉ, D. & VANHAEREN, H. 2021. Post-translational modifications regulate the activity of the growth-restricting protease *DA1. Journal of Experimental Botany,* 72, 3352-3366.

CHEN, Y., LIU, Y., ZHANG, J., TORRANCE, A., WATANABE, N., ADAMSKI, N. M. & UAUY, C. 2022. The *Triticum ispahanicum* elongated glume locus P2 maps to chromosome 6A and is associated with the ectopic expression of *SVP-A1. Theor Appl Genet,* 135, 2313-2331.

CHIA, T., CHIRICO, M., KING, R., RAMIREZ-GONZALEZ, R., SACCOMANNO, B., SEUNG, D., SIMMONDS, J., TRICK, M., UAUY, C., VERHOEVEN, T. & TRAFFORD, K. 2019. A carbohydrate-binding protein, *B-GRANULE CONTENT 1*, influences starch granule size distribution in a dose-dependent manner in polyploid wheat. *Journal of Experimental Botany,* 71, 105-115.

CUI, F., ZHAO, C., DING, A., LI, J., WANG, L., LI, X., BAO, Y., LI, J. & WANG, H. 2014. Construction of an integrative linkage map and QTL mapping of grain yield-related traits using three related wheat RIL populations. *Theoretical and Applied Genetics,* 127, 659-675.

DAOURA, B. G., CHEN, L. & HU, Y.-G. 2013. Agronomic traits affected by dwarfing gene "Rht-5" in common wheat (*'Triticum aestivum' L.*). *Australian Journal of Crop Science,* 7, 1270-1276.

DAVIÈRE, J.-M., WILD, M., REGNAULT, T., BAUMBERGER, N., EISLER, H., GENSCHIK, P. & ACHARD, P. 2014. Class I TCP-DELLA Interactions in Inflorescence Shoot Apex Determine Plant Height. *Current Biology,* 24, 1923-1928.

DEBERNARDI, J. M., TRICOLI, D. M., ERCOLI, M. F., HAYTA, S., RONALD, P., PALATNIK, J. F. & DUBCOVSKY, J. 2020. A GRF-GIF chimeric protein improves the regeneration efficiency of transgenic plants. *Nat Biotechnol,* 38, 1274-1279.

131

DESTA, B. & AMARE, G. 2021. Paclobutrazol as a plant growth regulator. *Chemical and Biological Technologies in Agriculture,* 8**,** 1.

DREISIGACKER, S., BURGUEÑO, J., PACHECO, A., MOLERO, G., SUKUMARAN, S., RIVERA-AMADO, C., REYNOLDS, M. & GRIFFITHS, S. 2021. Effect of Flowering Time-Related Genes on Biomass, Harvest Index, and Grain Yield in CIMMYT Elite Spring Bread Wheat. *Biology,* 10**,** 855.

ELLIS, H., SPIELMEYER, W., GALE, R., REBETZKE, J. & RICHARDS, A. 2002. "Perfect" markers for the *Rht-B1b* and *Rht-D1b* dwarfing genes in wheat. *Theor Appl Genet,* 105**,** 1038-1042.

ELLIS, M. H., REBETZKE, G. J., AZANZA, F., RICHARDS, R. A. & SPIELMEYER, W. 2005. Molecular mapping of gibberellin-responsive dwarfing genes in bread wheat. *Theor Appl Genet,* 111**,** 423-30.

ESTEN MASON, R., MONDAL, S., BEECHER, F. W. & HAYS, D. B. 2011. Genetic loci linking improved heat tolerance in wheat (*Triticum aestivum L.*) to lower leaf and spike temperatures under controlled conditions. *Euphytica,* 180**,** 181-194.

FAO 2021. *World Food and Agriculture – Statistical Yearbook 2021. Rome.*

FENN, M. A. & GIOVANNONI, J. J. 2021. Phytohormones in fruit development and maturation. *The Plant Journal,* 105**,** 446-458.

FERRERO, L. V., VIOLA, I. L., ARIEL, F. D. & GONZALEZ, D. H. 2019a. Class I TCP Transcription Factors Target the Gibberellin Biosynthesis Gene *GA20ox1* and the Growth-Promoting Genes *HBI1* and *PRE6* during Thermomorphogenic Growth in Arabidopsis. *Plant and Cell Physiology,* 60**,** 1633-1645.

FERRERO, V., VIOLA, I. L., ARIEL, F. D. & GONZALEZ, D. H. 2019b. Class I TCP Transcription Factors Target the Gibberellin Biosynthesis Gene *GA20ox1* and the Growth-Promoting Genes *HBI1* and *PRE6* during Thermomorphogenic Growth in Arabidopsis. *Plant Cell Physiol,* 60**,** 1633-1645.

FISCHER, R. A., BYERLEE, D. & EDMEADES, G. 2014. Crop yields and global food security: will yield increase continue to feed the world? ACIAR Monograph No. 158. Australian Centre for International Agricultural Research. *Canberra.*

FORD, B. A., FOO, E., SHARWOOD, R., KARAFIATOVA, M., VRÁNA, J., MACMILLAN, C., NICHOLS, D. S., STEUERNAGEL, B., UAUY, C., DOLEŽEL, J., CHANDLER, P. M. & SPIELMEYER, W. 2018. *Rht18* Semi dwarfism in Wheat Is Due to Increased *GA 2-oxidaseA9* Expression and Reduced GA Content. *Plant Physiology,* 177**,** 168-180.

FRADGLEY, N. S., GARDNER, K., KERTON, M., SWARBRECK, S. M. & BENTLEY, A. R. 2022. Trade-offs in the genetic control of functional and nutritional quality traits in UK winter wheat. *Heredity,* 128**,** 420-433.

GENG, J., LI, L., LV, Q., ZHAO, Y., LIU, Y., ZHANG, L. & LI, X. 2017. *TaGW2-6A* allelic variation contributes to grain size possibly by regulating the expression of cytokinins and starch-related genes in wheat. *Planta,* 246**,** 1153-1163.

GIL-HUMANES, J., WANG, Y., LIANG, Z., SHAN, Q., OZUNA, C. V., SÁNCHEZ-LEÓN, S., BALTES, N. J., STARKER, C., BARRO, F. & GAO, C. 2017. High-efficiency gene targeting in hexaploid wheat using DNA replicons and CRISPR/Cas9. *The Plant Journal,* 89**,** 1251-1262.

GOLAN, G., AYALON, I., PERRY, A., ZIMRAN, G., ADE-AJAYI, T., MOSQUNA, A., DISTELFELD, A. & PELEG, Z. 2019a. *GNI-A1* mediates trade-off between grain number and grain weight in tetraploid wheat. *Theor Appl Genet,* 132**,** 2353-2365.

GOLAN, G., AYALON, I., PERRY, A., ZIMRAN, G., ADE-AJAYI, T., MOSQUNA, A., DISTELFELD, A. & PELEG, Z. 2019b. *GNI-A1* mediates trade-off between grain number and grain weight in tetraploid wheat. *Theoretical and Applied Genetics,* 132**,** 2353-2365.

GRIFFITHS, S., WINGEN, L., PIETRAGALLA, J., GARCIA, G., HASAN, A., MIRALLES, D., CALDERINI, D. F., ANKLESHWARIA, J. B., WAITE, M. L., SIMMONDS, J., SNAPE, J. & REYNOLDS, M. 2015. Genetic Dissection of Grain Size and Grain Number Trade-Offs in CIMMYT Wheat Germplasm. *PLOS ONE,* 10**,** e0118847.

GROVER, G., SHARMA, A., GILL, H. S., SRIVASTAVA, P. & BAINS, N. S. 2018. *Rht8* gene as an alternate dwarfing gene in elite Indian spring wheat cultivars. *PLoS One,* 13**,** e0199330.

GUILLARME, D. & VEUTHEY, J.-L. 2017. Chapter 1 - Theory and Practice of UHPLC and UHPLC–MS. *In:* HOLČAPEK, M. & BYRDWELL, W. C. (eds.) *Handbook of Advanced Chromatography/Mass Spectrometry Techniques.* AOCS Press.

GUZMÁN, C., AUTRIQUE, E., MONDAL, S., HUERTA-ESPINO, J., SINGH, R. P., VARGAS, M., CROSSA, J., AMAYA, A. & PEÑA, R. J. 2017. Genetic improvement of grain quality traits for CIMMYT semi-dwarf spring bread wheat varieties developed during 1965–2015: 50 years of breeding. *Field Crops Research,* 210**,** 192-196.

HAJIHASHEMI, S., KIAROSTAMI, K., SABOORA, A. & ENTESHARI, S. 2007. Exogenously applied paclobutrazol modulates growth in salt-stressed wheat plants. *Plant Growth Regulation,* 53**,** 117-128.

HAMADA, H., LINGHU, Q., NAGIRA, Y., MIKI, R., TAOKA, N. & IMAI, R. 2017. An in planta biolistic method for stable wheat transformation. Sci Rep 7 (1): 11443.

HAYTA, S., SMEDLEY, M. A., DEMIR, S. U., BLUNDELL, R., HINCHLIFFE, A., ATKINSON, N. & HARWOOD, W. A. 2019. An efficient and reproducible Agrobacterium-mediated transformation method for hexaploid wheat (*Triticum aestivum L.*). *Plant Methods,* 15**,** 121.

HEDDEN, P. & SPONSEL, V. 2015. A Century of Gibberellin Research. *Journal of Plant Growth Regulation,* 34**,** 740-760.

HIRAYAMA, T. & MOCHIDA, K. 2022. Plant Hormonomics: A Key Tool for Deep Physiological Phenotyping to Improve Crop Productivity. *Plant and Cell Physiology*.

HIRAYAMA, T., SAISHO, D., MATSUURA, T., OKADA, S., TAKAHAGI, K., KANATANI, A., ITO, J., TSUJI, H., IKEDA, Y. & MOCHIDA, K. 2020. Life-Course Monitoring of Endogenous Phytohormone Levels under Field Conditions Reveals Diversity of Physiological States among Barley Accessions. *Plant and Cell Physiology,* 61**,** 1438-1448.

HOWE, K. L., CONTRERAS-MOREIRA, B., DE SILVA, N., MASLEN, G., AKANNI, W., ALLEN, J., ALVAREZ-JARRETA, J., BARBA, M., BOLSER, D. M., CAMBELL, L., CARBAJO, M., CHAKIACHVILI, M., CHRISTENSEN, M., CUMMINS, C., CUZICK, A., DAVIS, P., FEXOVA, S., GALL, A., GEORGE, N., GIL, L., GUPTA, P., HAMMOND-KOSACK, K. E., HASKELL, E., HUNT, S. E., JAISWAL, P., JANACEK, S. H., KERSEY, P. J., LANGRIDGE, N., MAHESWARI, U., MAUREL, T., MCDOWALL, M. D., MOORE, B., MUFFATO, M., NAAMATI, G., NAITHANI, S., OLSON, A., PAPATHEODOROU, I., PATRICIO, M., PAULINI, M., PEDRO, H., PERRY, E., PREECE, J., ROSELLO, M., RUSSELL, M., SITNIK, V., STAINES, D. M., STEIN, J., TELLO-RUIZ, M. K., TREVANION, S. J., URBAN, M., WEI, S., WARE, D., WILLIAMS, G., YATES, A. D. & FLICEK, P. 2020. Ensembl Genomes 2020-enabling non-vertebrate genomic research. *Nucleic Acids Res,* 48**,** D689-d695.

HU, M.-J., ZHANG, H.-P., CAO, J.-J., ZHU, X.-F., WANG, S.-X., JIANG, H., WU, Z. Y., LU, J., CHANG, C., SUN, G.-L. & MA, C.-X. 2016. Characterization of an *IAA-glucose hydrolase* gene *TaTGW6* associated with grain weight in common wheat (*Triticum aestivum L.*). *Molecular Breeding,* 36**,** 25.

HYLES, J., BLOOMFIELD, M. T., HUNT, J. R., TRETHOWAN, R. M. & TREVASKIS, B. 2020. Phenology and related traits for wheat adaptation. *Heredity,* 125**,** 417-430.

HYLES, J., VAUTRIN, S., PETTOLINO, F., MACMILLAN, C., STACHURSKI, Z., BREEN, J., BERGES, H., WICKER, T. & SPIELMEYER, W. 2017. Repeat-length variation in a wheat cellulose synthase-like gene is associated with altered tiller number and stem cell wall composition. *J Exp Bot,* 68**,** 1519-1529.

JEON, J.-S., RYOO, N., HAHN, T.-R., WALIA, H. & NAKAMURA, Y. 2010. Starch biosynthesis in cereal endosperm. *Plant Physiology and Biochemistry,* 48**,** 383-392.

JOBSON, E. M., JOHNSTON, R. E., OIESTAD, A. J., MARTIN, J. M. & GIROUX, M. J. 2019. The Impact of the Wheat *Rht-B1b* Semi-Dwarfing Allele on Photosynthesis and Seed Development Under Field Conditions. *Frontiers in Plant Science,* 10.

JOBSON, E. M., OHM, J.-B., MARTIN, J. M. & GIROUX, M. J. 2021. *Rht-1* semi-dwarfing alleles increase the abundance of high molecular weight glutenin subunits. *Cereal Chemistry,* 98**,** 337-345.

KAMRAN, M., WENNAN, S., AHMAD, I., XIANGPING, M., WENWEN, C., XUDONG, Z., SIWEI, M., KHAN, A., QINGFANG, H. & TIENING, L. 2018. Application of paclobutrazol

affect maize grain yield by regulating root morphological and physiological characteristics under a semi-arid region. *Scientific Reports,* 8**,** 4818.

KATYAYINI, N. U., RINNE, P. L. H., TARKOWSKÁ, D., STRNAD, M. & VAN DER SCHOOT, C. 2020. Dual Role of Gibberellin in Perennial Shoot Branching: Inhibition and Activation. *Frontiers in Plant Science,* 11.

KHUSH, G. S. 1995. Modern varieties — Their real contribution to food supply and equity. *GeoJournal,* 35**,** 275-284.

KICHEY, T., HIREL, B., HEUMEZ, E., DUBOIS, F. & LE GOUIS, J. 2007. In winter wheat (*Triticum aestivum L.*), post-anthesis nitrogen uptake and remobilisation to the grain correlates with agronomic traits and nitrogen physiological markers. *Field Crops Research,* 102**,** 22-32.

KIRBY, E. J. M. 1988. Analysis of leaf, stem and ear growth in wheat from terminal spikelet stage to anthesis. *Field Crops Research,* 18**,** 127-140.

KITAGAWA, S., SHIMADA, S. & MURAI, K. 2012. Effect of *Ppd-1* on the expression of flowering-time genes in vegetative and reproductive growth stages of wheat. *Genes & Genetic Systems,* 87**,** 161-168.

KORNHUBER, K., COUMOU, D., VOGEL, E., LESK, C., DONGES, J. F., LEHMANN, J. & HORTON, R. M. 2020. Amplified Rossby waves enhance risk of concurrent heatwaves in major breadbasket regions. *Nature Climate Change,* 10**,** 48-53.

KRASILEVA, K. V., VASQUEZ-GROSS, H. A., HOWELL, T., BAILEY, P., PARAISO, F., CLISSOLD, L., SIMMONDS, J., RAMIREZ-GONZALEZ, R. H., WANG, X., BORRILL, P., FOSKER, C., AYLING, S., PHILLIPS, A. L., UAUY, C. & DUBCOVSKY, J. 2017. Uncovering hidden variation in polyploid wheat. *Proceedings of the National Academy of Sciences,* 114**,** E913-E921.

KRAUS, T. E. & FLETCHER, R. A. 1994. Paclobutrazol Protects Wheat Seedlings from Heat and Paraquat Injury. Is Detoxification of Active Oxygen Involved? *Plant and Cell Physiology,* 35**,** 45-52.

KRONENBERG, L., YU, K., WALTER, A. & HUND, A. 2017. Monitoring the dynamics of wheat stem elongation: genotypes differ at critical stages. *Euphytica,* 213**,** 157.

KUCHEL, H., WILLIAMS, K. J., LANGRIDGE, P., EAGLES, H. A. & JEFFERIES, S. P. 2007. Genetic dissection of grain yield in bread wheat. I. QTL analysis. *Theor Appl Genet,* 115**,** 1029-41.

KUTZNER, B. & BUCHENAUER, H. 1986. Effect of various triazole fungicides on growth and lipid metabolism of *Fusarium moniliforme* as well as on gibberellin contents in culture filtrates of the fungus / Wirkung verschiedener Triazolfungizide auf Wachstum und Lipidstoffwechsel von Fusarium moniliforme sowie auf die Gibberellingehalte in Kulturfiltraten des Pilzes. *Zeitschrift für Pflanzenkrankheiten und Pflanzenschutz / Journal of Plant Diseases and Protection,* 93**,** 597-607.

LAIDIG, F., PIEPHO, H.-P., RENTEL, D., DROBEK, T. & MEYER, U. 2017a. Breeding progress, genotypic and environmental variation and correlation of quality traits in malting barley in German official variety trials between 1983 and 2015. *Theoretical and Applied Genetics,* 130**,** 2411-2429.

LAIDIG, F., PIEPHO, H.-P., RENTEL, D., DROBEK, T., MEYER, U. & HUESKEN, A. 2017b. Breeding progress, environmental variation and correlation of winter wheat yield and quality traits in German official variety trials and on-farm during 1983–2014. *Theoretical and Applied Genetics,* 130**,** 223-245.

LANGRIDGE, P., BRAUN, H., HULKE, B., OBER, E. & PRASANNA, B. M. 2021. Breeding crops for climate resilience. *Theoretical and Applied Genetics,* 134**,** 1607-1611.

LANGRIDGE, P. & REYNOLDS, M. 2021. Breeding for drought and heat tolerance in wheat. *Theoretical and Applied Genetics,* 134**,** 1753-1769.

LI, N. & LI, Y. 2016. Signaling pathways of seed size control in plants. *Current Opinion in Plant Biology,* 33**,** 23-32.

LI, Q., LI, L., LIU, Y., LV, Q., ZHANG, H., ZHU, J. & LI, X. 2017. Influence of *TaGW2-6A* on seed development in wheat by negatively regulating gibberellin synthesis. *Plant Sci,* 263**,** 226-235.

LI, Q., LI, L., YANG, X., WARBURTON, M. L., BAI, G., DAI, J., LI, J. & YAN, J. 2010. Relationship, evolutionary fate and function of two maize co-orthologs of rice *GW2* associated with kernel size and weight. *BMC Plant Biology,* 10**,** 143.

LIU, C., LI, D., LI, J., GUO, Z. & CHEN, Y. 2019. One-pot sample preparation approach for profiling spatial distribution of gibberellins in a single shoot of germinating cereal seeds. *The Plant Journal,* 99**,** 1014-1024.

LIU, H., LI, H., HAO, C., WANG, K., WANG, Y., QIN, L., AN, D., LI, T. & ZHANG, X. 2020. TaDA1, a conserved negative regulator of kernel size, has an additive effect with TaGW2 in common wheat (Triticum aestivum L.). *Plant Biotechnology Journal,* 18**,** 1330-1342.

LOBELL, D. B., SCHLENKER, W. & COSTA-ROBERTS, J. 2011. Climate Trends and Global Crop Production Since 1980. *Science,* 333**,** 616-620.

LU, G., CONEVA, V., CASARETTO, J. A., YING, S., MAHMOOD, K., LIU, F., NAMBARA, E., BI, Y. M. & ROTHSTEIN, S. J. 2015. OsPIN5b modulates rice (Oryza sativa) plant architecture and yield by changing auxin homeostasis, transport and distribution. *Plant J,* 83**,** 913-25.

LU, L., LIU, H., WU, Y. & YAN, G. 2020. Development and Characterization of Near-Isogenic Lines Revealing Candidate Genes for a Major 7AL QTL Responsible for Heat Tolerance in Wheat. *Frontiers in Plant Science,* 11.

LV, Q., LI, L., MENG, Y., SUN, H., CHEN, L., WANG, B. & LI, X. 2022. Wheat E3 ubiquitin ligase TaGW2-6A degrades TaAGPS to affect seed size. *Plant Science,* 320**,** 111274.

MANAL MOHAMED EMAM HASSAN, S. A.-A. F. A. A.-R. 2013. EFFECTS OF PACLOBUTRAZOL ON MITIGATION OF TEMPERATURE STRESS INDUCED BY MANIPULATION OF SOWING DATE IN WHEAT PLANT. *Egypt. J. Exp. Biol. (Bot.),* 9**,** 125.

MANGINI, G., GADALETA, A., COLASUONNO, P., MARCOTULI, I., SIGNORILE, A. M., SIMEONE, R., DE VITA, P., MASTRANGELO, A. M., LAIDÒ, G., PECCHIONI, N. & BLANCO, A. 2018. Genetic dissection of the relationships between grain yield components by genome-wide association mapping in a collection of tetraploid wheats. *PLOS ONE,* 13**,** e0190162.

MARCUSSEN, T., SANDVE, S. R., HEIER, L., SPANNAGL, M., PFEIFER, M., JAKOBSEN, K. S., WULFF, B. B. H., STEUERNAGEL, B., MAYER, K. F. X., OLSEN, O.-A., ROGERS, J., DOLEŽEL, J., POZNIAK, C., EVERSOLE, K., FEUILLET, C., GILL, B., FRIEBE, B., LUKASZEWSKI, A. J., SOURDILLE, P., ENDO, T. R., KUBALÁKOVÁ, M., ČÍHALÍKOVÁ, J., DUBSKÁ, Z., VRÁNA, J., ŠPERKOVÁ, R., ŠIMKOVÁ, H., FEBRER, M., CLISSOLD, L., MCLAY, K., SINGH, K., CHHUNEJA, P., SINGH, N. K., KHURANA, J., AKHUNOV, E., CHOULET, F., ALBERTI, A., BARBE, V., WINCKER, P., KANAMORI, H., KOBAYASHI, F., ITOH, T., MATSUMOTO, T., SAKAI, H., TANAKA, T., WU, J., OGIHARA, Y., HANDA, H., MACLACHLAN, P. R., SHARPE, A., KLASSEN, D., EDWARDS, D., BATLEY, J., LIEN, S., CACCAMO, M., AYLING, S., RAMIREZ-GONZALEZ, R. H., CLAVIJO, B. J., WRIGHT, J., MARTIS, M. M., MASCHER, M., CHAPMAN, J., POLAND, J. A., SCHOLZ, U., BARRY, K., WAUGH, R., ROKHSAR, D. S., MUEHLBAUER, G. J., STEIN, N., GUNDLACH, H., ZYTNICKI, M., JAMILLOUX, V., QUESNEVILLE, H., WICKER, T., FACCIOLI, P., COLAIACOVO, M., STANCA, A. M., BUDAK, H., CATTIVELLI, L., GLOVER, N., PINGAULT, L., PAUX, E., SHARMA, S., APPELS, R., BELLGARD, M., CHAPMAN, B., NUSSBAUMER, T., BADER, K. C., RIMBERT, H., WANG, S., KNOX, R., KILIAN, A., ALAUX, M., ALFAMA, F., COUDERC, L., GUILHOT, N., VISEUX, C., LOAEC, M., KELLER, B. & PRAUD, S. 2014. Ancient hybridizations among the ancestral genomes of bread wheat. *Science,* 345**,** 1250092.

MARES, D., DERKX, A., CHEONG, J., ZAHARIA, I., ASENSTORFER, R. & MRVA, K. 2022. Gibberellins in developing wheat grains and their relationship to late maturity α-amylase (LMA). *Planta,* 255**,** 119.

MASON, R. E., MONDAL, S., BEECHER, F. W., PACHECO, A., JAMPALA, B., IBRAHIM, A. M. H. & HAYS, D. B. 2010. QTL associated with heat susceptibility index in wheat (Triticum aestivum L.) under short-term reproductive stage heat stress. *Euphytica,* 174**,** 423-436.

MATSUURA, T., MORI, I. C., HIMI, E. & HIRAYAMA, T. 2019. Plant hormone profiling in developing seeds of common wheat (Triticum aestivum L.). *Breed Sci,* 69**,** 601-610.

MO, Y., VANZETTI, L., HALE, I., SPAGNOLO, E., GUIDOBALDI, F., AL-OBOUDI, J., ODLE, N., PEARCE, S., HELGUERA, M. & DUBCOVSKY, J. 2018. Identification and characterization of Rht25, a locus on chromosome arm 6AS affecting wheat plant height, heading time, and spike development. *Theoretical and Applied Genetics,* 131.

MOHAMMADI, V., ZALI, A. & BIHAMTA, M. 2008. Mapping QTLs for heat tolerance in wheat.

MOHAN, A., GRANT, N. P., SCHILLINGER, W. F. & GILL, K. S. 2021. Characterizing reduced height wheat mutants for traits affecting abiotic stress and photosynthesis during seedling growth. *Physiologia Plantarum,* 172**,** 233-246.

MOHAN, A., SCHILLINGER, W. F. & GILL, K. S. 2013. Wheat seedling emergence from deep planting depths and its relationship with coleoptile length. *PloS one,* 8**,** e73314-e73314.

MOORE, C. & REBETZKE, G. 2015. Genomic Regions for Embryo Size and Early Vigour in Multiple Wheat (Triticum aestivum L.) Populations. *Agronomy,* 5**,** 152-179.

MORA-RAMIREZ, I., WEICHERT, H., VON WIRÉN, N., FROHBERG, C., DE BODT, S., SCHMIDT, R.-C. & WEBER, H. 2021. The da1 mutation in wheat increases grain size under ambient and elevated CO2 but not grain yield due to trade-off between grain size and grain number. *Plant-Environment Interactions,* 2**,** 61-73.

MÜLLER, M. & MUNNÉ-BOSCH, S. 2011. Rapid and sensitive hormonal profiling of complex plant samples by liquid chromatography coupled to electrospray ionization tandem mass spectrometry. *Plant Methods,* 7**,** 37.

ORDON, F., & FRIEDT, W. (EDS.). 2019. *Advances in breeding techniques for cereal crops (1st ed.).*

ORTIZ-MONASTERIO R, J. I., DHILLON, S. S. & FISCHER, R. A. 1994. Date of sowing effects on grain yield and yield components of irrigated spring wheat cultivars and relationships with radiation and temperature in Ludhiana, India. *Field Crops Research,* 37**,** 169-184.

PALLOTTA, M., WARNER, P., FOX, R., KUCHEL, H., JEFFERIES, S. & LANGRIDGE, P. Marker assisted wheat breeding in the southern region of Australia. Proceedings of the Tenth International Wheat Genetics Symposium, 2003a. Istituto Sperimentale per la Cerealicoltura Puglia, Italy, 789-791.

PALLOTTA, M., WARNER, P., FOX, R., KUCHEL, H., JEFFERIES, S. & LANGRIDGE, P. 2003b. Proceedings of the 10th international wheat genetics symposium.

PARENT, B., BONNEAU, J., MAPHOSA, L., KOVALCHUK, A., LANGRIDGE, P. & FLEURY, D. 2017. Quantifying wheat sensitivities to environmental constraints to dissect genotype× environment interactions in the field. *Plant Physiology,* 174**,** 1669-1682.

PATRA, K., PARIHAR, C. M., NAYAK, H. S., RANA, B., SINGH, V. K., JAT, S. L., PANWAR, S., PARIHAR, M. D., SINGH, L. K., SIDHU, H. S., GERARD, B. & JAT, M. L. 2021. Water budgeting in conservation agriculture-based sub-surface drip irrigation in tropical maize using HYDRUS-2D in South Asia. *Sci Rep,* 11**,** 16770.

PEARCE, S., SAVILLE, R., VAUGHAN, S. P., CHANDLER, P. M., WILHELM, E. P., SPARKS, C. A., AL-KAFF, N., KOROLEV, A., BOULTON, M. I., PHILLIPS, A. L., HEDDEN, P., NICHOLSON, P. & THOMAS, S. G. 2011. Molecular characterization of Rht-1 dwarfing genes in hexaploid wheat. *Plant Physiol,* 157**,** 1820-31.

PEARCE, S., VANZETTI, L. S. & DUBCOVSKY, J. 2013. Exogenous Gibberellins Induce Wheat Spike Development under Short Days Only in the Presence of VERNALIZATION1 *Plant Physiology,* 163**,** 1433-1445.

PENG, J., RICHARDS, D. E., HARTLEY, N. M., MURPHY, G. P., DEVOS, K. M., FLINTHAM, J. E., BEALES, J., FISH, L. J., WORLAND, A. J., PELICA, F., SUDHAKAR, D., CHRISTOU, P., SNAPE, J. W., GALE, M. D. & HARBERD, N. P. 1999. 'Green revolution' genes encode mutant gibberellin response modulators. *Nature,* 400**,** 256-261.

PENG, Y., CHEN, L., LU, Y., WU, Y., DUMENIL, J., ZHU, Z., BEVAN, M. W. & LI, Y. 2015. The ubiquitin receptors DA1, DAR1, and DAR2 redundantly regulate endoreduplication by modulating the stability of TCP14/15 in Arabidopsis. *Plant Cell,* 27**,** 649-62.

PINTHUS, M. J., GALE, M. D., APPLEFORD, N. E. J. & LENTON, J. R. 1989. Effect of Temperature on Gibberellin (GA) Responsiveness and on Endogenous GA1 Content of Tall and Dwarf Wheat Genotypes. *Plant Physiology,* 90**,** 854-859.

POORTER, H., FIORANI, F., PIERUSCHKA, R., WOJCIECHOWSKI, T., VAN DER PUTTEN, W. H., KLEYER, M., SCHURR, U. & POSTMA, J. 2016. Pampered inside, pestered outside? Differences and similarities between plants growing in controlled conditions and in the field. *New Phytologist,* 212**,** 838-855.

PRIETO, P., OCHAGAVÍA, H., SAVIN, R., GRIFFITHS, S. & SLAFER, G. A. 2018. Dynamics of floret initiation/death determining spike fertility in wheat as affected by Ppd genes under field conditions. *J Exp Bot,* 69**,** 2633-2645.

QI, P.-F., JIANG, Y.-F., GUO, Z.-R., CHEN, Q., OUELLET, T., ZONG, L.-J., WEI, Z.-Z., WANG, Y., ZHANG, Y.-Z., XU, B.-J., KONG, L., DENG, M., WANG, J.-R., CHEN, G.-Y., JIANG, Q.-T., LAN, X.-J., LI, W., WEI, Y.-M. & ZHENG, Y.-L. 2019. Transcriptional reference map of hormone responses in wheat spikes. *BMC Genomics,* 20**,** 390.

QIN, L., HAO, C., HOU, J., WANG, Y., LI, T., WANG, L., MA, Z. & ZHANG, X. 2014. Homologous haplotypes, expression, genetic effects and geographic distribution of the wheat yield gene TaGW2. *BMC Plant Biology,* 14**,** 107.

QUINTERO, A., MOLERO, G., REYNOLDS, M. P. & CALDERINI, D. F. 2018. Trade-off between grain weight and grain number in wheat depends on GxE interaction: A case study of an elite CIMMYT panel (CIMCOG). *European Journal of Agronomy,* 92**,** 17-29.

RAY, D. K., MUELLER, N. D., WEST, P. C. & FOLEY, J. A. 2013. Yield Trends Are Insufficient to Double Global Crop Production by 2050. *PLoS One,* 8**,** e66428.

REBETZKE, G. J., BONNETT, D. G. & REYNOLDS, M. P. 2016. Awns reduce grain number to increase grain size and harvestable yield in irrigated and rainfed spring wheat. *Journal of experimental botany,* 67**,** 2573-2586.

REBETZKE, G. J., BRUCE, S. E. & KIRKEGAARD, J. A. 2005. Longer coleoptiles improve emergence through crop residues to increase seedling number and biomass in wheat (Triticum aestivum L.). *Plant and Soil,* 272**,** 87-100.

REBETZKE, G. J., ELLIS, M. H., BONNETT, D. G., MICKELSON, B., CONDON, A. G. & RICHARDS, R. A. 2012. Height reduction and agronomic performance for selected gibberellin-responsive dwarfing genes in bread wheat (Triticum aestivum L.). *Field Crops Research,* 126**,** 87-96.

REBETZKE, G. J., RICHARDS, R. A., FETTELL, N. A., LONG, M., CONDON, A. G., FORRESTER, R. I. & BOTWRIGHT, T. L. 2007. Genotypic increases in coleoptile length improves stand establishment, vigour and grain yield of deep-sown wheat. *Field Crops Research,* 100**,** 10-23.

REYNOLDS, M., ATKIN, O. K., BENNETT, M., COOPER, M., DODD, I. C., FOULKES, M. J., FROHBERG, C., HAMMER, G., HENDERSON, I. R., HUANG, B., KORZUN, V., MCCOUCH, S. R., MESSINA, C. D., POGSON, B. J., SLAFER, G. A., TAYLOR, N. L. & WITTICH, P. E. 2021a. Addressing Research Bottlenecks to Crop Productivity. *Trends in Plant Science,* 26**,** 607-630.

REYNOLDS, M., MANES, Y., IZANLOO, A. & LANGRIDGE, P. 2009. Phenotyping approaches for physiological breeding and gene discovery in wheat. *Annals of Applied Biology,* 155**,** 309-320.

REYNOLDS, M. P., LEWIS, J. M., AMMAR, K., BASNET, B. R., CRESPO-HERRERA, L., CROSSA, J., DHUGGA, K. S., DREISIGACKER, S., JULIANA, P., KARWAT, H., KISHII, M., KRAUSE, M. R., LANGRIDGE, P., LASHKARI, A., MONDAL, S., PAYNE, T., PEQUENO, D., PINTO, F., SANSALONI, C., SCHULTHESS, U., SINGH, R. P., SONDER, K., SUKUMARAN, S., XIONG, W. & BRAUN, H. J. 2021b. Harnessing translational research in wheat for climate resilience. *Journal of Experimental Botany,* 72**,** 5134-5157.

REYNOLDS, M. P., SLAFER, G. A., FOULKES, J. M., GRIFFITHS, S., MURCHIE, E. H., CARMO-SILVA, E., ASSENG, S., CHAPMAN, S. C., SAWKINS, M., GWYN, J. & FLAVELL, R. B. 2022. A wiring diagram to integrate physiological traits of wheat yield potential. *Nature Food,* 3**,** 318-324.

RICHARDS, R., REBETZKE, G., WATT, M., SPIELMEYER, W. & DOLFERUS, R. 2010. Breeding for improved water productivity in temperate cereals: Phenotyping, quantitative trait loci, markers and the selection environment. *Functional Plant Biology - FUNCT PLANT BIOL,* 37.

ROITSCH, T. & EHNEß, R. 2000. Regulation of source/sink relations by cytokinins. *Plant Growth Regulation,* 32**,** 359-367.

ROSEGRANT, M. W., RINGLER, C., ZHU, T., TOKGOZ, S. & BHANDARY, P. 2013. Water and food in the bioeconomy: challenges and opportunities for development. *Agricultural Economics,* 44**,** 139-150.

SAKUMA, S., GOLAN, G., GUO, Z., OGAWA, T., TAGIRI, A., SUGIMOTO, K., BERNHARDT, N., BRASSAC, J., MASCHER, M., HENSEL, G., OHNISHI, S., JINNO, H., YAMASHITA, Y., AYALON, I., PELEG, Z., SCHNURBUSCH, T. & KOMATSUDA, T. 2019. Unleashing floret fertility in wheat through the mutation of a homeobox gene. *Proceedings of the National Academy of Sciences,* 116**,** 5182-5187.

SAKUMA, S. & SCHNURBUSCH, T. 2020. Of floral fortune: tinkering with the grain yield potential of cereal crops. *New Phytologist,* 225**,** 1873-1882.

SANCHEZ-GARCIA, M., ROYO, C., APARICIO, N., MARTÍN-SÁNCHEZ, J. A. & ÁLVARO, F. 2013. Genetic improvement of bread wheat yield and associated traits in Spain during the 20th century. *The Journal of Agricultural Science,* 151**,** 105-118.

SÁNCHEZ-LEÓN, S., GIL-HUMANES, J., OZUNA, C. V., GIMÉNEZ, M. J., SOUSA, C., VOYTAS, D. F. & BARRO, F. 2018. Low-gluten, nontransgenic wheat engineered with CRISPR/Cas9. *Plant Biotechnol J,* 16**,** 902-910.

SCHMIDT, J., GARCIA, M., BRIEN, C., KALAMBETTU, P., GARNETT, T., FLEURY, D. & TRICKER, P. J. 2020. Transcripts of wheat at a target locus on chromosome 6B associated with increased yield, leaf mass and chlorophyll index under combined drought and heat stress. *PLoS One,* 15**,** e0241966.

SESTILI, F., PAGLIARELLO, R., ZEGA, A., SALETTI, R., PUCCI, A., BOTTICELLA, E., MASCI, S., TUNDO, S., MOSCETTI, I., FOTI, S. & LAFIANDRA, D. 2019a. Enhancing grain size in durum wheat using RNAi to knockdown GW2 genes. *Theor Appl Genet,* 132**,** 419-429.

SESTILI, F., PAGLIARELLO, R., ZEGA, A., SALETTI, R., PUCCI, A., BOTTICELLA, E., MASCI, S., TUNDO, S., MOSCETTI, I., FOTI, S. & LAFIANDRA, D. 2019b. Enhancing grain size in durum wheat using RNAi to knockdown GW2 genes. *Theoretical and Applied Genetics,* 132**,** 419-429.

SHEWRY, P. R., HASSALL, K. L., GRAUSGRUBER, H., ANDERSSON, A. A. M., LAMPI, A.-M., PIIRONEN, V., RAKSZEGI, M., WARD, J. L. & LOVEGROVE, A. 2020. Do modern types of wheat have lower quality for human health? *Nutrition Bulletin,* 45**,** 362-373.

SHEWRY, P. R., MITCHELL, R. A. C., TOSI, P., WAN, Y., UNDERWOOD, C., LOVEGROVE, A., FREEMAN, J., TOOLE, G. A., MILLS, E. N. C. & WARD, J. L. 2012. An integrated study of grain development of wheat (cv. Hereward). *Journal of Cereal Science,* 56**,** 21-30.

SHIFERAW, B., SMALE, M., BRAUN, H.-J., DUVEILLER, E., REYNOLDS, M. & MURICHO, G. 2013. Crops that feed the world 10. Past successes and future challenges to the role played by wheat in global food security. *Food Security,* 5**,** 291-317.

SIMMONDS, J., SCOTT, P., BRINTON, J., MESTRE, T. C., BUSH, M., DEL BLANCO, A., DUBCOVSKY, J. & UAUY, C. 2016. A splice acceptor site mutation in TaGW2-A1 increases thousand grain weight in tetraploid and hexaploid wheat through wider and longer grains. *Theor Appl Genet,* 129**,** 1099-112.

SINGH, M., KUMAR, M., ALBERTSEN, M. C., YOUNG, J. K. & CIGAN, A. M. 2018. Concurrent modifications in the three homeologs of Ms45 gene with CRISPR-Cas9 lead to rapid generation of male sterile bread wheat (Triticum aestivum L.). *Plant Molecular Biology,* 97**,** 371-383.

SLAFER, G. A. 2003. Genetic basis of yield as viewed from a crop physiologist's perspective. *Annals of Applied Biology,* 142**,** 117-128.

SLAFER, G. A., FOULKES, M. J., REYNOLDS, M. P., MURCHIE, E., CARMO-SILVA, E., FLAVELL, R., GWYN, J., SAWKINS, M. & GRIFFITHS, S. 2022. A 'Wiring Diagram' for sink-strength traits impacting wheat yield potential. *Journal of Experimental Botany*, erac410.

SNOWDON, R. J., WITTKOP, B., CHEN, T.-W. & STAHL, A. 2021. Crop adaptation to climate change as a consequence of long-term breeding. *Theoretical and Applied Genetics,* 134**,** 1613-1623.

SONG, X.-J., HUANG, W., SHI, M., ZHU, M.-Z. & LIN, H.-X. 2007. A QTL for rice grain width and weight encodes a previously unknown RING-type E3 ubiquitin ligase. *Nature Genetics,* 39**,** 623-630.

STEWART, B. A. & LAL, R. 2018a. Chapter One - Increasing World Average Yields of Cereal Crops: It's All About Water. *In:* SPARKS, D. L. (ed.) *Advances in Agronomy.* Academic Press.

STEWART, B. A. & LAL, R. 2018b. Increasing World Average Yields of Cereal Crops: It's All About Water.

SU, Z., HAO, C., WANG, L., DONG, Y. & ZHANG, X. 2011a. Identification and development of a functional marker of TaGW2 associated with grain weight in bread wheat (Triticum aestivum L.). *Theor Appl Genet,* 122**,** 211-23.

SU, Z., HAO, C., WANG, L., DONG, Y. & ZHANG, X. 2011b. Identification and development of a functional marker of TaGW2 associated with grain weight in bread wheat (Triticum aestivum L.). *Theoretical and Applied Genetics,* 122**,** 211-223.

SUKUMARAN, S., REYNOLDS, M. P. & SANSALONI, C. 2018. Genome-Wide Association Analyses Identify QTL Hotspots for Yield and Component Traits in Durum Wheat Grown under Yield Potential, Drought, and Heat Stress Environments. *Front Plant Sci,* 9**,** 81.

THOMAS, S. G. 2017. Novel Rht-1 dwarfing genes: tools for wheat breeding and dissecting the function of DELLA proteins. *Journal of Experimental Botany,* 68**,** 354-358.

TIAN, X., XIA, X., XU, D., LIU, Y., XIE, L., HASSAN, M. A., SONG, J., LI, F., WANG, D., ZHANG, Y., HAO, Y., LI, G., CHU, C., HE, Z. & CAO, S. 2022. Rht24b, an ancient variation of *TaGA2ox-A9*, reduces plant height without yield penalty in wheat. *New Phytol,* 233**,** 738-750.

TRICK, M., ADAMSKI, N. M., MUGFORD, S. G., JIANG, C.-C., FEBRER, M. & UAUY, C. 2012. Combining SNP discovery from next-generation sequencing data with bulked segregant analysis (BSA) to fine-map genes in polyploid wheat. *BMC Plant Biology,* 12**,** 14.

TUAN, P. A., KUMAR, R., REHAL, P. K., TOORA, P. K. & AYELE, B. T. 2018. Molecular Mechanisms Underlying Abscisic Acid/Gibberellin Balance in the Control of Seed Dormancy and Germination in Cereals. *Frontiers in Plant Science,* 9.

UAUY, C., PARAISO, F., COLASUONNO, P., TRAN, R. K., TSAI, H., BERARDI, S., COMAI, L. & DUBCOVSKY, J. 2009. A modified TILLING approach to detect induced mutations in tetraploid and hexaploid wheat. *BMC Plant Biology,* 9**,** 115.

URBANOVÁ, T., TARKOWSKÁ, D., NOVÁK, O., HEDDEN, P. & STRNAD, M. 2013. Analysis of gibberellins as free acids by ultra performance liquid chromatography-tandem mass spectrometry. *Talanta,* 112**,** 85-94.

VAN DE VELDE, K., RUELENS, P., GEUTEN, K., ROHDE, A. & VAN DER STRAETEN, D. 2017. Exploiting DELLA Signaling in Cereals. *Trends Plant Sci,* 22**,** 880-893.

VAN DE VELDE, K., THOMAS, S. G., HEYSE, F., KASPAR, R., VAN DER STRAETEN, D. & ROHDE, A. 2021. N-terminal truncated *RHT-1* proteins generated by translational reinitiation cause semi-dwarfing of wheat Green Revolution alleles. *Molecular Plant,* 14**,** 679-687.

VANHAEREN, H., CHEN, Y., VERMEERSCH, M., DE MILDE, L., DE VLEESCHHAUWER, V., NATRAN, A., PERSIAU, G., EECKHOUT, D., DE JAEGER, G., GEVAERT, K. & INZÉ, D. 2020. *UBP12* and *UBP13* negatively regulate the activity of the ubiquitin-dependent peptidases DA1, DAR1 and DAR2. *eLife,* 9**,** e52276.

VELU, G., SINGH, R. P., HUERTA, J. & GUZMÁN, C. 2017. Genetic impact of Rht dwarfing genes on grain micronutrients concentration in wheat. *Field Crops Research,* 214**,** 373-377.

VERMA, A., PRAKASH, G., RANJAN, R., TYAGI, A. K. & AGARWAL, P. 2021. Silencing of an Ubiquitin Ligase Increases Grain Width and Weight in indica Rice. *Frontiers in Genetics,* 11.

VIJAYALAKSHMI, K., FRITZ, A. K., PAULSEN, G. M., BAI, G., PANDRAVADA, S. & GILL, B. S. 2010. Modeling and mapping QTL for senescence-related traits in winter wheat under high temperature. *Molecular Breeding,* 26**,** 163-175.

WADDINGTON., S. R., CARTWRIGHT, P. M. & WALL, P. C. 1983. A Quantitative Scale of Spike Initial and Pistil Development in Barley and Wheat. *Annals of Botany,* 51**,** 119-130.

WALKOWIAK, S., GAO, L., MONAT, C., HABERER, G., KASSA, M. T., BRINTON, J., RAMIREZ-GONZALEZ, R. H., KOLODZIEJ, M. C., DELOREAN, E., THAMBUGALA, D., KLYMIUK, V., BYRNS, B., GUNDLACH, H., BANDI, V., SIRI, J. N., NILSEN, K., AQUINO, C., HIMMELBACH, A., COPETTI, D., BAN, T., VENTURINI, L., BEVAN, M., CLAVIJO, B., KOO, D.-H., ENS, J., WIEBE, K., N'DIAYE, A., FRITZ, A. K., GUTWIN, C., FIEBIG, A., FOSKER, C., FU, B. X., ACCINELLI, G. G., GARDNER, K. A., FRADGLEY, N., GUTIERREZ-GONZALEZ, J., HALSTEAD-NUSSLOCH, G., HATAKEYAMA, M., KOH, C. S., DEEK, J., COSTAMAGNA, A. C., FOBERT, P., HEAVENS, D., KANAMORI, H., KAWAURA, K., KOBAYASHI, F., KRASILEVA, K., KUO, T., MCKENZIE, N., MURATA, K., NABEKA, Y., PAAPE, T., PADMARASU, S., PERCIVAL-ALWYN, L., KAGALE, S., SCHOLZ, U., SESE, J., JULIANA, P., SINGH, R., SHIMIZU-INATSUGI, R., SWARBRECK, D., COCKRAM, J., BUDAK, H., TAMESHIGE, T., TANAKA, T., TSUJI, H., WRIGHT, J., WU, J., STEUERNAGEL, B., SMALL, I., CLOUTIER, S., KEEBLE-GAGNÈRE, G., MUEHLBAUER, G., TIBBETS, J., NASUDA, S., MELONEK, J., HUCL, P. J., SHARPE, A. G., CLARK, M., LEGG, E., BHARTI, A., LANGRIDGE, P., HALL, A., UAUY, C., MASCHER, M., KRATTINGER, S. G., HANDA, H., SHIMIZU, K. K., DISTELFELD, A., CHALMERS, K., KELLER, B., MAYER, K. F. X., POLAND, J., STEIN, N., MCCARTNEY, C. A., SPANNAGL, M., WICKER, T. & POZNIAK, C. J. 2020. Multiple wheat genomes reveal global variation in modern breeding. *Nature,* 588**,** 277-283.

WANG, W., SIMMONDS, J., PAN, Q., DAVIDSON, D., HE, F., BATTAL, A., AKHUNOVA, A., TRICK, H. N., UAUY, C. & AKHUNOV, E. 2018. Gene editing and mutagenesis reveal inter-cultivar differences and additivity in the contribution of *TaGW2* homoeologues to grain size and weight in wheat. *Theoretical and Applied Genetics,* 131**,** 2463-2475.

WANG, Y., CHENG, X., SHAN, Q., ZHANG, Y., LIU, J., GAO, C. & QIU, J.-L. 2014. Simultaneous editing of three homoeoalleles in hexaploid bread wheat confers heritable resistance to powdery mildew. *Nature biotechnology,* 32**,** 947-951.

WANG, Z., XU, Y., CHEN, T., ZHANG, H., YANG, J. & ZHANG, J. 2015. Abscisic acid and the key enzymes and genes in sucrose-to-starch conversion in rice spikelets in response to soil drying during grain filling. *Planta,* 241**,** 1091-1107.

WIERSMA, J. J., BUSCH, R. H., FULCHER, G. G. & HARELAND, G. A. 2001. Recurrent selection for kernel weight in spring wheat. *Crop Science,* 41**,** 999-1005.

WILKINSON, P. A., ALLEN, A. M., TYRRELL, S., WINGEN, L. U., BIAN, X., WINFIELD, M. O., BURRIDGE, A., SHAW, D. S., ZAUCHA, J., GRIFFITHS, S., DAVEY, R. P., EDWARDS, K. J. & BARKER, G. L. A. 2020. CerealsDB-new tools for the analysis of the wheat genome: update 2020. *Database (Oxford),* 2020.

WILKINSON, S., KUDOYAROVA, G. R., VESELOV, D. S., ARKHIPOVA, T. N. & DAVIES, W. J. 2012. Plant hormone interactions: innovative targets for crop breeding and management. *Journal of Experimental Botany,* 63**,** 3499-3509.

WRIGHT, S. T. 1961. A sequential growth response to gibberellic acid, kinetin and indolyl-3-acetic acid in the wheat coleoptile (*Triticum vulgare L.*). *Nature,* 190**,** 699-700.

WÜRSCHUM, T., LEISER, W. L., LANGER, S. M., TUCKER, M. R. & LONGIN, C. F. H. 2018. Phenotypic and genetic analysis of spike and kernel characteristics in wheat reveals long-term genetic trends of grain yield components. *Theoretical and Applied Genetics,* 131**,** 2071-2084.

XIA, T., LI, N., DUMENIL, J., LI, J., KAMENSKI, A., BEVAN, M. W., GAO, F. & LI, Y. 2013. The Ubiquitin Receptor *DA1* Interacts with the E3 Ubiquitin Ligase *DA2* to Regulate Seed and Organ Size in Arabidopsis *The Plant Cell,* 25**,** 3347-3359.

XIE, Q. & SPARKES, D. 2021a. Dissecting the trade-off of grain number and size in wheat. *Planta,* 254.

XIE, Q. & SPARKES, D. L. 2021b. Dissecting the trade-off of grain number and size in wheat. *Planta,* 254**,** 3.

XU, H., LIU, Q., YAO, T. & FU, X. 2014. Shedding light on integrative GA signaling. *Curr Opin Plant Biol,* 21**,** 89-95.

YANG, Z., BAI, Z., LI, X., WANG, P., WU, Q., YANG, L., LI, L. & LI, X. 2012. SNP identification and allelic-specific PCR markers development for *TaGW2*, a gene linked to wheat kernel weight. *Theoretical and Applied Genetics,* 125**,** 1057-1068.

YAO, F. Q., LI, X. H., WANG, H., SONG, Y. N., LI, Z. Q., LI, X. G., GAO, X.-Q., ZHANG, X. S. & BIE, X. M. 2021. Down-expression of *TaPIN1s* Increases the Tiller Number and Grain Yield in Wheat. *BMC Plant Biology,* 21**,** 443.

ZADOKS, J. C., CHANG, T. T. & KONZAK, C. F. 1974. A decimal code for the growth stages of cereals. *Weed research,* 14**,** 415-421.

ZHAI, H., FENG, Z., DU, X., SONG, Y., LIU, X., QI, Z., SONG, L., LI, J., LI, L., PENG, H., HU, Z., YAO, Y., XIN, M., XIAO, S., SUN, Q. & NI, Z. 2018. A novel allele of *TaGW2-A1* is located in a finely mapped QTL that increases grain weight but decreases grain number in wheat (Triticum aestivum L.). *Theoretical and Applied Genetics,* 131**,** 539-553.

ZHANG, N., FAN, X., CUI, F., ZHAO, C., ZHANG, W., ZHAO, X., YANG, L., PAN, R., CHEN, M., HAN, J., JI, J., LIU, D., ZHAO, Z., TONG, Y., ZHANG, A., WANG, T. & LI, J. 2017. Characterization of the temporal and spatial expression of wheat (*Triticum aestivum L.)* plant height at the QTL level and their influence on yield-related traits. *Theoretical and Applied Genetics,* 130**,** 1235-1252.

ZHANG, Y. & LENHARD, M. 2017. Exiting Already? Molecular Control of Cell-Proliferation Arrest in Leaves: Cutting Edge. *Mol Plant,* 10**,** 909-911.

ZHANG, Y., LI, D., ZHANG, D., ZHAO, X., CAO, X., DONG, L., LIU, J., CHEN, K., ZHANG, H., GAO, C. & WANG, D. 2018. Analysis of the functions of *TaGW2* homoeologs in wheat grain weight and protein content traits. *The Plant Journal,* 94**,** 857-866.

ZHAO, B., WU, T. T., MA, S. S., JIANG, D. J., BIE, X. M., SUI, N., ZHANG, X. S. & WANG, F. 2020. TaD27-B gene controls the tiller number in hexaploid wheat. *Plant Biotechnology Journal,* 18**,** 513-525.

ZHAO, C., LIU, B., PIAO, S., WANG, X., LOBELL, D. B., HUANG, Y., HUANG, M., YAO, Y., BASSU, S., CIAIS, P., DURAND, J.-L., ELLIOTT, J., EWERT, F., JANSSENS, I. A., LI, T., LIN, E., LIU, Q., MARTRE, P., MÜLLER, C., PENG, S., PEÑUELAS, J., RUANE, A. C., WALLACH, D., WANG, T., WU, D., LIU, Z., ZHU, Y., ZHU, Z. & ASSENG, S. 2017. Temperature increase reduces global yields of major crops in four independent estimates. *Proceedings of the National Academy of Sciences,* 114**,** 9326-9331.

ZHAO, J., ZHAI, Z., LI, Y., GENG, S., SONG, G., GUAN, J., JIA, M., WANG, F., SUN, G., FENG, N., KONG, X., CHEN, L., MAO, L. & LI, A. 2018. Genome-Wide Identification and Expression Profiling of the TCP Family Genes in Spike and Grain Development of Wheat (Triticum aestivum L.). *Front Plant Sci,* 9**,** 1282.

6. Supplementary materials

Table 1: Complete list of Paragon NILs and sister lines used in these study

#	Genotype	Sister Line	Gw2_A1	Gw2_B1	Gw2_D1	No.Mutations	Rep
	2019			**Alleles**			
1	Paragon WT	A	AA	BB	DD	0	1
2	Paragon WT	A	AA	BB	DD	0	2
3	Paragon WT	A	AA	BB	DD	0	3
4	Paragon single	A	aa	BB	DD	1	1
5	Paragon single	A	AA	bb	DD	1	1
6	Paragon single	A	AA	BB	dd	1	1
7	Paragon single	A	AA	bb	DD	1	2
8	Paragon single	A	aa	BB	DD	1	2
9	Paragon single	A	AA	BB	dd	1	2
10	Paragon single	A	AA	BB	dd	1	3
11	Paragon single	A	aa	BB	DD	1	3
12	Paragon single	A	AA	bb	DD	1	3
13	Paragon doubles	A	aa	BB	dd	2	1
14	Paragon doubles	A	AA	bb	dd	2	1
15	Paragon doubles	A	aa	BB	dd	2	2
16	Paragon doubles	A	AA	bb	dd	2	2
17	Paragon doubles	A	aa	BB	dd	2	3
18	Paragon doubles	A	AA	bb	dd	2	3
19	Paragon triples	A	aa	bb	dd	3	1
20	Paragon triples	A	aa	bb	dd	3	2
21	Paragon triples	A	aa	bb	dd	3	3
22	Paragon WT	B	AA	BB	DD	0	1
23	Paragon WT	B	AA	BB	DD	0	2
24	Paragon single	B	aa	BB	DD	1	1
25	Paragon single	B	AA	BB	dd	1	1
26	Paragon single	B	AA	bb	DD	1	1
27	Paragon single	B	aa	BB	DD	1	2
28	Paragon single	B	AA	BB	dd	1	2
29	Paragon single	B	AA	bb	DD	1	2
30	Paragon single	B	AA	BB	dd	1	3
31	Paragon single	B	AA	bb	DD	1	3
32	Paragon doubles	B	aa	bb	DD	2	1
33	Paragon doubles	B	aa	BB	dd	2	1
34	Paragon doubles	B	AA	bb	dd	2	1
35	Paragon doubles	B	aa	bb	DD	2	2
36	Paragon doubles	B	aa	BB	dd	2	2
37	Paragon doubles	B	AA	bb	dd	2	2
38	Paragon doubles	B	AA	bb	dd	2	3
39	Paragon doubles	B	aa	BB	dd	2	3
40	Paragon doubles	B	aa	bb	DD	2	3
41	Paragon triples	B	aa	bb	dd	3	1
42	Paragon triples	B	aa	bb	dd	3	2

			Alleles				
2020 and 2021							
#	Genotype	BC	GW2_A	GW2_B	GW2_D	*No.Mutations*	Rep
1	Paragon WT	BC2	AA	BB	DD	0	1
2	Paragon WT	BC2	AA	BB	DD	0	1
3	Paragon WT	BC4	AA	BB	DD	0	1
4	Paragon WT	BC4	AA	BB	DD	0	1
5	Paragon WT	BC2	AA	BB	DD	0	2
6	Paragon WT	BC2	AA	BB	DD	0	2
7	Paragon WT	BC4	AA	BB	DD	0	2
8	Paragon WT	BC4	AA	BB	DD	0	2
9	Paragon WT	BC2	AA	BB	DD	0	3
10	Paragon WT	BC4	AA	BB	DD	0	3
11	Paragon WT	BC2	AA	BB	DD	0	3
12	Paragon WT	BC4	AA	BB	DD	0	3
13	Paragon WT	BC4	AA	BB	DD	0	4
14	Paragon WT	BC2	AA	BB	DD	0	4
15	Paragon WT	BC2	AA	BB	DD	0	4
16	Paragon WT	BC4	AA	BB	DD	0	4
17	Paragon WT	BC2	AA	BB	DD	0	5
18	Paragon WT	BC2	AA	BB	DD	0	5
19	Paragon WT	BC4	AA	BB	DD	0	5
20	Paragon WT	BC4	AA	BB	DD	0	5
21	Paragon single	BC4	aa	BB	DD	1	1
22	Paragon single	BC4	AA	bb	DD	1	1
23	Paragon single	BC4	AA	BB	dd	1	1
24	Paragon single	BC4	aa	BB	DD	1	1
25	Paragon single	BC4	AA	bb	DD	1	1
26	Paragon single	BC4	AA	BB	dd	1	1
27	Paragon single	BC4	AA	bb	DD	1	2
28	Paragon single	BC4	aa	BB	DD	1	2
29	Paragon single	BC4	AA	BB	dd	1	2
30	Paragon single	BC4	AA	bb	DD	1	2
31	Paragon single	BC4	aa	BB	DD	1	2
32	Paragon single	BC4	AA	BB	dd	1	2
33	Paragon single	BC4	AA	BB	dd	1	3
34	Paragon single	BC4	AA	bb	DD	1	3
35	Paragon single	BC4	aa	BB	DD	1	3
36	Paragon single	BC4	AA	bb	DD	1	3
37	Paragon single	BC4	AA	BB	dd	1	3
38	Paragon single	BC4	aa	BB	DD	1	3
39	Paragon single	BC4	aa	BB	DD	1	4
40	Paragon single	BC4	AA	BB	dd	1	4
41	Paragon single	BC4	AA	bb	DD	1	4
42	Paragon single	BC4	AA	BB	dd	1	4
43	Paragon single	BC4	AA	bb	DD	1	4
44	Paragon single	BC4	aa	BB	DD	1	4

45	Paragon single	BC4	AA	bb	DD	1	5
46	Paragon single	BC4	aa	BB	DD	1	5
47	Paragon single	BC4	aa	BB	DD	1	5
48	Paragon single	BC4	AA	bb	DD	1	5
49	Paragon single	BC4	AA	BB	dd	1	5
50	Paragon single	BC4	AA	BB	dd	1	5
51	Paragon doubles	BC4	aa	bb	DD	2	1
52	Paragon doubles	BC4	aa	BB	dd	2	1
53	Paragon doubles	BC4	AA	bb	dd	2	1
54	Paragon doubles	BC4	aa	bb	DD	2	1
55	Paragon doubles	BC4	aa	BB	dd	2	1
56	Paragon doubles	BC4	AA	bb	dd	2	1
57	Paragon doubles	BC4	aa	bb	DD	2	2
58	Paragon doubles	BC4	aa	BB	dd	2	2
59	Paragon doubles	BC4	AA	bb	dd	2	2
60	Paragon doubles	BC4	aa	bb	DD	2	2
61	Paragon doubles	BC4	aa	BB	dd	2	2
62	Paragon doubles	BC4	AA	bb	dd	2	2
63	Paragon doubles	BC4	aa	BB	dd	2	3
64	Paragon doubles	BC4	aa	bb	DD	2	3
65	Paragon doubles	BC4	aa	BB	dd	2	3
66	Paragon doubles	BC4	AA	bb	dd	2	3
67	Paragon doubles	BC4	AA	bb	dd	2	3
68	Paragon doubles	BC4	aa	bb	DD	2	3
69	Paragon doubles	BC4	AA	bb	dd	2	4
70	Paragon doubles	BC4	aa	bb	DD	2	4
71	Paragon doubles	BC4	aa	BB	dd	2	4
72	Paragon doubles	BC4	aa	BB	dd	2	4
73	Paragon doubles	BC4	aa	bb	DD	2	4
74	Paragon doubles	BC4	AA	bb	dd	2	4
75	Paragon doubles	BC4	AA	bb	dd	2	5
76	Paragon doubles	BC4	aa	bb	DD	2	5
77	Paragon doubles	BC4	aa	BB	dd	2	5
78	Paragon doubles	BC4	AA	bb	dd	2	5
79	Paragon doubles	BC4	aa	bb	DD	2	5
80	Paragon doubles	BC4	aa	BB	dd	2	5
81	Paragon triples	BC2	aa	bb	dd	3	1
82	Paragon triples	BC2	aa	bb	dd	3	1
83	Paragon triples	BC4	aa	bb	dd	3	1
84	Paragon triples	BC4	aa	bb	dd	3	1
85	Paragon triples	BC4	aa	bb	dd	3	2
86	Paragon triples	BC2	aa	bb	dd	3	2
87	Paragon triples	BC2	aa	bb	dd	3	2
88	Paragon triples	BC4	aa	bb	dd	3	2
89	Paragon triples	BC2	aa	bb	dd	3	3
90	Paragon triples	BC4	aa	bb	dd	3	3

91	Paragon triples	BC4	aa	bb	dd	3	3
92	Paragon triples	BC2	aa	bb	dd	3	3
93	Paragon triples	BC4	aa	bb	dd	3	4
94	Paragon triples	BC2	aa	bb	dd	3	4
95	Paragon triples	BC2	aa	bb	dd	3	4
96	Paragon triples	BC4	aa	bb	dd	3	4
97	Paragon triples	BC4	aa	bb	dd	3	5
98	Paragon triples	BC2	aa	bb	dd	3	5
99	Paragon triples	BC2	aa	bb	dd	3	5
100	Paragon triples	BC4	aa	bb	dd	3	5